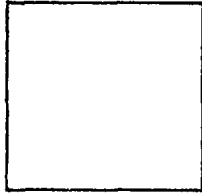


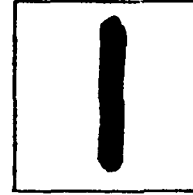
PHOTOGRAPH THIS SHEET

ADA083541

DTIC ACCESSION NUMBER



LEVEL



INVENTORY

FTD-ID (RS)T-0521-79
DOCUMENT IDENTIFICATION

DISTRIBUTION STATEMENT A
Approved for public release;
Distribution Unlimited

DISTRIBUTION STATEMENT

| | |
|--------------------|---|
| ACCESSION FOR | |
| NTIS | GRA&I <input checked="" type="checkbox"/> |
| DTIC | TAB <input type="checkbox"/> |
| UNANNOUNCED | <input type="checkbox"/> |
| JUSTIFICATION | |
| | |
| BY | |
| DISTRIBUTION / | |
| AVAILABILITY CODES | |
| DIST | AVAIL AND/OR SPECIAL |
| A | |

DISTRIBUTION STAMP

DTIC
ELECTE
S APR 24 1980 D
D

DATE ACCESSIONED

79 1 13 219

DATE RECEIVED IN DTIC

PHOTOGRAPH THIS SHEET AND RETURN TO DTIC-DDA-2

AE A 083541

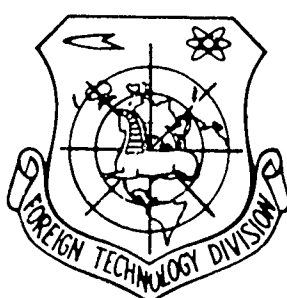
FOREIGN TECHNOLOGY DIVISION



DESIGN OF AIRCRAFT
(Selected Chapters)

by

A. A. Badyagin, S. M. Yeger, V. F. Mishin,
F. I. Sklyanskiy, N. A. Fomin



Approved for public release;
distribution unlimited.



FTD- ID(RS)T-0521-79

UNEDITED MACHINE TRANSLATION

FTD-ID(RS)T-0521-79

10 July 1979

MICROFICHE NR: *FTD-79-C 000 931*

DESIGN OF AIRCRAFT (Selected Chapters)

By: A. A. Badyagin, S. M. Yeger, V. F. Mishin,
F. I. Sklyanskiy, N. A. Fomin

English pages: 417

Source: Proyektirovaniye Samoletov, 2-ye
Izd-vo "Mashinostroyeniye" Moscow,
1972, pp. 1-14: 26-55; 69-85; 97-149;
189-225.

Country of origin: USSR

This document is a machine translation.

Requester: FTD/TQTA

Approved for public release; distribution unlimited.

THIS TRANSLATION IS A RENDITION OF THE ORIGINAL FOREIGN TEXT WITHOUT ANY ANALYTICAL OR EDITORIAL COMMENT. STATEMENTS OR THEORIES ADVOCATED OR IMPLIED ARE THOSE OF THE SOURCE AND DO NOT NECESSARILY REFLECT THE POSITION OR OPINION OF THE FOREIGN TECHNOLOGY DIVISION.

PREPARED BY:

TRANSLATION DIVISION
FOREIGN TECHNOLOGY DIVISION
WP-AFB, OHIO.

FTD- ID(RS)T-0521-79

Date 10 Jul 19 79

TABLE OF CONTENTS

| | |
|--|-----|
| U. S. Board on Geographic Names Transliteration System, Russian and English Trigonometric Functions..... | ii |
| Preface..... | 4 |
| Introduction..... | 21 |
| Chapter II. Basic and Relative Parameters of Aircraft, Equation of Relative Weights. The Effect of the most Important Parameters of Air- craft on its Flight Characteristics..... | 41 |
| Chapter IV. Approximate Methods of the Optimization of the Parameters of Aircraft..... | 113 |
| Section II. Selection of Scheme, Power Plant and Basic Parameters of Aircraft..... | 157 |
| Chapter VI. Airplane Design. Analysis and Selection of Diagram..... | 157 |
| Chapter VII. Basic Questions of the Design of the Power Plant of Aircraft..... | 222 |
| Chapter VIII. Determination of the Basic Parameters of Aircraft..... | 294 |
| Chapter XI. Special Features of the Design of Aero- space Aircraft..... | 314 |

U. S. BOARD ON GEOGRAPHIC NAMES TRANSLITERATION SYSTEM

| Block | Italic | Transliteration | Block | Italic | Transliteration |
|-------|------------|-----------------|-------|------------|-----------------|
| А а | <i>А а</i> | A, a | Р р | <i>Р р</i> | R, r |
| Б б | <i>Б б</i> | B, b | С с | <i>С с</i> | S, s |
| В в | <i>В в</i> | V, v | Т т | <i>Т т</i> | T, t |
| Г г | <i>Г г</i> | G, g | У у | <i>У у</i> | U, u |
| Д д | <i>Д д</i> | D, d | Ф ф | <i>Ф ф</i> | F, f |
| Е е | <i>Е е</i> | Ye, ye; E, e* | Х х | <i>Х х</i> | Kh, kh |
| Ж ж | <i>Ж ж</i> | Zh, zh | Ц ц | <i>Ц ц</i> | Ts, ts |
| З э | <i>З э</i> | Z, z | Ч ч | <i>Ч ч</i> | Ch, ch |
| И и | <i>И и</i> | I, i | Ш ш | <i>Ш ш</i> | Sh, sh |
| Й й | <i>Й й</i> | Y, y | Щ щ | <i>Щ щ</i> | Shch, shch |
| К к | <i>К к</i> | K, k | Ъ ъ | <i>Ъ ъ</i> | " |
| Л л | <i>Л л</i> | L, l | Ы ы | <i>Ы ы</i> | Y, y |
| М м | <i>М м</i> | M, m | Ь ь | <i>Ь ь</i> | ' |
| Н н | <i>Н н</i> | N, n | Э э | <i>Э э</i> | E, e |
| О о | <i>О о</i> | O, o | Ю ю | <i>Ю ю</i> | Yu, yu |
| П п | <i>П п</i> | P, p | Я я | <i>Я я</i> | Ya, ya |

*ye initially, after vowels, and after Ъ, Ь; e elsewhere.
When written as ë in Russian, transliterate as yë or ë.

RUSSIAN AND ENGLISH TRIGONOMETRIC FUNCTIONS

| Russian | English | Russian | English | Russian | English |
|---------|---------|---------|---------|----------|--------------------|
| sin | sin | sh | sinh | arc sh | sinh ⁻¹ |
| cos | cos | ch | cosh | arc ch | cosh ⁻¹ |
| tg | tan | th | tanh | arc th | tanh ⁻¹ |
| ctg | cot | cth | coth | arc cth | coth ⁻¹ |
| sec | sec | sch | sech | arc sch | sech ⁻¹ |
| cosec | csc | csch | csch | arc csch | csch ⁻¹ |

Russian English

rot curl
lg log

DOC = 79052101

PAGE 1

Page 1.

DESIGN OF AIRCRAFT.

A. A. Badyagin, S. M. Yeger, V. P. Mishin, P. I. Sklyanskiy, N. A.
Pomin.

Second edition, revised and supplemented

Page 2.

In the book are presented common/general/total bases and design concepts of aircraft, is examined the selection of diagram, power plant and basic parameters of aircraft. The second edition includes the new materials: the methods of optimum design with use of computers, the method of the gradients of takeoff weight for the evaluation of the designing solutions and conversion of weight characteristics, special feature/peculiarity of the design of aircraft with the shortened and vertical lift, passenger and aerospace aircraft.

Are considerably expanded and reworked the sections, which relate taking into consideration of the requirements of saving and for the design of basic aggregate/units.

Application/appendices to the book are supplemented by the characteristics of aircraft engines, by standard combined weight and enumeration of standard electronic equipment.

The book is intended for the students of aviation VUZ [Institute of Higher Education] can be useful for the engineers of the aircraft industry.

DOC = 79052101

PAGE 3

Tables - 30. Illust. - 393. List of lit. - 37 titles.

Page 3.

PREFACE.

In the years, which passed from the time of the publication of the textbook of N. A. Fomin "design of aircraft" (1961), substantially grew the technological level of aviation and. Appeared supersonic heavy aircraft, including passenger, usual became aircraft with on the variable in flight sweepback of wing, are introduced VTOL aircraft.

Questions of the design of aircraft within this time also obtained substantial development. Widely is applied the method of optimum design, system approach, use of computers and so forth.

The authors were aware in the fact that to write stable manual on the design of aircraft is extremely difficult. Each decade in aviation now whole epoch ! Therefore in this book in comparison with the analogous previous textbooks, considerable attention is given to the fundamental systematic questions which are not subjected to so quick ageing. At the same time the authors attempted to give material of reference character, necessary for license or pre-sketching design of aircraft.

The proposed manual corresponds to the program of course the "design of aircraft" for VU2.

Manual consists of two sections - common/general/total design of aircraft and design of its parts.

In the first section of a book three parts. In the first part are presented common/general/total bases and design concepts of aircraft. Here is given the method of the operation of low increases in parameters and characteristics of aircraft, which makes it possible comparatively simple to solve the large circle of tasks.

In the second part is examined the selection of diagram, power plant and basic parameters of aircraft. Primary attention is here given to the design jets. Separate chapters are dedicated to the special feature/peculiarities of the common/general/total design of passenger aircraft, aircraft with shortened and vertical takeoff and landing, and also to the design of the aerospace aircraft.

In third part one section is examined layout and position of center of gravity in aircraft.

Page 4.

In the second section of manual, is given the procedure of determining dimensions and weight of wing, fuselage, tail assembly and chassis/landing gear. Here are examined the common/general/total bases of the design of the aircraft components and basis of the design of the system of its control.

Chapters I, III, IV, V, VI, XIV are written by A. A. Badyagin, introduction, chapter II, VIII, XII, XIII by V. F. Mishin, chapter XVII, XIX - by P. I. Sklyanskiy. Chapters XVI and XVII are written by A. A. Badyagin and V. F. Mishin, chapter X is written by N. A. Fomin and N. K. Liseytsev, Chapter XV - by N. A. Fomin and by V. Ye. Rotin.

All concrete/specific/actual information on the design of aircraft and the selection of engine in the period of the preliminary development of aircraft is published in the open Soviet and foreign press. The authors with appreciation will accept the observations about the book, which should be guided to: Moscow, E-66, 1st Basmany per., 3, publishing house "Mashinostroyeniye".

Page 5.

BASIC DESIGNATIONS AND ABBREVIATIONS

a - speed of sound, expenditure/consumptions per 1 ton-kilometer;

α - angle of attack of wing;

B - track of landing gear;

b - wing chord, basis of chassis/landing gear;

b_0 - root wing chord;

b_n - end wing chord;

C - cost/value;

c_a - wing chord ratio in root;

c_n - thickness ratio at wing tip;

c_f - aerodynamic coefficient of friction;

c_m - coefficient of the aerodynamic pitching moment of wing profile;

c_{m_0} - coefficient c_m when $c_y=0$;

c_T - thrust coefficient;

c_p - specific hourly consumption of fuel/propellant of TRD [turbojet engine];

c_p - specific hourly consumption of fuel/propellant of TVD [turboprop engine];

c_x - drag coefficient;

c_{x_0} - drag coefficient when $c_y=0$;

c_{x_i} - the coefficient of induced drag;

c_{x_w} - coefficient of wave drag;

c_{x_p} - coefficient of profile drag;

c_v - lift coefficient;

c_v' - derivative c_v according to angle of attack α ;

D_0 - diameter of fuselage;

δ - angle of deflection of any control;

E - modulus of normal elasticity of material;

F - area of the washed by flow surface;

f - coefficient of friction, safety factor;

G - weight of aircraft;

G_0 - starting (takeoff) weight of aircraft

G_k - structural weight;

$\bar{G}_k = \frac{G_k}{G_0}$ - the over-all payload ratio of construction/design;

G_f - fuel load;

$\bar{G}_r = \frac{G_r}{G_0}$ - the over-all payload ratio of fuel/propellant;

g - acceleration of gravity; the weight of 1 m² of the surface of aggregate/unit;

γ - specific gravity/weight;

H - flight altitude;

χ - sweep angle of wing (on quarter-chord);

$\chi_{n.k}$ - sweep angle (on leading wing edge);

K - lift-drag ratio;

k - coefficient;

L - flying range, length;

l - wingspan;

λ - wing aspect ratio;

λ_i - elongation of any aircraft component;

M - Mach number;

m - mass of the flight vehicle: bypass ratio of TVRD;

m_x, m_y, m_z - coefficients of the aerodynamic moment of aircraft (in body coordinate system);

N - the total power of engines.

Page 6.

N_0 - starting power of engines (with $V=0$; $H=0$);

N_{0i} - starting power of one engine;

$\bar{N}_0 = N_0/G_0$ - relative starting power;

$n^p, n^q, n_y, n_x, n_z, n_A, n_E$ - load factors;

n_{te} - number engine;

n_{pass} - passengers' quantity;

P - gross thrust engine;

P_0 - the boost for launching of engines (with $V=0$; $H=0$);

P_{01} - the boost for launching of one engine;

$\bar{P}_0 = P_0/G_0$ - starting thrust-weight ratio;

$P_{s.p}$ - specific thrust of power plant;

p - the specific wing load (p_0 - with takeoff);

Q - the hourly consumption of fuel/propellant;

q - ram pressure, fuel consumption per kilometer;

ρ - mass air density; ρ_0 - in the surface of sea;

$\Delta = \rho/\rho_0$ - relative density of air;

R - radius of the Earth, radius of bank/turn and so forth;

S - wing area (with subfuselage part);

\bar{S}_i - relative area of any aircraft component (referred to wing area);

η - wing taper;

η_p - propeller efficiency;

T, K - temperature in degrees Kelvin;

T - the serviceable life of service; resource/lifetime;

t - time, temperature in degrees Celsius;

θ - flight path angle to the horizon;

V - flight speed;

V_{in} - orbital velocity;

V_v - the vertical velocity;

X - aerodynamic drag;

x_T - position the center of gravity of aircraft from leading edge/nose of *MAC*

x_F - position of the focus of aircraft from leading edge/nose of *MAC*;

Y - aerodynamic lift.

Contractions.

VKS - aerospace aircraft;

VP β - takeoff and landing strip;

GTD - gas turbine engine;

DTRD - turbofan engine;

ZhRD - liquid propellant rocket engine;

LPS - flight personnel;

PVRD - ramjet engine;

PD - piston engine;

PRD - solid propellant rocket engine;

SA - standard atmosphere;

MAC - mean aerodynamic chord;

SPS - supersonic passenger aircraft;

TVD - turboprop engine;

TVRD - turbofan engine;

TRD - turbojet engine;

TRDF - turbojet reheat engine;

EVM - electronic computer;

UPS - boundary layer control;

SVVP - VTOL aircraft;

SUVP - STOL aircraft.

Indices.

v - wave;

vzl. - takeoff (G_0 - takeoff weight);

v.o - vertical tail assembly;

g - nacelle, load, throat;

g.o - horizontal tail assembly;

dv - engine;

i - interference;

k - construction/design.

Page 7.

kach - rolling;

kom - commercial;

kr - wing;

kreys - cruising;

krit - critical (value);

m - midsection;

m.f - midsection of fuselage.

0 - initial value of value (or with start);

n - load;

n.v - climb;

n.z - navigational reserve;

ob.upr - equipment and control;

omyv - the washed surface;

op - tail assembly;

ost - cessation;

otr - breakaway;

pas - passenger;

pl - gliding/planning;

p.n - payload;

pos - landing;

pot - ceiling;

prerv - interrupted;

priv - given;

prob - landing run;

pust - empty;

rasch - calculation;

reys - voyaging speed;

razb - takeoff/run-up;

ras^hh - expended;

ri - control;

rch - knob/stick;

^Sg - the jettisonable load (in flight);

sk - slip;

sluzh - service;

sn - equipment;

s.u - power plant;

f - fuselage;

sh - chassis/landing gear;

ek - crew.

Page 8.

INTRODUCTION.

By design of aircraft, usually is understood the process development of the technical materials (documentation), which are determining its technical flight characteristics, diagram and construction/design of separate aggregate/units.

Designation/purpose, operating conditions and technical flight characteristics of the design/projected aircraft are determined by client and take shape in the form of special requirements.

Designing the aircraft encompasses the development of sketch and worker of projects. The work on the refinement of requirements for aircraft and possibility of their accomplishing, done prior to the beginning of the development of preliminary design, is called, preliminary (pre-sketching) design.

Sketch design consists in the development of the fundamental characteristics of aircraft, its aerodynamic and design concepts which make it possible to judge the advisability of further design.

Into the sketch design of aircraft, enters:

- a) the development of general views and layout cut/sections;
- b) the abbreviated development of the construction/design of the most important parts (aggregate/units);
- c) the development of schematic diagrams, systems of equipment and control, and also power plant;
- d) the calculation of the force of gravity (weight) and centering;
- e) aerodynamic design, stability analysis and controllability;
- f) approximate computation for the strength of the most important aircraft components.

Simultaneously with the development of preliminary design is constructed aircraft scale model full size. For the examination of mock-up by customer is assigned the board from different specialists, including crew.

After the conclusion of simulated board, which examines and

confirms preliminary design and aircraft scale model, is realize/accomplished the final connecting/fitting of construction/design with the arrangement/position of control and equipment, are more precisely formulated external enclosures. Then conduct the more complete crews of aircraft on strength, make and blast in the wind tunnels of model and according to the results of testings of model in wind tunnel they more precisely formulate aerodynamic design, stability analysis, spin and flutter. On the basis of the results of blasting, is more precisely formulated the airplane design, are performed the refined weight calculations, in this case, are establish/installed weight limits (greatest values of the weight of the structure of aircraft and its parts, the permissible from considerations designs).

Page 9.

Is working design - this is the concluding process of development of technical documentation. Working project gives all necessary materials about the technical flight data of future aircraft, about his strength and reliability; it contains equipment specifications and all necessary information for developing technology of the production of aircraft. It must be noted that is working the design of the experimental aircraft usually is terminated after the constructed specimen/sample of aircraft passed tests.

Into working design enters:

a) the development of the assembly and detail drawings of the construction/design of the separate aggregate/units (parts) of aircraft;

b) the development of the general view drawings of the aggregate/units of aircraft;

c) the refinement of calculations for the strength of all load-bearing elements;

d) the refinement of the calculations of the structural weight;

e) conducting the research and experimental works, connected with the implementation of new construction/designs, materials, etc.

Development of the working project of contemporary aircraft the extremely labor-consuming and complicated process whose accomplishing under force only to the large collective of the qualified technical-engineering workers of different specialties.

With experimental research works deal the laboratories of design bureaus and scientific research institutes. The final stage of experimental research works are usually the static and dynamic tests of construction/design for strength, lifetime, reliability of separate aggregate/units and systems. Hydraulic systems and other systems of equipment, system of control and recovery facilities aircrew in necessary order undergo bench tests under conditions, close to operational ones.

Entire immense volume of knowledge, necessary for designing the contemporary aircraft, was accumulated as a result of the more than half century work scientist different countries - aerodynamicists, material-strength engineers, metallurgists - and the engineering practice of design, construction and production of aircraft.

Accumulation of knowledge and engineering experience contributed to the perfection of aircraft, which was being accompanied by a change in the basic parameters and by an improvement in its fundamental flight characteristics.

By fundamental aircraft performance, is usually understood maximum speed of level flight V_{max} , ceiling H_{hor} , maximum vertical velocity V_{vmax} and maximum flying distance L_{max} . The basic parameters of aircraft include such parameters whose change substantially is

reflected in the characteristics of aircraft, namely: the takeoff weight of aircraft G_0 , wing area S , the specific wing load $p_0 = G_0/S$, horsepower loading G_0/N or thrust-weight ratio $\bar{P}_0 = P_0/G_0$.

Tables 0.1 and 0.2 depict the common/general/total picture of a change in some of these values over the years for heavy and light aircraft.

It is characteristic that one of the fundamental aircraft performance (the maximum speed of level flight) increased continuously from year to year.

A continuous increase in the maximum speed of flight became possible as a result of decreasing the aerodynamic drag of aircraft and decrease of the load, which is necessary on / hp of installed power.

Page 10.

The decrease of aerodynamic drag can be reached, in the first place, by the aerodynamic perfection of diagram and forms of aircraft, in the second place, by decrease to the known limit of carrying wing area (in the latter case the specific wing load p_0 is increased).

The most effective means of the decrease of load on 1 hp was an increase in the installed power during the decrease of the value of its specific gravity/weight, i.e., the ratio of the weight of installation toward its power $G_{c,y}/N_{max}$.

With an increase in the installed power usually grow/rose its weight, and also fuel load, necessary for achievement by given one of distance or duration of flight. At the same time grow/rose the weight of transportable ones by the aircraft of loads. All these factors, and increased requirements for the structural strength of aircraft, unavoidably led to an increase in the takeoff weight.

The decrease of the aerodynamic drag of aircraft was achieved to a considerable degree as a result of the aerodynamic perfection of wings, in particular wing airfoil/profiles.

The perfection of wings occurred simultaneously with the development of airplane design, which in 30-35 years underwent considerable changes.

Table 0.1. Change in the fundamental characteristics and parameters of heavy aircraft over the years.

| Год (1) | Наименование самолета (2) | (3) G_0 кгс | (4) S m^2 | (5) P_0 кгс/ m^2 | (6) V_{max} км/ч | (7) N_{max} л. с. | (8) G_0/N_{max} кгс/л. с. | (9) P_0 кгс | (10) P_0 кгс/кгс | H м |
|------------|--|---------------------|---------------------|----------------------------|--------------------------|---------------------------|-----------------------------------|---------------------|--------------------------|----------|
| 1910 | «Гаккел -III» (Россия) ⁽¹¹⁾ | 420 | 29 | 14,5 | 90 | 35 | 12,0 | — | — | 1 000 |
| 1915 | «Ил'я Муромец» (Россия) ⁽¹²⁾ | 5 600 | 160 | 35,0 | 115 | 740 | 7,5 | — | — | 3 000 |
| 1920 | Капрони (Италия) ⁽¹³⁾ | 4 500 | 100 | 45,0 | 180 | 600 | 7,5 | — | — | 4 000 |
| 1930 | ТБ-3 (СССР) | 18 000 | 230 | 78,5 | 240 | 2000 | 9,0 | — | — | 4 000 |
| 1940 | Боинг В-17 (США) ⁽¹⁴⁾ | 20 600 | 130 | 158,5 | 450 | 4000 | 5,2 | — | — | 9 000 |
| 1950 | Боинг В-29 (США) ⁽¹⁵⁾ | 47 000 | 161 | 292,0 | 600 | 8000 | 5,9 | — | — | 10 500 |
| 1950 | Стратоджет В-47 (США) ⁽¹⁵⁾ | 84 000 | 140 | 600 | 960 | — | — | 14 000 | 0,167 | 13 000 |
| 1956 | Конвэр В-58 (США) ⁽¹⁶⁾ | 63 500 | 140 | 450 | 2000 | — | — | 36 000 | 0,567 | — |
| 1965 | XB-70 (США) | 250 000 | 585 | 427 | 3200 | — | — | 81 500 | 0,326 | 20 000 |

Key: (1). Year. (2). Designation of aircraft. (3). kg. (4). m^2 . (5). kgf/m^2 . (6). km/h. (7). hp. (8). kg/hp . (9). kg. (10). kg/kg . (11). "Gakkel-III" (Russia). (12). "Il'ya Muromets" (Russia). (13). Caproni (Italy). (14). Boeing. (15). Stratojet. (16). Convair.

Table 0.2. Change in the fundamental characteristics and parameters of light aircraft over the years.

| Год (1) | Наименование самолета (2) | G_0 кгс (3) | S m^2 (4) | P_0 кгс/ m^2 (5) | V_{max} км/ч (6) | N_{max} л. с. (7) | G_0/N_{max} кгс/л. с. (8) | P_0 кгс (9) | \bar{P}_0 | H м |
|------------|---|---------------------|---------------------|----------------------------|--------------------------|---------------------------|-----------------------------------|---------------------|-------------|----------|
| 1910 | «Гаккель-III» (Россия) (10) | 420 | 29 | 14,5 | 90 | 35 | 12,0 | — | — | 1000 |
| 1915 | Ньюпор-21 (Франция) | 495 | 15 | 33,0 | 150 | 80 | 6,2 | — | — | 5000 |
| 1920 | Маргинсайд F.4 (Анг- лия) (12) | 1113 | 34,0 | 32,8 | 211 | 300 | 3,7 | — | — | 6800 |
| 1930 | И-5 (СССР) | 1300 | 19,0 | 67,0 | 275 | 525 | 2,5 | — | — | 8000 |
| 1940 | Мессершмитт 109 (13) (Германия) (14) | 2600 | 16,5 | 159 | 570 | 1100 | 2,3 | — | — | 11000 |
| 1950 | МиГ-15 (СССР) (15) | 4800 | 20,0 | 240 | 1050 | — | — | 2000 | 0,415 | 15000 |
| 1956 | Локхид F-104 (США) | 6800 | 17,0 | 400 | 2500 | — | — | 9000 | 1,32 | 21000 |

Key: (1). year. (2). Designation of aircraft. (3). kg. (4). m^2 . (5). kgf/m^2 . (6). km/h. (7). hp. (8). kg/hp . (9). kg. (10). "Gakkel'-III" (Russia). (11). Nieuport (France). (12). Martinside (England). (13). Messerschmidt (14). Germany. (15). MiG (USSR). (16). Lockheed (USA).

Page 11.

The applied previously extremely widely diagram of biplane already since 1925 began to be displaced by the aerodynamically more advanced diagram of cantilever monoplane with the thick wing profile (of type of N. Ye. Zhukovskiy's airfoil/profiles), which had thickness ratio $\bar{c}=0.20-0.24$.

Subsequently the development of wings followed already by means of the gradual decrease of the thickness ratio of their airfoil/profiles (Fig. 0.1). Tendency toward decrease of \bar{c} of wing

profile is explained by the fact that with decrease of c decreases profile and wave wing drag. Figures 0.2 show a change in the total coefficient of profile and wave drag c_x (when $\dot{c}_y=0$) wing in dependence on \bar{c} . Especially sharply change \bar{c} in the airfoil/profile affects the value of wave wing drag, which appears with speeds, close to the speed of sound (curve $M=1$).

Transfer/transition from the diagram of wing in the form of multi-stand biplane cell (Fig. 0.3a) to the cantilever wing of first thick (Fig. 0.3b), and then fine/thin airfoil/profile (Fig. 0.3c) contributed to the aerodynamic perfection of wing and decreased its overall height h . A change in the overall height substantially affects by weight of wing. With the decrease of the overall height of wing h , increase the forces, received with bending by the cell/elements of longitudinal wing skeleton, and therefore increases the weight of its structure. The application/use of fine/thinner airfoil/profiles must be it was lead to a considerable increase in the over-all payload ratio of wing construction, i.e., relation G_{np}/G_0 .

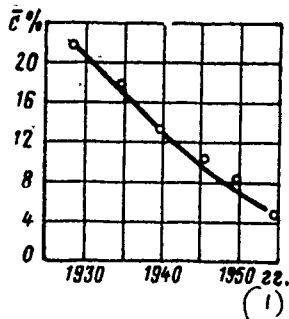


Fig. 0.1. Change in thickness ratio \bar{c} of the monoplane cantilever wing over the years.

Key: (1). yr.

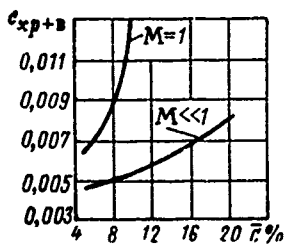


Fig. 0.2. Change in coefficient of profile and wave drag c_{xp+b} in dependence on thickness ratio with $M \ll 1$ and with $M = 1$ ($c_v = 0$)



Fig. 0.3. Diagrams of wings: a) multi-stand biplane; b) cantilever monoplane with thick wing (ratio of overall height toward semispan

$h/l=0.06$); c) cantilever monoplane with fine/thin wing (ratio of overall height toward semispan $h/l=0.035$).

Page 12.

In actuality, as shows statistics, the over-all payload ratio of the cantilever wings not only did not increase, but, on the contrary, it acquired tendency toward certain decrease. This fact is explained by the following reasons:

- 1) by the increase in the specific wing load p_0 , which occurred in the development of aircraft construction;
- 2) by a gradual increase in the specific strength of the materials, used in the construction of the aircraft;
- 3) by transfer/transition to the more rational structural load-bearing diagrams or wings, and also by perfection of the methods of the stress analyses of aircraft.

An increase in the load on wing p_0 sufficiently substantially affects a reduction/descent in the over-all payload ratio of wing.

Figures 0.4 show that curved $G_{1p}/G_0=f(p_0)$, obtained as a result of

processing of statistical data on lighters with approximately equal by the values of elongation λ , thickness ratio \bar{c} and load factor n_A .

The mechanical properties of the materials, which were being applied in aircraft construction, with years improved. The characteristic (criterion), which defines in the first approximation, advantages of material in ratio by weight, it can be, as is known, its specific strength σ/γ^1 .

FOOTNOTE 1. Specific strength with elongation characterizes the degree of the advantage of the application/use of material for aircraft construction. Usually during the determination of the value of specific strength, accept dimensionality σ in kg/mm^2 and γ in G/cm^3 . ENDFOOTNOTE.

The greater the specific strength, the more favorable material for application/use in construction/design. The specific strength of aviation materials steadily is increased.

As a result of an increase in the specific wing load, increases in the specific strength of materials, perfection of the design concepts of wings, methods for calculations and testing for designers it was possible during a considerable reduction/descent in aerodynamic wing drag to preserve its over-all payload ratio

approximately at one and the same level.

The decrease of aerodynamic wing drag in the total resistance of aircraft was achieved not only as a result of transfer/transition to the diagram of monoplane and decrease of thickness ratio of wing, but also as a result of the continuous perfection of the form of wing airfoil/profiles.

Large role in the decrease of aerodynamic wing drag played different means of its mechanization/high-lift devices (flaps, flaps, etc.), which made it possible to substantially increase the specific wing load without a considerable increase in the landing speed of auto/self-ku by wing without a considerable increase in the landing speed of aircraft. One should note also that an increase in the specific wing load became possible because of the perfection of the landing equipment of aircraft (application/use of wheel brakes, diagrams of nose-wheel landing gear, etc.), with which was allow/assumed certain increase in the landing speed.

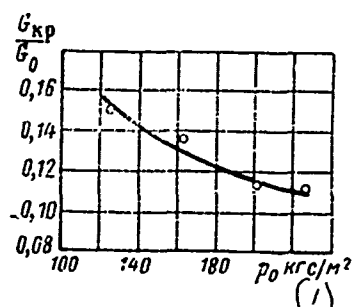


Fig. 0.4. Dependence of the over-all payload ratio of wing construction \bar{G}_{kp}/G_0 on the specific wing load p_0 of fighter-monoplanes, obtained as a result of treating the statistical data.

Key: (1). kgf/m².

Page 13.

Fight for the decrease of the aerodynamic drag of aircraft was conducted not only according to the line of a reduction/descent in wing drag, but also along the line of a reduction/descent in the drag of other aircraft components (fuselage, engine nacelles, chassis/landing gear, lamp/canopies, superstructures). Especially great work conducted on the decrease of drag of power plants. Won acceptance the cowlings of air-cooled engines with improved aerodynamics, the ducted radiators for cooling water and oil, arrange/located in fuselage or in wing.

Since 1931 the designers began to use extensively retractable landing gear.

In proportion to the perfection of technology of the manufacture of aircraft, became possible an improvement in the quality of finishing its external surfaces. For the laminarized enclosures this gave considerable effect in a reduction/descent in the frictional resistance.

Measures described above made it possible to considerably lower the drag coefficient of entire aircraft C_{x0} (Fig. 0.5) despite the fact that its value with an increase in the specific wing load p_0 must grow/rise¹.

FOOTNOTE ¹. Change p_0 differently affects the resistance of aircraft and drag coefficient C_{x0} , namely increase p_0 always conducts to increase C_{x0} , whereas X with increase p_0 at first decreases, and then at sufficiently large values p_0 it begins to increase. ENDFOOTNOTE.

From 1915 through 1950, i.e., in 35 years, the value of this coefficient was lowered from 0.033 to 0.015 (at subsonic flight speeds).

In parallel with the perfection of aircraft itself occurred the perfection of aircraft engine. For an improvement in the aircraft performance, it was necessary to increase the power of engine, to decrease its specific gravity/weight, to increase height, i.e., to retain power up to possible the high altitudes, and to decrease the specific fuel consumption.

An increase in the power of piston engine is connected with a gain in weight of the power plant of aircraft².

FOOTNOTE 2. Into the power plant of aircraft, enter: engines with attachment and screw/propellers, throttle circuit, of lubrication system and fuel feed with tanks, coolers, cowlings. ENDFOOTNOTE.

If the power which they want to obtain, it is very great, then the weight of power plant so increases that the application/use of a piston engine proves to be inexpedient.

In order to avoid this, should be created more light power plants (SU), than installation with piston engines (PD). As a result of investigations and development work, such a SU was created on the basis of turbine jet engines (TRD).

The weight advantages of power plants with TRD in comparison with installations with PD become especially clear during the comparison of the specific gravity/weight of these installations, i.e., weight on 1 kg of the engine thrust under conditions for flight in the earth/ground at different speeds (Table 0.3).

Large specific gravity/weight of power plants with PD and adverse characteristic of this type of engine on speed and height/altitude conditioned the practical limit of the maximum speed of "piston" aircraft approximately into 750 km/h.

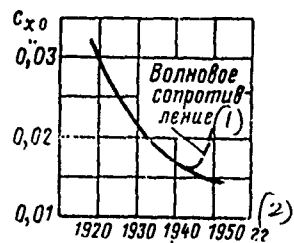


Fig. 0.5. Change in the value of drag coefficient without induced drag $c_{x0} (c_y=0)$ over the years.

Page 14.

Considerably smaller specific gravity/weight of power plants with TRD (it is at present equal to 0.25-0.35) and special feature/peculiarity of the characteristics of the thrust of these engines on speed and height/altitude they allowed aircraft not only to overcome sound barrier, but also to reach high supersonic speeds.

Table 0.3. Specific gravity/weight of SU with TRD and PD under conditions for flight in the earth/ground at the speeds, which correspond to different Mach numbers.

| V км/ч (1) | M | Удельный вес СУ кгс, кгс тяги (2) | | V км/ч (1) | M | Удельный вес СУ (2) кгс, кгс тяги (3) | |
|------------------|-----|--------------------------------------|---------------|------------------|------|--|---------------|
| | | ПД | ТРД (1916 г.) | | | ПД | ТРД (1916 г.) |
| 0 | 0 | 0,9 | 0,5 | 720 | 0,59 | 3,0 | 0,5 |
| 360 | 0,3 | 1,5 | 0,5 | 900 | 0,74 | 3,9 | 0,5 |

Key: (1). km/h. (2). Specific gravity/weight of SU kg/kg of thrust.

(3). g.

Page 26.

Chapter II.

Basic and relative parameters of aircraft, equation of relative weights. The effect of the most important parameters of aircraft on its flight characteristics.

Most important task of the design of aircraft - determination of its basic parameters: takeoff weight G_0 ; wing area S ; thrust P_0 or power N_0 of the power plant, required for obtaining the assigned/prescribed flight characteristics. These parameters serve as initial values for developing entire project of aircraft, and their correct selection causes optimum technical indices and flight-performance data of aircraft.

Page 27.

In certain cases during design to more conveniently use the relative parameters: the specific load on wing area $p_0 = G_0/S$; by thrust-weight ratio $\bar{P}_0 = P_0/G_0$; by the thrust, in reference to wing

area P_0/S ; by load on power G_0/N_0 .

§1. Equation of the over-all payload ratios of aircraft.

The complete (takeoff) weight of aircraft is composed of several differing in their special feature/peculiarities parts

$$G_0 = G_k + G_{c.v} + G_f + G_{c.o.r.}$$

where G_k - a weight of the structure of aircraft; $G_{c.v}$ - weight of power plant; G_f - fuel load; $G_{c.o.r.}$ - weight of equipment, equipment, crew and cargos.

Value G_k depends on the row/series of the parameters of aircraft and its parts, mainly, from the specific wing load p_0 , from wing aspect ratio λ , from the coefficient of calculated overload n_p , from the weight of aircraft, etc. Value $G_{c.v}$ depends on weight per horsepower, on the thrust level of aircraft, on the weight of tanks and so forth; G_f - from the specific consumption of fuel, distance of aircraft, from its cruising speed, from the weight of aircraft, etc. Value $G_{c.o.r.}$ it is direct with with the parameters and the characteristics of aircraft and with its weight it is not connected and is determined depending on the aircraft type and its designation/purpose.

If we divide both parts of the given equality to G_0 , then will

be the obtained equation

$$1 = \bar{G}_k + \bar{G}_{c.y} + \bar{G}_r + \bar{G}_{c.g.r.},$$

called the equation of the over-all payload ratios of aircraft or the equation of the weight balance of aircraft. In this case, the relationship/ratios

$$\bar{G}_k = \frac{G}{G_0}; \bar{G}_{c.y} = \frac{G_{c.y}}{G_0}; \bar{G}_r = \frac{G_r}{G_0}; \bar{G}_{c.g.r.} = \frac{G_{c.g.r.}}{G_0}$$

are respectively the over-all payload ratios of the construction/design of aircraft, power plant, reserve of fuel, equipment, crew and loads. The equation of over-all payload ratios, as it will be shown below, plays considerable role in the expansion/disclosure of the dependence between the parameters and the aircraft performance.

§2. Dependence of fundamental aircraft performance on the separate parameters.

Maximum speed.

The maximum speed of level jet flight (when it is not limited to heating construction/design, to flight safety, etc.) at height/altitude H , can be determined according to the formula

$$V_{\max} = \sqrt{\frac{16P}{c_r S \Delta}} = \sqrt{\frac{16\rho_0 P}{c_r \Delta}}, \quad (2.1)$$

where P - a full thrust of the power plant of aircraft at the given height/altitude H at speed V_{max} ;

S - a wing area;

c_x - the coefficient of the drag of aircraft at speed V_{max} ;

$\bar{P} = P/G_0$ - available thrust-weight ratio of aircraft with flight at height/altitude H with a speed of V_{max} ;

$\Delta = \rho/\rho_0$ - relative density of air at height/altitude H .

Page 28.

The thrust of jet engines (TRD and PVRD) depends on speed and flight altitude. During an increase in the velocity of flight V and of the corresponding to it Mach number ($V = aM$, where a - speed of sound), the thrust of engines P at speeds $M \leq 0.5$ somewhat decreases, and then, in dependence on the parameters of engine, it grows/rises, after which on large Mach numbers sufficiently sharply it falls. In the initial stage of the design of aircraft, it is convenient a change in the thrust to judge by the curve/graph of coefficient $\xi = P/P_0$, where P_0 - the starting (in work on the spot) thrust (for TRD - with $M=0$). The exemplary/approximate curve/graph of change ξ in M

for $H \geq 11000$ m is given in Fig. 2.1. Thus, the thrust of all engines at any speed with $H=0$ can be expressed thus:

$$P_V = \xi P_0.$$

A change in the thrust of TRD in height/altitude H occurs in accordance with the formula

$$P_H = P_0 \Delta^e,$$

where the exponent e at heights $H < 11000$ m somewhat lesser than unity ($e \approx 0,85-0,9$), and at heights $H \geq 11000$ m it is equal to unity. Subsequently presentation will be by larger part examined the tasks, connected with flight at height/altitudes $H > 11000$. Consequently, expression for the engine thrust at any speed and at any height/altitude $H > 11000$ it is possible to write thus:

$$P = m \xi P_0 \Delta,$$

where m - the numerical coefficient, determined by the change-in-thrust pattern at height/altitudes $H < 11000$ m, and $\xi = f(M)$ it will have identical character for engines with the similar parameters.

After dividing both parts of this equality to G_0 and after accepting $e = 0,85$ and $m = 1,2$, we will obtain

$$\text{1) для } H < 11000 \text{ м } \bar{P} = \xi \Delta^{0,85} \bar{P}_0; \quad (2.2)$$

$$\text{2) для } H \geq 11000 \text{ м } \bar{P} = 1,2 \xi \Delta \bar{P}_0. \quad (2.2')$$

Key: (1). for.

where $\bar{P}_0 = P_0 / G_0$.

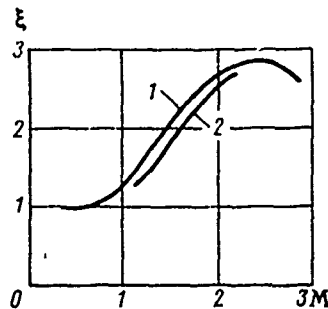


Fig. 2.1. Dependence ξ (ratio of thrust level in flight P toward thrust in work on the spot P_0) from speed for TRD (degree of an increase of the pressure in compressor $\pi_k=6$, the temperature of the gases before turbine $T_3=1200^\circ$, height $H \geq 11000$ m): 1 - without taking into account entry loss; 2 - taking into account entry loss.

Page 29.

After substituting into formula (2.1) obtained expression (2.2'), let us be able to write for height/altitudes $H \geq 11000$ m

$$V_{\max} = 15,7 \sqrt{\frac{\rho_0 \bar{P}_0 \xi}{c_x}} \text{ KM/h, (i)} \quad (2.3)$$

Key: (1). km/h.

OR

$$M_{\max} = 0,0148 \sqrt{\frac{\rho_0 \bar{P}_0 \xi}{c_x}}; \quad (2.3')$$

for height/altitudes $H < 11000$ m

$$V_{\max} = 14,4 \sqrt{\frac{\rho_0 \bar{P}_0 \xi}{c_x \Delta^{0,15}}} \text{ KM/ч}, \quad (2.4)$$

$$M_{\max} = \frac{4}{a} \sqrt{\frac{\rho_0 \bar{P}_0 \xi}{c_x \Delta^{0,15}}}, \quad (2.4')$$

Key: (1) . km/h.

where a - speed of sound at heights $H < 11000$ m.

In this case, $c_x = c_{x0} + c_{xi} = c_{x0} + D_0 c_y^2$,

where

$$D_0 = \frac{c_{xi}}{c_y^2}.$$

Ceiling.

For aircraft with TRD, static ceiling H_{not} is determined by the value of relative density on ceiling, which can be obtained according to the formula

$$\Delta_{\text{not}} = \frac{1,66 \sqrt{D_0 c_{x0}}}{\xi \bar{P}_0}, \quad (2.5)$$

of that escape/ensuing from obvious equality $\rho = \frac{G_0}{K_{\max}}$. Utilizing (2.2') and setting $K_{\max} = \left(\frac{c_y}{c_x}\right)_{\max} = 0,5 / \sqrt{D_0 c_{x0}}$, we will obtain formula (2.5).

Vertical rate of climb.

The maximum vertical velocity approximately can be expressed so [5]:

$$V_{y \max} \approx \frac{2}{3} \frac{P}{G_0} \sqrt{\frac{2P}{3\rho c_{x_0} S}}$$

Set/assuming for $H=0$ $\rho=1/8$; $P/G_0=\xi \bar{P}_0$; $P/S=p_0 \bar{P}_0 \xi$,

we will obtain

$$V_{y \max} = 1,53 \sqrt{\frac{p_0 (\bar{P}_0 \xi)^3}{c_{x_0}}}, \quad (2.6)$$

or for an engine with afterburning

$$V_{y \max} = 1,53 \sqrt{\frac{p_0 (\bar{P}_{0\phi} \xi)^3}{c_{x_0}}},$$

where $\bar{P}_{0\phi}$ - a thrust-weight ratio with afterburning.

Maximum range at speed $V_{\text{кретис}}$.

The work, produced by the engine thrust in flight of aircraft to distance of L , can be expressed thus:

$$U = 1,53 P_{cp} L,$$

where P_{cp} - average thrust on way of L .

Page 30.

This same work, expressed through mechanical heat equivalent of

the burned down fuel/propellant, is determined by the expression

$$U = 427 G_r H_r \eta_0$$

where H_r - fuel heating value;

G_r - weight of the burned down fuel/propellant;

η_0 - overall efficiency of power plant.

After equating the right lots of the obtained expressions, let us find

$$L = \frac{427 G_r H_r \eta_0}{P_{cp}}, \quad (2.7)$$

whence, in particular, is visible the dependence of distance L on calorific value H_r . Formula (2.7), however, cannot serve as basis for the examination of the effect of different parameters of aircraft on its distance and therefore let us turn to the detailed analysis of following formula [13] for aircraft with jet engines (TRD and PVRD):

$$L = 3,6 \int_{G_1}^{G_0} \frac{1}{c_p} \frac{c_y}{c_x} V \frac{dG}{G} \text{ KM}, \quad (2.8)$$

where V - a speed in m/s.

c_p - specific hourly consumption of fuel/propellant in kg per 1 kg of thrust;

G_1 - weight of aircraft at the end of the way; if we consider that in way the weight changes only due to the fuel consumption, then

$$G_1 = G_0 - G_r.$$

During the design of aircraft large interest is of the maximum flying distance. It is obvious that for achievement of maximum range it is necessary that in the assigned/prescribed ratio G_1/G_0 product $\frac{i}{c_p} \frac{c_y}{c_x} V$ in formula (2.8) would have maximum value. Let us explain, under what conditions expression $\frac{i}{c_p} \frac{c_y}{c_x} V$ has a maximum. Let us examine for this the factors, which affect the entering it values.

From theory of TRD, it is known that the specific fuel consumption depends on flight speed V , height/altitudes H (or Δ) and the degree of throttling/choking engine (or number of revolutions n). Graphically these dependences are represented in Fig. 2.2. As can be seen from this curve/graph, c_p with increase V increases (see Fig. 2.2a), with an increase in the height/altitude to $H=11000$ m — it is gradually decreased, at heights $H > 11000$ m c_p it remains the constant (see Fig. 2.2b).

During throttling/choking of engine, i.e., during gear down n , c_p noticeably it changes, at first decreasing, in this case minimum value c_p it is reached at the small degree of throttling/choking on the so-called cruise setting of engine, and then rapidly increasing (see Fig. 2.2c).

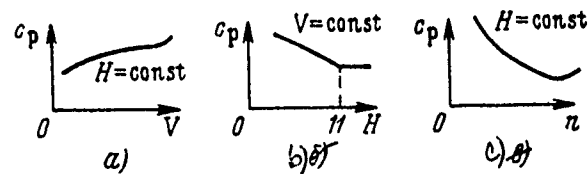


Fig. 2.2. Dependence c_p on speed V (a), height/altitude H (b) and number of revolutions of TRD n (c) for single-flow engines.

Page 31.

The value of relation c_y/c_x depends on flight conditions, i.e., from coefficient c_y , on which is accomplished the flight. The expression, which is determining c_y , can be obtained from the relationship/ratios

$$\frac{c_H}{c_x} = \frac{G_0}{P}; \quad \frac{G_0}{P} = \frac{1}{\bar{P}}.$$

whence $c_y = \frac{c_x}{\bar{P}}.$

Replacing in this equality c_x by its expression through c_{x_0} and $D_0 c_y^2$, we will obtain

$$c_y = \frac{c_{x_0} + D_0 c_y^2}{\bar{P}},$$

whence

$$c_y = \frac{\bar{P}}{2D_0} - \sqrt{\frac{\bar{P}^2}{4D_0^2} - \frac{c_{x_0}}{D_0}}. \quad (2.8')$$

After substituting expressions for (2.2) and (2.2') into formula (2.8'), we will obtain

$$c_y = \frac{\bar{P}_0 \xi \Delta^{0,85}}{2D_0} \sqrt{\frac{\bar{P}_0^2 \xi^2 \Delta^{1,7}}{4D_0^2} - \frac{c_{x_0}}{D_0}} \quad (H \leq 11000 \text{ m});$$

$$c_y = \frac{0,6\bar{P}_0 \xi \Delta}{D_0} \sqrt{\frac{0,36\bar{P}_0^2 \xi^2 \Delta^2}{D_0^2} - \frac{c_{x_0}}{D_0}} \quad (H > 11000 \text{ m}).$$

These formulas show that c_y depends on \bar{P}_0 , height/altitudes H (or Δ) and from the flight speed V , from which in turn, depend ξ , c_{x_0} , and at supersonic speeds and D_0 .

Figure 2.3 depicts the curve, which gives the representation of the character of change c_y in the level flight in height/altitudes in cruise setting of TRD. It is obvious, c_y on ceiling H_{not} will achieve greatest value $c_{y_{\text{not}}} = c_{y_{\text{opt}}}$, its value when K_{max} . With the decrease of height/altitude H , coefficient c_y decreases and respectively decreases quality c_y/c_x .

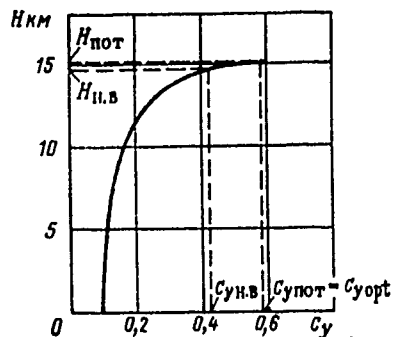


Fig. 2.3. Change c_y in the level flight with the completely open throttle/choke of TRD in dependence on height/altitude H ($H_{пт}$ - the most advantageous height/altitude).

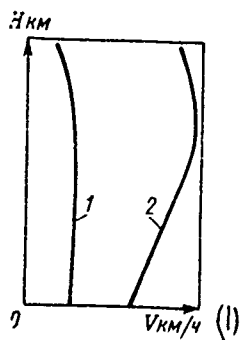


Fig. 2.4. Character of change in maximum speed in dependence on height/altitude H : 1 - transonic aircraft; 2 - supersonic aircraft.

Key: (1). km/h.

The speed of level flight V_{max} at given height/altitude for an aircraft with TRD, as noted, can be expressed by formulas (2.3) and (2.4).

After using values c_x of aircraft in blasting or approximate computation and by the curves of the dependence of coefficient ξ on speed, it is possible to graphically determine the speeds of level flight at different height/altitudes.

In this case for the row/series of the selected height/altitudes in the range from $H=0$ to $H=11000$ m, being assigned the value of speeds $V_{зад}$, we determine corresponding to them values c_x and ξ and, substituting in formula (2.4), we find values $V_{ист}$, through which we plot a curve in coordinates $V_{зад}$ and $V_{ист}$. Then, utilizing formula (2.3), let us perform the same operation for heights $H > 11000$ m. For each selected height/altitude we will obtain curve/graph in coordinates $V_{зад}$ and $V_{ист}$. After conducting on each curve/graph from the origin of coordinates ray/beam at an angle of 45° , we will obtain in the point of intersection of ray/beam and curve V value of speeds V at the selected height/altitudes H .

Figure 2.4 give typical curved changes in the height/altitude

of maximum speed for subsonic (1) and supersonic (2) aircraft. For both aircraft types characteristic is an increase in the speed in the height/altitudes to $H=11000$ m.

On the basis of aforesaid signs for aircraft with TRD are valid the following conclusions:

a) the specific consumption of fuel c_p with an increase in altitude to $H=11000$ m decreases and at heights $H>11000$ m becomes the constant (see Fig. 2.2);

b) coefficient c_y , which corresponds to level flight, with an increase in height/altitude H increases to c_{yopt} (see Fig. 2.3), reaching this value on the static ceiling. Together with c_y with an increase in altitude, increases aircraft quality/fineness ratio c_y/c_x , which on ceiling takes the maximum value;

c) the speed of the level flight V with an increase in altitude to $H=11000$ m increases.

Taking into account the given conclusion/derivations, it is possible to confirm that product $\frac{1}{c_p} \frac{c_y}{c_x} V$, flying range reach maximum value at heights $H>11000$ m.

Assuming that the specific consumption of fuel c_p for heights $H \leq 11\,000$ m can be expressed thus:

$$c_p \cong \psi \Delta^k c_{p0},$$

where $\psi = 1.05 + 0.1M + 0.05M^2$ is considered approximately the effect of Mach number of flight in the range from 0.8 to 3.0 on specific hourly consumption;

Δ - relative density of air;

$$k = 0,12;$$

c_{p0} - starting specific expenditure/consumption ($M=0$; $H=0$), we can for $H \geq 11\,000$ m write

$$c_p = 0,863 \psi c_{p0},$$

i.e., at heights $H > 11\,000$ m, specific expenditure/consumption does not depend on height/altitude.

Formula (2.8) now can be obtained in the following form:

$$L = 4,17 \int_{G_1}^{G_0} \frac{1}{\psi c_{p0}} \frac{c_y}{c_x} V \frac{dG}{G} \text{ KM.} \quad (2.9)$$

Page 33.

Keeping in mind that $\frac{c_y}{c_x} V$ on a change in weight G does not depend, let us integrate this expression, by assuming that $G_1 = G_0 - G_T$, $V = \text{const}$:

$$L = 4,17 \frac{1}{\psi c_{p_0}} \frac{c_y}{c_x} V \ln \frac{G_0}{G_0 - G_T},$$

or

$$L = 4,17 \frac{1}{\psi c_{p_0}} \frac{c_y}{c_x} V \ln \frac{1}{1 - \bar{G}_T}. \quad (2.9')$$

The maximum value of distance L_{\max} will occur at maximum value $\left(\frac{c_y V}{c_x}\right)_{\max}$.

Substituting for V expression (2.3), we will obtain

$$\frac{c_y V}{c_x} = 15,7 \frac{c_y}{c_x^{1,5}} V \sqrt{p_0 \bar{p}_0 \xi},$$

whence it follows that, since value $p_0 \bar{p}_0$ for this aircraft can be accepted constant/invariable $\left(\frac{c_y V}{c_x}\right)_{\max}$, it will occur when $\left(\frac{c_y}{c_x^{1,5}} \xi^{0,5}\right)_{\max}$. Consequently, for obtaining maximum range L_{\max} aircraft with TRD must fly under the conditions during which $\left(\frac{c_y}{c_x^{1,5}} \xi^{0,5}\right)_{\max}$.

Let us determine c_y , which corresponds to this conditions/mode. It is obvious, maximum range will be obtained when $\left(\frac{c_x^{1,5}}{c_y \xi^{0,5}}\right)_{\min}$. After elevating this fraction into degree of 2/3 and utilizing an analytical expression of the polar

$$c_x = c_{x_0} + D_0 c_y^2, \quad (2.10)$$

we will obtain

$$\left(\frac{c_x^{1,5}}{c_y \xi^{0,5}}\right)^{2/3} = \frac{c_{x_0}}{c_y^{2/3} \xi^{1/3}} + \frac{c_y^{4/3}}{\xi^{1/3}} D_0. \quad (2.11)$$

For a subsonic aircraft the coefficient ξ in speed varies little and it is possible in the first approximation, to accept $\xi \sim 1$, and $D_0 = \frac{1}{\pi \lambda_{3\phi}} = \text{const}$ and c_x depends only on c_y . Let us differentiate

expression (2.11) on c_y , will make equal to zero and we will obtain advantageous value $c_{y_{HB}}$ for conditions/mode L_{max} :

$$c_{y_{HB}} = 1,252 \sqrt{\lambda_{3\phi} c_{x_0}}.$$

Value $c_{y_{opt}}$, which corresponds to maximum quality, as is known, it will be equal to

$$c_{y_{opt}} = \sqrt{\pi \lambda_{3\phi} c_{x_0}} = 1,773 \sqrt{\lambda_{3\phi} c_{x_0}}. \quad (2.12)$$

Consequently,

$$c_{y_{HB}} = \frac{1,252 c_{y_{opt}}}{1,773} = 0,71 c_{y_{opt}}.$$

Thus, goal flight of subsonic aircraft must be conducted under the conditions, by which $c_{y_{HB}} = 0,71 c_{y_{opt}}$, but height/altitude H_{HB} is somewhat less H_{HOR} (see Fig. 2.3) in the engine operation in cruise setting.

Page 34.

Substituting (2.12) into the theoretical expression of polar (2.10), we will obtain after simple conversions value $c_{x_{HB}}$ for the conditions/mode of maximum range

$$c_{x_{HB}} = 1,5 c_{x_0}.$$

In transonic rate of speed ($M \sim 0.8-1.3$) the coefficient ξ noticeably changes. Furthermore, in this range c_{x_0} and D_0 depending on speed undergo considerable changes; therefore for a transonic aircraft the determination of value c_y of the conditions/mode of

maximum range, i.e., conditions/mode $\left(\frac{c_y}{c_x} V\right)_{\max}$, it can be carried out in a following simple graphic manner. Having a polar of aircraft on blasting or according to the data of approximate computations for speeds in the range $M \sim 0.8-1.3$, we plot a curve $c_x = c_x(M)$ for the row/series of heights $H > 11000$ m (Fig. 2.5). Then to this same curve/graph it is applied curve $c_P = c_P(M)$ for $H > 11000$ m, calculated by the formula

$$c_P = \frac{P}{Sg} = \frac{19,2\rho_0\bar{P}_0\xi}{(\alpha M)^2}. \quad (2.13)$$

Curve $c_P = c_P(M)$ we construct for this value of thrust-weight ratio \bar{P}_0 so that it would intersect curves $c_x = c_x(M)$ in transonic speed range. Values ξ we find from curve/graph $\xi = \xi(M)$, then the points of intersection of curves $c_x = c_x(M)$ and $c_P = c_P(M)$ will correspond to flight speed M at different height/altitudes H . Now, knowing M , it is possible for each of the undertaken height/altitudes to find values c_y from the formula

$$c_y = \frac{16\rho_0}{\Delta(\alpha M)^2}$$

and, therefore, to determine corresponding to them qualities $\frac{c_y}{c_x}$.

Further let us calculate for the row/series of values c_y of value $\frac{c_y}{c_x} V$ and let us construct curve $\frac{c_y}{c_x} V$ depending on c_y (Fig. 2.6)¹.

FOOTNOTE ¹. Figure 2.6 as an example give curve for a hypothetical transonic aircraft. ENDFOOTNOTE.

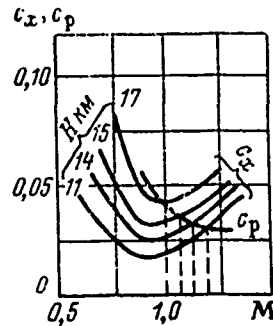


Fig. 2.5. Determination of dependence C_x on M from different height/altitudes for of an assigned/prescribed engine (auxiliary construction for obtaining the dependence, given in Fig. 2.6).

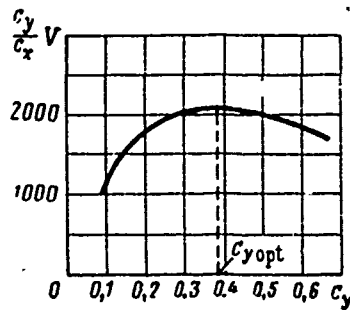


Fig. 2.6. Dependence $\frac{C_y}{C_x} V$ on C_y for determination C_y , corresponding to most advantageous flight conditions to maximum range.

Page 35.

With the aid of this curve let us determine coefficient C_{yRB} , to which

it corresponds

$$\left(\frac{c_y}{c_x} V\right)_{\max}$$

and in this case let us ascertain that $c_{y_{HB}} = c_{y_{opt}}$.

Consequently, in transonic zone the most advantageous conditions/mode for flight (with $n \neq \text{const}$) will be the conditions/mode of maximum quality, i.e., for achievement L_{\max} flight must occur with

$$c_y = c_{y_{opt}}$$

If the flight of transonic aircraft occurs at the speed, at which appears sufficiently noticeable wave drag, then conditions/mode when $c_{y_{opt}}$ with the completely open throttle/choke due to a sharp increase in the wave drag becomes unfavorable and maximum range is obtained during certain throttling/choking of engines, greater than in cruise setting.

For supersonic zone $c_{y_{HB}}$ it is possible to find by graphic method so, as this is described above.

The results of determination from this method $c_{y_{HB}}$ show that maximum $\left(\frac{c_y}{c_x} V\right)$ occurs with

$$c_{y_{HB}} = 0,73 c_{y_{opt}}$$

i.e., it is possible to approximately consider that the conditions/mode of maximum range for a supersonic aircraft is

analogous to the conditions/mode of the maximum range of subsonic aircraft. Allow/assuming certain unessential inaccuracy, it is possible during determination L_{\max} of supersonic aircraft in the first approximation to accept

$$c_{y_{\text{HB}}} = 0,71 c_{y_{\text{opt}}}$$

Thus, let us assume that the conditions/mode of maximum range is characterized both for the subsonic ones and for supersonic aircraft with TRD by coefficients $c_{y_{\text{HB}}} = 0,71 c_{y_{\text{opt}}}$ and $c_{x_{\text{HB}}} = 1,5 c_{x_0}$. To these values $c_{y_{\text{HB}}}$ and $c_{x_{\text{HB}}}$ corresponds the value $\left(\frac{c_y}{c_x}\right)_{\text{HB}}$:

$$\left(\frac{c_y}{c_x}\right)_{\text{HB}} = \frac{0,472}{c_{x_0}} c_{y_{\text{opt}}},$$

or, since $c_{y_{\text{opt}}} = \sqrt{\frac{c_{x_0}}{D_0}}$,

$$\left(\frac{c_y}{c_x}\right)_{\text{HB}} = \frac{0,472}{\sqrt{c_{x_0} D_0}}. \quad (2.14)$$

Page 36.

Substituting (2.14) in (2.9'), we will obtain

$$L_{\max} = 4,17 \frac{1}{\psi c_{p_0}} \frac{0,472}{\sqrt{c_{x_0} D_0}} V_{\text{крейс}} \ln \frac{1}{1 - \bar{G}_{\text{т.крейс}}}, \quad (2.15)$$

either

$$L_{\max} = 7,0 \sqrt{\rho_0 \bar{P}_0} \frac{1}{\psi c_{p_0} c_{x_0} \sqrt{D_0}} \ln \frac{1}{1 - \bar{G}_{\text{т.крейс}}},$$

or

$$L_{\max} = 584 \frac{1}{\psi c_{p_0}} \frac{M_{\text{крейс}}}{\sqrt{c_{x_0} D_0}} \ln \frac{1}{1 - \bar{G}_{\text{т.крейс}}}, \quad (2.15')$$

where cruising speed

$$V_{\text{кретс}} = 12,8 \sqrt{\frac{\rho_0 \bar{P}_0 \xi}{c_{x_0}}} \text{ км/ч} \quad (2.16)$$

and the corresponding to it number

$$M_{\text{кретс}} = 0,012 \sqrt{\frac{\rho_0 \bar{P}_0 \xi}{c_{x_0}}}. \quad (2.16')$$

Formulas (2.16) and (2.16') can be obtained via substitution in (2.3) and (2.3') values $c_{x_{\text{HB}}} = 1,5 c_{x_0}$.

Utilizing calculated or experimental data for ψ , c_{p_0} , c_{x_0} and D_0 for of assigned/prescribed value $\bar{G}_{\text{т.кретс}}$, it is possible with the aid of formula (2.15) to obtain dependence L_{max} on $M_{\text{кретс}}$ (Fig. 2.7).

Distance of takeoff/run-up $L_{\text{разб}}$ with takeoff.

The distance of takeoff/run-up $L_{\text{разб}}$ is expressed by following formula [13]:

$$L_{\text{разб}} = \frac{1}{2g} \int_0^{v_{\text{отр}}^2} \frac{dv^2}{\bar{P} - f - \frac{q}{\rho_0} (c_x - f c_y)}. \quad (2.17)$$

If we accept thrust-weight ratio \bar{P} on the takeoff/run-up of the constant/invariable and equal starting thrust-weight ratio $\bar{P} = \bar{P}_0$, and

expression $c_x - f c_y = 0$ in view of its smallness, then integral (2.17) can be calculated analytically in the form

$$L_{\text{pass}}^- = \frac{1}{2g} \frac{V_{\text{отр}}^2}{\bar{P}_0 - f}.$$

Since the value of velocity near with the breakaway

$$q_{\text{отр}} = \frac{\rho V_{\text{отр}}^2}{2} = \frac{V_{\text{отр}}^2}{16},$$

and

$$c_y = \frac{p_0}{q} = \frac{16 p_0}{V_{\text{отр}}^2},$$

that

$$V_{\text{отр}}^2 = \frac{16 p_0}{c_{y \text{ отр}}}$$

and

$$L_{\text{pass}}^- = \frac{0,82 p_0}{c_{y \text{ отр}} (\bar{P}_0 - f)}, \quad (2.17')$$

or with afterburning

$$L_{\text{pass}}^- \approx \frac{0,82 p_0}{c_{y \text{ отр}} (\bar{P}_{0\phi} - f)}.$$

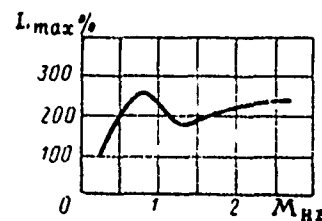


Fig. 2.7. Dependence of relative distance \bar{L}_{max} on number M_{HB} .

Page 37.

Dependence of flight characteristics on the parameters of aircraft $c_x, c_{x0}, D_0, \bar{P}_0, p_0$ and ϵ .

Examining formulas (2.3), (2.3'), (2.4), (2.4'), (2.5), (2.7), (2.16), (2.16'), (2.17), (2.17'), we can make the conclusion that the values of fundamental flight characteristics $V_{max}; V_{крет}; L_{max}; V_y; H_{гор}; L_{pass}$ depend on of the following parameters and coefficients c_x and $c_{x0}; D_0; \bar{P}_0, p$ and ϵ .

Let us examine each of the given parameters and we will attempt to establish/install, on what factors depends their value and how they affect fundamental aircraft performance.

Drag coefficient c_x corresponds to total aerodynamic drag of

aircraft X and can be expressed as follows:

$$c_x = \frac{X}{qS} = \frac{X_p + X_{B.KP} + X_{OH} + X_{B.OH} + X_\phi + X_{B.\phi} + X_r + X_{B.r} + X_i + X_H}{qS},$$

where q - velocity head of the incident flow;

X_p - shape drag and friction of wing;

$X_{B.KP}$ - wave wing drag;

X_{OH} - shape drag and friction of tail assembly;

$X_{B.OH}$ - wave drag of tail assembly;

X_ϕ - shape drag and friction of fuselage;

$X_{B.\phi}$ - wave drag of fuselage;

X_r - shape drag and friction of the engine nacelles of, those of the nacelles of chassis/landing gear and so forth;

$X_{B.r}$ - wave pod drag of engines, nacelles of chassis/landing gear;

X_i - induced drag, i.e., the resistance, which depends on angle of attack or c_y ;

$X_{\text{н}}$ - the interference drag, which appears as a result of mutual wing influence, fuselage, tail assembly, engine nacelles during flow.

Using the appropriate dimensionless coefficients, let us write the coefficient of the total drag of aircraft in the following form:

$$c_x = c_{x_p} + c_{x_{\text{в.кп}}} + (c_{x_{\text{он}}} + c_{x_{\text{в.он}}}) \frac{S_{\text{он}}}{S} + \\ + (c_{x_{\phi}} + c_{x_{\text{в.}\phi}}) \frac{S_{\text{м.}\phi}}{S} + (c_{x_r} + c_{x_{\text{в.}r}}) \frac{S_{\text{м.}r}}{S} + c_{x_{\text{н}}}$$

where $c_{x_{\text{он}}}$; $c_{x_{\text{в.он}}}$ - the drag coefficients, in reference to the area of tail assembly

$c_{x_{\phi}}$; $c_{x_{\text{в.}\phi}}$; c_{x_r} ; $c_{x_{\text{в.}r}}$ - the drag coefficients, in reference to the appropriate areas of the masection of fuselage $S_{\text{м.}\phi}$ and nacelles $S_{\text{м.}r}$.

It is convenient for analysis to present the coefficient of the total drag of aircraft c_x in the form of the sum of two coefficients c_{x0} and c_{x_i} , from which

$$c_{x0} = c_{x_p} + c_{x_{\text{в.кп}}} + (c_{x_{\text{он}}} + c_{x_{\text{в.он}}}) \frac{S_{\text{он}}}{S} + \\ + (c_{x_{\phi}} + c_{x_{\text{в.}\phi}}) \frac{S_{\text{м.}\phi}}{S} + (c_{x_r} + c_{x_{\text{в.}r}}) \frac{S_{\text{м.}r}}{S} + c_{x_{\text{н}}}$$

corresponds to the drag of aircraft which it has when $c_v=0$, and $c_{x_i} = D_0 c_v^2$ corresponds to the additional drag of the wing which is added

when $c_v \neq 0$. In this case, it is considered that supplementary resistance, that appears in tail assembly, fuselage, nacelles as a result of changing the angle of attack, is negligibly small.

Thus, the drag coefficient of aircraft c_x can be with sufficient approach/approximation examined by that consisting of two parts $c_x = c_{x0} + c_{xt}$.

Page 38.

From aerodynamics it is known that total frontal aerodynamic drag of aircraft changes according to Mach number both in its total quantity and on the relationship/ratio between components of the separate means of the resistance: form, friction, wave, interference and inductive.

On the curve/graph of Fig. 2.8, is shown the character of a change of coefficient c_x in dependence on Mach number in aircraft with various forms (on curve/graph to each value c_x it corresponds its value $c_v = \frac{P_0}{q}$). Entire speed range of contemporary aircraft in dependence on the character of change c_x can be broken into three zones: the first (from $M=0$ to $M = M_{\text{крит}}$) - subsonic, the second (from $M_{\text{крит}}$ to $M \sim 1.2$) - transonic, the third (from $M=1.2$ to $M=5$) - supersonic.

Let us examine how changes the relationship/ratio between components c_x in each of the above-mentioned zones.

In the first, subsonic, zone the drag, which does not depend on the angle of attack of the wing to which corresponds coefficient c_{x0} , is encompassed: the shape drag, friction, interference drag. To this resistance is added the resistance inductive, which depends on the angle of attack (from c_y), to which corresponds coefficient c_{xi} :

$$c_{xi} = D_0 c_y^2 = D_0 \frac{p^2}{q^2} = \frac{256 p^2}{(\alpha M)^2 \Delta \pi \lambda}$$

From this formula it is evident that with assigned magnitudes p , λ and Δ with decrease of M c_{xi} considerably it increases (Fig. 2.9). From resistance, to which corresponds c_{x0} , large value in this zone resistive of friction. Therefore for the low-speed aircraft, which possess the maximum speed in the first zone, for decrease c_x should be to apply wings with sufficiently great lengthening λ and accepted the moderate specific wing loads. For decreasing the frictional resistance for similar aircraft, is expedient the application/use of such forms of its parts, with which would be provided the low value of accelerating pressure gradients on the surfaces, streamlined with flow. Last/latter circumstance contributes to the preservation/retention/maintaining of a laminar boundary layer in the

large sections of the surface of the streamlined bodies and, therefore, it brings in to the decrease of frictional resistance.

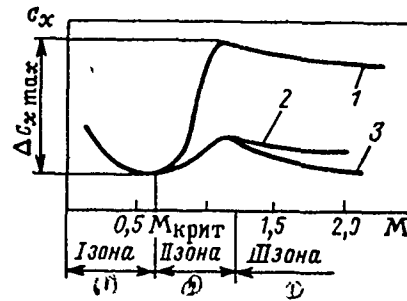


Fig. 2.8. Change c_x of the aircraft in dependence on Mach number: 1 - subsonic aircraft; 2 - supersonic aircraft with the rounded wing leading edge; 3 - supersonic aircraft with the pointed wing leading edge.

Key: (1). zone.

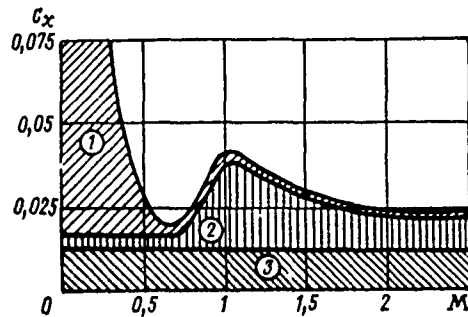


Fig. 2.9. Character of change in components of coefficient total drag of aircraft in dependence on Mach number for medium altitudes ($H \approx 10000$ m, $\rho = 250$ kgf/m², $\lambda = 3.2$): 1 - induced drag, which depends on spread/scope; 2 - shape drag and wave drag; 3 - frictional

resistance.

Page 39.

For this, is necessary the application/use of the laminarized wing profiles and laminarized enclosures of fuselages and nacelles. However, one should remember that for the laminarized airfoil/profiles are characteristic lowered/reduced values $c_{y\max}$, therefore the gain in frictional resistance can be considerably lowered as a result of the need for increase S for the satisfaction of the requirements, presented to takeoff and landing characteristics.

The secondly, transonic, to zone the resistance, to which corresponds coefficient c_{x0} , upon reaching of Mach number, called critical $M_{\text{крит}}$ as a result of emergence and violent increase in the wave drag sharply increases (see Fig. 2.8). For a subsonic aircraft with the subsonic forms of wing, fuselage, nacelles and tail assemblies, this increase can be in ten or more times. An increase in the resistance occurs sufficiently sharply; therefore the phenomenon was called characteristically name "sound barrier". For the aircraft, the value of maximum speed of which is located in the second zone, is expedient the application/use of forms, which facilitate the decrease of an increase in the wave drag (Fig. 2.10), i.e., the sweptback

wings and tail assemblies, wings and tail assemblies of low elongation (with $M > 1$), especially triangular planform, and also application/use for wings and tail assembly of airfoil/profiles with small thickness ratio ($\bar{c} = 0.06 - 0.08$) and with the low concavity also of fuselages with great lengthening.

The application/use of these forms can ensure a comparatively small value of increase $\Delta c_{x_{max}}$ (see Fig. 2.8).

In the third, supersonic, zone the wave drag, called by bow shocks, comprises considerable portion in total drag of the aircraft to which corresponds $c_x = c_{x0} + c_{x1}$. Imparting to aircraft components - to wing, fuselage, to tail assembly and so forth - especially supersonic forms, which ensure the emergence of oblique bow waves, i.e., the application/use of fine/thin wing profiles and tail assembly ($\bar{c} = 0.03 - 0.05$) with the pointed leading edges, the enclosures of fuselages with the pointed, strongly elongated nose section and great lengthening and the like (Fig. 2.11) substantially decreases the wave drag of aircraft.

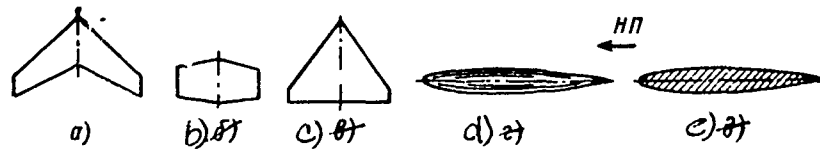


Fig. 2.10. Wing planform, its airfoil/profile and the form of fuselage, that are applied on transonic aircraft ($M \approx 1.0$): a) the sweptback wing; b) trapezoidal low-aspect-ratio wing; c) delta low-aspect-ratio wing; d) fuselage with great lengthening; e) wing profile (laminar), thickness ratio $\bar{c} = 0.10$.

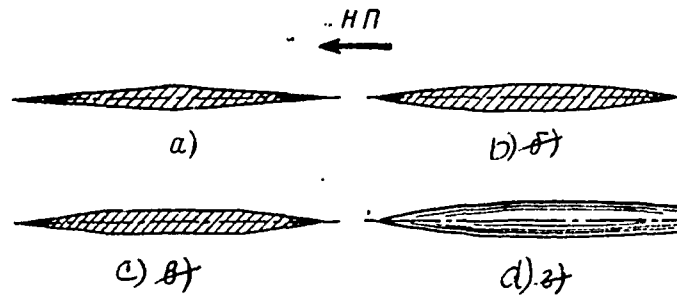


Fig. 2.11. Forms of wing profiles (a, b and c) and fuselage (d), advisable for supersonic speeds ($M > 1.5$).

Page 40.

However, one should consider that the wing profiles with acute/sharp leading edges possess unsatisfactory properties in the relation to

the landing data of aircraft and therefore their to apply without the special high-lift device or wing (drooped noses) does not follow. In supersonic zone is relatively great the frictional resistance to value of which, as is known, affects the smoothness of the fairing of body and therefore wings and supersonic fuselage must have least possible surface roughness. For supersonic aircraft is expedient the application/use of low-aspect-ratio wings ($\lambda < 2.5$), since the latter on supersonic aircraft plays an insignificant role. On the other hand, the wings of such type make it possible in supersonic range to lower wave drag. Taking into account during design effect on value c_x and c_{x0} of the examined above factors, designer must remember also that value c_{x0} depends on the specific wing load p_0 . Let us assume that are designed completely similar aircraft of one and of the same weight G_0 , but with different in the area of wings ($G_0 = \text{const}$; $S_{\text{HP}} = \text{var}$). The areas of maximum cross sections of fuselage and engine nacelles ($S_{\text{M}\phi}$ and $S_{\text{M}r}$) will be identical, but the ratios of the areas of tail assembly and area of their wings are permanent $S_{\text{OH}}/S = \text{const}$.

It is possible also to consider that

$$\frac{c_{x_{\text{OH}}} + c_{x_{\text{OH}}}}{c_{x_{\text{P}}} + c_{x_{\text{HP}}}} = \gamma = \text{const}$$

and

$$c_{x_{\phi}} + c_{x_{\text{H}\phi}} = c_{x_r} + c_{x_{\text{H}r}}$$

Furthermore, for similar aircraft is correct the equality

$$\frac{S_{M,\phi}}{S} + \frac{S_{M,r}}{S} = \frac{P_0}{G_0/\Sigma S_M} = \frac{P_0}{k_1},$$

where ΣS_M - sum of the areas of maximum cross sections of fuselage and engine nacelles

$$k_1 = \frac{G_0}{\Sigma S_M}.$$

Then, set/assuming

$$1 + \gamma \frac{S_{on}}{S} = k_0$$

and disregarding the coefficient c_{x_n} , we can write

$$c_{x_0} = (c_{x_p} + c_{x_{n,p}}) k_0 + (c_{x_\phi} + c_{x_{n,\phi}}) \frac{P_0}{k_1}.$$

For subsonic speeds ($c_{x_{n,p}}=0$; $c_{x_{n,\phi}}=0$) will be used the following formula:

$$c_{x_0} = k_0 c_{x_p} + c_{x_\phi} \frac{P_0}{k_1}, \quad (2.18)$$

FOOTNOTE 1. In the practice of preliminary (sketch) design c_{x_0} it is determined either by calculation according to approximation methods, or from the blasting of similar by airplane design. ENDFOOTNOTE.

and for supersonic speeds can be used the approximation formula

$$c_{x_0} \cong 5,0 k_0 c^2 \frac{1}{\sqrt{M^2 - 1}} + c_f + c'_{x_\phi} \frac{P_0}{k_1}, \quad (2.18')$$

where $c'_{x_\phi} = c_{x_\phi} + c_{x_{n,\phi}}$.

Page 41.

On the basis of formulas (2.1b) and (2.18') it is possible to judge the effect on c_{x0} the specific wing load p_0 . Formula (2.18') gives the representation of considerable effect on value c_{x0} at supersonic speeds of thickness ratio of wing \bar{c} , which enters into formula in square.

The second coefficient, which characterizes the aerodynamic properties of aircraft, is coefficient D_0 , entering the formula, sufficiently precise for the flight speed range of the aircraft

$$c_x = c_{x0} + D_0 c_y^2 = c_{x0} + D_0 \frac{p^2}{q^2}.$$

Value D_0 depends on different factors depending on that, what zone includes the speed of the design/projected aircraft. In the first zone (subsonic) coefficient D_0 is equal to

$$D_0 = \frac{k_2}{\pi \lambda_{\text{эф}}},$$

where $k_2 = 1.02$ for the tapered wings with elongation $\lambda > 3$; $k_2 = 1.6$ for delta wings with elongation $\lambda \leq 4$.

FOOTNOTE 1. Let us recall that $D_0 = 1/c_y^*$. ENDFOOTNOTE.

Consequently, as was already noted above, for the aircraft whose speeds can be related to the first zone, must be used average/mean ($\lambda=4-7$) and large ($\lambda=7-12$) wing aspect ratios. Is especially important the application/use of large ones λ for aircraft with large flying range.

In supersonic, the transonic zone coefficient D_0 can be expressed thus:

$$D_0 = 0,25B_0 \sqrt{M^2 - 1}.$$

Coefficient B_0 , is expressed by the following formulas:

for the direct/straight tapered wing

$$B_0 = \frac{1}{1 - \frac{1}{2\lambda \sqrt{M^2 - 1}}};$$

for a delta wing with the supersonic leading edges

$$B_0 = 1;$$

for a delta wing with the subsonic edges

$$B_0 = \frac{1}{\pi} \left(\frac{4}{\lambda \sqrt{M^2 - 1}} + \frac{\lambda \sqrt{M^2 - 1}}{1,8} \right).$$

Thus, D_0 at subsonic and transonic speeds ($M < 1$) is expressed the dependence of aerodynamic drag when $c_y = 0$ on wing planform (λ and η), and at supersonic speeds - from wing planform and speed (M). Consequently, designer can attain decrease c_{x0} and D_0 by the final adjustment of the aerodynamic shape of wing, fuselage, tail assembly

of aircraft. In this case, as we saw above, for each speed range, were characteristic special shapes of airfoil/profiles, wing in plan/layout, fuselage, etc. Decrease c_{x0} and L_0 (at the constant values of other parameters), as it follows from the examination of formulas (2.3); (2.3'); (2.5); (2.6); (2.15); (2.15'); (2.16); (2.16'), leads to an improvement in the aircraft performance

$$V_{\max}(M_{\max}); V_{\text{крет}}(M_{\text{крет}}); H_{\text{гор}}, V_{y \max}, L_{\max}.$$

Page 42.

The following parameter, which considerably affects all fundamental flight characteristics, is the thrust-weight ratio

$$\bar{P} = \frac{P}{G_0}$$

or the in question during design starting (for TRD) or initial (PVRD) thrust-weight ratio

$$\bar{P}_0 = \frac{P_0}{G_0}. \quad (2.19)$$

It is easy to see that expression (2.19) has the definite meaning only in such a case, when are determined P_0 and G_0 . During the design of aircraft, these values must be found, moreover task is complicated by the fact that G_0 proves to be the value, dependent on P_0 , and P_0 , and its turn, it depends on G_0 . Thus, for the design/projected aircraft to determine \bar{P}_0 by formula (2.19) is impossible. If we express \bar{P}_0 , after using formulas (2.3') and (2.16'), then

$$\bar{P}_{0n} = \frac{4650M_{\max}^2 c_x}{\xi \rho_0}; \quad (2.20)$$

$$\bar{P}_{0n} = \frac{6950M_{\text{крит}}^2 c_{x_0}}{\xi \rho_0} \quad (2.20')$$

they will determine those values of thrust-weight ratio which are required for obtaining respectively given ones M_{\max} and $M_{\text{крит}}$ with given ones c_x ; c_{x_0} ; ρ_0 and ξ . The thrust-weight ratio, expressed (2.20) and (2.20'), let us call required thrust-weight ratio. After determining the value of required thrust-weight ratio \bar{P}_{0n} , of that ensuring assigned magnitude M_{\max} or $M_{\text{крит}}$, designer it must know well the ways which lead to equality \bar{P}_{0n} and thrust-weight ratio of "that arrange/located" \bar{P}_{0p} , i.e., the thrust-weight ratio which it is possible to virtually ensure at the values of the parameters of aircraft and power plant accepted and during the assign/prescribed to structural strength. The guarantee of equality value \bar{P}_{0p} to value \bar{P}_{0n} is one of the basic tasks of the design of aircraft, which the designer to final sum must solve in design. In order to know, how it is possible to influence value \bar{P}_{0p} , it is necessary to explain the dependence of available thrust-weight ratio \bar{P}_{0p} on different parameters, for which we will use the equation of the over-all payload ratios of the aircraft

$$\bar{G}_k + \bar{G}_{c,y} + \bar{G}_T + \bar{G}_{c,s,r} = 1.$$

We will obtain for the second and third members of the left side of equation $\bar{G}_{c,y}$ and \bar{G}_T the expressions, establishing their

dependence on different parameters.

For $\bar{G}_{c,y}$ it follows from the determination

$$\bar{G}_{c,y} = \frac{G_{c,y}}{G_0} = \frac{G_{c,y} P_0}{G_0 P_0} = r_0 \bar{P}_0, \quad (2.21)$$

where $r_0 = \frac{G_{c,y}}{P_0}$ - the specific gravity/weight of the power plant of aircraft (referred to boost for launching P_0).

For the over-all payload ratio of fuel/propellant \bar{G}_T it is possible to obtain dependence on the parameters as follows.

Page 43.

The complete fuel reserve on the aircraft to which corresponds over-all payload ratio \bar{G}_T , it consists: of the fuel/propellant, expended in cruise $G_{T,крещ}$, of the fuel/propellant, required for taxiing, takeoff/run-up, takeoff, lift and landing $G_{T,л}$, of the fuel/propellant, required to acceleration/dispersal $G_{T,р}$ and navigational reserve $G_{T,н.з}$. Consequently, the complete reserve

$$G_T = G_{T,крещ} + G_{T,л} + G_{T,р} + G_{T,н.з}$$

Transfer/converting to over-all payload ratios, let us have

$$\bar{G}_T = \bar{G}_{T,крещ} + \bar{G}_{T,л} + \bar{G}_{T,р} + \bar{G}_{T,н.з}$$

For aircraft with TRD and PVRD the over-all payload ratio of the fuel/propellant, expended to the cruise (with given one L_{max}), we will obtain, solving equation (2.15) relatively $\bar{G}_{T,крещ}$: $\bar{G}_{T,крещ} = 1 - e^{-\frac{L_{max}}{A}}$,

where

$$A = 7,0 \frac{1}{\psi c_{p0}} \sqrt{\rho_0 \bar{P}_0} \frac{1}{c_{x_0} \sqrt{D_0}} = \frac{584 M_{крещ}}{\psi c_{p0} \sqrt{c_{x_0} D_0}},$$

or according to the linearized formula (replacement of logarithmic curve by two straight lines)

$$\bar{G}_{т.крещ} = R \psi c_{p0} \frac{L_{max} \sqrt{c_{x_0} D_0}}{M_{крещ}} + u,$$

where u - the coefficient, depending on values $\bar{G}_{т.крещ}$; $R=0,00145$ and $u=0$ when $\bar{G}_{т.крещ} \leq 0,3$; $R=0,00100$ and $u=0,09$ when $0,5 > \bar{G}_{т.крещ} > 0,3$. With given one of duration of flight t' , will be real the formula (for H , which corresponds Δ) $\bar{G}_{т.крещ} = \psi \bar{P}_0 \Delta t'$. Knowing $\bar{G}_{т.крещ}$, it is possible to determine further $\bar{G}_{т.п.}$, $\bar{G}_{т.р.}$ and $\bar{G}_{т.н.з.}$ $\bar{G}_{т.п.} = 0,0009 H_{крещ}$, where $H_{крещ}$ they determine, after finding

$$\Delta_{крещ} = \frac{1,76 \sqrt{c_{x_0} D_0}}{\xi \bar{P}_0}.$$

With large ones to numbers $M \geq 2$ the over-all payload ratio of the fuel reserve, required by acceleration/dispersal $\bar{G}_{т.р.}$, is determined from the formula

$$\bar{G}_{т.р.} = \psi c_{p0} \bar{P}_0 \Delta t', \text{ where } t' = \frac{1}{g} \int_{V_1}^{V_2} \frac{dV}{\bar{P}_{расч} - \bar{P}_{пот}},$$

and Δ corresponds to the height/altitude of acceleration/dispersal. For the aircraft of subsonic and transonic ones, $\bar{G}_{т.р.}$ very little can be disregarded.

The over-all payload ratio of the navigational fuel reserve is

determined from approximation formula [30]

$\bar{G}_{т.н.э} = 0,10\bar{G}_{т.крейс}$ (for military aircraft); $\bar{G}_{т.н.э} = (0,15 - 0,20)\bar{G}_{т.крейс}$ (for passenger aircraft).

Thus, for the over-all payload ratio of fuel/propellant on aircraft \bar{G}_t can be written following of formula.

If is assign/prescribed flying range, then

$$\bar{G}_t = S \left(1 - e^{-\frac{L_{\max}}{\lambda}} \right) + u, \quad (2.22)$$

where $S = 1,1$; $u = 0,0009H_{крейс} + \psi c_{р0} \bar{P}_0 \Delta l'$ (если $M_{крейс} \geq 2,0$);
 $S = 1,15 - 1,2$; $u = 0,0009H_{крейс}$ (если $M_{крейс} < 2,0$).

Key: (1). if.

Page 44.

If $\bar{G}_{т.крейс} \leq 0,5$, then

$$\bar{G}_t = SR_{р0} \frac{L_{\max} \sqrt{c_{x0} D_0}}{M_{крейс}} + u, \quad (2.23)$$

where $S = 1,1$; $u = 0,0009H_{крейс} + \psi c_{р0} \bar{P}_0 \Delta l'$ (если $\bar{G}_{т.крейс} \leq 0,3$ и $M_{крейс} \geq 2,0$);
 $S = 1,15 - 1,2$; $u = 0,0009H_{крейс}$ (если $\bar{G}_{т.крейс} \leq 0,3$ и $M_{крейс} < 2,0$);
 $u = 0,0009H_{крейс} + \psi c_{р0} \bar{P}_0 \Delta l' + 0,09$ (если $\bar{G}_{т.крейс} > 0,3$ и $M_{крейс} > 2,0$);
 $u = 0,0009H_{крейс} + 0,09$ (если $\bar{G}_{т.крейс} > 0,3$ и $M_{крейс} < 2,0$).

Key: (1). if. (2). and.

If is assign/prescribed duration of flight t' , then

$$\bar{G}_r = S \psi \xi \bar{P}_0 \Delta c_{p0}' + u, \quad (2.23')$$

where $S=1.1$; $u=0.0009 H_{\text{up}} \text{etc.}$

For aircraft with TVD, it is possible to apply the formula

$$\bar{G}_r = 0,00057 S L_{\text{max}} c_e \sqrt{\frac{c_{x_0}}{\lambda}}, \quad (2.23'')$$

where $S=1.15-1.2$.

Utilizing formulas (2.21), (2.23) and (2.23') and the equation of over-all payload ratios, we will obtain following of formula for available thrust-weight ratio \bar{P}_{op} :

if task is duration of flight t' , then

$$\bar{P}_{op} = \frac{1 - \bar{G}_K - \bar{G}_{c.z.r}}{r_0 + S \psi \xi c_{p0} \Delta t'}, \quad (2.24)$$

and if is assign/prescribed flying range L_{max} , then

$$\bar{P}_{op} = \frac{1 - \bar{G}_K - \bar{G}_{c.z.r}}{r_0} - \frac{1}{r_0} \left[\frac{SR \psi c_{p0} L_{\text{max}} \sqrt{c_{x_0} D_0}}{M_{kp}} + u \right]. \quad (2.24')$$

These formulas give the clear representation of the dependence of available thrust-weight ratio \bar{P}_{op} of the row/series of design parameters.

For determining the quantitative effect of a change in one or the other parameter to available thrust-weight ratio \bar{P}_{op} can be used

following of the formula:

$$\bar{P}'_0 = \bar{P}_0 \frac{1 - \varepsilon_1 \bar{G}_k}{1 - \bar{G}_k}; \quad \bar{P}'_0 = \bar{P}_0 \frac{1 - \varepsilon_2 \bar{G}_r}{1 - \bar{G}_r};$$

$$\bar{P}'_0 = \bar{P}_0 \frac{1 - \varepsilon_3 \bar{G}_r}{1 - \bar{G}_r}; \quad \bar{P}'_0 = \frac{\bar{P}_0}{1 + \bar{G}_{c,y} (\varepsilon_4 - 1)},$$

where

$$\varepsilon_1 = \frac{\bar{G}'_k}{\bar{G}_k}; \quad \varepsilon_2 = \frac{c'_{p0}}{c_{p0}}; \quad \varepsilon_3 = \frac{L'_{max}}{L_{max}}; \quad \varepsilon_4 = \frac{r'_0}{r_0};$$

\bar{P}'_0 - new value \bar{P}_0 , obtained, if we \bar{G}_1 increase on $\Delta \bar{G}_1$.

If we increase thrust-weight ratio \bar{P}_0 by installation on the aircraft of two engines instead of one, then when $L_{max} = \text{const}$

$$G_{c,y,r} = \text{const} \quad \text{and} \quad \bar{G}'_k = \varepsilon_1 \bar{G}_k;$$

$$\bar{P}'_0 = \frac{1 - (\bar{G}_k \varepsilon_1 + \bar{G}_r)}{\frac{0,5 \bar{G}_{c,y,r}}{\bar{P}_0} + r_0 \varepsilon_4}.$$

Page 45.

The formulas given above easily can be obtained from the equation of over-all payload ratios, which we will write in the abstract/removed form $\bar{G}_1 + \bar{G}_2 + \bar{G}_3 + \bar{G}_4 = 1$; if we increase \bar{G}_1 on $\Delta \bar{G}_1$, then \bar{G}_2 ; \bar{G}_3 and \bar{G}_4 will be changed and equation will be written as follows:

$$\bar{G}_1 + \Delta \bar{G}_1 + \bar{G}_2 + \bar{G}_3 + \bar{G}_4 = 1.$$

Then

$$\bar{G}_i = \bar{G}_i \left(1 - \frac{\Delta \bar{G}_i}{1 - \bar{G}_i} \right); \quad \Delta \bar{G}_i = -\bar{G}_i \frac{\Delta \bar{G}_i}{1 - \bar{G}_i},$$

and

$$G'_0 = G_0 \frac{1}{1 - \frac{\Delta \bar{G}_i}{1 - \bar{G}_i}}.$$

Assuming that $P' = P$, we will obtain

$$\bar{P}'_0 = \bar{P}_0 \left(1 - \frac{\Delta \bar{G}_i}{1 - \bar{G}_i} \right),$$

or generally

$$\bar{P}'_0 = \bar{P}_0 \left(1 - \frac{\Delta \bar{G}_i}{1 - \bar{G}_i} \right).$$

Examining formulas (2.24) and (2.24'), it is possible to make the conclusion that the equality of the thrust-weight ratio of that arrange/located \bar{P}_{0p} and the thrust-weight ratio of required \bar{P}_{0n} at these values of all other parameters, entering the formulas indicated, possibly only at one specific required value of the over-all payload ratio of the construction/design of aircraft $\bar{G}_{k,n}$, expression for which we will obtain from formulas (2.24) and (2.24'):

$$\bar{G}_{k,n} = 1 - \bar{G}_{c.s.r} - \bar{G}_{0p} (r_0 + S\psi c_{p0}'),$$

or

$$\bar{G}_{k,n} = 1 - \bar{G}_{c.s.r} - \bar{P}'_{0p} r_0 - SR\psi c_{p0} \frac{L_{\max} \sqrt{c_{x_0} D_0}}{M_{kp}} - u.$$

If an aircraft with these parameters and characteristics to carry out is possible, then will be satisfied the equality

$$\bar{P}'_{0p} = \bar{P}_{0n}.$$

According to formulas (2.20) and (2.20') we can find the value of the

over-all payload ratio or construction/design $\bar{G}_{k.n}$, required for guaranteeing assigned magnitudes M_{max} , M_{kp} and L_{max} in assigned/prescribed parameters c_{x0} , ρ_0 , c_{p0} and other,

$$\bar{G}_{k.n} = 1 - \bar{G}_{c.s.r} - \frac{4650 M_{max}^2 c_x}{\xi \rho_0} (r_0 + S \xi \Delta c_{p0} t'); \quad (2.25)$$

with preset time t' of flight or

$$\bar{G}_{k.n} = 1 - \bar{G}_{c.s.r} - \frac{6950 M_{kp}^2 c_{x0}}{\xi \rho_0} r_0 - SR \xi c_{p0} \frac{L_{max} \sqrt{c_{x0} D_0}}{M_{kp}} - u \quad (2.25')$$

with given one L_{max} .

Page 46.

The available over-all payload ratio of construction/design $\bar{G}_{k.p}$ can be expressed approximately by formula (2.26) for aircraft with the direct/straight or sweptback wing of the large or average/mean elongation

$$\bar{G}_{k.p} = (0,027 \varphi m \lambda \frac{G_0^{1.2}}{\cos \lambda} \sqrt{\frac{\lambda}{\rho_0} + \frac{5,5}{\rho_0}}) (1 + \beta_1 \lambda \phi m + \beta_2) + 0,065 \quad (2.26)$$

or for delta-wings airplane or the low elongation

$$\bar{G}_{k.p} = (0,049 \varphi m \lambda G_0^{1.2} \sqrt{\frac{\lambda}{\rho_0} + \frac{5,5}{\rho_0}}) (1 + \beta_1 \lambda \phi m + \beta_2) + 0,065. \quad (2.26')$$

Here $\varphi = 1 - \frac{3(\eta + 1)}{\eta + 2} (\bar{z}_1 \varepsilon_1 \bar{G}_r + \bar{z}_2 \varepsilon_2 \bar{G}_{c.y})$ - coefficient of discharging the wing

where η - wing taper;

ε_1 - portion of the fuel/propellant, arranged/located in wing.

\bar{z}_1 - relative, in the portions of semispan, coordinate of the center of gravity of fuel/propellant in wing (relative to the axis of the symmetry of aircraft).

ϵ_2 - portion of the weight of power plant in wing.

\bar{z}_2 - relative coordinate in the portions of semispan the center of gravity of power plant.

$\mu = 1 + \epsilon \left(\frac{\sigma_r}{\sigma_r'} - 1 \right)$ - coefficient of the weight increase of the construction of the aircraft as a result of the account of kinetic heating.

ϵ - the ratio of the weight of the load-bearing loaded in flight elements toward the weight of an entire structure of aircraft (in the first approximation, can be accepted $\epsilon=0,5$);

$\frac{\sigma_r}{\sigma_r'}$ - relation of yield points at normal temperature and during kinetic heating.

n_A - coefficient of calculated g-force.

G_0 - gross weight of aircraft in t.

$\beta_1 = 0.07 - 0.09$ - for supersonic aircraft.

$\beta_1 = 0.065 - 0.08$ - for heavy subsonic and transonic aircraft.

$\beta_1 = 0.08 - 0.115$ - for transonic transport aircraft.

$m = 1$ - for supersonic aircraft.

$m = 1.2 - 1.3$ - for subsonic and near-sonic aircraft.

$\beta_2 = 0.27$ - for supersonic aircraft.

$\beta_2 = 0.15$ - for subsonic and transonic aircraft.

λ_ϕ - fineness ratio of fuselage.

For aircraft of the specific type and with the known discharging of wing can be used approximation simplified formula (2.26'')

$$\bar{G}_{k,p} = \beta \frac{G_0^{1/2}}{\rho_0^{1/2}} + \frac{15}{\rho_0} + 0,065, \quad (2.26'')$$

where G_0 - in t.

$\beta = 1.6$ - for fighters.

$\beta=0.7-0.8$ - for passenger aircraft with two TVD with discharging of wing.

$\beta=0.4-0.5$ - for passenger aircraft with four TVD with the large discharging of wing¹.

FOOTNOTE 1. Large discharging - discharging wing by a large quantity of loads (engines, fuel/propellant). To large discharging corresponds the low value of the coefficient of discharging ϕ . ENDFCOTNOTE.

Page 47.

$\beta=0.55$ - for passenger aircraft with two TRD with discharging of wing only by fuel/propellant.

$\beta=0.35$ - for passenger aircraft with four TRD with the large discharging of wing.

$\beta=0.35$ - for carriers with four TRD with the large discharging of wing.

It is obvious, designer in design, selecting these or other the

values of the parameters, entering formulas (2.26), (2.26'), it can attain the equality of the available over-all payload ratio of construction/design $\bar{G}_{K,D}$ to required value $\bar{G}_{K,D}$, thereby having successfully solved the basic task of design.

Let us examine as it affects an increase in thrust-weight ratio \bar{P}_0 by fundamental flight characteristics

$V_{max}(M_{max}); V_{kp}(M_{kp}); H_{not}; L_{max}; V_{y,max}$ and L_{p236} .

We will use formula (2.20) for graphing of dependence M_{max} on \bar{P}_0 . Since during increase \bar{P}_0 coefficients c_x and ξ as a result of change M will change, then, being assigned by graphic or computed values M_{max} , for each value M_{max} let us obtain c_x and ξ . Substituting these values in (2.20), let us find the appropriate values \bar{P}_0 and as a result will construct the graph/diagram of dependence M_{max} on \bar{P}_0 according to formula (2.12). We see that during increase \bar{P}_0 value M_{max} steadily grows. The same can be obtained, also, for $M_{specific}$. Utilizing formula (2.5), the dependence of relative density of air on height/altitude H and taking into account that the flight on ceiling occurs on maximum quality K_{max} , for which

$$c_x = 2c_{x_0},$$

we can construct the graph/diagram of dependence H_{not} on \bar{P}_0 . For this, after writing formula (2.20) for the case of flight at velocity, which corresponds to Mach number on ceiling,

$$\bar{P}_0 = \frac{4650M^2 \cdot 2c_{x_0}}{\xi p_0} = \frac{9300M^2 c_{x_0}}{\xi p_0},$$

are assigned by the row/series of values M , determining for each value by calculation or according to the curve/graphs

$$c_{x_0} = f(M); \quad \xi = f(M) \text{ and } D_0 = f(M)$$

and, after substituting these values into formula (2.5), we will obtain data for the curve/graph

$$H_{\text{not}} = f(\bar{P}_0),$$

from which evident that with an increase \bar{P}_0 ceiling H_{not} of aircraft increases (Fig. 2.13).

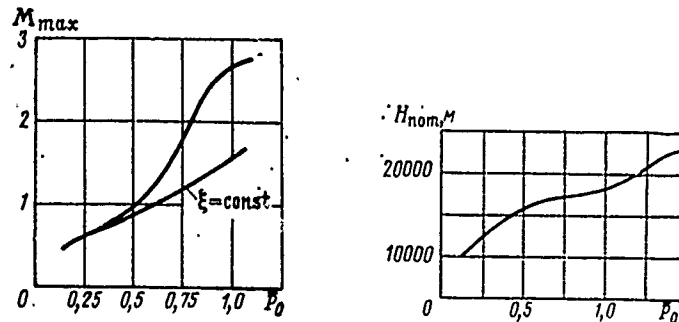


Fig. 2.12. Change in the maximum speed of flight, which corresponds to number M_{max} of aircraft with TRD in dependence on the starting thrust-weight ratio \bar{P}_0 ($H=11000$ m).

Fig. 2.13. Dependence of ceiling H_{nom} on starting thrust-weight ratio \bar{P}_0 .

Page 48.

Value L_{max} thrust-weight ratio \bar{P}_0 affects through M_{kpefc} . Substituting in formula (2.15') of value $M_{kpefc} = f(\bar{P}_0)$ and corresponding values c_{x0} , D_0 and ψ , it is possible to obtain curve/graph $L_{max} = f(\bar{P}_0)$ (see Fig. 2.7), from which it is evident that distance L_{max} first increases, and then during the appearance of wave drag (at transonic speeds) it begins sharply to decrease, with further increase \bar{P}_0 , again it begins to grow to some limit.

In a similar manner it is easy to arrive at the conclusion that $V_{y\max}$ with an increase \bar{P}_0 grows, and takeoff run length $L_{\text{посб}}$ during increase \bar{P}_0 decreases. Parameter value designer usually selects in the beginning of design on the basis of common/general/total considerations or special calculations. This dimensional-weight parameter has complicated effect on fundamental flight characteristics both directly, entering into formula which is determining the value of characteristic, and through other parameters (\bar{P}_0 and c_{x0}).

Let us examine, first, what effect exerts directly change p_0 to the given above aircraft performance without taking into account the effect of this change to its other parameters (\bar{P}_0, c_{x0}).

On the basis of the dependences, expressed by formulas (2.18) and (2.19), it is possible to write

$$c_x = k_0 c_{xp} + c_{x\phi} \frac{p_0}{k} + D_0 \left(\frac{p_0}{q} \right)^2. \quad (2.27)$$

After dividing both parts (2.27) on $c_y = \frac{p_0}{q}$, we will obtain expression for the required thrust-weight ratio

$$\bar{P}_0 = k_0 c_{xp} \frac{1}{p_0} + c_{x\phi} \frac{q}{k} + D_0 \frac{p_0}{q}, \quad (2.28)$$

where

$$k_0 = 1 + \gamma \frac{S_{\text{on}}}{S}; \quad \gamma = \frac{c_{x\text{on}} + c_{x\text{n.on}}}{c_{xp} + c_x},$$

whence

$$p_0^2 + \frac{q}{D_0} \left(c_{x\phi} \frac{q}{k} - \bar{P}_0 \right) p_0 + \frac{q^2}{D_0} c_{xp} k_0 = 0,$$

OR

$$p_0 = \frac{q}{2D_0} \left(\bar{P}_0 - c_{x\phi} \frac{q}{k} \right) - \sqrt{\frac{q^2}{4D_0} \left(c_{x\phi} \frac{q}{k} - \bar{P}_0 \right)^2 - \frac{q^2}{D_0} c_{x\rho} k_0}. \quad (2.29)$$

Using formula (2.29), it is possible to construct the graph/diagram of dependence q or M on p_0 under the condition of independence \bar{P}_0 on p_0 (i.e. when $\bar{G}_R = \text{const}$ with change p_0) (see Fig. 2.14, 2.15). Curves give the possibility to make the following conclusions:

1) increase p_0 conducts to time of ripening M (or q)¹, but to certain limit p_0 , which increases with an increase \bar{P}_0 ;

2) with increase p_0 the intensity of increase M (i.e. dM/dp_0) or q decreases; with an increase \bar{P}_0 dM/dp_0 , it grows.

FOOTNOTE 1. Besides the specially stipulated cases, everywhere has in mind increase p_0 during decrease of S and $c_0 = \text{const}$. ENDFOOTNOTE.

Page 49.

3) increase p_0 to large values, the close p_0 (with given one of thrust-weight ratio \bar{P}_0), is irrational, since in this case increase M

is small, and the exaggerated values p_0 can lead to the inadmissible increase in landing speed V_{noc} and distances of take-off and landing run.

Effect p_0 thrust-weight ratio \bar{P}_0 affects as follows. During increase p_0 , available over-all payload ratio \bar{G}_R [see (2.26), (2.26'), (2.26'')] decreases, available thrust-weight ratio \bar{P}_{op} [see (2.24) and (2.24')] it increases, and p_0 is shift/sheared to large values and intensity of increase M (or q) increases. Over-all payload ratio $\bar{G}_{c.o.r}$ during change \bar{G}_R on $-\Delta\bar{G}_R$ will increase on

$$\Delta\bar{G}_{c.o.r} = -\bar{G}_{c.o.r} \frac{\Delta\bar{G}_R}{1-\bar{G}_R}$$

To ceiling H_{not} or on relative density Δ_{not} , corresponding to ceiling H_{not} , specific load p_0 affects through c_x [see (2.27)] and through \bar{P}_{op} [see (2.24) and (2.24')] as a result of effect p_0 on \bar{G}_R , entering expressions (2.26) and (2.26'). Having this in form and analyzing formula (2.5)

$$\Delta_{not} = \frac{1,66 \sqrt{c_{x_0} D_0}}{\xi \bar{P}_0},$$

it is possible to make the following conclusions:

- 1) increase p_0 leads to increase c_{x_0} , since

$$c_{x_0} = k_0 c_{xp} + c_{x\phi} \frac{p_0}{k_1}.$$

Consequently, in subsonic and transonic aircraft ceiling H_{not} with

increase p_0 will descend. Since during increase p_0 the over-all payload ratio of construction/design \bar{C}_k decreases and respectively increases available thrust-weight ratio \bar{P}_{op} , then the intensity of the decrease of ceiling during increase p_0 will be small;

2) increase p_0 for supersonic aircraft leads in certain cases to an increase in static ceiling H_{not} . Occurs this on following reason. Speed on ceiling, i.e., when $\left(\frac{c_y}{c_x}\right)_{max}$, is equal to

$$V_{not} = 11,1 \sqrt{\frac{p_0 \bar{P}_{op} \bar{C}_k}{c_{x_0}}} \approx M_{not} = 0,0104 \sqrt{\frac{p_0 \bar{P}_{op} \bar{C}_k}{c_{x_0}}}$$

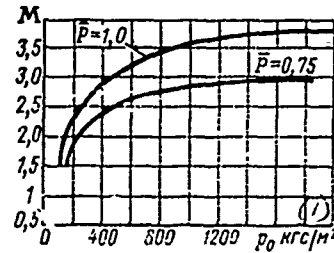
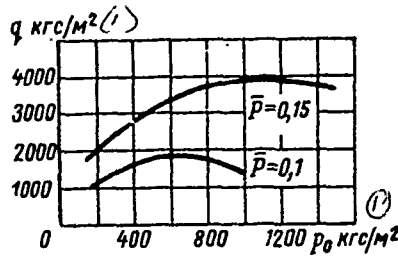


Fig. 2.14. The effect of velocity head on value p with different values of thrust-weight ratio \bar{P} under conditions when wave drag is absent ($\lambda=4$; $c_{xP}=0,007$)

Key: (1). kgf/m^2 .

Fig. 2.15. Effect p_0 on value M at different values of thrust-weight ratio \bar{P} of aircraft ($H=10000$ m).

Key: (1). kgf/m^2 .

Page 50.

Consequently, increase p_0 with the constant/invariable thrust-weight ratio \bar{P}_0 and at the speeds, which correspond $M > 1.5$, will lead to an increase in the speed on ceiling $V_{\text{ПOT}}$ or $M_{\text{ПOT}}$ (effect on $V_{\text{ПOT}}$ increases c_{x0} , as show calculations, it is less than the effect of increase p_0). But with an increase in the speed (with $M > 1.5$) will increase to

certain limit the coefficient ξ of the dependence of the engine thrust in speed. This increase with $M=1.5-2.5$ (but with boosting TRD and on the large ones M) will be so/such perceptibly, which

$$\Delta_{\text{not}} = \frac{1,66 \sqrt{c_{x_0} D_0}}{\xi \bar{P}_0}$$

during increase p_0 and, therefore, increase c_{x_0} will nevertheless decrease, ceiling H_{not} will in this case increase. During increase p_0 , the available over-all payload ratio of construction/design \bar{C}_k will, as we already saw, decrease, available \bar{P}_{op} will increase, and Δ_{not} will be they decrease, i.e., H_{not} will increase.

With increase p_0 , increases $V_{y \text{ max}}$ - the maximum vertical velocity in the earth/ground. This is easy to see from the formula

$$V_{y \text{ max}} = 1,53 \sqrt{\frac{p_0 (\bar{P} \xi)^3}{c_{x_0}}}$$

Since $c_{x_0} = k_0 c_{xp} + c_{x\phi} \frac{p_0}{k_1}$, that $\frac{p_0}{c_{x_0}}$ it is possible to write thus: $\frac{1}{\frac{k_0}{p_0} c_{xp} + \frac{c_{x\phi}}{k_1}}$,

from which it is clear that during increase p_0 fraction

$\frac{p_0}{c_{x_0}}$ - increases, i.e., $V_{y \text{ max}}$ - increases. $V_{y \text{ max}}$ increases and because decreases in this case \bar{C}_k and, therefore, grows available thrust-weight ratio \bar{P}_{op} .

Increase p_0 contributes to increase L_{max} . In this case, increase L_{max} will occur to certain sufficiently large value p_0 , after which the distance will begin to decrease. For subsonic and transonic

aircraft in the formula

$$L_{\max} = 7,0 \sqrt{\rho_0 \bar{P}_0 \xi} \frac{1}{\psi c_{p0} c_{x0} \sqrt{D_0}} \ln \frac{1}{1 - \bar{G}_T}$$

of value ξ, ψ and D_0 , it is possible to accept being independent of the speed (change they at transonic speed little), then, obviously, L_{\max} achieves the greatest value with similar ρ_0 , with which $\sqrt{\rho_0} c_{x0}$ will achieve its maximum value, and $\frac{c_{x0}}{\sqrt{\rho_0}}$ - a minimum value. After making first-order derivative $\frac{c_{x0}}{\sqrt{\rho_0}}$ on ρ_0 equal to zero and utilizing formula (2.18), we will obtain

$$\rho_{0\text{HB}} = k_0 \frac{c_{xp}}{c_{x\phi}} \frac{G_0}{\Sigma S_M}. \quad (2.30)$$

However, this solution does not consider effect ρ_0 on \bar{G}_K and, as a result, to available thrust-weight ratio \bar{P}_{0p} . Applying graphic methods, it is possible to find $\rho_{0\text{HB}}$ taking into account effect ρ_0 on \bar{P}_0 .

Page 51.

For a supersonic aircraft value $\rho_{0\text{HB}}$ in flight to maximum range let us find graphically, after constructing the curve of function L_{\max} :

$$L_{\max} = \frac{584 M_{\text{крет}} c}{\psi c_{p0} \sqrt{c_{x0} D_0}} \ln \frac{1}{1 - \bar{G}_T}$$

of argument ρ_0 . In this case, one should consider that entering the formula values $M_{\text{крет}}, c_{x0}, \bar{G}_T$ are functions ρ_0 , and ψ, c_{x0}, D_0 change in

dependence on M .

After assigning p_0 , $M_{кретс}$ and c_{x0} let us determine, utilizing formulas (2.26'') and (2.20'), arrange/located $\bar{G}_{к,р}$

$$\bar{G}_{к,р} = \beta \frac{G_0^{1,2}}{p_0^{1,2}} + \frac{15}{p_0} + 0,065,$$

required thrust-weight ratio $\bar{P}_{он} = \frac{6950 M_{кретс}^2 c_{x_0}}{p_0 \xi}$,

and

$$D_0 = 0,25 B_0 \sqrt{M^2 - 1}$$

$$\bar{G}_{c,y} = \bar{P}_0 r_0.$$

During the satisfactory solution of the task of design, available thrust-weight ratio $\bar{P}_{оп}$ will be equal to required thrust-weight ratio $\bar{P}_{он}$, the available over-all payload ratio of fuel/propellant will be

$$\bar{G}_{т,р} = 1 - \bar{G}_к - \bar{G}_{c,y} - \bar{G}_{c,э,г},$$

where by value $\bar{G}_{c,э,г}$ we are assigned. Then $L_{max} = \frac{584 M_{кретс}}{\psi c_{p0} \sqrt{c_{x_0} D_0}} \ln \frac{1}{1 - \bar{G}_{т,р}}$ and p_0 will serve as the coordinates of the first point of curve L_{max} on p_0 . We are further assigned by the new value p'_0 and, utilizing the taken and calculated above values for \bar{P}_0 ; $\bar{G}_к$; $\bar{G}_{т,р}$, let us find

$$\bar{G}'_к = \bar{G}_к + \Delta \bar{G}_к = \beta \frac{(G'_0)^{1,2}}{(p'_0)^{1,2}} + \frac{15}{p'_0} + 0,065;$$

$$M'_{кретс} = 0,012 \sqrt{\frac{p'_0 \bar{P}'_0 \xi'}{c_{x_0}}};$$

$$c'_{x_0} = k_0 c_{xp} + c_{x\phi} \frac{p'_0}{k_1}, \quad \bar{P}'_0 = \bar{P}_0 \frac{1 - \varepsilon \bar{G}_к}{1 - \bar{G}_к}; \quad \varepsilon = \frac{\bar{G}'_к}{\bar{G}_к},$$

where $G'_0 = G_0 \frac{1}{1 - \frac{\Delta \bar{G}_к}{1 - \bar{G}_к}}$.

$M'_{крелс}$ we find graphically, after constructing curve $M'_{крелс. истр} = f(M'_{крелс. зад})$ and ray/beam from the origin of coordinates at an angle of 45° to axle/axes. In this case, $M'_{крелс. зад}$ - Mach number, by which we are assigned, selecting values ξ and c_{x_0} and $M'_{крелс. истр}$ - Mach number, which we obtain according to formula for

$$M'_{крелс} = 0,012 \sqrt{\frac{p'_0 p'_0 \xi'}{c_{x_0}}}$$

FOOTNOTE 1. According to curves $\xi = f(M)$ and $c'_{x_0} = f(M)$, which are assign/prescribed or calculated. ENDFCOTNOTE.

Knowing $M'_{крелс}$ and after determining D_0 , ψ and \bar{G}'_r from $\bar{G}'_r = \bar{G}_r \left(1 - \frac{\bar{G}'_k - \bar{G}_k}{1 - \bar{G}_k}\right)$, let us find for p'_0

$$L'_{max} = \frac{584 M'_{крелс}}{\psi c_{p_0} \sqrt{c'_{x_0} D_0}} \ln \frac{1}{1 - \bar{G}'_r}$$

Page 52.

Figures 2.16 give the curve, constructed thus. In this case, was considered increase \bar{G}_k on the large Mach numbers, which was being obtained as a result of kinetic heating.

As can be seen on Fig. 2.16, distance with an increase p_0 always

grows up to very large values p_0 ($p_{opt}=900$ kgf/m²). The decrease of distance during further increase p_0 is connected with an incidence/drop in the coefficient ξ .

Note. In the practice of the design of long-range aircraft, such large values p_0 ($p_0=900$ kgf/m²) are not applied on following the considerations:

1) maximum $L_{max}=f(p_0)$ is very flat, i.e., L_{max} grows near p_{opt} it is weak.

2) very large values p_0 make takeoff and landing characteristics worse of aircraft.

During increase p_0 , the takeoff run length L_{take} increases.

Examining formula (2.17')

$$L_{take} \approx \frac{0,82 p_0}{c_{y\text{отр}}(\bar{P}_0 - f)},$$

it is possible to say following. During increase p_0 , increases that arrange/located \bar{P}_{0p} as a result of the decrease of that arrange/located \bar{C}_x . Drag coefficient

$$c_x = k_0 c_{xp} + c_{x\phi} \frac{p_0}{k_1} + D_0 \left(\frac{p_0}{q} \right)^2$$

during increase p_0 increases, since p_0/k_1 - increases, and $p_0/q = c_y$ remains constant/invariable, since the angle of attack of aircraft on

takeoff/run-up depends only on the geometric parameters of chassis/landing gear and remains constant/invariable.

Comparing formulas (2.17'), (2.26) and (2.25'), it is not difficult to draw the conclusion that during increase p_0 the denominator of fraction (2.17') grows more slowly than numerator and, therefore, L_{pass} increases with increase p_0 .

Coefficients ξ and ψ_1 characterizing the dependence of thrust and specific consumption of fuel of engine on the speed of flight are determined by the selected parameters of engine and virtually, during the design of aircraft under the existing engine, they are located out of the effect of the designer of aircraft.

From formulas (2.3); (2.5); (2.6); (2.15') it is evident that an increase in the coefficient ξ at the constant values of other parameters leads to increase M_{max} ; $M_{\text{крейс}}$; $H_{\text{пот}}$; $V_{y \text{ max}}$; L_{max} . However, it is necessary to keep in mind that the rational value ξ will be such, which with given ones M_{max} or $M_{\text{крейс}}$ will be determined from the formula

$$\xi = \frac{4650M_{\text{max}}^2 c_x}{\bar{P}_0 p_0} \quad \text{or} \quad \xi = \frac{6950M_{\text{крейс}}^2 c_{x_0}}{\bar{P}_0 p_0} .$$

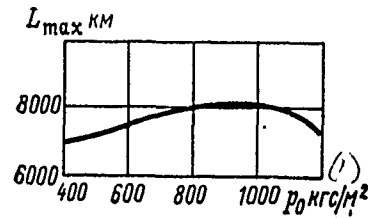


Fig. 2.16. Dependence of maximum range L_{max} on specific load p_0 taking into account effect p_0 on the over-all payload ratio of construction/design \bar{G}_K (p_0 =var; \bar{G}_K =var)

Key: (1). kgf/m².

Page 53.

In this case, must be observed the condition

$$\bar{P}_0 = \frac{0,82p_0 + L_{расч} c_{y\text{отр}} f}{L_{расч} c_{y\text{отр}} \epsilon_\phi}$$

where $\epsilon_\phi = \frac{\bar{P}_{0\phi}}{\bar{P}_0}$ - coefficient of afterburning.

$\bar{P}_{0\phi}$ - thrust-weight ratio on takeoff with afterburning.

$L_{расч}$ - assigned/prescribed distance of takeoff/run-up.

f - coefficient of friction.

After conducting conversions in expressions (2.25) and (2.25'),

it is possible to write for or assigned/prescribed duration of flight t'

$$4650M_{\max}^2 c_x (r_0 + S\psi\xi\Delta c_{p0}') - \xi p_0 (1 - \bar{G}_k - \bar{G}_{c.s.r}) = 0 \quad (2.31)$$

and for of assigned/prescribed distance L_{\max}

$$6950M_{\text{кретс}}^3 c_{x_0} r_0 - M_{\text{кретс}} \xi p_0 (1 - \bar{G}_k - \bar{G}_{c.s.r} - u) + \\ + SRc_{p0}' \xi p_0 L_{\max} \sqrt{c_{x_0} D_0} = 0. \quad (2.31')$$

Equations (2.31) and (2.31') give the demonstrative representation of the dependence of the most important aircraft performance M on different parameters and they make it possible to determine the value M_{\max} or $M_{\text{кретс}}$ which virtually possibly for an aircraft in assigned/prescribed parameters $\bar{G}_{\text{кр}}$, $\bar{G}_{c.s.r}$, p_0 , c_{x_0} , c_{p_0} , r_0 , L_{\max} , t' and so forth.

Solving first equation (2.31), we will obtain for M_{\max} with mission time t'

$$M_{\max} = \sqrt{\frac{\xi p_0 (1 - \bar{G}_k - \bar{G}_{c.s.r})}{4650 c_x (r_0 + S\psi\xi\Delta c_{p0}')}}. \quad (2.32)$$

Note. For determining value M_{\max} it is possible to use this graphic procedure. After assigning several values of M , they determine the cooresponding to them ξ , c_x and ψ . Last/latter values substitute in formula (2.32) and calculate values M_{\max} . In terms of the selected values of M and the corresponding to them values M , calculated according to formula, is plotted a curve in coordinates $M_{\text{кретс}}$ and $M_{\text{кретс}}$ (Fig. 2.17), intersection with which with the straight

line, carried out from the origin of coordinates at an angle of 45° , will give unknown value M_{\max} , $M_{\text{зад}}$ and $M_{\text{кр}}$ (all values must be undertaken on one scale).

Value $M_{\text{кр}}$ can be found also, using by graphical solution (Fig. 2.18), after taking as functions for plotting of curves following:

$$\left. \begin{aligned} 6950M_{\text{кр}}^3 c_{x_0} r_0 &= \theta_1; \\ M_{\text{кр}} \xi p_0 (1 - \bar{\sigma}_k - \bar{\sigma}_{\text{с.э.г}} - u) - \\ - SR \xi L_{\max} c_{p0} p_0 \sqrt{c_{x_0} D_0} &= \theta_2. \end{aligned} \right\} \quad (2.33)$$

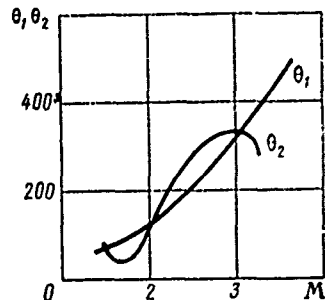
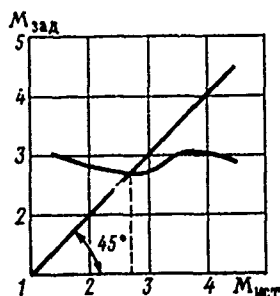


Fig. 2.17. Example of graphical solution of equations (2.29).

Fig. 2.18. Example of graphical solution of equations (2.29').

Page 54.

The point of intersection of these curves on curve/graph in coordinates M and θ_1 and θ_2 will determine unknown value $M_{k, \text{petic}}$. At some values of values, can be obtained three values $M_{k, \text{petic}}$. In this case, to each of them will correspond its value of thrust-weight ratio \bar{P}_0 , determined on

$$\bar{P}_0 = \frac{6950 M_{k, \text{petic}}^2 c_{x_0}}{p_0 \xi}$$

The presence of several solutions is explained by the complexity of the functions

$$\xi = f(M); \quad \psi = f(M); \quad c_{x_0} = f(M).$$

Examining equations (2.31) and (2.31'), it is not difficult to draw the important conclusion that assigned magnitude M can be

obtained only during the specific combinations of the parameters, entering these equations. If the parameters at assigned magnitudes M_{Rpellec} and L_{max} or t' satisfy equations (2.31) and (2.31'), then the real realization of this aircraft is possible. But if equations are not satisfied, then the design/projected aircraft virtually it is not possible to carry out. Besides in addition to this, the named equations reveal/detect direct effect on M of such parameters of aircraft as G_{10} , r_0 , c_{p0} etc. All this tells about the large value of the equation of the over-all payload ratios of aircraft for setting of the regular dependences between the flight characteristics and the most important parameters of aircraft.

Subsequently we will call equations (2.31) and (2.31') the fundamental equations of the design/projected aircraft.

On the basis of entire of that presented in this chapter, it is possible to make following conclusions.

1. Speeds V_{max} and V_{Rpellec} (or number M_{max} and M_{Rpellec}) increase, if \bar{P}_0 in constant/invariable other parameters increases. The available thrust-weight ratio increases with:

a) the decrease of specific gravity/weight of the power plant Γ_0 .

b) the decrease of the over-all payload ratio of the construction/design of aircraft $G_{R,P}$ (arrange/located).

c) the decrease of the specific fuel consumption by engine c_{p0} (substantially for long-range aircraft).

One should, however, remember that the maximum speed of aircraft V_{max} is sometimes limited to not available thrust-weight ratio P_{op} , but permissible for reasons of strength by velocity head or temperature of kinetic heating.

2. Speeds V_{max} and $V_{крет}$ can be increased (, other conditions being equal,) as a result of increase in specific wing load p_0 , but in this case, it is necessary to consider that with an increase p_0 intensity of increase in speed V (or Mach number) sufficiently sharply descends, and at value p_0^* , increase V ceases. At the same time with very large p_0 substantially deteriorate takeoff and landing characteristics of aircraft ($V_{нос}$, V_y , $L_{разб}$ and $L_{проб}$).

3. Speeds V_{max} and $V_{крет}$ can be increased during decrease of drag coefficient c_{x0} . The methods of decrease c_{x0} change in dependence on rate of speed (subsonic, transonic, supersonic).

4. Static ceiling of aircraft $H_{\text{нот}}$ increases ($\Delta_{\text{нот}}$ - it decreases), if as a result of indicated in p. 1 measures thrust-weight ratio \bar{P}_0 increases.

5. Static ceiling $H_{\text{нот}}$ of subsonic aircraft decreases, if specific load p_0 increases (in this case c_x increases). For a supersonic aircraft with TRD, increase p_0 in certain cases leads to increase $H_{\text{нот}}$. Decrease c_{x0} at the constant values of other parameters leads to certain control $H_{\text{нот}}$.

Page 55.

6. Vertical velocity $V_{y \text{ max}}$ intensely increases during increase \bar{P}_0 . Decrease c_{x0} at the constant values of other parameters increases $V_{y \text{ max}}$.

7. Maximum range L_{max} with increase in cruising values $M_{\text{кретч}}$ in subsonic range increases [see formula (2.15) and Fig. 2.7]; with further increase $M_{\text{кретч}}$ (with preservation/retention/maintaining of other conditions) in near-sonic range L_{max} it sharply decreases, but during further increase $M_{\text{кретч}}$ in supersonic range L_{max} gradually it grows. An increase in the specific wing load p_0 , which leads to

increase $M_{кретс.}$ decrease \bar{C}_R and, therefore, to increase \bar{C}_T in subsonic and supersonic range ($M < 1$ and $M > 1.5$) to certain value ρ_{opt} (see Fig. 2.16) leads to increase L_{max} .

8. Distance of takeoff/run-up L_{pass} increases with increase p_0 and decreases with increase \bar{P}_0 .

9. Fundamental equations of aircraft show that between flight characteristics and most important parameters of aircraft there are laws, analyzing which it is possible to find rational solutions.

Page 69.

Chapter IV.

APPROXIMATE METHODS OF THE OPTIMIZATION OF THE PARAMETERS OF AIRCRAFT.

In the preceding/previous chapter were examined the methods of the simultaneous optimization of the basic parameters and characteristics of aircraft, based on use of computers. However, during design are encountered the cases when there is not possibilities to utilize computers and it is necessary to select the basic parameters of aircraft, applying the approximation methods of optimization. Most commonly used from these methods are examined in present chapter.

Page 70.

§ 1. Determination of the particular optima of the parameters of aircraft.

To task it is placed as follows. Are known

- the designation/purpose of aircraft and its diagram;
- type and engine characteristic;
- value of payload and fundamental flight characteristics, provided for by requirements for aircraft.

It is required to determine the particular optima of any which interest designer parameters, for example the parameters of wing, fuselage or power plant. During finding of the particular optimum of any of the parameters, the remaining parameters are considered known from statistics or previous approximate computations and are considered as constant values. This method, called the method of the "freezing" of the parameters, is applied during optimization of one of them.

If is defined the optimum of any of the parameters at the given values of payload, distance and flight mach number, then by the approximate criterion of optimization, as was noted in chapter I, can be the value of the takeoff weight of aircraft. In this case the

optimum of the parameter will correspond to the minimum of takeoff weight.

When known values are payload and takeoff weight (assign/prescribed or found in the first approximation), then the criterion of optimization can be flying range and the optimum of the parameters will correspond in this case to the maximum of distance.

Are possible other more complicated criteria, which consider the cost-effectiveness/efficiency of aircraft, for example, the prime cost of transportation.

During the determination of optima, one should consider the limitations, placed on parameters and characteristics of the aircraft (see Chapter III).

The algorithms, given in chapter III, especially when is averaged coefficient c_x (Go), they can be utilized it goes without saying and for the optimization of several parameters of aircraft on the basis of calculations without use of computers.

Is of interest the emergence of the optima of the separate parameters of aircraft components.

As examples let us examine the emergence and approximate grapho-analytic determination of the particular optima of the following parameters of aircraft:

- wing aspect ratio λ ;
- wing chord ratio \bar{c} ;
- sweep angle of wing χ ;
- load on 1 m² of wing with takeoff p_0 ;
- fineness ratio of fuselage λ_ϕ ;
- bypass ratio of TVRD m .

Optimum wing aspect ratio. On wing aspect ratio, depend, in essence, two values - weight of wing and fuel load. With an increase in elongation ($\lambda \geq 3$) grows the weight of wing in other constant/invariable parameters (including wing area), since increase the bending and torsional moments, and also the shearing forces. If as the criterion of optimization to accept takeoff weight, then increase λ adversely will affect this criterion (takeoff weight will increase).

On the other hand, with an increase λ inductive wing drag [17], required thrust of engines and weight of required fuel/propellant will decrease. The weight of power plant it is possible to approximately consider being independent of wing aspect ratio. Thus, the optimum of wing aspect ratio approximately can be determined by the minimum of the sum of the weights of wing and fuel/propellant.

Page 71.

Graphical solution of the task of selection λ_{opt} is given in Fig. 4.1 and does not require special explanation.

The obtained optimum λ of wing is, as a rule, moderated in sharpness, and change in the evaluation criteria to 10/o in comparison with its outer limit gives the possibility to step back from λ_{opt} to 8-10o/o.

Besides graphic, and possible the approximate analytical solution, determined from the condition of extremum with $M \neq f(\lambda)$

$$\frac{\partial G_{sp}}{\partial \lambda} + \frac{\partial G_r}{\partial \lambda} = 0. \quad (4.1)$$

For example, for subsonic nonmaneuverable jets, taking into account satisfaction of condition (4.1), it is possible to obtain the

following equation:

$$\lambda_{opt}^3 [1 + (0,018 + 0,14\chi^{max})\lambda_{cp}] = \frac{10^4 (c_x)_{min} (\bar{c}_0)^{1,5} (\rho_0 \cos \chi^0)^3}{87G_0} \left[\frac{(c_p)_{cp} \left(L_{расч} + \frac{4}{b} L_{расч}^{2/3} \right)}{\varphi (V_{кретс} - 50) \frac{\eta + 4}{\eta + 1}} \right]^2 = E, \quad (4.2)$$

where χ^{max} and χ^0 - a sweepback of wing along 1/4 chords in radians and in degrees respectively;

$(c_p)_{cp} = (0,92 - 0,94)(c_p)_{кретс}$ - average/mean for flight time specific hourly consumption of fuel/propellant in kg/kg·h;

ϕ - coefficient of discharging wing;

$b = 1.05 - 1.20$ - coefficient, depending on aircraft type (with the decrease of tonnage values b decrease; approximately $b \approx 1.05 + G_0 \cdot 10^{-3}$, where G_0 in t).

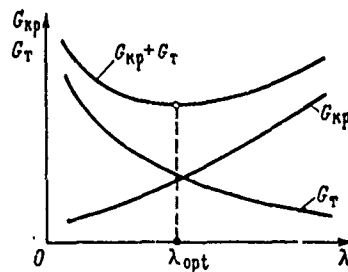


Fig. 4.1. Diagram of the emergence of optimum wing aspect ratio.

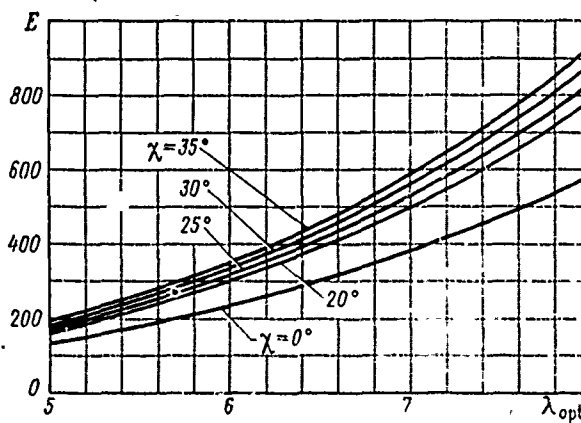


Fig. 4.2. Curve/graph for determining optimum wing aspect ratio of subsonic nonmaneuverable aircraft.

Page 72.

Curve/graph for determination λ_{opt} from formula (4.2) is given in Fig. 4.2.

The analysis of formula (4.2) makes it possible to make the following conclusions:

- with an increase in the calculated flying range L_{pacv} and the specific hourly consumption of fuel/propellant c_D , grows optimum wing aspect ratio. For subsonic aircraft the marked trend in development of TVRD, foreseen reduction/descent c_D , entails decrease λ_{opt} in other constant/invariable parameters of aircraft;

- during increase $c_{x_{min}}$ in the aircraft (or c_{x_0} in the absence of the twist of wing) optimum aspect ratio of wing increases;

- with an increase in calculated cruising speed λ_{opt} descends;

- increase when $L_{pacv} = \text{const}$ takeoff weight (G_0) as a result of increasing the payload decreases optimum wing aspect ratio;

- with an increase in the values of such parameters as ρ_0 , \bar{c}_0 , η , and also with the decrease of angle χ value λ_{opt} increases. Generally, if a change in any parameter leads to the decrease of the over-all payload ratio of wing, then this change increases λ_{opt} , and vice versa;

- great effect on λ_{opt} exert load on wing p_0 and its sweepback χ .

As show the results of calculations, the accuracy/precision of

determination λ_{opt} from approximation formula (4.2) composes $\pm 10\%$.

Optimum wing chord ratio. Let us examine how affects average/mean on spread/scope wing chord ratio \bar{c}_{cp} the of payload and flying range. Let us consider that the law of a change in the wing chord ratios in spread/scope is known ¹.

FOOTNOTE ¹. The solution of the task of the optimum law of change \bar{c} in the wingspan is given in § 3 of this chapter. ENDFOOTNOTE.

Change \bar{c}_{cp} has effect mainly by weight of wing and its aerodynamic resistance. With increase \bar{c}_{cp} the weight of the wings of contemporary aircraft in its other constant/invariable parameters decreases as a result of an increase in the overall height h of wing. In by increase h at the constant value of bending moment M_{HOR} axial forces $P = M_{HOR}/h$, applied to beam flanges (or to the panels of caisson), decrease and respectively decrease required cross sections and weight of longitudinal load-bearing elements ².

FOOTNOTE ². For some wing constructions, increase \bar{c}_{cp} entails an increase in the weight of ribs. However, this fact does not have vital importance, since the over-all payload ratio of the longitudinal structural assembly of contemporary wings is considerably more than the over-all payload ratio of ribs.

ENDFOOTNOTE.

Thus, increase \bar{c}_{cp} leads to the decrease of the takeoff weight of aircraft.

On the other hand, with increase \bar{c}_{cp} grows profile and wave wing drag, which increases required thrust and fuel consumption with assigned/prescribed flight mach number.

Consequently, at some values of parameters and characteristics of aircraft is possible the existence of optimum value \bar{c}_{cp} (Fig. 4.3).

Having dependences $G_{kp}(\bar{c}_{cp})$ and $G_r(P_{notp})$, where $P_{notp} = G \frac{c_x}{c_y}$ and $c_x = f(\bar{c}_{cp})$, it is possible graphically to find $(\bar{c}_{cp})_{opt}$.

The solution of this task leads to following results (\bar{c} - everywhere along flow):

for supersonic aircraft

$$(\bar{c}_{cp})_{opt} = (2,5 - 3,5)\%; (\bar{c}_0)_{opt} = (3 - 4)\%;$$

for subsonic aircraft with TVRD

$$(\bar{c}_{cp})_{opt} = (9 - 12)\%; (\bar{c}_0)_{opt} = 10 - 13\%.$$

Page 73.

Optimum \bar{c} of wing is usually not strong. Change in the evaluation criteria to 10/0 gives the possibility to step back from $(\bar{c}_{cp})_{opt}$ to 10-120/0.

During the design of subsonic aircraft, determination \bar{c}_{opt} somewhat becomes complicated by that fact that the flight speed, which corresponds usually $M_{крит}$, depends on \bar{c}_{cp} or on c_0 . In particular, with increase \bar{c}_0 in the wing flight speed is necessary to decrease. Therefore, if flight speed enters into evaluation criteria of aircraft as, for example, into prime cost t-km, then during determination $(\bar{c}_0)_{opt}$ must be also taken into account dependence $V_{пенс}(\bar{c}_{cp})$.

Optimum sweepback of wing. The sweepback of wing χ of subsonic aircraft affects, first of all, the weight of wing, fuselage and power plant. Increase χ in the constant/invariable remaining parameters leads to the weight increase of wing due to an increase in the structural/design spread/scope (in the direction of 1/4 chords) and the torsional moment in root cross sections. End wing sections it is also necessary to amplify for torsion in order to avoid the reversal of ailerons. Furthermore, if the longitudinal structural assembly of the sweptback wing approaches at angle the former/frames of fuselage, then the part of the bending moment from wing is transferred by fuselage, increasing its weight 1 , and is greater, the greater χ .

FOOTNOTE ¹. The weight of fuselage increases also in connection with an increase in the length of its tail section, the caused increase in the sweepback of wing. ENDFOOTNOTE.

Finally, with increase χ decrease values \bar{c}_y^* and \bar{c}_{y0rp} , which leads to an increase in the required starting thrust-weight ratio of aircraft.

However, despite all the enumerated deficiency/lacks increase in the sweepback of the wing of subsonic aircraft gives the important advantage: appears the possibility to increase flight speed due to an increase in number M_{kpr} and reduction/descent c_x , which favorably affects the cost-effectiveness/efficiency of aircraft. Appears as if counterweight to the adverse effect of an increase in the sweepback of wing by the weight characteristics of aircraft. Therefore possibly the existence of the optimum sweepback of wing along 1/4 chords, the corresponding to the minimum prime costs t-km (Fig. 4.4).

If we solve the task of $(\chi)_{opt}$ graphically, taking into account all contradictory dependences, it is possible to obtain approximately following of value $(\chi)_{opt}$ for the subsonic jets:

the aircraft of the low and average/mean distance (≤ 1500 km) -

DOC = 79052104

PAGE

125

20-25°;

the aircraft of average/mean distance (2000-3000 km) - 30-35°;

the aircraft of the large distance (≥ 5000 km) - 35-37°.

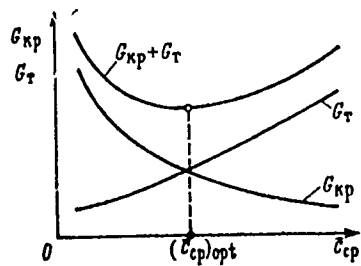


Fig. 4.3.

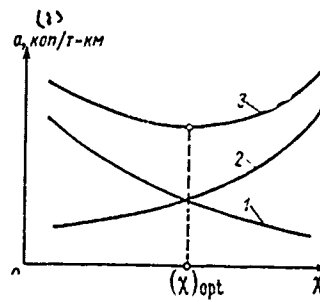


Fig. 4.4.

Fig. 4.3. Diagram of emergence of optimum average/mean wing chord ratio.

Fig. 4.4. Diagram of emergence of optimum sweepback of wing:

1 - effect of flight speed; 2 - gravity effect of construction/design and power plant; 3 - total effect on prime cost of transportation.

Key: (1). a, kopecks/ton-kilometer.

Page 74.

One should consider that the optimum values of sweepback depend also on other parameters of wing, mainly, from c_0 , λ , p_0 . With increase p_0 and \tilde{c}_0 value $(\lambda)_{opt}$ they grow, while from an increase λ -

they fall. Respectively are selected values $(\chi)_{opt}$ in the recommended limits.

As far as aircraft are concerned supersonic with low-aspect-ratio wing, effect of sweepback on front/leading stern $\chi_{ll,k}$ by weight of wing and fuselage more complicated than in the subsonic aircraft (sweepback of the wing of supersonic aircraft is measured according to leading edge). Increase $\chi_{ll,k}$ in the delta wing, for example, always leads to a gain in weight of wing and fuselage, but beginning with the specific sweepback it leads even to a reduction/descent in the weight of these aggregate/units. Stronger effect has value $\chi_{ll,k}$ on lift-drag ratio and fuel load. Approximately it is possible to consider that the optimum sweepback of wing on M_{pacu} corresponds to the maximum of lift-drag ratio and is equal (see the Table).

| | | | | | |
|-----------------------|-----|-----|-----|-----|-----|
| M_{pacu} | 2,0 | 2,3 | 2,5 | 2,7 | 3,0 |
| $(\chi_{ll,k})_{opt}$ | 60 | 65 | 69 | 72 | 75 |

If sweepback on leading edge changes on spread/scope, then the given data should be accepted as average values.

The optimum of the sweepback of wing is, as a rule, very strong. Change in the evaluation criteria to 10/o gives the possibility to step back from χ_{opt} in all on 3-4°.

Optimum load on 1 m² of wing with takeoff. Load on 1 m² of wing with takeoff ($p_0 = G_0/S$) most strongly affects by weight of wing and power plant, and also by weight of fuel/propellant. Schematically this effect is shown in Fig. 4.5.

During increase p_0 , decreases the wing area, which leads in other constant/invariable parameters to a reduction/descent in its weight. At the same time with increase p_0 , it is necessary to increase the starting thrust-weight ratio of aircraft (\bar{P}_0) in order to fulfill requirements along the length of takeoff/run-up or length VPP (accelerate-stop distance). Increase \bar{P}_0 leads to the weight increase of power plant.

Effect p_0 by weight of fuel/propellant is more complicated, but relatively weak. Occurs optimum p_0 by fuel load, which corresponds to the minimum of its expenditure/consumption (point 1 in Fig. 4.5).

Thus, the contradictory effect p_0 on G_{HP} , $G_{c.y}$ and G_r leads to the existence of the optimum of load on 1 m² of wing.

Possibly analytical determination $(p_0)_{opt}$ in the first and second approach/approximations.

In the first approximation, the rational value of load on 1 m²

can be obtained from the considerations of similarity in dependence on takeoff weight. Really/actually, wing area is proportional to the square of the linear dimensions

$$S = a^2,$$

and takeoff weight in the first approximation, it is possible to consider proportional to the cube of the size/dimensions:

$$G_0 = b^3, \quad (4.3)$$

where $(a, b) = \text{const.}$

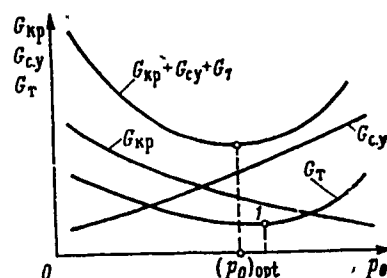


Fig. 4.5. The diagram of the emergence of optimum load on the m^2 of the wing:

1 - optimum according to per-kilometer expenditure/consumption.

Page 75.

Consequently,

$$p_0 = G_0 / S = cl. \quad (4.4)$$

Substituting from (4.3) $l = \sqrt{G_0 / b}$ in (4.4), we will obtain

$$p_0 = \xi G_0^{1/3}, \quad (4.5)$$

where $\xi = \text{const.}$

For subsonic nonmaneuverable aircraft coefficient $\xi \approx 10$, if G_0 in kg, and p_0 in kgf/m^2 (Fig. 4.6).

From the curve/graph of Fig. 4.6, it is evident that the curve $p_0 = 10 G_0^{1/3}$ very satisfactorily reflect/represents statistics $p_0 (G_0)$.

However, it does not explain the spread of values p_0 with $G_0 = \text{const}$. For example, with $G_0 = 43-44$ t there is range $p_0 = 315-505$ kgf/m². The spread of values p_0 with $G_0 = \text{const}$ can be explained, if to consider the dependence of load on 1 m² of wing on the conditions for takeoff and landing - assigned/prescribed length of VFP, c_v with breakaway and during landing. With $G_0 = \text{const}$ there are aircraft, designed on VFP of different length, different speed with landing approach and different degree of the high-lift device of wing ($c_{v\text{отр}}$ or $c_{v\text{нос}}$).

Dependence $p_0 (L_{\text{ВПП}}, c_{v\text{отр}})$ of transport aircraft is described, for example, by the following equation, obtained from the coincidence of the conditions of the interrupted and continued takeoff with given one by the climb angle ($\sin \theta_{\text{отк}}$) in the case of the failure of one engine [3]:

$$p_0 = k_1 g \rho_0 c_{v\text{отр}} (L_{\text{ВПП}} + L_{\text{КПБ}}) \left[\frac{1}{k_2} \left(\frac{1}{K_{\text{отр}}} + \sin \theta_{\text{отк}} \right) - \frac{f_{\text{КВМ}} + \mu}{k_1} \right] \text{ кгс/м}^2, \quad (4.6)$$

where $k_1 \approx 0.86-0.01$ m;

$k_2 \approx 0.83-0.017$ m;

m - bypass ratio of TVRD;

$K_{\text{отр}}$ - lift-drag ratio with breakaway;

$g = 9.81$; $\rho_0 = 0.114$ ^{with} $\rho_{\text{атм}} = +30^\circ \text{C}$, $\rho_{\text{атм}} = 730$ ^{mm. Hg} ~~mm-рт.ст.~~;

$L_{\text{КПБ}}$ - length of clear zone (250-400 m);

$f_{\text{кат}}$ - rolling friction coefficient of wheels;

μ - average/mean air resistance in the section of the final takeoff, in reference to takeoff weight ($\mu \approx 0.03-0.05$).

Values $\sin \theta_{\text{отк}}$ depend on a number of engines and are given by the technical requirements (see the Table).

| $n_{\text{дв}}$ | 2 | 3 | 4 |
|----------------------------|-------|-------|-------|
| $\sin \theta_{\text{отк}}$ | 0,025 | 0,027 | 0,030 |

If design conditions is takeoff run length with MSA, then formula for determining the load on 1 m^2 of wing takes the form

$$p_0 = g \rho_0 c_{\mu \text{отр}} L_{\text{разб}} (k_3 \bar{P}_0 - f_{\text{кат}} - \mu) \text{ кгс/м}^2, \quad (4.7)$$

where $k_3 \approx 0.92-0.95$.

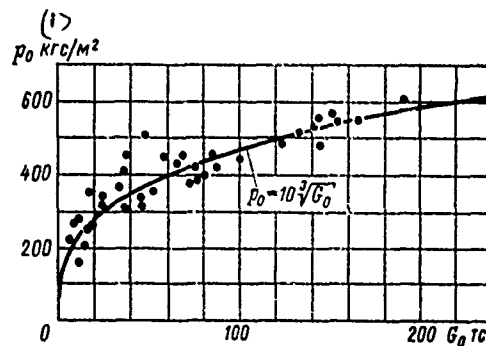


Fig. 4.6. Change of the load on the m^2 of wing in dependence on the takeoff weight of subsonic aircraft.

Key: (1). kgf/m^2 .

Page 76.

From the condition of given speed with landing approach or landing speed

$$p_0 = c_v \frac{\rho_0 V^2}{2k_4} \text{ kgf/m}^2. \quad (4.8)$$

Here c_v and V are taken with landing approach or during landing; k_4 - coefficient, that considers the decrease of landing weight in comparison with takeoff ($k_4 \leq 1$).

Formulas (4.6) - (4.8) can be used for determining the optimum (rational) load on 1 m^2 of wing in the second approach/approximation.

In third approach/approximation $(p_0)_{\text{opt}}$ it is determined taking

into account effect p_0 by weight of wing, power plant and fuel/propellant (see Fig. 4.5) and differs from the calculation of the second approach/approximation insignificantly (to 3-50/o), moreover the parameters whose increase leads to a gain in weight of wing (G_0, χ, λ), cause also increase $(p_0)_{opt}$ and, on the contrary, the parameters whose increase leads to the reduction of the weight of wing (\bar{c}_0, η), they contribute to an incidence/drop in value $(p_0)_{opt}$.

The optimum of load on 1 m^2 of wing is, as a rule, strong. Change in the evaluation criteria to 10/o of outer limit gives the possibility to step back from $(p_0)_{opt}$ in all to 4-60/o.

Optimum fineness ratio of fuselage. Fineness ratio of fuselage λ_ϕ , i.e. the ratio of the length of fuselage toward diameter on midsection 1 , affects, first of all, by weight of fuselage itself, and also by weight of chassis/landing gear, tail assembly and fuel/propellant. The discrepancy of effect λ_ϕ by weight of these components leads to formation $(\lambda_\phi)_{opt}$ (Fig. 4.7).

The graphical solution of the task of $(\lambda_\phi)_{opt}$ is conducted either at a constant volume of fuselage v_ϕ , when, for example, is known the quantity of fuel/propellant, which must be placed in fuselage or in permanent floor space $S_{\text{пол}}$ - in the case of transport or commercial airplanes when are known dimensions and composition of loads or

number of passengers and condition of their arrangement/position (level of comfort). In each of these cases, the diameter of fuselage, entering the weight formulas, is calculated differently:

from condition $v_\phi = \text{const}$

$$D_\phi = \sqrt[3]{\frac{v_\phi}{a\lambda_\phi}}; \quad (4.9)$$

from condition $S_{\text{пол}} = \text{const}$

$$D_\phi = \sqrt{\frac{101}{b\lambda_\phi}}. \quad (4.10)$$

Here (a, b) = const - coefficients.

Formulas for determining the over-all payload ratio of the fuselage and other aggregate/units, necessary for graphic determination $(\lambda_\phi)_{\text{opt}}$, are given in chapter XVI-XVIII.

In the first approximation, it is possible to utilize also formulas for $\bar{G}_m(\lambda_\phi)$ and $\bar{G}_{\text{on}}(\lambda_\phi)$, given below.

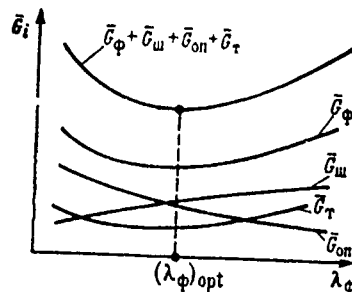


Fig. 4.7. Diagram of the formation of optimum fineness ratio of fuselage in of assigned/prescribed volume or assigned/prescribed floor space.

Page 77.

The over-all payload ratio of chassis/landing gear is connected with fineness ratio of fuselage with the dependence of the height/altitude of struts on λ_ϕ (Fig. 4.8)

$$\bar{G}_w \approx c_1 + c_2 \lambda_\phi - c_3 \lambda_\phi^2, \quad (4.11)$$

where c_1, c_2, c_3 - coefficients, which depend on designation/purpose and airplane design.

For example, for commercial airplanes:

$$c_1 = 0,024 - 0,026; c_2 = 0,0018 - 0,0019; c_3 = 3,5 \cdot 10^{-5} - 3,6 \cdot 10^{-5}.$$

The over-all payload ratio of tail assembly is the function of fineness ratio of fuselage in connection with the fact that the area of tail assembly is proportional to the length of the fuselage

$$\bar{G}_{on} \approx \frac{g_{on}}{p_0} \frac{c_4}{D_\phi \lambda_\phi}, \quad (4.12)$$

where g_{on} - weight of 1 m² of tail assembly in kgf/m²;

p_0 - load on 1 m² of wing;

$c_4=10-15$ - for transport aircraft.

The over-all payload ratio of fuel/propellant also depends on fineness ratio of fuselage (see Fig. 4.7) as a result of the dependence of the aerodynamic drag of fuselage and engine thrust on λ_ϕ . In subsonic zone, for example, the coefficient of the aerodynamic drag of fuselage in the first approximation, can be calculated from following the formula:

$$c_{x\phi} \approx 0,008\lambda_\phi + \frac{0,5}{\lambda_\phi^2}. \quad (4.13)$$

Investigations show that the optimum of fineness ratio of fuselage is not too acute/sharp. If we consider permissible a change in the evaluation criteria to 10% of outer limit, then appears the possibility to step back from $(\lambda_\phi)_{opt}$ to 1-1.5 (to 10-15%).

Optimum bypass ratio of TVRD. The bypass ratio of turbofan engines m , equal to the ratio of the air flow rate through the fan toward the air flow rate through the gas-producing part, affects, first of all, the specific hourly consumption and fuel load, by

aerodynamic pod drag (as a result - also by weight of fuel/propellant) and weight of TVRD themselves. Schematically this effect with $M < 1$ is shown in Fig. 4.9.

In the first approximation, it is possible to consider that for subsonic aircraft $m_{opt} = 4-6$, moreover with an increase in the flying range (or the over-all payload ratio of fuel/propellant) value m_{opt} grows.

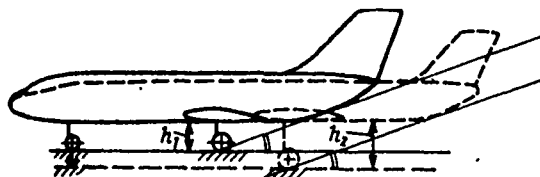


Fig. 4.8. Dependence of the height/altitude of chassis/landing gear on the length (elongation) of fuselage ($h_2 > h_1$).

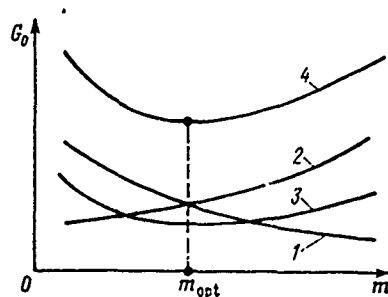


Fig. 4.9. Dependence of takeoff weight on bypass ratio of TVRD:

- 1 - during change in specific hourly consumption of fuel/propellant;
- 2 - during change in pod drag; 3 - during change in weight of engines; 4 - total change.

Page 78.

§ 2. Consecutive optimization of several parameters.

With the aid of computers it is possible to carry out a simultaneous optimization of a large quantity of parameters.

Without the application/use of computers, is possible the consecutive approximate optimization only of several parameters of aircraft. For this purpose is utilized the particular optimization of the parameters, examined in the preceding/previous paragraph.

At first is found the particular optimum of any from the parameters at other "frozen" parameters, known from statistics or from approximate computations. Then it is optimized by the second of the assigned parameters. In this case, is accepted the obtained earlier optimum value of the first parameter. The optimization of the third parameter is conducted at the values of the particular optima, found earlier. Thus are located the optima of the remaining parameters and characteristics.

This procedure of consecutive optimization is undoubtedly approximated, since after the particular optimization of each of the subsequent parameters the optima of the preceding/previous parameters must somewhat be changed (on the basis of the solution of the equation of weight balance, which connects all parameters and characteristics of aircraft). Therefore after the first cycle of calculations according to the optimization of the parameters, should be, generally speaking, calculated the second approach/approximation, during which are accepted the values of the parameters, obtained in the first approximation, (in the first cycle of calculations). It is

usually completely sufficiently two-three cycles of calculations, the optima of the parameters were stabilized at the specific level of values.

§ 3. Variational problems. Optimum distribution of wing chord ratios according to spread/scope.

During the solution of series of problems when it is required to find not the only outer limit of the parameter, but the optimum law of its change (i.e. to optimize functional), are applied the methods of the calculus of variations. As a classical example of the use of the calculus of variations serves the task of optimum trajectory, for example of the law of a change in the speed of aircraft in height/altitude during lift or reduction/descent. The optimum law $V(H)$ corresponds to the extremum of any functional - the fuel load or duration of ascent to base altitude, etc.

As another example of the use of an apparatus of the calculus of variations during the design of aircraft serves the determination of the optimum law of bending (twist) of median surface of the wing of supersonic aircraft for obtaining the maximum lift-drag ratio.

In many of these tasks, in final form it is possible to obtain with the specific assumptions of expression for optimum laws of a

change in the functions.

Let us examine as an example of the use of a classical method of variation problem calculus of the optimum law of a change in the wing chord ratios in spread/scope. As the subject of investigation, let us take subsonic aircraft with trapezoidal ($\chi \geq 0^\circ$) wing.

Task is placed as follows.

With some known parameters of wing and aircraft ($G_0, S, \lambda, \eta, D_\phi$) and assigned/prescribed flight conditions (V, H, L) to find the optimum law of a change in the wing chord ratios in spread/scope, i.e. to find $[\bar{c}_z(z)]_{opt}$.

Page 79.

Evaluation criteria of laws $\bar{c}_z(z)$ with $(V, H, L) = \text{const}$ will be incremental value in the takeoff weight. Optimum law $\bar{c}_z(z)$ corresponds to the minimum of increase in the takeoff weight or to the minimum of quite takeoff weight under given conditions. The variation character of the task in question escape/ensues from physical considerations.

In fact, if, for example, thickness ratio \bar{c}_z remains constant on spread/scope (with $S, \lambda, \eta = \text{const}$), then the weight of wing will be

less than in the case when \bar{c}_z decreases from one root to with $\bar{c}_0 = \text{const}$. However, the aerodynamic drag of "thick" wing with $\bar{c}_z = \bar{c}_0 = \text{const}$ is more than wing drag with decreasing value \bar{c}_z on spread/scope. It is also known that on the value of aerodynamic drag depends the takeoff weight of aircraft, i.e. there is a completely specific weight equivalent, resistance (see Chapter V), the change in the aerodynamic drag considerably more strongly affecting G_0 than the same in value change in the weight of wing. From these considerations it is evident that version $\bar{c}_z(z) = \text{const}$, apparently, will not be best.

On the other hand, if we intensely attenuate of wing on spread/scope, then aerodynamic resistance decreases, and the weight of wing, on the contrary, will increase with $\bar{c}_0 = \text{const}$. It is obvious, must exist the optimum law of change $\bar{c}_z(z)$, under which the takeoff weight will be minimum.

Let us compose the functional of task, on the basis of the calculation of wing to bending and the calculation of its profile drag when $M \leq M_{\text{крит}}$.

Air loads we consider proportional to chords. As a result of the smallness of the over-all payload ratios of the spar webs (conditional beam) and ribs, and also due to the smallness of the effect of dependence $\bar{c}_z(z)$ by weight of walls and ribs during the

solution of task we will not consider their weight. We consider also that material, working to the common/general/total bending of wing, together with walls forms the caisson, sufficient for the perception of the torsional moments.

Thus, during the compilation of functional let us consider only the weight of material, working to common/general/total bending wing, and also component of aerodynamic drag, which depends on \bar{c} , i.e. profile drag (when $M \leq M_{крит}$). The calculation gross weight wing or common/general/total aerodynamic resistance (taking into account inductive) is not necessary.

We will use communication/connection between a change in weight and aerodynamic wing drag, on one hand, and change in the takeoff weight - with another:

$$\Delta G_0 \approx \Delta G_{кр.нзг} \frac{\partial G_0}{\partial G_{кр.нзг}} + \Delta X_{кр.проф} \frac{\partial G_0}{\partial X_{кр.проф}} = \Delta G_{кр.нзг} x_G + \Delta X_{кр.проф} x_X,$$

where ΔG_0 - change in the takeoff weight of aircraft;

x_G - derivative of takeoff weight in connection with a change in the weight of aircraft components (see Chapter V), - weight of wing ($x_G = \partial G_0 / \partial G_l \approx \partial G_0 / \partial G_{кр}$);

x_X - the derivative of takeoff weight in connection with a change in the parasitic aerodynamic drag of aircraft components (see Chapter

V), - the profile drag of wing ($\alpha_{X_0} = \partial G_0 / \partial X_{\text{кр.проф}}$).

$$\Delta G_{\text{кр.изг}} = G_{\text{кр.изг} 0} - G_{\text{кр.изг} i}; \quad \Delta X_{\text{кр.проф}} = X_{\text{кр.проф} 0} - X_{\text{кр.проф} i};$$

$G_{\text{кр.изг} 0}$ and $X_{\text{кр.проф} 0}$ - weight of material, working to bending wing, and the profile drag of initial wing respectively;

$G_{\text{кр.изг} i}$ and $X_{\text{кр.проф} i}$ - the same for a wing, the differing from initial by dependence $\bar{c}(z)$.

Page 80.

In this case

$$(G_{\text{кр.изг} 0}, X_{\text{кр.проф} 0}) = \text{const.}$$

Let us designate

$$\alpha_G G_{\text{кр.изг} 0} = N_1 = \text{const}; \quad \alpha_{X_0} X_{\text{кр.проф} 0} = N_2 = \text{const.}$$

Then we have

$$-\Delta G_0 = \alpha_G G_{\text{кр.изг} i} + \alpha_{X_0} X_{\text{кр.проф} i} - N_1 - N_2. \quad (4.14)$$

The weight of the flanges of longeron/spars (panels), receiving the bending of wing, taking into account discharging will be [22]

$$G_{\text{кр.изг} i} = \frac{4\gamma\varphi}{\xi f \sigma_{\text{ср}}} \int_0^{\frac{l-D_\phi}{2}} \frac{M_z}{c_z} dz, \quad (4.15)$$

where c_z - the greatest profile thickness of wing in cross section z ;

λ - the specific gravity/weight of material;

ϕ - coefficient of discharging;

ϵ - coefficient, which considers the effective height/altitude of flanges (panels) in comparison with maximum;

f - coefficient, which considers the decrease of average/mean voltage/stress in comparison with maximum;

σ_{cp} - average/mean voltage/stress in upper and lower regiment (panel), determined from the relationship/ratio

$$\frac{1}{\sigma_{cp}} = \frac{1}{2} \left(\frac{1}{\sigma_p} + \frac{1}{\sigma_{cж}} \right).$$

Here σ_p - ultimate tension;

$\sigma_{cж}$ - allowable stress during compression.

In formula (4.15) M_z - the bending moment in the current cross section z :

$$M_z = \frac{G_0 n_p}{3} \frac{1}{l} \frac{2b_{\kappa} + b_z}{b_0 + b_{\kappa}} z^2, \quad (4.16)$$

where b_{κ} - end wing chord;

b_0 - wing chord along the axis of aircraft;

b_z - current wing chord;

z - coordinate on spread/scope from wing tip.

After placing M_z (4.16) into formula (4.15) and simple conversions from condition $\sigma_{cp}(z) = \text{const}$, we will obtain

$$G_{\text{кр.нзг } l} = \frac{4n_p \gamma \psi G_0}{3\xi f \sigma_{cp} l (\eta + 1)} \left[2 \int_0^{\frac{l-D_\phi}{2}} \frac{z^2 dz}{\bar{c}_z b_z} + \int_0^{\frac{l-D_\phi}{2}} \frac{z^2 dz}{\bar{c}_z b_k} \right]. \quad (4.17)$$

$$\text{Here } \bar{c}_z = \frac{c_z}{b_z}; \quad \eta = \frac{b_0}{b_k}.$$

Let us manufacture in (4.17) the replacement of variables, after designating $z' = dz/d\bar{c}_z$.

Page 81.

Then

$$G_{\text{кр.нзг } l} = N_3 \int_{\frac{\bar{c}_k}{\bar{c}_0}}^{\bar{c}_0} \left(\frac{2z^2 z'}{\bar{c}_z b_z} + \frac{1}{b_k} \frac{z^2 z'}{\bar{c}_z} \right) d\bar{c}_z, \quad (4.18)$$

where \bar{c}_0 - wing chord ratio along side fuselage ¹ without taking into account overflows;

$$N_3 = \frac{4n_p \gamma \psi G_0}{3\xi f \sigma_{cp} l (\eta + 1)} = \text{const.}$$

FOOTNOTE ¹. Is assumed that to the side of fuselage from the axle/axis of aircraft wing chord ratio it does not vary. ENDFOOTNOTE.

Here γ is accepted in kg/m^3 ; G_0 - in kg; σ_{cp} - in kgf/m^2 ; $\lambda = 0.85-0.90$; $f=0.80-0.85$.

The variable part of aerodynamic wing drag $X_{кр.проф}$, entering equation (4.14), can be found as follows:

$$X_{кр.проф} = c_{xp} S q. \quad (4.19)$$

For determining the coefficient of profile drag of wing when $M \leq M_{крит}$ we will use known formula A. A. Dorodnitsyn - L. G. Loytsyanskiy [15]

$$c_{xp} = 2c_f \eta_c n_1, \quad (4.20)$$

where c_f - coefficient of the friction of plate;

n_1 - empirical coefficient ($n_1 \approx 1.485$);

$$\eta_c = \eta_c(\bar{c}_z, \bar{x}_t);$$

\bar{x}_t - relative coordinate of the transfer/transition of laminar boundary layer into turbulent (in chord from leading edge/nose).

For values $\bar{x}_t = 0.25-0.30$:

$$\eta_c \approx 1 + 3,3\bar{c}_z.$$

Value $2c_f$ we take according to Schlichting [15]:

$$2c_f = \frac{0,91}{(\lg Re)^{2,58}}.$$

Substituting the value of coefficients into formula (4.20), we will obtain for wing $c_{\bar{c}_z} = \text{const}$

$$c_{xp} = \frac{1,35(1 + 3,3\bar{c}_z)}{(\lg Re)^{2,58}}.$$

If $\bar{c}_z = \bar{c}_z(z)$, then

$$c_{xp} = \frac{1,35 [1 + 3,3 (\bar{c}_z)_{cp}]}{(\lg Re)^{2,58}}, \quad (4.21)$$

where average/mean value \bar{c}_z is equal

$$(\bar{c}_z)_{cp} = \frac{2}{1 - D_\phi} \int_0^{1 - D_\phi} \bar{c}_z dz. \quad (4.22)$$

Substituting (4.21) and (4.22) in (4.19), after conversions we will obtain

$$X_{кр.проф. l} = Sq \left[\frac{8,9}{(\lg Re)^{2,58} (1 - D_\phi)} \int_{\frac{c_k}{c_0}}^{\frac{c_0}{c_k}} \bar{c}_z z' d\bar{c}_z \cdot \frac{1,35}{(\lg Re)^{2,58}} \right]. \quad (4.23)$$

Page 82.

Formula (4.14) taking into account (4.18) and (4.23) will take the form

$$\begin{aligned} -\Delta G_0 = & x_0 N_3 \int_{\frac{c_k}{c_0}}^{\frac{c_0}{c_k}} \left(\frac{2z^2 z'}{c_z b_z} + \frac{1}{b_k} \frac{z^2 z'}{c_z} \right) d\bar{c}_z + \\ & + x_{X_0} N_4 \int_{\frac{c_k}{c_0}}^{\frac{c_0}{c_k}} \bar{c}_z z' d\bar{c}_z + x_{X_0} N_5 - N_1 - N_2, \end{aligned} \quad (4.24)$$

where $N_4 = \frac{8,9 Sq}{(1 - D_\phi) (\lg Re)^{2,58}} = \text{const};$

$$N_5 = \frac{1,35 Sq}{(\lg Re)^{2,58}} = \text{const}.$$

It is combined firstly and secondly term in (4.24)

$$\begin{aligned} -\Delta G_0 = & \int_{\frac{c_k}{c_0}}^{\frac{c_0}{c_k}} \left[x_0 N_3 \left(\frac{2z^2 z'}{c_z b_z} + \frac{1}{b_k} \frac{z^2 z'}{c_z} \right) + x_{X_0} N_4 \bar{c}_z z' \right] d\bar{c}_z + \\ & + x_{X_0} N_5 - N_1 - N_2. \end{aligned} \quad (4.25)$$

Here $(x_{X_0}, N_5, N_1, N_2) = \text{const}.$

Finally the functional of this task takes the form

$$F = \frac{2x_0 N_3 z^2 z'}{\bar{c}_z b_z} + \frac{x_0 N_3}{b_k} \frac{z^2 z'}{\bar{c}_z} + x_{X_0} N_4 \bar{c}_z z'. \quad (4.26)$$

The condition of optimum $\bar{c}_z(z)$ is the equation of Euler [35], which in the expanded/scanned form is record/written as follows:

$$\frac{\partial^2 F}{(\partial z')^2} z'' + \frac{\partial^2 F}{\partial z' \partial z} z' + \frac{\partial^2 F}{\partial z' \partial \bar{c}_z} - \frac{\partial F}{\partial z} = 0. \quad (4.27)$$

After calculating the derivatives, provided for (4.27), we will obtain

$$-2x_0 N_3 \frac{z^2}{(\bar{c}_z)^2 b_z} - \frac{x_0 N_3}{b_k} \frac{z^2}{(\bar{c}_z)^2} + x_{X_0} N_4 = 0. \quad (4.28)$$

Since functional (4.26) is linear relative to first-order derivative z' , the solution (4.28) is degenerated and it takes the form of the usual algebraic equation where b_z - known function from z .

From (4.28) we have unknown optimum law $\bar{c}_z(z)$

$$(\bar{c}_z)_{opt} = z \sqrt{\frac{x_0 N_3}{x_{X_0} N_4} \left(\frac{2}{b_z} + \frac{1}{b_k} \right)}. \quad (4.29)$$

It is more convenient, however, to deal not concerning the absolute values of coordinate z , but concerning relative ones

$$\bar{z} = \frac{z}{\frac{1 - D_\phi}{2}}.$$

Page 83.

Let us replace in formula (4.29) the appropriate. Besides in

addition to this, let us take b_k and b_z the form:

$$b_k = \frac{2}{\eta+1} \frac{S}{l} = \frac{2}{\eta+1} \sqrt{\frac{G_0}{\rho_0 \lambda}}; \quad b_z = \frac{2}{\eta+1} \sqrt{\frac{G_0}{\rho_0 \lambda}} [1 + (\eta-1)\bar{z}],$$

and in coefficient of N_6 let us take air density according to the formula of Vetchinkin V. P.

$$\rho = \rho_0 \frac{20-H}{20+H},$$

where H in km.

Then solution (4.29) after conversions will take the form

$$(\bar{c}_z)_{opt} = \frac{\bar{z}}{2} \left(\sqrt{\frac{\lambda G_0}{\rho_0}} - D_\phi \right) \sqrt{N_6 \left[\frac{2}{1 + (\eta-1)\bar{z}} + 1 \right]}, \quad (4.30)$$

where

$$N_6 = \frac{8 \cdot 10^{-3} \rho_0 (20+H)}{V^2 (20-H)} \left(\frac{x_0}{x_{x_0}} \right) \sqrt{\frac{\lambda}{G_0}} \left(1 - D_\phi \sqrt{\frac{\rho_0}{\lambda G_0}} \right) [\lg \text{Re}]^{2.58}. \quad (4.31)$$

In formulas (4.30) and (4.31) spread/scope $l = \sqrt{\frac{\lambda G_0}{\rho_0}}$;

$$G_0 - \text{in kgf}, \quad \rho_0 - \text{in kgf/m}^2, \quad H - \text{in km}, \quad V - \text{in m/s}, \quad D_\phi - \text{in } \frac{1}{\text{m}}.$$

In the limits of one class of aircraft ($\lg \text{Re}$) ~~2.58~~ it changes insignificantly and it is possible to take as its equal to: 180 - for the aircraft of short distance; 200 - for the aircraft of average/mean distance; 220 - for the aircraft of large distance.

With $\bar{z}=1$ we have $(\bar{c}_0)_{opt}$:

$$(\bar{c})_{\bar{z}=1} = [\bar{c}_0]_{opt} = \frac{1}{2} \left(\sqrt{\frac{\lambda G_0}{\rho_0}} - D_\phi \right) \sqrt{N_6 \left(\frac{2}{\eta} + 1 \right)}. \quad (4.32)$$

From formulas (4.32) and (4.31) it is evident that with increase ϕ , κ_0 , H, λ the optimum wing chord ratio in root (along side fuselage) increases; with increase V, κ_{x_0} , D_ϕ values $(\bar{c}_0)_{opt}$ decrease; with increase ρ_0 value $(\bar{c}_0)_{opt}$ decrease; with increase G_0 in value $(\bar{c}_0)_{opt}$ they increase.

Thus, if an increase in the parameter leads to an increase in the weight of wing, then this increase it leads also to increase of $(\bar{c}_0)_{opt}$ and vice versa.

It must be noted that solution (4.30) does not depend on the sweepback of wing, since area S when $(b, \bar{z}) = const$ does not depend on x if chords are taken along flow.

The characteristic feature of the obtained solution is the fact that with $\bar{z}=0$ (at wing tip) the optimum thickness ratio also must be equal to zero. This is explained by the fact that the bending moment at wing tip is equal to zero. By the way, if we consider not only bending strength of wing, but also for torsion, then the indicated special feature/peculiarity of the solution will not be changed, since the torsional moment at wing tip is also equal to zero.

Virtually, however, it cannot be made $\bar{c}_{z=0}=0$, since will not be reached the necessary rigidity of end cross sections for the torsion (is feasible the reversal of ailerons and wing flutter). Besides in addition to this, when $\bar{c} \leq 0.08$ the lift effectiveness of airfoil/profiles sharply fall, hinders the high-lift device of wing, appear other structural/design difficulties. Taking into account the

satisfaction of these all requirements is selected value \bar{c}_k .

Page 84.

Thus, formula (4.30) can be virtually used only in root wing sections, to 30-35% of spread/scope, and for the remaining part of the wing should be accepted either $\bar{c}_z = \bar{c}_k = 0.08-0.09 = \text{const}$ or law, close to linear 1 , in this case, at wing tip, it is necessary to ensure $\bar{c}_k = 0.08-0.09$.

FOOTNOTE 1 . Since it is necessary to consider the required volume of wing for the arrangement/position of fuel/propellant. ENDFOOTNOTE.

Examples of theoretical optimum law $\bar{c}_z(\bar{z})$, the constructed according to formula (4.30), and practical optimum law where in end and wing center sections $\bar{c}_z = \bar{c}_k = \text{const}$, they are given in Fig. 4.10.

Besides the examined above case, when average/mean design stresses $\sigma_{cp} = \text{const}$ on the wingspan, is of also interest the case, characteristic for the sweptback wings when $\frac{(\sigma_{cp})_z}{\epsilon_z} = \text{const} = d$ on spread/scope. The solution in this case does not differ in principle from (4.29)-(4.30) and it takes the form

$$(\bar{c}_z)_{opt} = \sqrt[3]{\frac{2z^2}{b_z} \left(\frac{2}{b_z} + \frac{1}{b_k} \right) \frac{E_B}{x_{X_0} N_4}}, \quad (4.33)$$

where $E_B = \frac{4\gamma\varphi G_0 n_p x_G}{3\epsilon_f d l (\eta + 1)} = \text{const}$;

$$x_{X_0} N_4 = \text{const}.$$

DOC = 79052104

PAGE ~~42~~ 154

Comparison shows that under condition $(\sigma_{cp})_z/c_z = \text{const}$ optimum values \bar{c}_z on the average on (5-7)% are more than under condition $(\sigma_{cp})_z = \text{const}$.

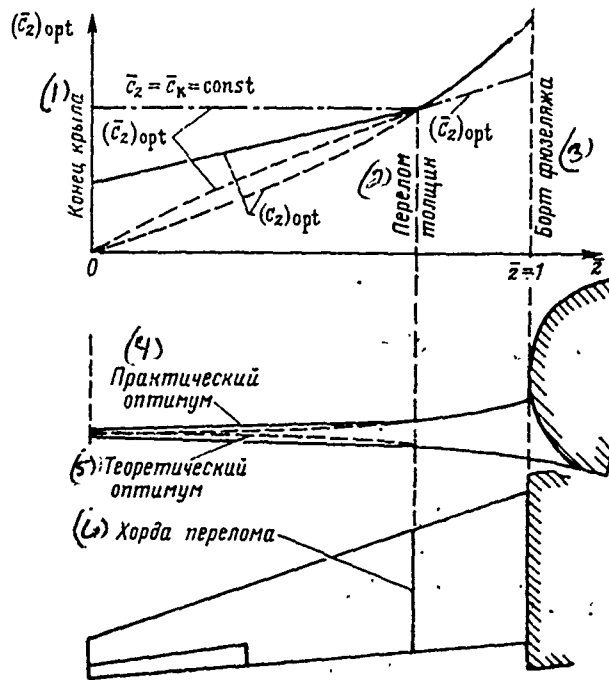


Fig. 4.10. Diagram of a change in the optimum values of the relative and greatest absolute thickness of the tapered wing in the spread/scope:

----- theoretical optimum taking into account the bending strength of wing;

———— practical optimum taking into account the rigidity of wing to torsion and bending.

Key: (1). Wing tip. (2). Break of thicknesses. (3). Side of fuselage. (4). Practical optimum. (5). Theoretical optimum. (6). Chord of

break.

Page 85.

Thus, the examined variational problem gives the possibility to base to theoretically and obtain virtually (with correction for the guarantee of rigidity of wing) the optimum law of a change in the wing chord ratio in spread/scope.

Analogous variational problems can be solved and in connection with supersonic aircraft during the determination of optimum laws $\bar{c}_z(z)$ of wing, sectional areas of fuselage along the length and the like taking into account a change in the aerodynamic, weight and rigid characteristics of aggregate/units with some assigned magnitudes, for example, with assigned/prescribed volume for the arrangement/position of fuel/propellant.

Page 97.

Section II.

SELECTION OF SCHEME, POWER PLANT AND BASIC PARAMETERS OF AIRCRAFT.

Chapter VI.

AIRPLANE DESIGN. ANALYSIS AND SELECTION OF DIAGRAM.

Airplane design is determined by relative position, form and quantity of basic aggregate/units of aircraft - wing, fuselage, tail assembly and engines.

By a quantity of aggregate/units, are distinguished following of the diagram: biplane and monoplane (Fig. 6.1a, b); with one or two fuselages (Fig. 6.1c, d); with one or two surfaces of horizontal or vertical tail assembly (Fig. 6.1e); with one or several engines. Are possible airplane designs without wing (the "flying fuselage")¹, without fuselage ("the flying wing"), and also without horizontal

tail assembly ("bobtailed aircraft").

FOOTNOTE 1. At the speeds, which correspond $M \gg 5$, the fuselage little is inferior to wing according to lift effectiveness. At low speeds the lift can be created by the thrust of special engines.

ENDFOOTNOTE.

Page 98.

These diagrams are given in Fig. 6.1f, g, n, o, t.

The form of aggregate/units can change in flight (transformed diagrams, Fig. 6.1h, i, j).

Let us incidentally note that the aircraft, designed by diagram "bobtailed aircraft", in the world was for the first time created in our country (aircraft BiCh-3, 1926, designer E. I. Cheranovskiy).

The characteristic feature of diagram is created by wing planform - aircraft with direct/straight, swept, delta wings, with the wing of variable on the spread/scope of sweepback (Fig. 6.1k-m).

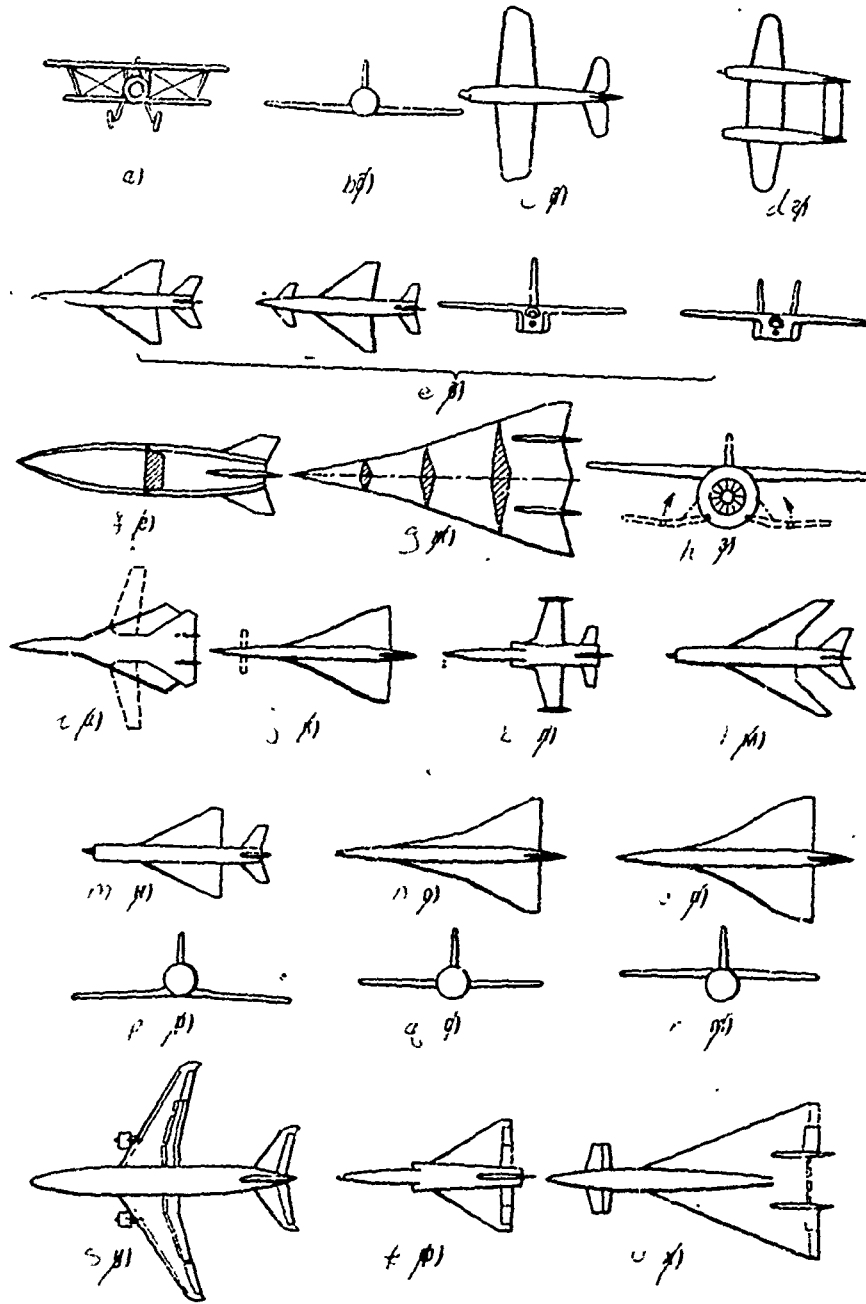


Fig. 6.1. Standard airplane designs.

Page 99.

The distinctive special feature/peculiarity of the diagram creates wing arrangement relative to fuselage on height/altitude (Fig. 6.1p, q, r) - low wing monoplane, midwing monoplane, high wing monoplane.

Most important differences according to aerodynamic, weight and operating characteristics creates mutual wing arrangement and horizontal tail assembly along the length of fuselage - diagram normal, or classical (Fig. 6.1s), "bobtailed aircraft" (Fig. 6.1t) ¹ and the diagram of "weft" (Fig. 6.1u).

FOOTNOTE ¹. The role of horizontal tail assembly here perform elevons on rear the lump of wing. ENDFOOTNOTE.

Less important sign/criterion of diagram is the arrangement of engines on the aircraft (see § 4).

How to explain this diversity of diagrams? Basic reason - in the diversity of requirements for aircraft, in the continuous development of the possibilities of their satisfaction. Each of the diagrams reflects designer's tendency to in the best way satisfy operational requirements in this state of development of aviation and technology.

This tendency it leads sometimes to the solutions, which do not justify itself in practice. As an example of this solution can serve the diagram of the unsymmetric aircraft BV-141 (firm Blom and Foss), constructed in Germany into 1938 (Fig. 6.2).

By interesting in this diagram is represented the idea to radically improve pilot's survey/coverage on single-engine reconnaissance aircraft.

From entire diversity of the questions, connected with the selection of airplane design, let us examine further following most important and actual/urgent ones:

- analysis and selection of the diagram of supersonic aircraft;
- analysis and selection of the diagram of subsonic aircraft;
- airplane design to by the wing of the variable in flight sweepback;
- arrangement of engines on aircraft.

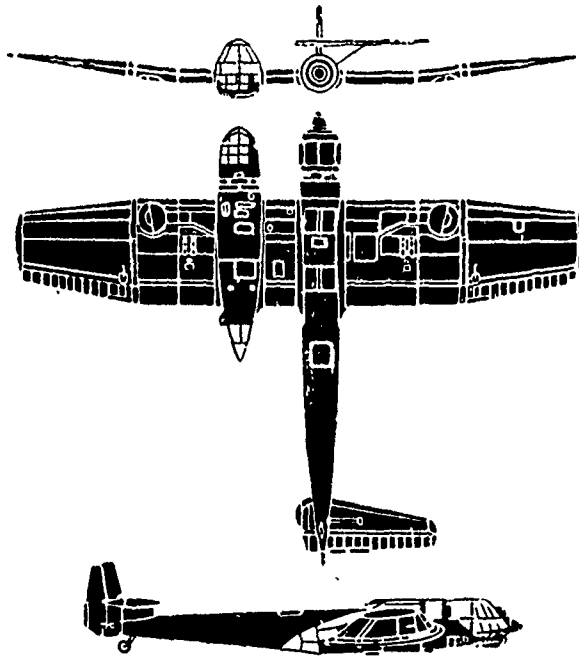


Fig. 6.2. Unsymmetric aircraft BV-141 of firm Blom and Foss. Basic data: $G_0=4400$ kg; $G_{\text{нyчr}}=2670$ kg; $S=53.1$ m²; $l=17.46$ m; $v_{\text{max}}=450$ km/h; $v_{\text{кpеtиc}}=350$ km/h; motor BMW-801; $N_0=1600$ - hp.

Page 100.

The formulation of the problem of the selection of diagram and parameters of aircraft is examined in § 1 of chapter III. Let us recall only that during the assigned/prescribed operational requirements and other limitations, placed by the stress standards, rigidity and operation, it is necessary among entire diversity of

diagrams and parameters of aircraft to select such, which they would lead to the outer limit of evaluation criteria of aircraft. As evaluation criteria, are considered: the cost-effectiveness/efficiency of operation (commercial airplanes), combat effectiveness or cost/value of accomplishing operation. The approximate criterion is the value of takeoff weight. The best airplane design of any designation/purpose in the first approximation, corresponds to the minimum of takeoff weight¹ during all assigned/prescribed limitations [4, 25].

FOOTNOTE¹. During more detailed comparison should be considered also the effect of diagram on manufacturability and the maintainability of construction/design, convenience in the operation and comfort of the crew and passengers. ENDFOOTNOTE.

Among many diagrams, at first are take/selected (on the basis of precomputations and experiment) several most interesting ones, which compete. Then they are in detail investigated quantitatively (on evaluation criteria) and it is qualitative (according to the sign/criteria, which did not enter the algorithm of optimization).

§ 1. Analysis and selection of the diagram of supersonic aircraft.

Let us examine nonmaneuverable long-range aircraft with the

fixed/recorded wing ², and also aircraft of maneuverable class.

FOOTNOTE ². Airplane design with the variable sweepback of wing is examined in § 3 of this chapter. ENDFOOTNOTE.

Let us consider that the aircraft have a usual running take-off and running landing ³.

FOOTNOTE ³. The diagrams of VTOL aircraft and STOL are examined in chapter X, the diagram air space aircraft - in chapter XI.

ENDFOOTNOTE.

When selecting of the diagram of nonmaneuverable long-range aircraft, considerable attention is given to the value of maximum lift-drag ratio K_{max} in cruise, since from it directly depends either flying range with known relative all fuel/propellants ($\bar{G}_T = \text{const}$), or value \bar{G}_T and G_0 with $L = \text{const}$.

Maximum lift-drag ratio can be increased, for example, due to the decrease of the midsections or the noncarrying parts, decrease of the washed surface of aircraft, and also by a reduction/descent in the so-called trim drag. The first two methods do not require special explanations. Let us pause in more detail at the dependence of lift-drag ratio on trim drag, which depends substantially on airplane

design.

Let us examine the classical (normal) diagram and the diagram of "weft".

From the trimmed conditions of aircraft, we will obtain:

- for a classical diagram (Fig. 6.3a)

$$\frac{Y_{r.o}}{Y_{kp}} = - \frac{x_n - x_T}{x_{r.o} - x_T};$$

- for the diagram of "weft" (Fig. 6.3b)

$$\frac{Y_{r.o}}{Y_{kp}} = - \frac{x_n - x_T}{x_{r.o} + x_T}.$$

Assuming that $x_n - x_T = \Delta x$,

$x_{r.o} - x_T = L_{r.o}$ (for a classical diagram);

$x_{r.o} + x_T = L_{r.o}$ (for the diagram of "weft"), and relating values Δx and $L_{r.o}$ to b_{CAx} , we will obtain

$$\frac{Y_{r.o}}{Y_{kp}} = \frac{\overline{\Delta x}}{\overline{L_{r.o}}}.$$

Page 101.

At supersonic speeds, as is known, the airfoil center of pressure is considerably moved back/ago and $\overline{\Delta x}$ it increases, and relation $Y_{r.o}/Y_{kp}$ can reach value by 0.15-0.20 (in subsonic

conditions/mode 0.03-0.05). Hence it follows that the balance in supersonic conditions/modes leads to an essential increase in the resistance, connected with horizontal tail lift.

The total drag of aircraft taking into account balance is equal

$$X = X_0 + X_{I_{кр}} + X_{балан} = X_0 + X_{I_{кр}} + X_{I_{г.о.}}$$

After dividing both parts of the equation to qS [we consider that

$q_{кр} = q_{г.о.}$ and $(c_y^a)_{кр} = (c_y^a)_{г.о.}$], we will obtain

$$c_x = c_{x_0} + c_{x_{I_{кр}}} + c_{x_{балан}} = c_{x_0} + c_{x_{I_{кр}}} + c_{x_{I_{г.о.}}} \bar{S}_{г.о.},$$

or, since for classical diagram $c_y = c_{y_{кр}} + c_{y_{г.о.}} \bar{S}_{г.о.}$ and for the diagram

of "weft" $c_y = c_{y_{кр}} - c_{y_{г.о.}} \bar{S}_{г.о.}$, that respectively

$$c_x = c_{x_0} + D_0 (c_{y_{кр}} + c_{y_{г.о.}} \bar{S}_{г.о.})^2 + D_0 c_{y_{г.о.}}^2 \bar{S}_{г.о.}; \quad (6.1)$$

$$c_x = c_{x_0} + D_0 (c_{y_{кр}} - c_{y_{г.о.}} \bar{S}_{г.о.})^2 + D_0 c_{y_{г.о.}}^2 \bar{S}_{г.о.}; \quad (6.1')$$

where $D_0 = 1/c_y^a$.

From Fig. 6.3 it follows that

$$(c_{y_{кр}} + c_{y_{г.о.}} \bar{S}_{г.о.}) \bar{\Delta x} = c_{y_{г.о.}} \bar{L}_{г.о.} \bar{S}_{г.о.} \text{ -- для классической схемы;} \quad (1)$$

$$(c_{y_{кр}} - c_{y_{г.о.}} \bar{S}_{г.о.}) \bar{\Delta x} = c_{y_{г.о.}} \bar{L}_{г.о.} \bar{S}_{г.о.} \text{ -- для схемы "утка".} \quad (2)$$

Key: (1). for a classical diagram. (2). for diagram of "weft".

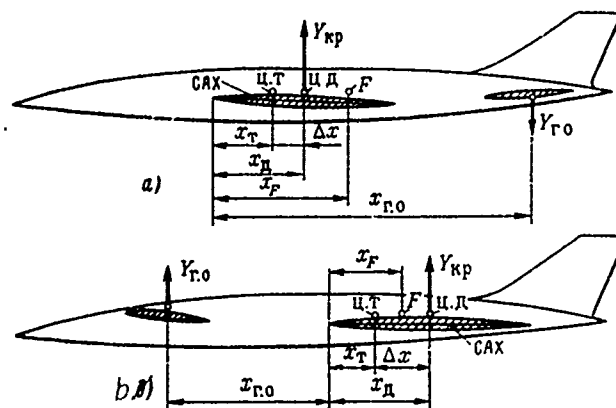


Fig. 6.3. The longitudinal balance of the aircraft of classical (normal) diagram (a) and diagram of "weft" (b): F - focus of aircraft.

Page 102.

From these expressions we will obtain

$$c_{y_{r.o.}} = \frac{c_{y_{кр}} \bar{\Delta x}}{\bar{S}_{r.o.} (\bar{L}_{r.o.} \mp \bar{\Delta x})}$$

For a classical diagram in denominator, is taken minus, for the diagram of "weft" - plus.

Let us substitute value $c_{y_{r.o.}}$ in (6.1) and (6.1'). After conversion we will obtain for the classical diagram

$$c_x = c_{x_0} + D_0 c_{y_{кр}}^2 \left[1 + \frac{\bar{\Delta x}^2}{(\bar{L}_{r.o.} - \bar{\Delta x})^2} \left(1 + \frac{1}{\bar{S}_{r.o.}} \right) + \frac{2\bar{\Delta x}}{\bar{L}_{r.o.} - \bar{\Delta x}} \right]; \quad (6.2)$$

for the diagram of "weft"

$$c_x = c_{x_0} + D_0 c_{y_{kp}}^2 \left[1 + \frac{\bar{\Delta x}^2}{(\bar{L}_{r.0} + \bar{\Delta x})^2} \left(1 + \frac{1}{\bar{S}_{r.0}} \right) - \frac{2\bar{\Delta x}}{\bar{L}_{r.0} + \bar{\Delta x}} \right]. \quad (6.2')$$

Thus, $c_x = c_{x_0} + D_{0\text{бал}} c_{y_{kp}}^2$, where $D_{0\text{бал}} = (1 + \omega) D_0$, moreover ω - coefficient, which considers the effect of balance on the resistance of aircraft. For the classical diagram

$$\omega = \frac{\bar{\Delta x}^2}{(\bar{L}_{r.0} - \bar{\Delta x})^2} \left(1 + \frac{1}{\bar{S}_{r.0}} \right) + 2 \frac{\bar{\Delta x}}{\bar{L}_{r.0} - \bar{\Delta x}}; \quad (6.3)$$

for the diagram of "weft"

$$\omega = \frac{\bar{\Delta x}^2}{(\bar{L}_{r.0} + \bar{\Delta x})^2} \left(1 + \frac{1}{\bar{S}_{r.0}} \right) - 2 \frac{\bar{\Delta x}}{\bar{L}_{r.0} + \bar{\Delta x}}. \quad (6.3')$$

Maximum aerodynamic aircraft quality/fineness ratio, as is known, it is equal

$$K_{\max} = \frac{1}{2} \sqrt{\frac{1}{c_{x_0} D_0}}.$$

Taking into account the trim drag

$$K_{\max} = \frac{1}{2} \sqrt{\frac{1}{c_{x_0} D_{0\text{бал}}}},$$

or

$$K_{\max} = \frac{1}{2} \sqrt{\frac{1}{c_{x_0} D_0 (1 + \omega)}}.$$

The given above formulas make it possible to draw a conclusion about the considerable effect of value ω on aerodynamics of aircraft. Is than more ω , the greater the trim drag and the greater the loss of lift-drag ratio.

During the analysis of trim drag, it is convenient to utilize a concept of the focus of aircraft. As is known, $\bar{x}_F - \bar{x}_T = -m_z^{c_y}$, where $m_z^{c_y}$ - derivative of the coefficient of the pitching moment of aircraft in c_y (reserve of longitudinal static stability);

$$\bar{x}_F = x_F / b_{CAX}; \quad \bar{x}_T = x_T / b_{CAX}$$

Page 103.

The greater the margin of stability $m_z^{c_y}$, the more and the balancing losses of lift-drag ratio, since increases

$$\bar{x}_F - \bar{x}_T = (\Delta x \pm \bar{S}_{r,0} \bar{L}_{r,0}) \frac{1}{1 + \bar{S}_{r,0}} \quad (\text{here in brackets plus sign it corresponds to normal diagram, and minus - to a diagram of "weft").$$

For the stabilization of supersonic aircraft in subsonic conditions/mode value $m_z^{c_y}$ is selected in limits 0.02-0.05, but in supersonic conditions/modes as a result of the movement of focus, back/ago longitudinal static stability considerably increases (if we do not take the special measures, indicated below), especially on the aircraft of normal diagram. Aircraft "bobtailed aircraft" occupies certain mid-position according to the greatest shift/shear of focus back/ago upon transfer from ONE $M < 1$ to $M > 1$ (Fig. 6.4). For the aircraft of this diagram with flat/plane wing (the flat surface of

wing chords) $\bar{x}_F \approx 0,35$ and $\bar{x}_T \approx 0,3$ with $M < 1$, but with $M \gg 1$ $\bar{x}_F \approx 0,5$. Thus, "bobtailed aircraft" with flat/plane wing has with $M \gg 1$

$$m_z^{cy} = -0,15, \quad \text{if } \bar{x}_T = 0,30.$$

Effect m_z^{cy} on relative maximum lift-drag ratio $\bar{K}_{\max} = K_{\max} / (K_{\max})_{m_z^{cy}=0}$ of the aircraft of two diagrams is shown in Fig. 6.5. These curve/graps are constructed at typical values \bar{L}_{r0} and \bar{S}_{r0} the aircraft of normal diagram and diagram of "weft". It is evident that the aircraft of classical diagram (with flat/plane wing) has the large losses of maximum aerodynamic quality, than the aircraft of the diagram of "weft".

This fact brought recently to thought about the advisability of applying the diagram of "weft" for heavy long-range aircraft (for example, the aircraft XB-70 "Valkyrie", USA). Then it was explained that losses K_{\max} from balance can be substantially decreased or even eliminated for the diagrams in question, if we use the following constructive solutions:

1) the "floating" or removed with $M < 1$ horizontal tail assembly in forepart/nose aircraft component.

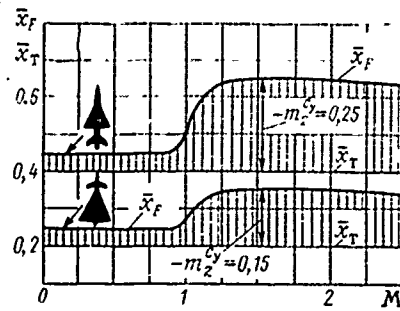


Fig. 6.4

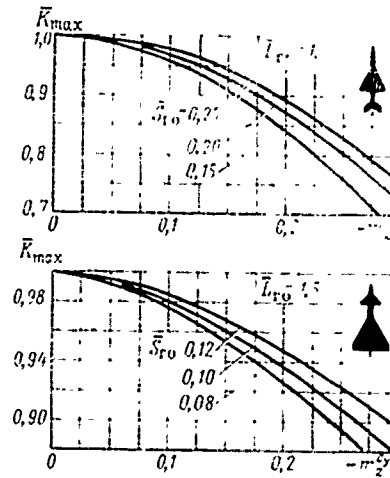


Fig. 6.5

Fig. 6.4. Change in the longitudinal stability factor of the aircraft of normal diagram and diagram of "weft" (wing flat/plane).

Fig. 6.5. Dependence of relative lift-drag ratio on degree of longitudinal static stability (wing flat/plane):

$$\bar{K}_{max} = K_{max}(K_{max})_{m_z^y = 0}$$

Page 104.

At subsonic speed this tail assembly either is removed into fuselage or as weathervane, is installed at zero or certain permanent positive angle of attack and does not affect, thus, to the position of the focus of aircraft. The aircraft of the diagram of "weft", for example, with this tail assembly with $M < 1$ and $\alpha_{r,0} = 0^\circ$ ($Y_{r,0} = 0$) is,

actually, "bobtailed aircraft". At supersonic speed the tail assembly is jammed at the specific angle of attack and it displaces the focus of aircraft forward to value $\Delta \bar{x}_F = \bar{S}_{r.o} \bar{L}_{r.o}$ (here $\bar{S}_{r.o}$ and $\bar{L}_{r.o}$ are related to tail assembly - destabilizer). In this case $m_z^{c_y}$ with $M < 1$ and with $M \gg 1$ it can have the identical values of order 0.03-0.05, that also requires (Fig. 6.6);

2) root overflows on wing (Fig. 6.7) before the center of gravity of aircraft. With $M > 1$ the effectiveness of overflows due to increase (c_y^2 наплыв) increases. Therefore with an increase in Mach number of flight, the focus of aircraft is moved forward and with the calculated Mach number the longitudinal stability factor decreases to acceptable size/dimensions;

3) the strain of median surface of wing (surface of chords). Wing seemingly is adjusted to basic conditions/mode (c_y, M) of the flight, by which the losses to balance are brought to the minimum (Fig. 6.8);

4) the deflect/diverted with $M \gg 1$ ends of the swept or delta wing; wing tips are converted into supplementary fins and do not participate in lift formation.

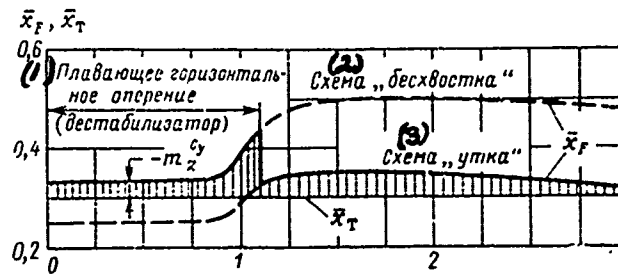


Fig. 6.6. Application/use of the floating horizontal tail assembly on the aircraft of the diagram of "weft".

Key: (1). Floating horizontal tail assembly (destabilizer). (2). Diagram "bobtailed aircraft". (3). Diagram, "weft".

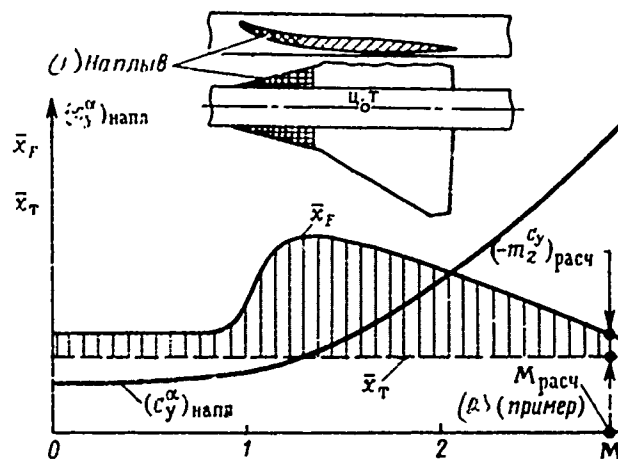


Fig. 6.7. Application/use of overflow in root of wing.

Key: (1). Overflow. (2). example.

Page 105.

The focus of aircraft with this operation is shift/sheared forward to value $\bar{\Delta x}_F = S_R \bar{L}_R$ where S_R - the relation to the area of the deflect/diverted part of the wing toward gross wing area;

$\bar{L}_R = L_R / b_{CAX}$; L_R - distance from the center of gravity of aircraft to the center of pressure of the deflect/diverted part of the wing (along the axis of aircraft).

All examined higher methods of decreasing the longitudinal stability factor of aircraft at supersonic speed the basic during limitation displacements of focus with the aid of an additional increase (creation) in the lift before the center of gravity of aircraft or with the aid of its decrease after the center of gravity. Besides these methods, it is possible to utilize some more, in principle different from preceding/previous, given in p. 5;

5) the displacement back/ago of the center of gravity of aircraft (following by the displacement of focus) via the pumping of fuel/propellant from front/leading tanks into rear balancing tank. This solution is utilized usually in combination with those enumerated above. Its deficiency/lack lies in the fact that for the rapid pumping of fuel/propellant are required the very powerful/thick (usually - several ten kilowatts) and heavy pumps, and also the fuel

lines of large productivity. When after the pumping of fuel/propellant it is back/ago necessary to specially decrease the flight speed prior to $M < 1$, it is necessary to apply the emergency discharge of the transferred fuel/propellant to avoid the pitch instability in subsonic zone (Fig. 6.9).

The presented methods allow to a greater or lesser extent to solve the problem of lift-drag ratio taking into account balance. For the diagrams of "weft" and "bootailed aircraft" it is solved more successfully, for a normal diagram - it is less successfully in connection with the large snift/sneer of the focus of aircraft back/ago.

Let us examine now three diagrams of nonmaneuverable supersonic aircraft ("weft", "tailless" and normal) from other point of view.

On the safety of operation, the aircraft of the diagram of "weft" is inferior to the aircraft of other diagrams. Reasons for this following.

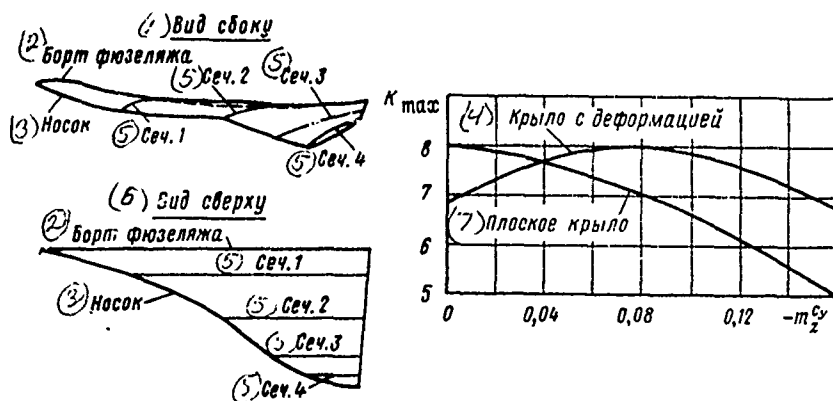


Fig. 6.8. The effect of the strain of the wing of the aircraft of diagram "bobtailed aircraft" on the maximum lift-drag ratio of supersonic aircraft with $M=2$ (cross sections 1-4 and the "side of fuselage" at the sight assembly are average/mean lines of the corresponding wing profiles).

Key: (1). Side view. (2). Side of fuselage. (3). Leading edge/nose. (4). Wing with strain. (5). Section. (6). Plan view. (7). Flat/plane wing.

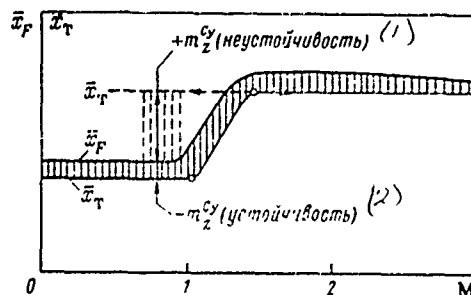


Fig. 6.9. Displacement of center of gravity of aircraft back/ago.

Key: (1). instability. (2). stability.

Page 106.

1. From condition $(M_z)_{\text{des r.o}} = (M_z)_{i.o}$ for diagram of "weft" we have:
if $m_z^c \geq \frac{(\bar{S}_{r.o})^2 \bar{L}_{i.o}}{1 - (\bar{S}_{i.o})^2}$, then $c_{y_{i.o}} \geq c_{y_{sp}}$.

At typical values $\bar{S}_{r.o} \leq 0,15$, $\bar{L}_{r.o} \leq 2$ we have $c_{y_{r.o}} \geq c_{y_{sp}}$ if $-m_z^c > 0,046$. Usually in the diagram of "weft" when $M < 1 - m_z^c > 0,046$. Therefore loss of lift at high angles of attack begins, as a rule, first on tail assembly ($c_{y_{r.o}} > c_{y_{sp}}$). In this case $Y_{sp} < G$ (at equilibrium $Y_{i.p} = G - Y_{r.o}$) and the aircraft of the diagram of "weft" together with peck (torque/moment $Y_{i.p}$ to dive relative to the center of gravity of aircraft, see Fig. 6.3) it loses altitude (it sags).

2. Spinning properties of aircraft of diagram of "weft" are worse than aircraft of other diagrams.

3. Aircraft of diagram of "weft" possesses insufficient dynamic stability (it is difficult to extinguish short-period vibrations).

It would seem that wing area on this aircraft it is possible to select less than on the aircraft of other diagrams, since horizontal tail assembly creates positive lift. However, of this advantage the

aircraft of the diagram of "weft" is deprived. The fact is that the possibility of the high-lift device of wing is here limited by the trimmed conditions and flow separation from tail assembly. Moreover, the lift of wing as a result of downwash from tail assembly decreases by 10-15%. Therefore acceptable takeoff and landing characteristics of the aircraft of the diagram of "weft" are achieved by an increase in the wing area ¹.

FOOTNOTE ¹. Is possible also the "super-mechanization/high-lift device" of horizontal tail assembly (UPS). However, in this case, grow/rises taper after tail assembly, falls Y_{np} , it appears stability problem of flow at the engine inlet, etc. ENDFOOTNOTE.

In any case of the gain of area and weight of wing in comparison with normal diagram, this diagram does not give.

Aircraft "bobtailed aircraft" (and also the "flying wing") has following of the advantage:

- is lesser than the loss of lift-drag ratio from balance with $M > 1.2$ than in the aircraft of normal diagram;

- the smaller cost/value of construction/design (to 10-15%) due to the absence of horizontal tail assembly as independent

aggregate/unit.

It should be noted that generally horizontal tail assembly it is necessary to nonmaneuverable supersonic aircraft mainly at high angles of attack (takeoff, landing, output/yield from disruption/separation, etc.). In the cruising flight of the function of horizontal tail assembly successfully they can fulfill flaps (in the diagram "bobtailed aircraft" - elevons).

However, during takeoff and landing, of diagram "bobtailed aircraft" is inferior to the aircraft of normal diagram, since the wing of tailless aircraft does not allow/assume mechanization/high-lift device ².

FOOTNOTE ². For the longitudinal balance of aircraft elevons it is necessary to deflect/divert upward, to the side, opposite to the flap deflection. ENDFOOTNOTE.

For an improvement in the takeoff and landing characteristics of the aircraft of diagram "bobtailed aircraft" ($L_{\text{pass}}, L_{\text{npob}}, V_{\text{отр}}, V_{\text{noc}}$) it is necessary to increase wing area (due to low values c_D , Fig. 6.10).

Certain positive effect it is possible to attain, if on the aircraft of diagram "bobtailed aircraft" to use advanced in nose

section during takeoff and landing small wing (the so-called "pen", Fig. 6.1j). Its area usually does not exceed 1.5-20% of wing area.

When selecting of the diagram of supersonic nonmaneuverable aircraft the important value acquires the sum of the weight of wing, fuselage, tail assembly and fuel/propellant.

Page 107.

On the aircraft of normal diagram, it is possible to obtain gain in the weight of wing due to its smaller area (if allow/assumes volume for the arrangement/position of fuel/propellant), but at the same time it is possible to lose in the weight of fuselage and fuel/propellant (decreases lift-drag ratio as a result of losses to balance), and also in the weight of tail assembly.

On aircraft "bobtailed aircraft", on the contrary, is obtained the smaller fuel load and fuselage (there are no loads on fuselage from horizontal tail assembly), but larger weight of wing.

In each specific case the balance of these weights can be either on the side of normal diagram or on the side of diagram "bobtailed aircraft". Everything depends on the concrete/specific/actual limitations: values of distance and Mach number of flight, length of

VPP and the like. To give any final recommendations regarding this question is not impossible. It is at present clear only, that the diagram of "weft" on the aircraft of the class in question did not justify those hopes which for it were laid.

When selecting of the position of wing relative to fuselage on height/altitude on supersonic nonmaneuverable aircraft one should consider that the low wing monoplane has a row/series of structural/design and operational advantages before the high wing monoplane:

- more conveniently to fasten and to retract the landing gear;
- increases coefficient c_v during takeoff and landing as a result of more effective ground effect ($\Delta c_v \approx 0,1$);
- is provided buoyancy during ditching.

If the conditions for load and unloading (jettisoning) purposeful load do not dictate unambiguously high wing arrangement, then one should approach the diagram of low wing monoplane or semi-low-wing monoplane especially because coefficient c_{x0} of supersonic aircraft - low wing monoplane virtually does not differ from c_{x0} high wing monoplane.

Maneuverable supersonic aircraft ¹ must satisfy following basic requirements.

FOOTNOTE ¹. Here are examined aircraft with usual takeoff and landing and fixed/recorded geometry of wing. ENDFOOTNOTE.

- maximum reserve thrust for guaranteeing of rapid acceleration/dispersal and necessary vertical velocity;
- the high-lift device of wing in entire speed range for guaranteeing of a rapid turn and change in altitude;
- the velocity of landing approach with poor visibility must not require too high a qualification of the pilots.

When selecting of the diagram of maneuverable supersonic aircraft, should be considered these requirements.

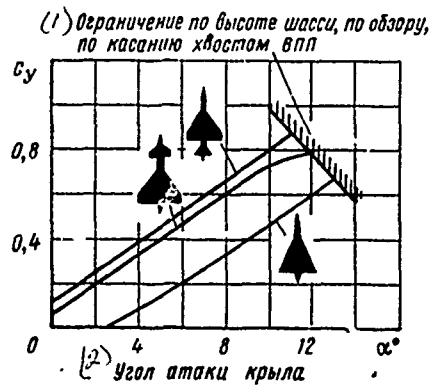


Fig. 6.10.

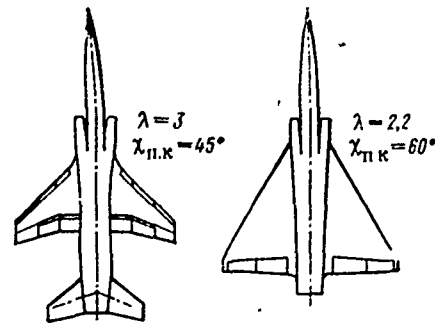


Fig. 6.11.

Fig. 6.10. Lift coefficient with takeoff (without taking into account ground effect).

Key: (1). Limitation on the height/altitude of chassis/landing gear, on survey/coverage, on the contact by tail of VPP. (2). Angle of attack of wing.

Fig. 6.11. Standard diagrams of maneuverable supersonic aircraft (to Table 6.1).

Page 108.

For a comparison let us take two diagrams - normal and "bobtailed aircraft" (Fig. 6.11) with the following initial data: the calculated number $M=2.2$; the radius of action 550 km; takeoff run length - not more than 750 m; approach speed not more than 280 km/h;

crew 1 man/person; purposeful load 1500 kg; power plant - one TRD
[turbojet engine].

The results of comparison are given in Table 6.1. Table 6.1 shows the advantage of normal diagram by takeoff weight (in essence, due to smaller wing area). This advantage is reached as a result of the fact that the wing of the aircraft of normal diagram allow/assumes powerful/thick mechanization/high-lift device (for example, double-slotted extension flaps and deflected leading edge/nose), whereas the wing of "bobtailed aircraft" does not allow/assume mechanization/high-lift device.

Parameter $\rho_0/c_{y \text{ доп}}$, the characteristic radius of turn (here $c_{y \text{ доп}}$ - permissible from the condition of stalling or buffeting lift coefficient), is virtually identical with respect to value for both diagrams. The characteristic parameter of acceleration/dispersal - g-force $n_x = \frac{P-X}{G}$ - is more in normal diagram due to smaller wing area. Calculations show that the time of climb with simultaneous acceleration/dispersal to $M_{\text{расч}}$ ($H=15 \text{ km}$; $M_{\text{расч}}=2,2$) aircraft "bobtailed aircraft" has to 250/o more than the aircraft of normal diagram.

Due to comparatively small load on the m^2 of wing the aircraft "bobtailed aircraft" is more sensitive to the vertical gusts of air (it is more g-force n_y from gusts, than in the aircraft of normal

diagram), which impedes piloting, tires the pilot and decreases the resource/lifetime of construction/design (especially in flight at low altitudes).

The advantage of diagram "bobtailed aircraft" - somewhat smaller takeoff run length ¹ - cannot change the advantage of normal diagram.

FOOTNOTE ¹. Upon this setting of the task where $V_{max} = \text{const}$. ENDFCOTNOTE.

One should emphasize that the obtained conclusion/derivations are not the consequence of initial data accepted, faster they reflect an organic deficiency/lack in the "bobtailed aircraft" - the unresolved problem of the high-lift device of wing. Conclusion/derivations are sufficiently common/general/total for the formulation of the problem accepted of the comparison of the aircraft of different diagrams with the identical degree of the safety of operation, determined to a considerable extent by approach speed.

Table 6.1. Comparison of two diagrams of maneuverable supersonic aircraft.

| (2) Схема | (1) Параметры | | | | | | | | | | | |
|--------------------------|-----------------------------|---------------------------|-----------------------------|--|----------------|--------------------------------|--------------------|--------------------|-----------------------|--------------------------------|---|-------------------|
| | (3) G ₀ в кгс | (4) S в м ² | (3) P ₀ в кгс | (5) P ₀ в кгс/м ² | P ₀ | V _{зар} в км/ч (6) | c _{у зах} | c _{у отр} | L _{разб} в м | n _x (H=0, M=0,9) | P ₀ /c _{у доп} (M=0,9) | C _{нуст} |
| (8) Нормальная | 13 850 | 23,5 | 10 300 | 585 | 0,745 | 280 | 1,35 | 1,2 | 750 | 0,58 | 585 | 0,610 |
| (9) «Бесхвост- ка» | 14 400 | 50,5 | 11 500 | 285 | 0,800 | 280 | 0,66 | 0,66 | 610 | 0,48 | 570 | 0,618 |

Key: (1). Parameters. (2). Diagram. (3). in kg. (4). in m². (5). in kgf/m². (6). km/h. (7). м. (8). Normal. (9). Bobtailed aircraft.

§ 2. Analysis and selection of the schematic of subsonic aircraft.

For the lifetime of aviation, it is known numerous attempts to use diagrams "bobtailed aircraft" and "weft" for subsonic aircraft [24]. However, these attempts, as a rule, concluded with the experimental models or the short runs of aircraft.

Page 109.

The normal diagram of subsonic aircraft maintained testing by time and by practice it is now classical.

The basic reasons for the failures of the aircraft of diagrams "bohtailed aircraft" and "weft" were connected with insufficient stability and controllability, with impossibility or limitedness of the high-lift device of wing. Flight safety on such aircraft was worse, but drag and weight - are not less (due to an increase in the wing area), than in the aircraft of normal diagram.

Let us examine following of the variety of the normal diagrams:

a) the diagrams, created by wing arrangement on the height/altitude of the fuselage (see Fig. 6.1f, g, r);

b) diagram with the application/use of a twin-boom fuselage instead of the usual single-beam (see Fig. 6.15) ¹.

FOOTNOTE 1. The diagrams of the arrangement/position of engines on subsonic aircraft are examined in § 4. ENDFOOTNOTE.

To the advantages of diagram with high wing arrangement they are related:

- decrease of aerodynamic drag from interference, especially for a circular fuselage (Fig. 6.12);

- the decrease of distance from fuselage to the earth/ground, which creates the row/series of operational conveniences;
- good survey/coverage of the earth/ground from passenger compartment;
- a reduction/descent in the probability of breakdown of the engines, arranged/located on wing, as a result of the incidence/impingement of solid particles with VPP during takeoff and landing (Fig. 6.13).

For decreasing the harmful wing-root interference effect, usually are installed the fillets. And the nevertheless lift-drag ratio of high wing monoplane with circular fuselage to 4-50/o is more than in low wing monoplane (, other conditions being equal,). In the case of the rectangular cross section of fuselage and on midwing monoplane fillets it is possible not to install.

In spite of the aerodynamic advantages of average/mean wing arrangement, this diagram rarely is applied for contemporary subsonic aircraft for layout reasons: wing usually is passed to the zone of pilot's, passenger or cargo compartment.

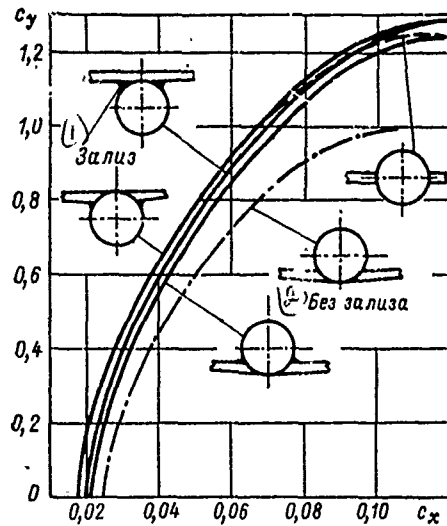


Fig. 6.12.

Fig. 6.12. Polars of aircraft in different position of wing on the height/altitude of fuselage.

Key: (1). Fillet. (2). Without fillet.

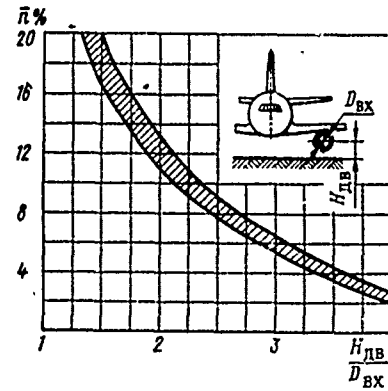


Fig. 6.13.

Fig. 6.13. Percentage of before the appointed time removed engines (TRD) depending on their distance to VPP.

Page 110.

On military transport and cargo aircraft high wing arrangement is most acceptable from an operational point of view, it gives the possibility to substantially decrease the distance from the sex/floor of cargo compartment to the earth/ground and to facilitate loading

and unloading.

The diagram of wing arrangement on the height/altitude of fuselage affects, as can be seen from Fig. 6.13, to the resource/lifetime of engines, if they are arranged/located on wing. This effect can be approximately estimated according to the formula

$$T_{\text{дв}} \approx T_{\text{дв.стена}} \left(\frac{100 - \bar{n}}{100} \right), \quad (6.4)$$

where $T_{\text{дв}}$ - average/mean resource/lifetime of the engines, establish/installed on aircraft, in hours;

$T_{\text{дв.стена}}$ - average/mean resource/lifetime, establish/installed on stand, in hours;

\bar{n} - is taken from curve/graph (Fig. 6.13) in terms of the average/mean value of height/altitude $H_{\text{дв}}$ for all engines, establish/installed on aircraft, in percentages.

Calculations according to formula (6.4) show that the service life of engines on high-wing monoplane can be to 10-15% more than on low wing monoplane. Therefore the prime cost of transportation, which depends on $T_{\text{дв}}$ (see Chapter 1), on high-wing monoplane descends. However, in absolute value the cost-effectiveness/efficiency of the operation of high-wing monoplane in the majority of the cases is obtained somewhat worse than low wing monoplane, due to weight

losses. These losses are explained by the following reasons:

- on high-wing monoplane is necessary to specially amplify the lower part of the fuselage in the case of crash landing without chassis/landing gear;

- increases the weight of the load-bearing elements (former/frames) of fuselage, receiving loads from wing and chassis/landing gear (if basic landing gear struts are connected to fuselage);

- by 30-50% increases required fin-and-rudder area in connection with a deterioration in the lateral stability of high-wing monoplane at high angles of attack, when tail assembly falls into wake from wing (Fig. 6.14).

In sum the weight of the structure of high-wing monoplane-aircraft increases by 2.5-3% of takeoff weight, if all landing gear struts are fastened to fuselage, and to 0.7-1.0%, if basic struts are fastened to wing.

When in the case of emergency alighting it is required to ensure the buoyancy (which the high-wing monoplane in contrast to low wing monoplane does not possess), then is necessary to install special

pneumatic floats which also increase the weight of high-wing monoplane.

During the final solution of a question of wing arrangement concerning the height/altitude of fuselage, it is necessary to consider, thus, the row/series of the contradictory factors: high wing monoplane has the best aerodynamic and operating characteristics, but it is inferior to low wing monoplane by the structural weight. Therefore it is necessary to make the detailed calculation of weight and cost-effectiveness/efficiency of aircraft of both diagrams. But if speech occurs about the design of military transport or cargo aircraft, then for layout and operational reasons should be given preference to high wing arrangement.

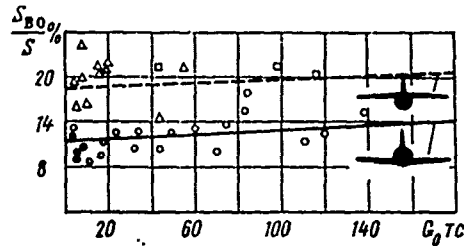


Fig. 6.14. The relative fin-and-rudder area of high-wing monoplane and aircraft-low wing monoplane: \circ - aircraft-low wing monoplanes; Δ - high-wing monoplanes; \square - military transport high-wing monoplanes.

Page 111.

During the design of multipurpose (for national economy) and cargo aircraft, appears the need for estimating advantages and deficiency/lacks in the twin-boom design of fuselage (with nacelle) instead of the usual fuselage (Fig. 6.15).

The advantage of twin-boom design is convenience in load and unloading of nacelle. However, the realization of such, is at first glance, tempting diagram it is struck into the row/series of the difficulties, connected with a deterioration in aerodynamics and a gain in weight of construction/design.

Calculations show that the aerodynamic drag of aircraft with twin-boom fuselage to 10-15% is more than usual due to the larger washed surface and the oblique airflow of beams by flow from screw/propellers (on aircraft with PD and TVD). If we decrease the washed surface of beams, after reducing the size/dimensions of their cross section, then appears the problem of the rigidity of the attachment of horizontal tail assembly and weight of beams themselves.

From the condition of equal sagging/deflection at the end of the usual and twin-boom fuselage (i.e. with equal flexural rigidity) it is possible to obtain in the first approximation, the following relationship/ratio:

$$G_{II} = G_I \cdot h_1^2 / h_{II}^2,$$

where G_I - weight of the tail section (to wing spar) of usual fuselage;

G_{II} - weight of beams;

h_1 - height/altitude of the cross section of usual fuselage in bearing edge (in wing spar);

h_{II} - height/altitude of structural section in bearing edge of its on wing.

Moving to the weight of the entire fuselage we have:

$$(G_{\phi})_{II} = (G_{\phi})_I \left[1 + \bar{G}_1 \left(\frac{h_1^2}{h_{II}^2} - 1 \right) \right]. \quad (6.5)$$

Here $(G_{\phi})_I$ - weight of usual fuselage;

$(G_{\phi})_{II}$ - weight of girder fuselage (together with nacelle);

\bar{G}_1 - ratio of the weight of the tail section of the usual fuselage toward its gross weight $\bar{G}_1 = G_1 / (G_{\phi})_I$.

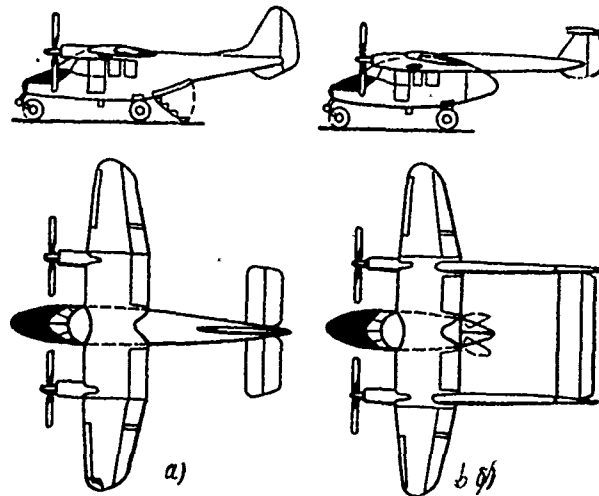


Fig. 6.15. Usual (a) and twin-boom (b) airplane designs with TVD.

Page 112.

In aircraft in weight to 6-8 t $\bar{G}_1=0,25-0,3$. If, for example, $h_1/h_H=1,5$, then the weight of twin-boom fuselage, as it follows from formula (6.5), there will be to 31-37% greater than usual fuselage (with equal flexural rigidity).

Besides a gain in weight and aerodynamic drag, the aircraft with twin-boom fuselage has other deficiency/lacks:

- cost/value of fuselage is more (to 10-15%) due to special equipment for manufacture and assembly of beams;

- beam occupy the part of the spread/scope of the high-lift device of wing; therefore wing area is necessary to increase by 5-7o/o for achievement of identical takeoff and landing characteristics with usual aircraft;

- weight of control line grow/rises by 20-25o/o.

As a result it is possible to draw a conclusion about the inexpediency of the application/use of a twin-boom fuselage, on the basis of weight and aerodynamic characteristics.

§ 3. Airplane desig. with the wing of the variable in flight sweepback.

The variable in flight sweepback of wing is a special case of the alternating/variable geometry of aircraft. Idea this is not new. Even at the glow of aviation French designer Clement Ader constructed the model airplane (1904), in which changed the sweepback of wing and horizontal tail assembly "for the regulation of speed".

Aircraft mono- biplane (see Fig. 6.1h) was constructed in us into 1940 (designers V. V. Nlikitini V. V. Shevchenko). In 1931 near

Paris, tested the aircraft of the construction/design of Makhonin with the variable wing area by means of the advancement of arms. The wingspan varied from 13 to 21.1 m, wing area increased from 21 m² to 33 m². The weight of the mechanization/high-lift device, connected with the telescopic separation of this wing, was 850 kg (170/o of design take-off weight).

Already in forties in many countries started work according to the creation of aircraft with the wing of variable in flight sweepback.

At present this idea became the same customary as the idea of retractable landing gear or extension flaps.

How do we explain, however, that throughout the entire history of the development of aviation attempts have been made to create an aircraft geometry which is changeable in flight? The cause of this phenomenon lies in the contradiction between the unchangeable nature of the form of the aircraft and the changing flight conditions with respect to speed and altitude.

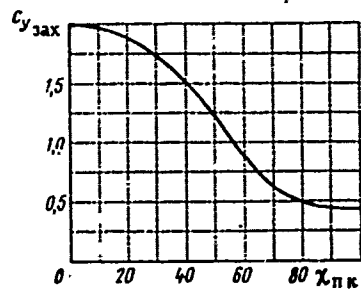


Fig. 6.16

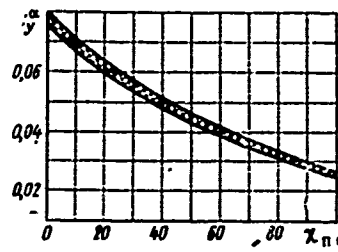


Fig. 6.17

Fig. 6.16. Dependence $c_{v \max}$ with landing approach on the sweepback of wing on leading edge (mechanization/high-lift device: Two-slot flaps and slats; $\alpha=12^\circ$).

Fig. 6.17. Character change c_y of aircraft in dependence on sweepback wing ($M<1$).

Page 113.

Diagram of aircraft with the fixed/recorded geometry is designed for the narrow flight envelope, and output/yield from this range makes aircraft far not optimum. The tendency to adapt the geometry of aircraft toward the changing flight conditions led to the creation of the diagrams of the variable geometry (the "managed diagrams").

The rapid development of this idea is recently explained by the practical requirements for aircraft with the very large flight envelope (multimode aircraft).

Aircraft with the wing of the variable in flight sweepback has following of advantage.

1. On supersonic aircraft it is possible to considerably improve takeoff and landing characteristics due to increase in elongation and c_y^* , and also effect of high-lift device of wing at minimum sweep angle (Fig. 6.16). So, when $\chi_{\text{п.к}} = 20^\circ$, $\lambda = 6-7$, utilized coefficients c_y 2-2.5 times more than on aircraft with $\chi_{\text{п.к}} = 60^\circ$, $\lambda = 2.3$. Increase c_y gives the possibility to decrease $V_{\text{отр}}$ and $V_{\text{пoc}}$ by 40-60% and L_{pas6} and $L_{\text{пoc6}}$ - 2-2.5 times.

2. More average/mean during flight lift-drag ratio substantially grow/rises in connection with increase K_{max} in subsonic conditions/modes

$$K_{\text{cp}} = \frac{1}{L} \int_0^L K dL \approx K_{M<1} \frac{L_{M<1}}{L} + K_{M>1} \frac{L_{M>1}}{L}. \quad (6.6)$$

If, for example, on long-range aircraft with

$\chi_{\text{п.к}} = \text{var}$, $K_{M<1} = 15$, $K_{M>1} = 8$, $L_{M<1}/L = 0,2$, $L_{M>1}/L = 0,8$, then according to formula (6.6) $K_{\text{cp}} = 9,4$.

On aircraft with the fixed/recorded low-aspect-ratio wing when $K_{M<1} = 10$, $K_{M>1} = 8$ we have under the same conditions $K_{\text{cp}} = 8,4$, i.e. per unit it is less.

Increase K_{cp} (when $\chi_{\text{п.к}} = 30-35^\circ$) gives the possibility either to increase flying range with $G_0 = \text{const}$ or to decrease the takeoff weight with $L = \text{const}$ due to a reduction/descent in the fuel load.

3. G-force from vertical gusts of air with $M=0.9-1.2$ (near earth/ground) can be lowered on $\Delta n_y=1.0-1.5$ because of decrease c_y^* with increase in sweepback of wing (with $45-50^\circ$ on aircraft with $\chi_{n.R}=\text{const}$ to $70-75^\circ$ and more on aircraft with $\chi_{n.R}=\text{var}$, Fig. 6.17).

Let us recall that $\Delta n_y = \xi c_y^* \rho V W_y \frac{1}{G/S}$, where $\xi = \text{const}$, W_y - the speed of gust.

The decrease of g-force from gusts, as noted above, favorably affects the accuracy/precision of piloting, is decreased pilot's enervation and it contributes to an increase in the resource/lifetime of construction/design.

4. With increase in sweepback of wing to $75-90^\circ$, decreases its effective thickness ratio along flow, which leads to certain reduction/descent in coefficient c_{x0} , to decrease of booster duration of aircraft and weight of corresponding fuel/propellant.

All enumerated advantages of aircraft with variable sweep wing it is possible to obtain only at a cost of gains in weight of the construction/design: due to hinge joint, rotary part of the wing (less favorable to structure diagram in area of hinge joint), due to

drives and high-lift device of wing. In sum these weight expenditures compose 3.5-4.5o/o of takeoff weight.

When selecting of airplane design with variable sweep wing, is of interest such diagram when wing in the position of the greatest sweepback with the aid of special flaps completely "pours" with horizontal tail assembly, creating with it single steady airfoil/profile. Aircraft becomes "bobtailed aircraft". In this diagram it is possible to increase the true altitude of airfoil/profile due to the summation of the wing chords and tail assembly ($\bar{c} = \text{const}$).

Page 114.

As a result descends the structural weight, especially hinge joint, increases the volume of wing for the arrangement/position of fuel/propellant, is simplified the resolution of the problem of the guarantee of the required rigidity.

In conclusion let us give as an example the results of the calculations of the supersonic passenger aircraft of four diagrams (Table 6.2), including diagrams with the variable sweepback of wing.

From Table 6.2 it is evident that the takeoff weight of aircraft

with $\chi_{u.R} = \text{var}$ is somewhat more than in the aircraft of normal diagram. Basic reason for this - gain in weight of the construction of the aircraft with variable sweep wing.

During the comparison of diagrams, it was assumed that the approach speed must be not more than 275 km/h. In aircraft from $\chi_{u.R} = \text{var}$ $V_{3ax} = 255$ km/h, since wing area more was selected it not from the condition of approach speed, but from the condition of the arrangement/position of the necessary fuel reserve.

Table 6.2. Comparison of four diagrams of supersonic passenger aircraft $L_{расч} = 6600$ км; $M_{расч} = 2,7$; $G_{ком} = 22$ тс; $L_{ВПП} = 3250$ м

| (2) Параметры | (1) Схема | | | | |
|-----------------------------------|-----------|-------|-------|-----|--------------------|
| G_0 в тс | | 380 | 362 | 346 | 340 |
| G_0 в % (4) | | 112 | 106,5 | 102 | 100 |
| $G_{пуст}$ в тс | | 162 | 152 | 145 | 137 |
| S в м ² (5) | | 730 | 670 | 925 | 730 |
| ρ_0 в кгс/м ² (6) | | 520 | 540 | 375 | 465 |
| $V_{зах}$ в км/ч (7) | | 255 | 255 | 275 | 275 |
| $\chi_{п.к}$ в град (8) | | 20-72 | 20-72 | 75 | 50 |
| | | | | | $\chi_{напл} = 74$ |

Key: (1). Diagram. (2). Parameters. (3). in t. (4). v. (5). in m². (6). in kgf/m². (7). in km/h. (8). in deg.

§ 4. Arrangement of engines on aircraft.

On aircraft of one and the same designation/purpose, are applied different diagrams of the layout of engines (Fig. 6.18). This bears out the fact that each of the diagrams has advantages, and deficiency/lacks 1.

FOOTNOTE 1. The diagram, which has only deficiency/lacks, is not competitive. ENDFOOTNOTE.

Let us examine the advantages and the deficiency/lacks in the arrangement on the aircraft of the most widely used turbojet engines.

During the design of maneuverable supersonic aircraft, compete two diagrams: the combined (single, Fig. 6.18a, b) and separate power plant (Fig. 6.18c, d).

The advantages of the combined with fuselage power plant in comparison with separate following:

- is less aerodynamic resistance (in comparison with diagram d);
- of minimum run up/turning torque/moment in the case of failure one of the engines (diagram b);
- increases the aspect ratio of the high-lift device of wing;
- is improved the possibility of the suspension of load under wing (in comparison with diagram d).

Page 115.

Deficiency/lacks in the combined power plant:

- is more extent and weight of air intakes (due to bending of channels);
- it is more than the loss of velocity head;
- the complexity of installation and disassembly of engine and its aggregate/units;
- increases the probability of multiple failure of two established/installed rows of engines;
- the difficulty of the arrangement/position of a relatively larger quantity of fuel/propellant.

Version c of the arrangement/position of engines differ significantly from versions b and d, representing extreme two given solutions.

Diagram c combines in itself the advantages of antipodes b and d:

- a comparatively short, simple and light air intake;
- small base drag;

- separate engines;
- the favorable possibilities of the suspension of load under wing;
- large volume in middle aircraft component for the arrangement/position of fuel/propellant.

During the design of multimode aircraft with the wing of alternating/variable sweepback, diagram d virtually is eliminated due to difficulty to preserve the position of the axle/axis of engines in the process of the turn of wing.

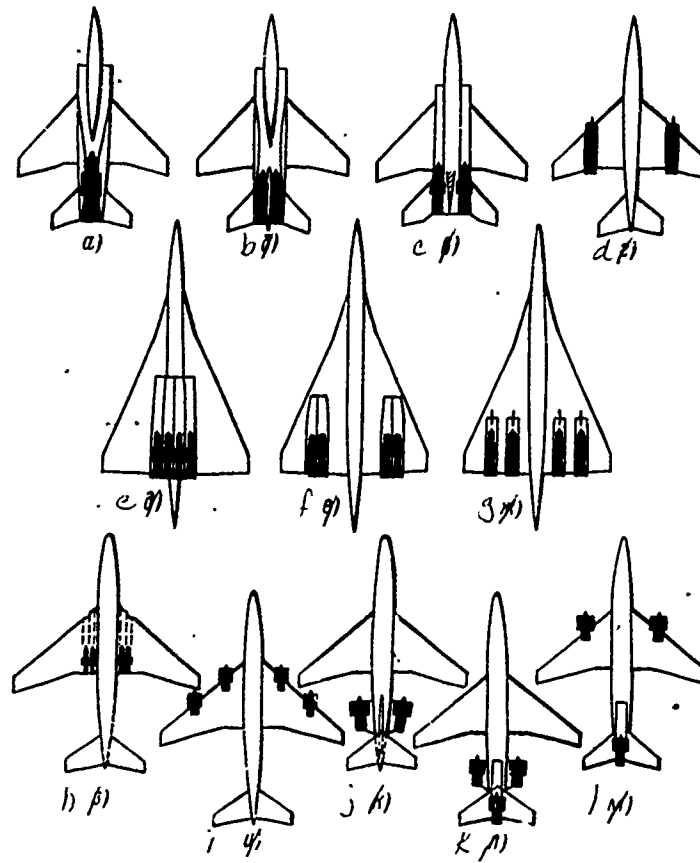


Fig. 6.18. Standard diagrams of the layout of the engines: a-d) maneuverable supersonic aircraft; e-g) the nonmaneuverable supersonic aircraft of large distance; h-l) subsonic transport aircraft.

Page 116.

On nonmaneuverable supersonic long-range aircraft, occur the same problems of selection - single or separate power plant (Fig.

6.18e, f, g).

Diagrams e and f are approximately equivalent. On aerodynamics is somewhat better diagram e, but it loses by weight due to long air intakes (for an improvement in the entry conditions, in particular for decreasing the boundary layer thickness, air intake it is necessary to lengthen). Diagram e differ significantly from f in the relation to the noise, created by engines on the earth/ground with takeoff (mutual screening of jets), and also in the relation to safety in the case of the failure of engine (lesser turning moment). However, in diagram f, is better discharging wing from the weight of the power plant (is somewhat easier wing). Is important the fact that the sprays and solid particles with VPP from the wheels of leading gear can not reach air intakes in diagram f (angle of spray from the axle/axis of aircraft is taken as as the equal to 15°).

Diagram g has following of the advantage:

- short and light air intakes;
- failure of one of the engines does not affect the operation of the adjacent engine (since engines are not connected with single air intake as in diagrams e and f);

- are simpler maintenance and replacement of engines.

Deficiency/lack in diagram g - smaller increase in the lift "from the compression", created on the lower wing surface by shock wave from air intakes (positive interference). In diagrams e and f, the effect of an increase in the lift "from compression" ($+\Delta c_y$) composes ~20% while in diagram g approximately half (it is proportional to wing area, which is located under the action of shock waves). To at the same time arrange engines in diagram g nearer to leading wing edge (for an increase in the fields of compression under wing) is not impossible due to the adverse effect of jet on wing construction (thermal and sonic effect of jet causes the decrease of the service life of construction/design).

Approximate solution of the task of the optimum selection of the diagram of the arrangement/position of engines taking into account different contradictory factors can be obtained by the method of the gradients of takeoff weight, presented in chapter V.

A final sitting of engines can be made only after the careful and detailed studying of the diverse variants taking into account the model tests, in which is imitated the engine operation. The typical patterns of the arrangement of engines on subsonic aircraft are shown in Fig. 18.6 h-1.

The arrangement/position of engines in root of the wing (diagram h) widely was applied on heavy subsonic jets of military and civil/civilian designation/purpose (aircraft of Tu-16, Tu-104, Tu-124, etc.; English aircraft "Volcano", "Victor", "Comet", etc.). This diagram of installation of engines together with the positive qualities (failure of one or two engines on the one hand does not cause the sharp turning and heeling moments, the high arrangement of air intakes, small external aerodynamic resistance) has a number of essential deficiency/lacks (especially for passenger aircraft). They include:

- a) the proximity of exhaust jet to fuselage covering, strong noise in passenger compartment;
- b) long air intakes by 5-60% decrease the engine thrust;
- c) the fire, which arose on engines, can be extended to passenger compartment and fuel tanks (is required the intensive fire-fighting protection);

d) in the case of destroying compressor blades or turbine there is possible the damage/defeat of passenger compartment and fuel tanks (special armoring is required);

e) the presence of air intakes on the leading wing edge and exhaust ducts on trailing edge decreases the possibilities of the high-lift device of wing;

f) hinders the creation of reversing gears of thrust;

g) hinders approach to engines;

h) substantially decreases the volume of wing for the arrangement/position of fuel/propellant.

The enumerated deficiency/lacks led to the fact that the engine installation in root of the wing now is not applied.

The arrangement/position of engines on pylons under wing (diagram I) is widely common on subsonic aircraft. This diagram of installation of engines has following of the advantage:

- engines unload wing construction in flight, decreasing bending to turning the torque/moments from external loads, which leads to the

reduction of the weight of wing to 10-15o/o;

- engines damp the oscillation/vibrations of wing in flight in the turbulent atmosphere;

- engines are anti-flutter balancers;

- convenience in the replacement of one type of engine by others (with large size/dimensions);

- light access to engine during maintenance.

The arrangement/position of engines on pylons has the deficiency/lacks:

- in the failure of engine, especially external, is created the large run up/turning horizontal moment;

- so that during the landing with bank (to 4°) outboard engines clear the earth/ground, is required the creation of the transverse angle of V wing (2-3°), which makes the stability characteristics worse and aircraft handling with the sweptback wing;

- during the low arrangement of engines relative to the surface

of airfield is possible the incidence/impingement into the air intakes of sand, dust and small/fine stones, which will fuse to the resource/lifetime of the engines [see formula (6.4)]. For elimination this necessary to apply special measures, for example, the cutoff of the vertical airflow, which heave from the earth/ground to air intakes, by air jet, take/selected from the compressor of engine, which is connected with gain in weight and decrease of the engine thrust;

- pylon engine mount impedes the use of flaps on entire wingspan, since with takeoff exhaust jets of engines can break them ($-\Delta c_{v_{opt}} = 0,08-0,12$).

The arrangement/position of engines on aft fuselage section was for the first time used by firm Sud-Aviation (France) on the aircraft of "Caravelle". This diagram of installation of engines (diagrams j and k) received wide acceptance on Soviet and foreign passenger aircraft (Il-62 VC-10, Yak-40, Tu-154, etc.).

The arrangement/position of engines on aft fuselage section is allowed:

- to ensure aerodynamically pure/clean wing, which increases aerodynamic aircraft quality/fineness ratio by 6-9o/o;

- to maximally utilize wingspan for the arrangement/position of the means of mechanization/high-lift device (flaps, slats, etc.), which improves takeoff and landing characteristics of aircraft;

- to determine of dihedral wing from the conditions of guaranteeing the optimum characteristics of transverse and directional stability and controllability;

- to decrease of run up/turning torque/moment with cessation one of the engines.

Page 118.

Besides in addition to this, diagrams j and k are allowed:

- to improve passengers' comfort due to the decrease of noise, since engine nacelles are installed behind pressurized cabin;

- to raise fire safety, since engines are distant from passenger compartment and from the fuel tanks (flame from the ignited in flight engine departs back/ago, clearing any load-bearing structural elements of aircraft);

- to raise (in comparison with the engine installation radically of wing) operating characteristics of power plant and entire aircraft as a whole due to sufficiently good conditions for an approach to engines;

- to protect engines from the incidence/impingement in them of foreign objects because of the high arrangement of air intakes from the earth/ground (increases the resource/lifetime of engines);

- to create the best conditions for the crash landing of aircraft.

However, the diagram of installation of engines on aft fuselage section has the essential deficiency/lacks, connected with a gain in weight of the construction of the aircraft as a result of:

a) strengthening the construction/design of aft fuselage section due to supplementary mass and inertia loads of the engines (weight of fuselage construction increases approximately by 10-150/o);

b) gain in weight of wing (approximately to 10-150/o) due to the absence of unloading of wing by engines;

c) increase in the length of fuselage due to the need for the attachment of engines.

Furthermore, in this diagram the center of gravity of the empty and loaded aircraft substantially do not coincide, in consequence of which appear the difficulties of the layout (is required either the fourth support with parking or large and heavy horizontal tail assembly for a breakaway with takeoff), appears also the need for laying fuel lines from tanks to engines near passenger compartment, which causes the danger of the incidence/impingement of vapors of kerosene into cabin/compartment and increases the weight of conduit/manifolds.

It should be noted that with the bypass ratio of engines it is more than 3.5-4.0, when substantially grow/rises the diameter of fan, installation of four engines by diagram j becomes extremely difficult. In this case it is better to apply either diagram k or compound configuration l. Last/latter diagram combines in itself the advantages of the underwing and feed engine installation. A deficiency/lack in two last/latter diagrams is the difficulty of the modification of the power plant: for an engine with large diameter, is required the alteration of aft fuselage section together with air

intake.

Table 6.3 gives an example of comparison by takeoff weight and according to cost-effectiveness/efficiency of the operation of hypothetical aircraft in 300 passenger places with three versions of the arrangement of engines. Practical flying range with the greatest payload was assumed to be the equal to 3000 km. Comparison was conducted with $(H, V, L_{BPH}, V_{max}) = \text{const.}$

From Table 6.3 it is evident that by takeoff weight and according to cost-effectiveness/efficiency of transportation the aircraft with the engines, arranged/located by diagram l, has advantage in comparison with diagrams i and k. Advantage is obtained, in essence, due to smaller over-all payload ratio of power plant ¹ in comparison with diagram i and of the smaller structural weight in comparison with diagram k ².

FOOTNOTE ¹. Thrust-weight ratio is less of the condition of failure of one engine; therefore is less the weight of power plant.

². In diagram l, wing is unloaded by weight of engines, but fuselage experience/tests smaller loads from one engine. ENDFOOTNOTE.

In conclusion one should emphasize that the selection of




DOC = 79052105

PAGE *220*

airplane design is the complicated creative process in which more than is somewhere opened all knowledge, experience and ability of designer.

Table 6.3. Comparison of three diagrams of the layout of engines

 $L_{расч} = 3000 \text{ км}; V = 950 \text{ км/ч}; L_{ВПП} = 2600 \text{ м}; V_{зах} = 240 \text{ км/ч}.$

| (2) / (1) Схемы |  |  |  |
|--------------------|---|---|---|
| Параметры | | | |
| G_0 в тс (3) | 140 | 136 | 138 |
| G_0 в % (4) | 103 | 100 | 101,5 |
| a в коп/т-км (5) | 9,07 | 8,80 | 8,9 |
| a в % (4) | 103 | 100 | 101 |

Key: (1). Diagrams. (2). Parameters. (3). in t. (4). v. (5). in kopecks/ton-kilometer.

Page 119.

Chapter VII.

BASIC QUESTIONS OF THE DESIGN OF THE POWER PLANT OF AIRCRAFT.

Into the power plant of aircraft, enter:

- 1) engines with aggregate/units and systems;
- 2) air intakes;
- 3). fuel system ¹.

FOOTNOTE ¹. Detailed list of the systems, entering the power plant of aircraft, is shown in appendix I. ENDFOOTNOTE.

Theory and design of the systems of power plant (engines, air intakes, nozzles, fuel systems, etc.) in detail are illuminated in specialized literature. In this chapter are examined in essence questions of the design of the power plant, directly connected with the common/general/total design of aircraft.

§ 1. Selection of engine for the power plant of aircraft.

For the power plant of contemporary aircraft, are applied jet engines (VRD), piston engines (PD) and liquid-rocket engines (ZhrD [liquid propellant rocket engine]). Jet engines in turn, are divided into gas-turbine (GTD [gas-turbine engine]) and ramjet/direct-flow (PVRD [ramjet engine]).

Widest use in aviation at present have GTD. This class of aircraft engines includes:

- turbojet engines (TRD);
- turbojet engines with afterburner (TRDF [turbojet engine with afterburner]);
- turbofan engines (TRDD [turbofan engine]), these engines are called also turbofan (TVRD);
- turboprop engines (TVD).

Piston engines are now placed only on very light aircraft.

The fluid-reactive engines are applied in aviation exclusively on experimental aircraft.

The selection of engine for power plant is conducted in the period of the sketch design of aircraft.

Page 120.

To estimate suitability of one or the other type of engine for the design/projected aircraft is possible, examining a change of the fundamental engine characteristics in the assigned/prescribed speed range and flight altitudes.

Characteristics of aircraft engines.

Fundamental characteristics, on which is realized/accomplished comparative evaluation when selecting of engine, are: the altitude-speed characteristics $P=f(M, H)$ and $c_p=f(M, H)$, the flow rate per second of air G_u , weight per horsepower $\gamma_{\text{лп}}$ and overall dimensions (length and maximum/overall diameter) of engine ¹.

FOOTNOTE ¹. The characteristics of aircraft engines, necessary for

accomplishing the diploma project, are given in appendix III.
ENDFOOTNOTE.

First TRD (with centrifugal compressor) had boost for launching (with $V=0$ and $H=0$) less than 2700 kg and the sufficiently large specific fuel consumption. At present aircraft engines are capable of developing boost for launching to 30000 kg (GE 4/J5). One ought not, of course, to assume that TRD with small thrust gradually died off. Contemporary aircraft engines depending on designation/purpose can have very small thrust, for example TRDD AI-25, established/installed on aircraft Yak-40, it develops thrust 1500 kg, and thrust TRD Bristol Siddeley BS-347 is equal only 63.6 kg (weight of engine 13.6 kg).

Contemporary GTD depending on designation/purpose can have the boost for launching, equal to $P_{0max} \approx 50$ to kg - smallest full thrust: $P_{0max} \approx 30'000$ - kg - greatest full thrust.

Simultaneously with an increase in the boost for launching decreased the starting specific consumption of fuel GTD. To 1946 majority TRD with single-stage centrifugal compressor had a compression ratio, equal to approximately four, and therefore the specific consumption of fuel of these TRD (in nonafterburning conditions/mode) exceeded 1.3 kg/kg•h).

Contemporary GTD have the starting specific fuel consumption, which is changed in the range

$c_p = 0,5 - 0,7$ кгс/кгс·ч — нефорсажный режим: (1)

$c_p = 1,7 - 2,0$ кгс/кгс·ч — форсажный режим: (2)

by Key: (1). kg/kg·h - nonafterburning conditions/mode. (2). kg/kg·h - afterburner conditions/mode.

It is possible to assume that as a result of further perfections TRDD will be reached the specific fuel consumption of less than 0.5 kg/kg·h, and on TRDD with large bypass ratio ($m=5-8$) the value of the starting specific fuel consumption will approach 0.3 kg/kg·h.

The important parameter, which characterizes the perfection of engine, is its specific gravity/weight on boost for launching, i.e., the ratio of dry weight of power plant toward maximum boost for launching $\gamma_{дв} = G_{дв}/P_0$.

Contemporary GTD can have specific gravity/weight $\gamma_{дв} = 0,15 - 0,23$.

It should be noted that the specific gravity/weight of contemporary TRD virtually does not depend on the value of boost for launching, for example, TRD GE 4/J5 ($P_0 = 28700$ kg) has $\gamma_{дв} = 0,166$; TRD

J85=13 ($P_0=1850$ kg) it has $\gamma_{\text{TB}}=0,163$. Specific gravity/weight TRDD is proportional to value $\sim P_0^{0,15}$, and also it depends on bypass ratio.

Sometimes instead of the weight per horsepower, is examined reciprocal value (i.e. thrust-to-weight ratio), which is called the weight specific thrust of engine $P_{\text{yH}}=1/\gamma_{\text{TB}}$.

The basic size dimensions of engine are its length and maximum/overall diameter (on compressor, on entry, on nozzle, etc.). The diameter of engine frequently determines the frontal area of fuselage or nacelle, which in the final analysis is reflected in the lift-drag ratio of entire aircraft. Therefore, other conditions being equal, always is given up preference to engine with smaller diameter.

Page 121.

The dependence of the diameter of engine on boost for launching can be written in the form

$$D_{\text{in}} \approx (1,62 + 0,275m^{0,75}) \sqrt{\frac{P_0}{20000}} \text{ m}, \quad (7.1)$$

where P_0 - in kg; m - bypass ratio.

The tasks, fulfilled by contemporary aviation, require the power plant of the aircraft of high cost-effectiveness/efficiency over a wide range of speeds and flight altitudes. However, the greatest

cost-effectiveness/efficiency of aircraft engine is provided in such a case, when it is designed for a comparatively small altitude-speed range. By this is explained the division of engines into subsonic, supersonic ones and hypersonic ones.

Engines for subsonic aircraft.

The oldest type of engines for subsonic aircraft it is, as is known, piston engine. At present are produced only low-power piston engines ($N=100-340$ hp) and are installed on very light aircraft (tourist, sport, etc.). However, also on light aircraft PD it began to be replaced by other types of engines.

A continuous increase in the launching weight of aircraft requires the appropriate increase in the installed power. Figures 7.1a give the curve of an increase in the required power in the cruise setting of flight, beginning with the aircraft of the 40's. During the examined/considered period the required power increased approximately 20 times. Weight per horsepower according to thrust horsepower in cruise setting considerably decreased (Fig. 7.1b), moreover by jump - with the advent of GTD. Contemporary TRDD develops thrust horsepower on 1 kg of weight 3-4 times more than PD.

As can be seen from Fig. 7.1c, contemporary GTD (at doubly

larger cruising flight speed) in the value of the specific expenditure/consumption of fuel were equaled with best PD.

Figures 7.1d show a change in the initial velocity of engine plants on 1 hp of thrust horsepower. With implementation GTD, the cost/value of engine plants sharply was lowered, in spite of an essential increase in the power of engines.

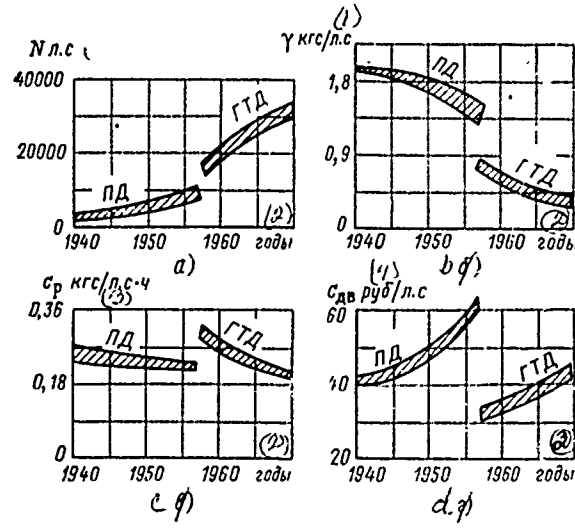


Fig. 7.1. Development of subsonic aircraft engines during period 1940-1970.

Key: (1). kg/hp. (2). year. (3). kgf/hp•h. (4). rubles/hp.

Page 122.

At present turboprop engine finds in aviation increasingly smaller use. In order to compete with contemporary TRDD [turbofan engine], further perfection of TVD must be directed toward an increase in the specific power and the decrease of the fuel consumption. However, in this case, appear the difficulties, connected with propeller: it is difficult to create the screw/propeller, which has sufficiently high efficiency at the increased power of engine, but it is not less difficult to solve the problem of a decrease in the common/general/total noise level and vibrations on aircraft during the installation of a similar screw/propeller.

Now most promising engine for the power plant of subsonic aircraft is TRDD (turbofan engine).

TRDD makes it possible to have in cruise to 10-15% smaller specific fuel consumption, than the straight ^{Turbo engine} jet (Fig. 7.2).

Advantage of TRDD is also the higher ratio of takeoff thrust

toward cruising, therefore, with equal with TRD cruising thrusts (determined by gross weight and by aerodynamic aircraft quality/fineness ratio), TRDD provides to aircraft the best takeoff data.

A resource/lifetime of this type of engines at present is most high. Service life between sorting/partitions for TRDD is equal to 8000-10000 h.

First TRDD were developed on the basis of existing TRD and they had small bypass ratio $m=0.6-1.4^1$.

FOOTNOTE 1. By the degree (coefficient) of bypass configuration, as is known, is understood the ratio of the flow rate per second of air in outer duct toward the flow rate per second of air in internal duct/contour. ENDFOOTNOTE.

Contemporary TRDD are characterized by higher bypass ratio $m=3-6$. They have a row/series of fundamentally new constructive solutions (possibility of independent rpm control of each cascade/stage of compressor); in the construction/design of engines, widely are utilized new structural materials (in particular, they are used the plastics, reinforced by the filaments of graphite, boron, etc.). These and other innovations make it possible to bring

compression ratio in compressor to 25 and more, which increases the cost-effectiveness/efficiency of engine.

Cost-effectiveness/efficiency of TRDD and its fundamental characteristics depend also on the bypass ratio of engine.

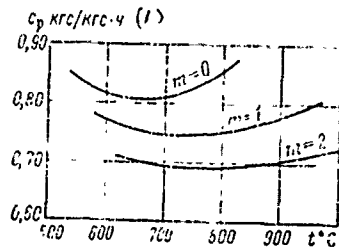


Fig. 7.2,

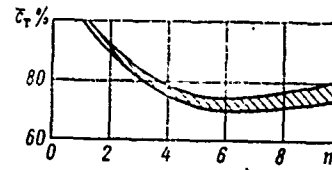


Fig 7.3

Fig. 7.2. The typical dependence between the temperature of the gas before the turbine and the specific consumption of fuel by TRD and TRDD (under conditions for cruise): m - bypass ratio.

Key: (1). kgf/kgf·h.

Fig. 7.3. Effect of bypass ratio on value \bar{c}_r of TRDD (\bar{c}_r - relative expenditures for fuel/propellant).

Page 123.

The specific hourly consumption of fuel/propellant in the first approximation, can be expressed as follows:

$$c_p \approx 0,9 \left[\frac{0,82}{1 + 0,525 \sqrt[3]{m}} + M(0,494 - 0,0145H) \right] \text{ kgf/kgf}\cdot\text{ч}, \quad (7.2)$$

Key: (1). kgf/kgf·h.

where m - bypass ratio;

M - flight mach number;

H - flight altitude, km.

Specific gravity/weight of TRDD approximately can be written in the form

$$\gamma_{TRDD} \approx 0,23 - 0,03m + 0,0082m^{1,5}. \quad (7.3)$$

The diameter of engine will be determined according to expression (7.1).

The drag coefficient of engine nacelle of TRDD with an increase in the bypass ratio decreases, which is evident from the expression

$$C_{x_{m.r}} \approx \frac{0,16}{\sqrt{m}}. \quad (7.4)$$

Figure 7.3 shows the effect of bypass ratio on cost-effectiveness/efficiency of TRDD (as unity is accepted cost-effectiveness/efficiency of TRDD with $m=1-1.5$).

At present for heavy subsonic aircraft are applied TRDD with bypass ratio $m=4-8$.

The subsonic engines include also special hoisting TRD and TRDD

for VTOL aircraft. According to the principle of the creation of vertical and horizontal thrusts, the power plants of VTOL aircraft are divided into single and compound/composite ones. Single power plants serve for vertical takeoff and landing and for the level flight (one and the same engine creates vertical, and horizontal thrusts). These engines, as a rule, were intended for installation on supersonic aircraft.

The compound/composite power plants of VTOL aircraft have engines for the creation of vertical thrust on takeoff and landing (hoisting) and engines for obtaining the horizontal thrust (march). As sustainer engines are utilized usual TRD and TRDD.

Lift engines in the parameters of working process and construction/design considerably differ from sustainer engines. These engines have specific gravity/weight approximately 3-3.5 times less than the specific gravity/weight of usual GTD [gas-turbine engine] (which is reached, first of all, due to a considerable reduction/descent in the resource/lifetime of engine).

The advantages of hoisting TRDD in comparison with hoisting TRD are;

- smaller exhaust gas velocities (and consequently, the smaller

destructive action of gas jet on the launching pad);

- best cost-effectiveness/efficiency under conditions of the vertical lift, landing and hovering (in hoisting TRDD with low-pressure fan the specific fuel consumption is almost three times less than in hoisting TRD). True, this TRDD, possessing the indicated advantages in comparison with hoisting TRD, is inferior to it according to diameter and by blockaded volume.

Engines for supersonic aircraft.

Most economical during supersonic flight are two types of engines - TRD and TRDD.

In order to ensure the smallest fuel consumption and highest efficiency over a wide range of Mach numbers (from takeoff to maximum speed), TRD has, as a rule, afterburner, and TRDD - afterburning in secondary circuit (Fig. 7.4).

For an endurance flight in supersonic conditions/mode, are examined usually two speed ranges: speed range, which correspond to number $M \approx 2$ whose advantage lies in the fact that the airframe of aircraft can have construction/design from usual aluminum alloys, and the speed range, which correspond to number $M \approx 3$, which although

creates the specific problems, promises the higher cost-effectiveness/efficiency of flight.

Page 124.

One should consider that for the flight speed, which corresponds to a number $M \approx 2$, it is possible to utilize TRD and TRDD; compression ratio in compressor for both types of engines it must be $\pi_{\kappa} \approx 9-10$.

Absence of essential difference in characteristics of TRD and TRDD on supersonic speeds to a certain degree is explained by the fact that during an increase in the coefficient of bypass configuration from 0 to 0.5-0.7 specific fuel consumption decreases insignificantly (approximately by 10%). Further increase in the coefficient of bypass configuration progressively makes the engine characteristics worse. One should, however, remember that we are dealing with prolonged supersonic flight.

Some supersonic aircraft (multipurpose fighters, etc.) frequently accomplish prolonged subsonic flight. In this case all advantages on side of TRDD. The bypass ratio of such engines (in order not to make characteristic worse with $M > 1$) must be small: $m = 0.7-1.2$, while compression ratio - $\pi_{\kappa} = 12-16$.

At the flight speed, which corresponds to number $M \approx 3$, single-circuit and bypass engines also do not have large differences. Therefore and it is possible to apply engines of both types. However, the difference is in the fact that at this speed the engines (both TRD and TRDD) with low compression ratio in compressor ($\pi_k = 3-4$ with $M \approx 3$) they have the smaller specific consumption of fuel (Fig. 7.5).

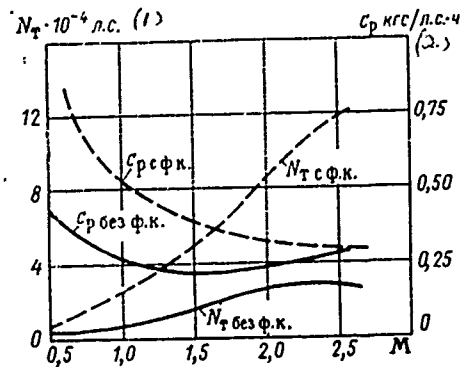


Fig. 7.4. The dependence of thrust horsepower and specific consumption of fuel of TRD "Olympus" (England - France) on flight Mach number (with afterburner, also, without afterburner), H=11 km.

Key: (1). hp. (2). kgf/hp·h.

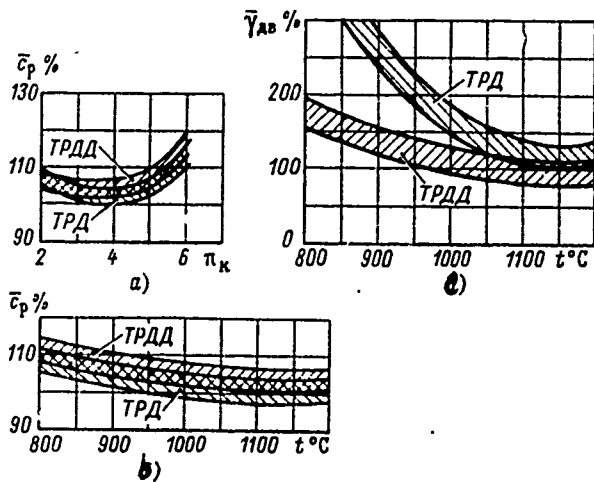


Fig. 7.5. Characteristics of TRD and TRDD, which are determining their cost-effectiveness/efficiency with $M \approx 3$; H=20 km.

Engine for hypersonic aircraft.

The application/use of gas turbine engines for aircraft power plants is limited, as is known, by a number $M \approx 3.5$. For flight at high speeds by the best cost-effectiveness/efficiency will possess PVRD [ramjet engine] with subsonic combustion ($M \leq 8$) and PVRD with supersonic combustion ($M > 8$).

Rocket engines, works on chemical fuel/propellant (ZhRD [liquid propellant rocket engine]), achieved now this level of the development when further increase in the specific impulse becomes ever slower and being expensive. Moreover, the specific impulse of ZhRD remains insufficient for its installation on hypersonic aircraft (Fig. 7.6).

The cost-effectiveness/efficiency of engine in the first approximation, can be estimated in the value of its specific impulse J_T (since $c_p = 3600/J_T$ kgf/kgf·h).

It must be noted that, in spite of the increase of the specific fuel consumption per supersonic speeds, the overall efficiency of engine increases. Overall efficiency, as is known, are considered all

losses in the energy conversion of fuel/propellant into useful thrust work. For hydrocarbon fuel (kerosene) the expression overall efficiency jet engine can be written in the form

$$\eta_n = 0,00082V/c_p. \quad (7.5)$$

The overall efficiency of the engine of subsonic aircraft ($M=0.85$) composes approximately 240/o. At the flight speed, which corresponds to number $M=2$, it grow/rises already to ~380/o (which exceeds the thermal efficiency of the best contemporary power stations), while with $M=3$ $\eta_n \approx 46\%$. Increase efficiency is continued also in flight at hypersonic speeds with PVRD.

Most promising ones for hypersonic aircraft are compound engines - direct-flow turbine (TRD+PVRD). TRD must work to the speed, which corresponds to number $M \approx 3.5$, then gas-turbine circuit is closed, and at hypersonic speeds engine will work as PVRD.

The examined above fundamental characteristics of aircraft engines (different types) can have the specific differences, caused by the design features of concrete/specific/actual specimen/samples. For example, two one-type engines with identical boost for launching can have the different values of specific gravity/weight, specific consumption of fuel, diameter of engine, etc. If all characteristics in one engine are better, a question of the selection of engine is solved unambiguously. However, in practice this case is encountered

DGC = 79052106

PAGE 243

rarely. As a rule, during the comparison of several engines it proves to be that one characteristics are better in one engine, others - are better in another engine, etc. How in that case to select concrete/specific/actual engine for the design/projected aircraft?

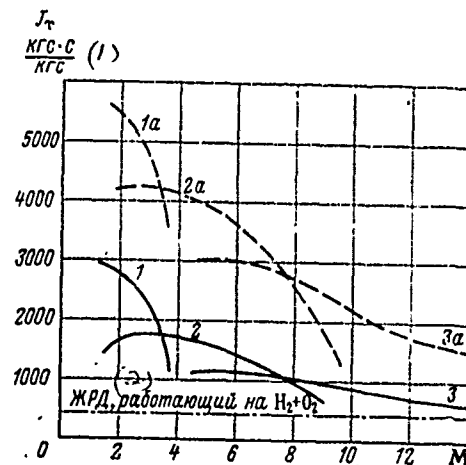


Fig. 7.6. The dependence of specific impulse (on fuel/propellant) from flight mach number for different types of engines, workers on kerosene (1; 2; 3) and hydrogen (1A; 2a; 3a): 1; 1a - GTD; 2; 2a - PVRD with subsonic combustion; 3; 3a - PVRD with supersonic combustion.

Key: (1). $\text{kgf} \cdot \text{s} / \text{kgf}$. (2). ZNRD, that works on $\text{H}_2 + \text{O}_2$.

Page 126.

There are methods of comparison of engines according to their fundamental characteristics, for example, is examined the product of the specific parameters: $\gamma_{\text{дв}}, c_p, D_{\text{дв}}/P_0$ or is compared the total weight of engine plant and fuel/propellant ($G_{\text{дв}} + G_{\text{топ}}$) and so forth. However, these methods bear the approximate character and they do not make it

possible to solve the presented question with sufficient accuracy/precision.

In order to select one or another engine, it is necessary to make detailed airplane performance computation with each engine, after determining flight (and others) characteristics of aircraft, and to estimate the degree of fulfilling the requirements, presented to this aircraft.

For contemporary civil/civilian and military aircraft (as a rule, heavy) is specially design/projected engine based on given characteristics of aircraft. The designers of aircraft and the designers of engine carry out great joint operation on the solution of the questions, connected with installation of this engine on this aircraft.

Only after accomplishing of the indicated works a question of the selection of engine can be solved finally.

The necessary quantity of engines for the power plant of aircraft depends on a whole series of the factors, caused designation/purpose of aircraft as well as by its basic parameters and flight characteristics.

The discrepancy of the effect of a number of engines on safety, cost-effectiveness/efficiency and regularity of flights leads to the fact that the selection of a number of engines, until now, remains the insufficiently developed question of the design of aircraft.

In general terms requirements for all aircraft when selecting of a number of engines can be formulated thus:

- aircraft must possess the necessary starting thrust-weight ratio;

- aircraft must possess sufficient reliability and cost-effectiveness/efficiency.

§2. Air intakes of contemporary aircraft.

The functions of air intake in the system of power plant of contemporary aircraft are reduced to following:

- to ensure the stable operation of engine in all flight conditions;

- to ensure air compression, which enters the air intake, converting kinetic energy of the incident flow into pressure.

As is known, at the subsonic flight speeds an increase in the air pressure in engine circuit occurs in basic in compressor of TRD (approximately five times more than in diffuser). With an increase in the speed of the function of compressor, gradually they transfer/convert to air intake; with number $M=1.2-1.4$, the air intake and compressor to identical degree compressible flow. At high supersonic flight speeds ($M>3$) the role of compressor becomes already unessential, and compression ratio in input device reaches order 40:1.

By the compression ratio of air in turbojet engines it is accepted to call the ratio of air pressure at the end compression, i.e., after compressor, toward the atmospheric pressure

$$\pi = \frac{p_k}{p_H} = \frac{p_a}{p_H} \frac{p_k}{p_a} = \pi_n \pi_k,$$

where p_k - compressor discharge pressure (at the burner inlet);

p_H - atmospheric pressure;

p_a - pressure at the entry into compressor;

π_{BX} - compression ratio in air intake;

π_k - compression ratio in compressor.

Page 127.

A change in values π_{bx} and π_k during an increase in the speed for air intake and TRD, designed for cruising flight speed with $M=3.0$, occur/flow/lasts approximately as follows:

| M | 0 | 1 | 2 | 2,2 | 2,5 | 2,7 | 3,0 |
|------------|----|---|---|-----|-----|-----|-----|
| π_{bx} | ~1 | 2 | 7 | 10 | 15 | 20 | ~30 |
| π_k | ~8 | 6 | 5 | 4,7 | 4,4 | 4,2 | ~4 |

to the air intake of supersonic aircraft at present is abstract/removed the role of the adjustable compressor.

In diffuser the pressure so grow/rises (for example, with $M \approx 2.2$ $\pi_{bx} = 10$) its distribution on internal surface is such, that is created the thrust, equal to 60-75% of entire thrust of power plant (Fig. 7.7).

During braking of flow, always take the place of loss of pressure, caused by friction, vortex formation (flow breakaway in the nonuniform velocity field), by heat exchange, while during stagnation of supersonic flow, appear the wave losses, caused by the emergence of shock waves. As a result of air-intake loss, actually attainable values π_{bx} prove to be lesser than theoretically possible ones. For example, with number $M=3$ it is possible to obtain $\pi_{bx} \approx 30$ instead of $\pi_{bx,ид} \approx 38$, which would be in the ideal case (without losses).

The losses of pressure, which appear during air compression in input device, it is accepted to estimate by the value of the total pressure recovery coefficient (in the theory of engines for convenience in the calculations they frequently use not the static, but total pressures). The total pressure recovery coefficient is equal to

$$\tau_{\text{BВ}} = \frac{\pi_{\text{BВ}}}{\pi_{\text{HX.HX}}} = \frac{p_a^*}{p_H^*},$$

where p_a^* - pressure of the completely stagnant flow at the end of the air intake (at the entry into compressor);

p_H^* - the free-stream total head of air.

So that the air intake of contemporary aircraft would effectively fulfill its functions, it must provide:

- possible the higher values of the total pressure recovery coefficient;
- a sufficiently uniform field of inlet velocities into compressor;
- stable (without separations of flow and pulsations of

pressure) operation in all conditions/modes of operation;

- least possible external resistance.

Subsonic air inlets.

The accumulated experience of construction and operation of the subsonic air inlets makes it possible to obtain the very high values of the total pressure recovery coefficient in similar input devices - $\sigma_{Bx}=0,97-0,98$.

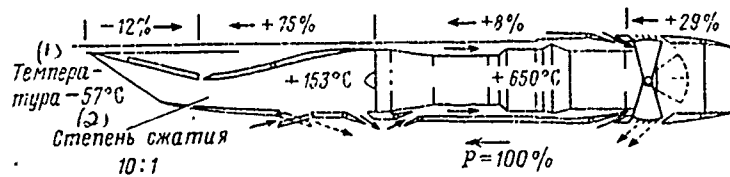


Fig. 7.7. Distribution of thrust and aerodynamic drag along the length of engine nacelle with number $M=2.2$.

Key: (1). Temperature. (2). Compression ratio.

Page 128.

During the design of the subsonic air inlets, their parameters are selected for basic flight conditions.

The size/dimensions of the inlet of diffuser are determined by the air flow rate through the intake area. According to the law of conservation of mass, the per-second weight flow rate of air in cross section H-H and $Bx-Bx$ (Fig. 7.8) will be identical:

$$G_b = F_H V_H \gamma_H = F_{Bx} V_{Bx} \gamma_{Bx}$$

where V - a rated speed of flight at height/altitude H .

Intake area it is possible to express thus:

$$F_{bx} = \frac{G_b}{V_{bx} \gamma_{bx}}, \quad (7.6)$$

where G_b - the flow rate per second of air by engine, for which is design/projected the air intake (it is assign/prescribed in the engine characteristics);

V_{bx} - air speed at the entry into air intake;

$\gamma_{bx} = \rho_{bx} g$ - the specific gravity/weight of air at entry.

Value V_{bx} in the first approximation, can be determined in the form

$$V_{bx} = V \bar{V}_{bx},$$

where $\bar{V}_{bx} = 0,3-0,7$ - relative air speed at the entry into air intake.

The smaller values of value \bar{V}_{bx} are accepted for the long and bent channels (in order to have small hydraulic losses), large values \bar{V}_{bx} - for short channels and GTD with high inlet velocities into compressor.

An increase in the air density ρ_{bx} during braking from V to V_{bx} is determined from special gas-dynamic tables.

In the period of precomputations (and also during diploma design) the size/dimensions of inlet can be determined through the

relative diameter of the entry

$$\bar{D}_{\text{ex}} = 1,1 \sqrt{\frac{1}{\frac{1 - \bar{V}_{\text{ex}}^2}{1 - M^2} + 1}} \quad (7.7)$$

Here $\bar{D}_{\text{ex}} = D_{\text{ex}}/D_r$;

D_{ex} - the diameter of the entry of air intake;

D_r - maximum outside diameter of nacelle, moreover

$$D_r \approx (1,2 - 1,3) D_{\text{BH}}$$

where D_{BH} - maximum inner diameter of nacelle.

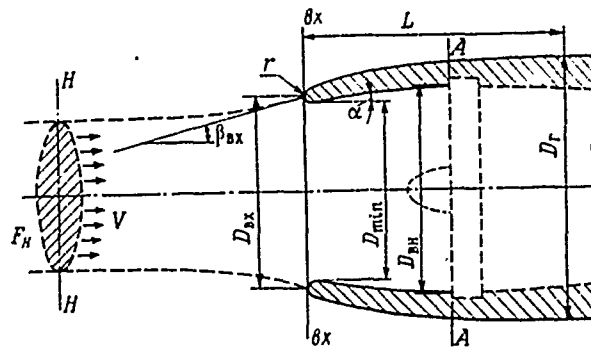


Fig. 7.8. Diagram of the subsonic air inlet.

Page 129.

It is possible to accept $D_{BH} \approx D_{RB}$ - the diameter of engine (on compressor).

The profiling of entering edge is realize/accomplished in order to obtain the even flow of nacelle and to avoid flow separations at entry.

The angle of indraft of external jet boundary to the entry into the air intake of its relatively axle/axis in the first approximation, can be determined through the relative rate of entry

$$\beta_{ax} = 22 \sqrt{\frac{1}{V_{ax}} - 1}, \quad (7.8)$$

where β_{ax} - in degrees.

The radius of curvature of air-intake lip, which ensures even flow, approximately can be accepted

$$r_{min} = (0,04 - 0,05) \sqrt{F_{ax}} \quad (7.9)$$

The profiling of air duct is provided for for obtaining the greatest value of value σ_{ax} and uniform field of inlet velocities into compressor (cross section A-A).

If the expansion of channel (after entry) too greatly or channel has sharp rotations and bendings, flow can be separated from walls, which will lead to considerable to eddy losses. Another reason for losses in subsonic diffuser - air friction against the walls of channel. However, if flow breakaway it does not proceed, then losses from friction prove to be comparatively small.

If diffuser is done with rectilinear walls, then the half-angle of its solution/opening must be

$$\alpha \leq 4 - 5^\circ.$$

If channel has rotations and bendings, then in last/latter section (before the engine) the axle/axis of channel must coincide with the axle/axis of compressor. The length of this cylindrical part of the channel must be not less $(0.5 - 0.1) D_{DB}$.

The profiling of the external enclosures of air intake must ensure to it minimum drag. Therefore the external enclosures of air

intake are shaped independent of internal ones.

The relative external length of entry, advisable from the point of view of external flow, it can be expressed as the function of flight mach number

$$\bar{L} = L/D_r \approx 1,5M^2, \quad (7.10)$$

where L - a distance from the leading edge/nose of nacelle to cylindrical part.

It must be noted that the given above dependences, which are determining the basic parameters of air intake, are approximated. It is theoretically very complicated to consider all special feature/peculiarities of real flow; therefore recommendation regarding profiling, for example air duct, they are establish/installed in essence experimentally.

Supersonic air inlet.

In the supersonic air inlet of the losses, which appear during air compression, they are composed of wave losses (in the system of jumps), eddy losses and losses from friction.

However, basic value compose the wave losses

$$\sigma_{hx} = (0,9 - 0,95) \sigma_{ck},$$

where $\sigma_{ck} = \sigma_1 \sigma_2 \dots \sigma_n = \prod_{l=1}^n \sigma_l$ - a total pressure recovery coefficient in the system of jumps;

σ_l - total pressure recovery coefficient in one jump.

Depending on the form of the cross section of entry, the supersonic air inlet can be divided into two types: two-dimensional (flat/plane) and three-dimensional (circular, semicircular, etc.). Depending on the position of oblique shocks, the air intakes are of the external, internal and mixed compression (all three types can be two-dimensional, and three-dimensional Fig. 7.9).

The first multishock air intakes of supersonic aircraft were external compression. In comparison with the air intakes of internal compression, they are sufficiently simple in regulation, they do not require complicated starting system, they possess weight advantages; however, efficiency in them are below (air intakes with external compression have also great aerodynamic resistance). For example with $M=3$, is obtained

$$\sigma_{hx} = 0,75 - \text{external compression};$$

$\alpha_{in} = 0,95$ - internal compression;

$\alpha_{bx} = 0,85$ - mixed compression.

The parameters and the size/dimensions of the supersonic air inlet are selected for basic flight conditions (as a rule, supersonic cruise).

Intake area. The throughput of air intake (diffuser) is estimated by the coefficient of expenditure/consumption ϕ , which are the ratio of the real air flow rate toward maximally possible, i.e.

$$\phi = \frac{G_n}{G_{n, \max}}$$

The coefficient of expenditure/consumption ϕ is numerically equal to the relation to the area of air jet in the undisturbed flow (cross section H-H) to intake area into air intake (Fig. 7.10)

$$\phi = \frac{F_H}{F_{bx}},$$

moreover the intake area of the supersonic air inlet is considered complete sectional area $v_{kh} - v_{kh}$. The area of directly entrance slit is defined as

$$F_{in} = F_{bx} - F_{\tau},$$

where F_{τ} - a sectional area of body, which creates the shock envelope.

For the creation of the system of jumps in air intakes, can be used both the flat/plane bodies (wedge) - for the two-dimensional inlets and circular bodies (cone, semicone, fourth of cone) - for the three-dimensional air intakes of the corresponding form.

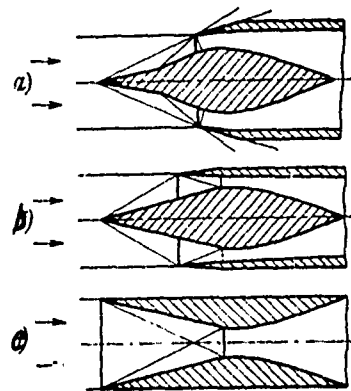


Fig. 7.9. The methods of forming the shock waves: a) air intake with external compression - all oblique shocks are arranged/located outside; b) the air intake of the mixed compression - oblique shocks are arranged/located inside, and within air intake; c) air intake with internal compression - all oblique shocks are arranged/located inside.

Page 131.

However, the geometric parameters of all air intakes are analogous; therefore longitudinal section, for example semicircular and two-dimensional inlets, it will be virtually equally, and the longitudinal section of circular air intake will be characterized by only the symmetry of the lower and upper part of the cross section.

In design conditions of the work of air intake, external oblique

shock waves are focused on the leading edge of cowling, i.e., occurs the equality

$$\varphi = \frac{G_B}{G_{B,max}} = \frac{F_H V \gamma_H}{F_{Bx} V \gamma_H} = 1,$$

whence
$$F_{Bx} = \frac{G_B}{V \rho_H g}, \quad (7.11)$$

where G_B - the flow rate per second of air;

V - flight speed of aircraft;

ρ_H - air density at flight altitude;

$$g = 9.81 \text{ m/s}^2.$$

The complete air flow rate through the air intake is equal to

$$G_{B\Sigma} = G_B + G_{B,n.c} + G_{B,nep},$$

where G_B - air flow rate through the engine;

$G_{B,n.c}$ - air of boundary layer, poured from the surfaces of compression (wedge, cone, etc.);

$G_{B,nep}$ - air, passed from diffuser back in the atmosphere through bypass (anti-surge) shutter/doors.

However, with sufficient for sketch design accuracy/precision it is possible to accept

$$G_{\text{вз}} \approx G_{\text{в}}$$

The flow rate of air (physical) through the engine is equal to

$$G_{\text{в}} = G_{\text{в.нр}} \frac{p_a^*}{p_0} \sqrt{\frac{T_0}{T_H^*}}, \quad (7.12)$$

where $G_{\text{в.нр}}$ - the given air flow rate;

$$p_a^* = p_H^{\text{вз}}$$

p_0, T_0 - respectively pressure and temperature of surrounding air with $H=0; V=0$.

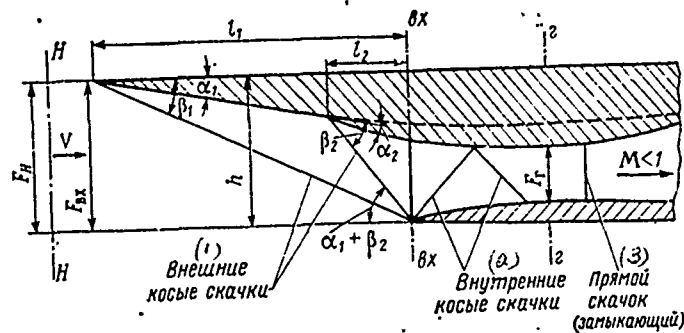


Fig. 7.10. Diagram of the supersonic air inlet of the mixed compression (design conditions of flow).

Key: (1). External oblique shocks. (2). Internal oblique shocks. (3). Normal shock (closing).

Page 132.

Expressing the pressure and the total stagnation temperature through the flight mach number

$$p_H^* = p_H (1 + 0,2M^2)^{3,5}; \quad T_H^* = T_H (1 + 0,2M^2),$$

where p_H^* , T_H^* - respectively the pressure and the total stagnation temperature incident flow at flight altitude;

p_H , T_H - respectively pressure (static) and temperature of surrounding air at flight altitude,

we will obtain

$$G_s = G_{n,np} \frac{\sigma_{bx} \rho_H (1 + 0,2M^2)^3}{1,033} \sqrt{\frac{288}{T_H}} \quad (7.13)$$

The resultant expression for determining the intake area of the supersonic air inlet will take the form

$$F_{bx} = G_{n,np} \frac{\sigma_{bx} \rho_H (1 + 0,2M^2)^3}{10,14V \rho_H} \sqrt{\frac{288}{T_H}} \quad (7.14)$$

where F_{bx} - is expressed in m^2 ;

$G_{n,np}$ - in kgf/s (values of the given air flow rate are given in appendix III);

ρ_H - in kg/cm^2 ;

V - in m/s ;

ρ_H - in $kg \cdot s^2/m^4$;

T_H - in K.

The minimally necessary number of jumps in the air intake of supersonic aircraft (depending on the rated speed of flight) must be;

$M \leq 1,3$ - one normal shock;

$M \leq 1.5$ - system 1 oblique shock +1 normal shock;

$M \leq 2.0$ - system of 2 oblique shocks +1 normal shock;

$M \leq 2.5$ - system of 3 oblique shocks +1 normal shock;

$M \leq 3.0$ - system of 4 oblique shocks +1 normal shock;

$M \leq 3.5$ - system of 5 oblique shocks +1 normal shock.

The arrangement of oblique shocks, as it was noted above, depends on the type of air intake. During the mixed compression usually of 1-3 oblique shocks, are arranged/located *outside* the others - within air intake.

The angles of stepped wedge (cone) - $\alpha_1, \alpha_2, \alpha_3$ and so forth select by such form, in order to in design conditions of the work of air intake the external oblique shocks (the first it is compulsory) they were focused on the leading edge of cowling. To focus jumps is possible, obviously, at different angles α , since the angles of the slope of jumps β depend on these angles. However, the great value of coefficient σ_{ck} is obtained only at the identical intensity of jumps,

which is defined as the relation to the speed of the flow before the jump toward the speed of flow after jump.

Therefore angles $\alpha_1, \alpha_2, \alpha_3$ and so forth must ensure the equality

$$\frac{V}{V_1} = \frac{V_1}{V_2} = \frac{V_2}{V_3} = \dots,$$

where V - speed of the undisturbed flow (flight speed);

V_1 - speed of flow after the 1st oblique shock;

V_2 - speed of flow after the 2nd oblique shock, etc.

Page 133.

The speed of flow after i oblique shock V_i is connected with the speed of the flow before the abruptly following dependence:

$$V_i = V_{i-1} \frac{\cos \beta_i}{\cos (\beta_i - \alpha_i)}, \quad (7.15)$$

where V_{i-1} - a speed of the flow before the i oblique shock. For the first oblique shock, therefore, let us have

$$V_1 = V \frac{\cos \beta_1}{\cos (\beta_1 - \alpha_1)}, \quad (7.16)$$

where V - flight speed.

Flow mach number after the i oblique shock is determined as follows:

$$M_i^2 = \frac{5 + M_{i-1}^2}{7M_{i-1}^2 \sin^2 \beta_i - 1} + \frac{5M_{i-1}^2 \cos^2 \beta_i}{5 + M_{i-1}^2 \sin^2 \beta_i}, \quad (7.17)$$

where M_{i-1} - flow mach number before the i oblique shock (for the 1st oblique shock - flight mach number).

The relationship/ratio between the angle of rotation of flow (by wedge angle, cone) and the angle of the slope of jump is expressed by the formula

$$\operatorname{tg} \alpha_i = \operatorname{ctg} \beta_i \frac{M_{i-1}^2 \sin^2 \beta_i - 1}{1 + M_{i-1}^2 (1.2 - \sin^2 \beta_i)} \quad (7.18)$$

Knowing a quantity of oblique shocks, from the preceding/previous equations it is possible to determine the necessary values of the angles of stepped wedge (cone), which ensure identical intensity in jumps.

Special attention should be paid to the angle of the slope of the first surface of compression α_1 , since it actually determines the carrying out of cone (wedge) - distance from the apex/vertex of wedge to intake plane.

For contemporary supersonic air inlet (depending on calculated flight mach number) the value of angle α_1 is equal to:

| | | | |
|--------------|---|------|---------|
| α_1 | M | <2,5 | 2,5-3,5 |
| (1) Клин | | ~9 | ~7 |
| (2) Конус | | ~15 | ~11 |

Key: (1). Wedge. (2). Cone.

Angle α_2 is approximately equal to angle α_1 :

$$\alpha_2 = \alpha_1 \pm (0^\circ + 2^\circ).$$

Table 7.1 for some values of angles α gives the appropriate values of angles β (depending on flow mach number before the jump).

The length of the step/stages of cone (wedge) easily is determined, if are known angles α and β and size/dimension h .

Distance along the axis from intake plane to the apex of the cone (wedge) will be equal

$$l_1 = h / \operatorname{tg} \beta_1. \quad (7.19)$$

Table 7.1.

| α° \ M | | α° \ M | | | | | | | α° \ M | | α° \ M | | | | | | |
|--------------------|----|--------------------|-----|-----|------|-----|-----|-----|--------------------|----|--------------------|-----|-----|------|-----|-----|-----|
| | | 1,5 | 2,0 | 2,2 | 2,35 | 2,7 | 3,0 | 3,5 | | | 1,5 | 2,0 | 2,2 | 2,35 | 2,7 | 3,0 | 3,5 |
| Клин (1) | 5 | 47 | 34 | 31 | 29 | 25 | 23 | 20 | Конус (2) | 9 | 42 | 31 | 28 | 26 | 23 | 21 | 19 |
| | 7 | 50 | 37 | 33 | 31 | 27 | 25 | 22 | | 11 | 43 | 32 | 29 | 27 | 24 | 22 | 20 |
| | 9 | 54 | 39 | 35 | 33 | 29 | 27 | 24 | | 13 | 44 | 33 | 30 | 28 | 25 | 23 | 21 |
| | 11 | 58 | 41 | 37 | 35 | 31 | 29 | 26 | | 15 | 45 | 34 | 31 | 30 | 27 | 25 | 23 |

Key: (1). Wedge. (2). Cone.

Page 134.

Distance from intake plane to the beginning of the second step/stage of cone (in Fig. 7.10 - size/dimension l_2) let us find, after conducting from the point of the focusing of the 2nd jump ray/bam at angle $(\alpha_1 + \beta_2)$ to the incident flow, etc.

The throat area of air intake F_r (in cross section g-g) must decrease during an increase in the velocity of flight. Physically this is completely obvious: with an increase in the flight mach number grow/rises pressure ratio of air in the system of jumps, and consequently, are increased pressure and air density in throat, that also leads to the need of decreasing its area (otherwise air in

throat will be expanded and π_{BX} will be lowered).

Usually is calculated the necessary relative throat area

$$\bar{F}_r = \frac{F_r}{F_{BX}}.$$

The value of value \bar{F}_r , depending on flight mach number in the first approximation, can be taken

| | | | | | |
|-------------|-----|------|------|------|-----|
| M | 1,5 | 2,0 | 2,5 | 3,0 | 3,5 |
| \bar{F}_r | 0,5 | 0,42 | 0,35 | 0,32 | 0,3 |

The obtained as a result of sketch design parameters of the supersonic air inlet compulsorily are checked and are corrected in experimental tests.

Regulation of the supersonic airs inlet.

The supersonic airs inlet must provide the high values of the total pressure recovery coefficient σ_{BX} in considerably larger speed range, than subsonic air intakes. Therefore they have a control system whose task lies in the fact that to provide the matched operation of air intake and engine (the capacity of air intake must correspond to the capacity of engine).

Otherwise can arise the unstable fluctuating work (surging, "buzzing/itch" of air intake). In this case, strongly descends coefficient σ_{ax} . At supersonic speeds the task of air inlet control is reduced to hold the system of jumps (especially terminal normal shock after throat) in assigned/prescribed position. This can be made a change in the throat area and a bypass of excess air into the surrounding atmosphere. Air bleeding into the atmosphere is realized/accomplished by discovery/opening the special shutter/doors established/installed on canal surface (after throat) of air intake. These shutter/doors were called anti-surge or bypass ones. During the supersonic cruise of the shutter/door of air bleeding, they are opened slightly and the part of the air bronzes in the atmosphere, preventing thereby the emergence of the surging of air intake.

At takeoff and small subsonic flight speeds, required throat area proves to be more than value $F_{r,max}$ of that determined by the structural/design possibilities (this is explained by relatively low air density in throat). Therefore in spite of the completely opened throat, there is not enough air for normal operation of the engine. In order not to disturb engine power rating, with takeoff and at low subsonic flight speeds they are open/disclosed additionally auxiliary (takeoff) shutter/doors and inspiratory reserve it proceeds to engine, passing the throat (auxiliary and bypass shutter/doors are

shown in Fig. 7.16).

Page 135.

Structurally control system is fulfilled:

a) for changing the throat area:

- by displacement/movement of cone forward - back/ago (circular air intakes);

- by displacement/movement of mobile ramps (the two-dimensional inlets);

- by change in the diameter of inner body (circular air intakes);

b) for supplementary suction or air bleeding:

- by opening of supplementary holes in channel after throat (auxiliary and bypass shutter/doors - on all supersonic air inlet).

Air inlet control is realized/accomplished by an automatic system. The diagram of a similar system is shown in Fig. 7.11. In

system there are two main chains of control of inner body and shutter/doors of bypass, with the aid of which is realized/accomplished the regulation of Mach number in throat and the positions of closing shock wave.

3. Arrangement/position of air intakes on aircraft.

On contemporary aircraft the engines frequently are placed in the special external nacelles where the air intake directly adjoins the compressor of engine. The layout of engine and air intake is fulfilled together with the layout of engine nacelle.

During the engine installation within fuselage or wing, the air intake is separate/liberated from engine by air duct and the layout of air intake is fulfilled separately.

By the main requirement, presented to the layout of air intakes on jets, as it was already noted, it is: the guarantee of a uniform field of inlet velocities into compressor and obtaining of the high values of the total pressure recovery coefficient σ_{bx} .

The essential nonuniformity of the field of the speeds of flow can cause the vibration of compressor blades and their breakage. Even the permissible nonuniformity of the field of speeds decreases the

resource/lifetime of compressor and engine as a whole. The basic source, calling the nonuniformity of the field of the speeds in air intake, is friction (caused by the ductility/toughness/viscosity of air). The presence of friction, as is known, is caused the appearance of the boundary layer on fairing, the speed in which sharply falls from the speed of the undisturbed flow to zero.

During supersonic flow the boundary layer, interacting with shock waves, disturbs their definition: appear the local separations of flow from walls; boundary layer, passing through jumps, even more greatly increases its thickness; in the places of the inflation/swelling/bulging of boundary layer, are formed new weak oblique shocks (λ - jumps), etc.

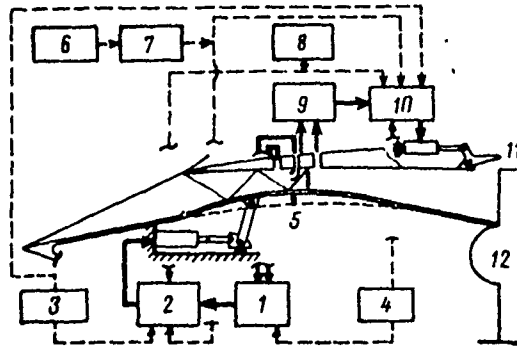


Fig. 7.11. The hypothetical control system of the supersonic air inlet (are shown basic and auxiliary functions): 1 - sensor of Mach number in throat; 2 - regulator of inner body; 3 - manual of control; 4 - sensor of surging; 5 - inner body; 6 - sensor of "disruption/separation"; 7 - launch control; 8 - sensor of Mach number; 9 - position detector of jump; 10 - regulator of bypass shutter/doors; 11 - bypass shutter/doors; 12 - engine; \longrightarrow - basic functions; $- - - \rightarrow$ - auxiliary functions.

Page 136.

The deviation from the design diagram of flow, caused by the ductility/toughness/viscosity of air, in the final analysis leads to the nonuniformity of the field of speeds and reduction/descent σ_{Dr} . Therefore all contemporary air intakes have a system of the branch/removal (drain) of boundary layer. Is driven out both the boundary layer, which was being formed on the surface of fuselage (or

wing), and the boundary layer, which arose on the surfaces of compression - cone (wedge) and internal surface of cowling (Fig. 7.12).

Boundary layer thickness δ , as is known, it depends on the speed of flow, on the coefficient of the ductility/toughness/viscosity of air and on the length of the contact of flow with the washed surface

$$\delta = f(V, \nu, x).$$

During the design of air intake for the reliable removal/distance of boundary layer the height/altitude of drainage slots ($h_1, h_2 \dots$) they accept

$$h \approx 0,01l,$$

where l - length of surface, at which is formed the boundary layer.

If, for example, air intake will close abut to the surface of fuselage (i.e. $h_1=0$), then the total pressure recovery coefficient with $M=2.5$ decreases by 25-30%, which will lead in final analysis to a reduction/descent in the engine thrust to ~45% and to an increase in the specific fuel consumption per ~15%.

For final equalization of velocity fields after the throat of the supersonic air inlet, are establish/installed the vortex generators (small plates). Place and need for the installation of vortex generators is determined in the process of the finishing of air intake (during wind tunnel tests).

The guarantee of a boundary-layer bleed is one of the special feature/peculiarities of the layout of contemporary air intakes.

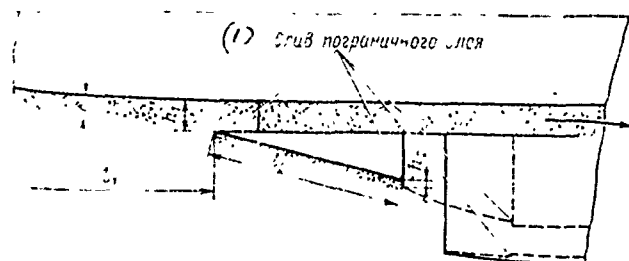


Fig. 7.12. Diagram of the branch/removal of boundary layer.

Key: (1). Boundary-layer bleed.

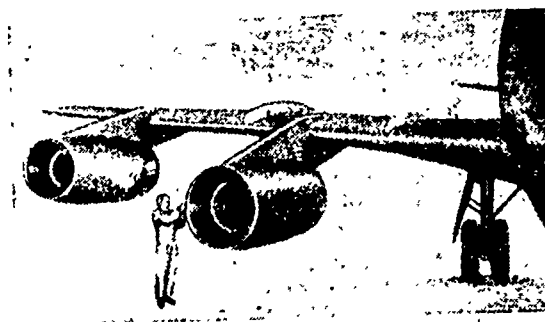


Fig. 7.13. Pylon suspension of TRDD under wing.

Page 137.

Depending on the place of arrangement/position on aircraft, are applied the following basic types of air intakes:

- 1) frontal air intakes (mainly, circular);

2) the off-axis inlets (circular, semicircular, flat/plane, etc.);

3) wingtip air intakes (mainly, flat/plane).

Frontal air intakes are placed either in to the nose of fuselage on light aircraft or in to the nose of the engine nacelle, suspend/hung from pylon under the wing of heavy aircraft (Fig. 7.13). The major advantage of frontal air intakes lies in the fact that they provide the high uniformity of velocity fields, and during supersonic flight in design conditions, furthermore, they make it possible to strictly maintain/withstand the assigned/prescribed position of the shock envelope.

However, frontal air intakes have a number of deficiency/lacks. If on heavy nonmaneuverable aircraft during entire cruise angle of attack is not changed, and consequently, the system of jumps at the entry into air intake retains assigned/prescribed position, then on light aircraft during maneuver accomplishment with large g-force, when angle of attack considerably increases, the focusing of jumps is disturbed, which leads to the nonuniformity of the field of speeds and to a reduction/descent in the total pressure recovery coefficient. Briefly stated, frontal air intakes at high angles of attack work insufficiently effectively.

The second deficiency/lack in the frontal air intakes bears layout character. Placing air intake in to the nose of fuselage, it is necessary to occupy large internal volumes in fuselage under the air duct (actually entire fuselage from nose to tail is gashed by air and engine circuit), which, naturally, complicates the layout of aircraft. Furthermore, frontal air intake does not make it possible to place in to the nose of fuselage the antenna of large-diameter radar (antenna is limited to the size/dimensicns of intake cone).

The off-axis inlets in form or entry differ in terms of great variety.

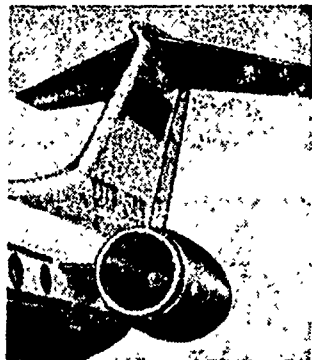


Fig. 7.14.

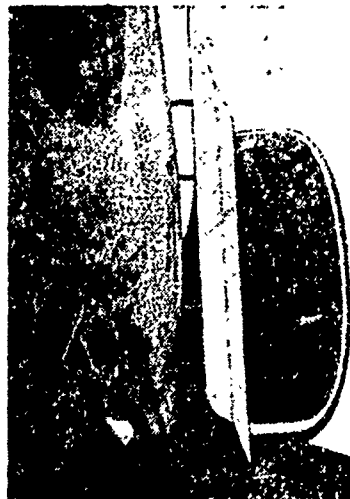


Fig 7.15.

Fig. 7.14. Engine nacelle of the aircraft of Tu-134.

Fig. 7.15. Air intake of fighter-bomber of (Phantom- II) (on surface of fuselage is visible bay for arrangement/position of rocket "Sparrow". On inside of cowling, is establish/installed PVD of the control system of air intake).

Page 138.

On subsonic aircraft in essence, are applied either the circular air intakes or the air intakes the entry form of which is close to the rectangular (deviation from circle is explained by the tendency to preserve wing profile); these air intakes are called also wing, since they are actually arrange/located in root of the wing.

The presence of boundary layer on the surface of fuselage requires the creations of drainage slots with the layout of the off-axis inlets on aircraft, for which entire engine nacelle is moved aside and is fastened to fuselage to pylon (Fig. 7.14).

It must be noted that the pylon makes it possible to only organize boundary-layer bleed, without providing, however, working conditions of frontal air intake, since wing downwashes, wake from the wing and other aircraft components create the local conditions for flow, different from the undisturbed flow.

On supersonic aircraft in essence, are applied flat/plane (Fig. 7.15) and semicircular lateral air intakes (although are encountered other entry forms). The arrangement/position of air intakes on each side of fuselage not only considerably reduced the length of air duct, but also it completely freed the nose of fuselage for the installation of radar station. During the clear organization of boundary-layer bleed, the off-axis inlets work very effectively (however during maneuver accomplishment at supersonic speed with large slip angles one of the air intakes can render/show the darkened forward fuselage).

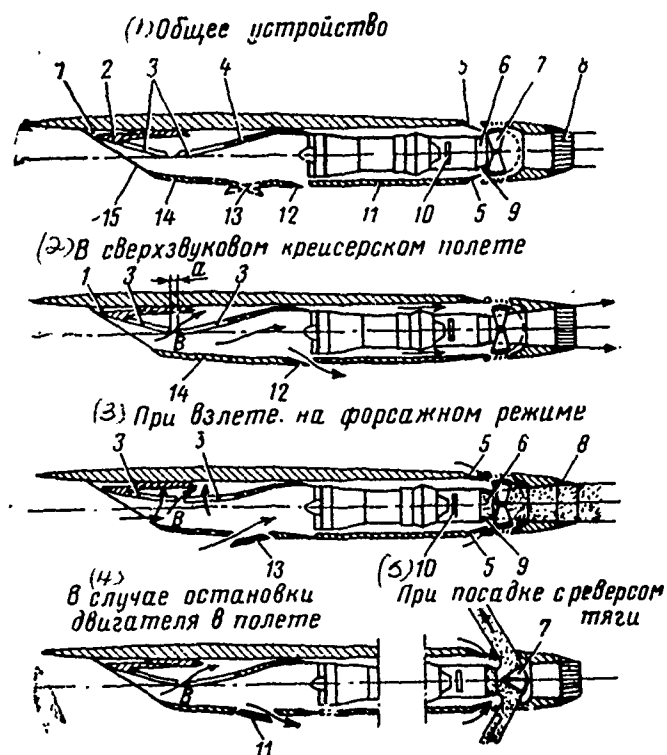


Fig. 7.16. The general-arrangement diagram of the engine nacelle of the heavy supersonic aircraft: 1 - slot for a boundary-layer bleed from the wing surface; 2 - the fixed plane of wedge; 3 - mobile ramps; 4 - subsonic air intake duct; 5 - supplementary air intake; 6 - primary nozzle; 7 - reverser of thrust; 8 - adjustable secondary nozzle; 9 - silencer; 10 - injector of afterburner; 11 - wall under engine; 12 - bypass (anti-surge) shutter/door; 13 - auxiliary (takeoff) shutter/door; 14 - cowling; 15 - vertical partition/baffle, which divides the air intakes of two engines; a) slot for a boundary-layer bleed from the plane of wedge; c) air of boundary layer.

Key: (1). General arrangement. (2). In supersonic cruise flight. (3). With takeoff in afterburning regime. (4). In the case of engine shutdown in flight. (5). During thrust reversal landing.

Page 139.

Wingtip air intakes on the existing aircraft (XB-70, Tu-144, "Concorde") have flat/plane entry. Air intake is the forward section of the engine nacelle, establish/installed under wing. In Fig. 7.16 shown longitudinal section of the engine nacelle of aircraft "Concorde".

A deficiency/lack in the wingtip air intakes is poor work on large negative angles of attack (in this case they are overshadowed by wing).

§4. The fuel system of aircraft.

The fuel system of contemporary aircraft encompasses the following basic cell/elements: fuel tanks, conduit/manifolds, pumps, valves, tap/cranes, filters and the system of different automatic machines, sensors, measuring meters, etc.

Designation/purpose of fuel system - to ensure the feed of fuel/propellant to engines in all possible for this aircraft flight conditions (on height/altitude, speed, g-forces, etc.) in a necessary quantity and with the necessary pressure. On supersonic aircraft (especially intended for a prolonged supersonic flight) the fuel system fulfills another row/series of important functions, providing cooling the system of conditioning, hydraulic system, etc., and also it can decrease the margin of the stability of aircraft, parrying the shift/shear of focus upon transfer from subsonic to the supersonic flight (see Chapter VI).

As main fuel for jet engines of contemporary aircraft, is applied the hydrocarbon fuel (improved types of kerosene). For hypersonic and aerospace aircraft are of interest cryogenic fuel/propellants (in essence liquid hydrogen).

At the high flight velocities, when the direction of heat flux in the construction of the aircraft changes to opposite, fuel/propellant (especially placed in wing tank compartments) is heated. For example, in cruise at velocity, which corresponds to number $M=3$, the heat flux, which proceeds from sheathing/skin, becomes this essential (mean temperature of sheathing/skin

~260°C) that it could heat kerosene to boiling point. The application/use of the thermal insulation (laminar honeycomb sandwich construction also considerably decreases heat flux) makes it possible to avoid the excessive heating of fuel/propellant; however, its temperature at high speeds ($M > 3$) nevertheless so is increased that hydrocarbon fuel cannot perform the role of coolant for cooling of construction/design and systems of aircraft.

One of the deficiency/lacks in the hydrocarbon fuel is its thermal instability at high temperatures (for example, for kerosene this limit it is equal to approximately 200°C). If the limit indicated is reached even to short period, then can be formed certain number of deposits of solid particles in heat exchangers, filters, injectors of engines and so forth with their possible blocking. In this connection one should speak about the superiority of liquid hydrogen as fuel/propellants for hypersonic aircraft.

At hypersonic speeds hydrogen before the feed into engine can be used for cooling the construction of the aircraft. And then the considerable difficulties, connected with the application/use of hydrogen, will be to some degree compensated.

The fact is that liquid hydrogen, possessing the irrefutable advantage before the kerosene: energy content per unit weight approximately 2.5 times more, specific heat is 7 times higher (liquid hydrogen - distinct coolant), it has a number of essential deficiency/lacks. A larger deficiency/lack in hydrogen - low density in the liquid state, that constitutes 0.1 of density of kerosene; therefore energy content per unit volume in hydrogen is approximately 4 times less. Another deficiency/lack is the low boiling point of liquid hydrogen, equal to -253°C . Therefore flight vehicles with this fuel/propellant will have large volumes, moreover fuel/propellant must be placed in the cryogenic tanks, which additionally increase weight and volume of apparatus.

The comparison of the characteristics of kerosene and hydrogen is given in table 7.2.

Differences in the physical and thermodynamic properties of hydrogen and kerosene have great effect on the possible compromise solutions, which connect the flight characteristics and the construction of the aircraft.

The arrangement/position of fuel/propellant to a considerable extent determines the overall design of aircraft, since the fuel reserve on contemporary aircraft can reach 50% and more from

takeoff weight (on Il-62 value $\bar{G}_{T,max}=0,51$; on XB-70 - $\bar{G}_{T,max}=0,57$). Is placed fuel/propellant in special fuel tanks which are divided into basic, expenditure ones and balancing ones (depending on designation/purpose and aircraft type expenditure and balancing tanks in fuel system can and not be provided for).

According to structural/design sign/criteria fuel tanks are divided into three types: rigid, soft and tank compartments of the construction of the aircraft. The major advantage of soft rubber tanks lies in the fact that they allow better than rigid tanks, to utilize a volume, they are more technologically effective and convenient in production and operation (they it is possible to coagulate and to install through handholes). Flexible tanks, furthermore, they do not fear vibrations, do not give torn edges with the leakage (small holes even are involve/tightened by a special layer of rubber), they possess good thermal insulation properties.

The advantage of rigid tanks is smaller weight in comparison with flexible tanks (together with containers). Rigid tanks are autonomous from the construction of the aircraft, they it is possible to comparatively easily repair.

Hermetically sealed tank compartments (tank-construction/design) make it possible to most rationally utilize

internal volumes of aircraft, since there is no fuel tank as such, and fuel/propellant fills into the section of wing or fuselage, covered with from within kerosene resistant (and temperature change resisting) sealing compound. The application/use of tank compartments makes it possible to increase the fuel reserve on board aircraft. However, tank compartments possess the increased vulnerability, which reduces the reliability of fuel system, it is difficult to repair them. Fuel/propellant in tank compartments directly undergoes the effect of the low temperatures in flight at subsonic speeds and high temperatures in flight at high supersonic speeds.

Table 7.2.

| (1) Характеристика топлива | (2) Керосин | (3) Водород |
|---|----------------|----------------|
| (4) Теплота сгорания в ккал/кгс | 10 290 | 28 700 |
| (5) Теплота сгорания в ккал/л | 8 700 | 2 100 |
| (6) Плотность в жидком состоянии в гс/см ³ | 0,833 | 0,0735 |
| (7) Удельная теплосемкость, в ккал/кгс·град | 0,46 | 2,7—3,7 |
| (8) Температура кипения (при давлении 1 кгс/см ²) в °С | +187—+237 | -253 |

Key: (1). Propellant property. (2). Kerosene. (3). Hydrogen. (4). Heat of combustion in kcal/kg. (5). Heat of combustion in kcal/l. (6). Density in the liquid state in g/cm³. (7). Specific heat, in kcal/kgf·deg. (8). Boiling point (at pressure 1 kg/cm²) in °C.

Page 141.

One of the basic requirements for the layout of fuel tanks on aircraft is the guarantee of a center-of-gravity location of aircraft during the consumption of fuel/propellant within the permissible limits. If aircraft is intended for a prolonged supersonic flight, then in the fuel system of this aircraft for decreasing the stability margin can be provided for the installation of the special balancing tanks (tanks, arranged/located on the largest possible removal/distance in front and from behind from the center of gravity of aircraft); by the pumping over of fuel/propellant from front/leading balancing tanks into rear ones it is possible to

approach the center of gravity focus of the aircraft (stability margin can be decreased also by the forced shift/shear of focus forward). If aircraft short-term emerges to supersonic speed, then the installation of the system of the decrease of the reserve of directional stability of the pumping of fuel/propellant on this aircraft, obviously, is unsuitable.

In Fig. 7.17 shown typical change in the center-of-gravity location and focus of aircraft in dependence on the speed (or time) of flight.

The permissible range of centering is held in flight because of the symmetrical arrangement of fuel tanks relative to the center of gravity of aircraft and specific sequence of the consumption of fuel/propellant of them. Can arise the question: it is not possible whether for decreasing value m_z^c to ensure this system of the consumption of fuel/propellant so that the center of gravity at supersonic speed would pass established/installed maximally rear with $M < 1$ position (\bar{x}_{T2}) and it did approach the focus of aircraft, for example due to the consumption of fuel/propellant only from front/leading tanks? However, this it is not possible to make on two reasons: first, if fuel/propellant from front/leading tanks will be developed (but not to be pumped over into rear ones), then the center of gravity will be shift/sheared back/ago very slowly and effect from

the decrease of the stability margin considerably will be lowered; in the second place, when the center of gravity will be located from behind position \bar{x}_{22} and through any reason it will be necessary to rapidly lower speed and to pass to subsonic flight, then it is necessary to also rapidly return the center of gravity of aircraft to the subsonic position (otherwise aircraft will become unstable), but to rapidly return the center of gravity to subsonic position it is possible only by the pumping of fuel/propellant into front/leading tanks. Therefore the system of the shift/shear of the center of gravity of aircraft with the aid of the pumping over of fuel/propellant from front/leading balancing tanks into rear ones compulsorily must provide the rapid reverse/inverse pumping of fuel/propellant upon transfer from supersonic flight to subsonic. On aircraft "Concorde" during acceleration/dispersal in transonic conditions/mod \bar{a} after 5 min it is approximately pumped over 9200 ν of fuel/propellant of four front/leading balancing tanks into rear tank. The reverse/inverse pumping of fuel/propellant upon transfer to subsonic flight speed is conducted still more rapidly - after 4 min.

The feed/supply of engines by fuel/propellant it is possible to accomplish from any fuel tanks, but most frequently for this are utilized the special service tanks, into which in the determined order is pumped over the fuel/propellant from basic tanks.

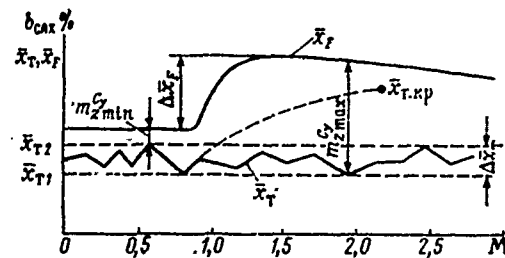


Fig. 7.17. A typical change in the center-of-gravity location and aerodynamic focus of aircraft in the flight: \bar{x}_{T1} - a maximally front/leading position center of gravity; \bar{x}_{T2} - a maximally rear position center of gravity; $\Delta \bar{x}_T$ - permissible range of position of center of gravity in aircraft; $\Delta \bar{x}_F$ - shift/shear of aerodynamic focus upon transfer from subsonic to supersonic flight; $\bar{x}_{T,sp}$ - possible position center of gravity in supersonic cruise (after the pumping of fuel/propellant from front/leading balancing tanks into rear ones).

Page 142.

Fuel system with service tank has the definite advantages, especially for the aircraft of the military designation/purpose: it possesses larger reliability, since during the malfunction of basic tanks in reserve remains service tank (to 20% of entire fuel/propellant) whose protection can be provided via armoring; one service tank (or several) to more easily equip with special devices for uninterrupted feed/supply of engine during accomplishing of the

acrobatic maneuvers, etc.

Fuel tanks can be placed both in the fuselage and in the wing of aircraft. Both that and other layout has definite advantages and deficiency/lacks. Therefore, for some aircraft fuel/propellant is placed in essence in wing, for others - in fuselage. Wing fuel tanks have the large area of the beaten surface, which leads to the smaller life of fuel system. This is a basic deficiency/lack in this arrangement of fuel tanks. However, during the arrangement/position of fuel/propellant in wing, its weight unloads wing in flight, thanks to which is obtained the specific gain in the weight of wing construction. Furthermore, during the arrangement/position of fuel/propellant in wing fuselage virtually completely can be engaged under payload which has large value first of all for passenger and transport aircraft. Therefore on all passenger, transport and heavy military aircraft fuel tanks are placed mainly in wing (Fig. 7.18).

The arrangement/position of fuel/propellant in fuselage can prove to be more advisable for military aircraft (especially low-flying). Arrange/locating fuel tanks in the fuselage above the center section, by engine, chassis/landing gear, etc., which serve seemingly protective shield from the antiaircraft fire, it is possible to raise the life of aircraft.

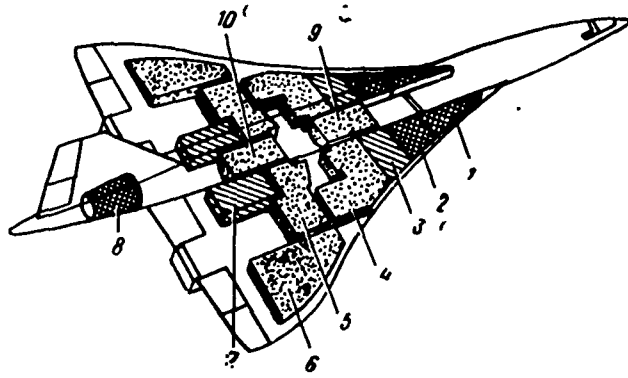


Fig. 7.18. The arrangement/position of fuel tanks on supersonic passenger aircraft "Concorde", France - England: 1; 2; 8 - balancing tanks; 3; 7 - service tanks; 4, 5, 6, 9, 10 - basic tanks.

Page 143.

Chapter VIII.

DETERMINATION OF THE BASIC PARAMETERS OF AIRCRAFT.

In present chapter is given determination of the basic parameters mainly of military aircraft. The determination of the parameters of passenger aircraft, vertical-taking off and aerospace aircraft is given in the special chapters of the book.

As already mentioned, the basic parameters of aircraft they are:

- complete (takeoff) weight G_0 ;
- wing area S ;
- thrust P_0 or power N_0 of SU, required for obtaining assigned/prescribed flight-performance data.

For determining these parameters on the initial stage of the design of aircraft, find the relative parameters p_0 and \bar{P}_0 .

§1. Determination of the value of the specific wing load.

In Chapter II, was shown, that the value of the specific wing load p_0 substantially affects the aircraft performance and its takeoff weight G_0 . In particular, the assigned/prescribed takeoff and landing characteristics can be decisive during determination p_0 . The takeoff-and-landing characteristics of aircraft include:

the landing speed

$$V_{noc} = A \sqrt{\frac{p_{noc}}{c_{y\ noc}}};$$

unstuck speed with the takeoff

$$V_{отр} = B \sqrt{\frac{p_0}{c_{y\ отр}}};$$

approach speed

$$V_{зак} = C \sqrt{\frac{p_{noc}}{c_{y\ зак}}},$$

where A, B and C - the constant coefficients, which consider air density and ground effect on c_y aircraft;

p_{noc} - the specific wing load during landing;

$c_{y\ noc}$; $c_{y\ отр}$ - lift coefficients which correspond to the landing angle of attack and to angle of attack with the breakaway of aircraft;

$C_{y_{max}}$ - lift coefficient at the angle of attack, which corresponds to approach speed.

High speed V_{noc} leads to the need for the creation of large airfields and complicates aircraft handling during landing. High speed V_{orp} leads to an increase in the size/dimensions of airfield or to the need of applying the takeoff accelerators, while high speed V_{max} impedes piloting during landing, which decreases the performing characteristics of the design/projected aircraft.

Permissible value V_{noc} depends on the designation/purpose of aircraft and possibility of applying on it of the landing parachutes and similar to them braking devices, and also reverse-thrust devices.

In the first approximation, on the basis of the statistical data, published abroad, it is possible to accept following of value V_{noc} :

for the military aircraft ... 180-250 km/h

for the military transport aircraft ... 120-150 km/h

for the trainer and sports airplanes ... 60-100 km/h.

FOOTNOTE 1. Maximum value V_{noc} is limited to permissible for the camera/chambers of wheels peripheral speed (V_{noc} less than 400 km/h).

ENDFOOTNOTE.

Allowable speed V_{3ax} usually is determined from the conditions of flight safety. For military aircraft it is possible to accept following of the value:

$$V_{3ax} = 200 - 280 \frac{(1)}{4} \text{ km/h.}$$

Key: (1). km/h.

Page 144.

It is usually considered that speed V_{3ax} must exceed the speed of disruption/separation, which corresponds $c_{y \max}$ to 20-30%, i.e.

$$c_{y \max} = \frac{c_{y \max}}{(1,2 + 1,3)^2} = (0,7 + 0,6) c_{y \max}.$$

In the first approximation, value p_0 should be selected in accordance with ^{value of} velocity V_{noc} or V_{3ax} .

Since the expendable in flight load (fuel/propellant, jettisonable loads, etc.) composes 25-60% of takeoff weight and, therefore, aircraft up to the torque/moment of landing proves to be considerably facilitated, then is expedient the value of specific

load p_{noc} , determined by the weight of aircraft at the moment of landing, to connect with V_{noc} and V_{sax} . Taking into account this, it is possible to use for determining value p_0 the following formulas:

$$p_0 = \frac{c_{y\text{ noc}} V_{\text{noc}}^2}{180 (1 - 0,8\bar{G}_r - \bar{G}_{c,r})}, \quad (8.1)$$

or

$$p_0 = \frac{c_{y\text{ sax}} V_{\text{sax}}^2}{208 (1 - 0,8\bar{G}_r - \bar{G}_{c,r})}, \quad (8.2)$$

where \bar{G}_r - the over-all payload ratio of fuel/propellant ($\bar{G}_r = G_r/G_0$);

$\bar{G}_{c,r}$ - the over-all payload ratio of jettisonable loads ($\bar{G}_{c,r} = G_{c,r}/G_0$).

In the absence on the initial stage of the design of blowoff data, it is possible to use following approximate values $c_{y\text{ noc}}$:

- for the straight wings with powerful/thick mechanization/high-lift device (slat and double-slotted extension flap) $c_{y\text{ noc}} = 2,2 - 2,5$;

- for sweptback wings ($\chi = 25 - 35^\circ$) with powerful/thick mechanization/high-lift device $c_{y\text{ noc}} = 1,8 - 2,0$;

- for sweptback wings ($\chi = 40 - 45^\circ$) with movable double-slotted flaps and slats $c_{y\text{ noc}} = 1,5 - 1,8$;

- for delta wings ($\chi_{\text{н.к}}=55-60^\circ$) with powerful/thick mechanization/high-lift device $c_{y\text{noc}}=1,0-1,2$.

The necessary value of specific load p_0 in the majority of the cases is determined from landing conditions. At the same time one should check, how obtained a value p_0 provides other assigned/prescribed flight characteristics. If, for example, is assign/prescribed a cruising speed or number $M_{\text{кретс}}$ at height/altitude $H_{\text{кретс}}$ ($\Delta_{\text{кретс}}$), then

$$p_0 = 3960 M_{\text{кретс}}^2 \Delta_{\text{кретс}} \sqrt{\frac{c_{x_0}}{D_0}} \text{ кгс/м}^2, \quad (8.3')$$

Key: (1). кгф/м^2 .

where

$$c_{x_0} = c_{x_p} k_0 + c_{x_\phi} \frac{p_0}{k_1}; \quad (8.3)$$

$$k_0 = 1,35; \quad k_1 = \frac{G_0}{\Sigma S_M}.$$

Taking into account (8.3') formula (8.3) is reduced to quadratic equation relative to p_0 . During the solution is taken real root (+ p_0).

Page 145.

Are given below the exemplary/approximate statistical values of

specific loads p_0 on the wing:

the fighters of the normal diagram ... 400-600 kgf/m²;

the fighters of the tailless diagram ... 250-300 kgf/m²;

bombers average/mean ... 350-550 kgf/m²;

bombers heavy ... 550-650 kgf/m²;

military transport aircraft with TRD heavy ... 500-650 kgf/m²;

the lungs the transport, sport and trainer aircraft ...
150-180 kgf/m²;

academic, transfer (with TRD) ... 100-150 kgf/m²;

aircraft for agriculture ... 80-120 kgf/m².

§2. Determination of the required thrust-weight ratio of aircraft.

During design the required thrust-weight ratio of aircraft $\bar{P}_0 = P_0/G_0$ is determined usually from the guarantee of the assigned/prescribed conditions:

- speed (Mach number) of flight at rated altitude $H_{\text{расч}}$;
- the takeoff run length or accelerate-stop distance;
- acceleration/dispersal for the specific time from the speed, which corresponds to number $M < 1$ to the speed, which corresponds to number $M_{\text{расч}} > 1$, and also from other conditions.

As calculated thrust-weight ratio is considered great from these conditions value \bar{P}_0 .

At assigned magnitudes $M_{\text{расч}}$, $H > 11$ km and selected value p_0 the required thrust-weight ratio

where

$$\bar{P}_0 = \frac{4650 M_{\text{расч}}^2 c_x}{\xi p_0}; \quad (8.4)$$

$$c_x = c_{x_0} + D_0 \frac{p_0^2}{294 \cdot 10^5 M_{\text{расч}}^4 \Delta^2}; \quad (8.5)$$

$$\xi = \frac{P}{P_0} \quad (1) \quad (\text{см. стр. 28});$$

Key: (1). (see Page 28).

Δ - relative density of air on to base altitude H .

If is known cruising number $M_{\text{крейс}}$ at height/altitude $H_{\text{крейс}} > 11$ км, then the starting required thrust-weight ratio

$$\bar{P}_0 = \frac{6950 M_{\text{крейс}}^2 c_{x_0}}{\xi P_0}, \quad (8.6)$$

while value $H_{\text{крейс}}$ can be found from $\Delta_{\text{крейс}}$:

$$\Delta_{\text{крейс}} = \frac{1,76 \sqrt{D_0 c_x}}{\xi \bar{P}_0}. \quad (8.7)$$

For the aircraft, intended for low altitudes, starting thrust-weight ratio is determined from following the formula:

$$\bar{P}_0 = \frac{7200 M^2 c_x}{\xi P_0}, \quad (8.8)$$

where $c_x = c_{x_0} + D_0 \frac{P_0^2}{525 \cdot 10^6 M^4}$,

(Mach number assign/prescribed).

Page 146.

From the condition of guaranteeing the assigned/prescribed takeoff run length, starting thrust-weight ratio is equal to

$$\bar{P}_0 = \frac{P_0}{0,9 c_{y \text{ отпр}} \rho_0 g L_{\text{разб}}} + 1,1 f_{\text{кан}} + 0,033, \quad (8.9)$$

where $c_{y \text{ отпр}} = 1,1 - 1,2$ - for the supersonic aircraft of normal diagram with the wing of moderate sweepback (35-45°);

$c_{y \text{ отпр}} = 0,65 - 0,67$ - for the aircraft of diagram "bobtailed aircraft" with

delta wing;

$c_{y\text{отр}} = 1,8-2$ - for military transport subsonic aircraft, and also light multipurpose aircraft;

$f_{\text{нач}}$ - rolling friction coefficient of wheels (with takeoff with concrete runway $f_{\text{нач}} = 0,03$; with takeoff from unpaved airfield $f_{\text{нач}} = 0,1$).

From safety condition takeoff (after breakaway) with one failed engine ($n_{\text{дв}} \geq 2$)

$$\bar{P}_0 = \frac{1,5}{1 - \frac{1}{n_{\text{дв}}}} \left[\left(\frac{c_x}{c_y} \right)_{\text{отр}} + \sin \theta \right]. \quad (8.10)$$

Here θ - smallest permissible climb angle

$$\begin{aligned} (\sin \theta = 0,024 - \text{для } n_{\text{дв}} = 2; \quad \sin \theta = 0,027 - \text{для } n_{\text{дв}} = 3; \\ \sin \theta = 0,03 - \text{для } n_{\text{дв}} = 4). \end{aligned}$$

Key: (1). for.

For the majority of the types of supersonic aircraft (except VTOL aircraft and STOL) starting thrust-weight ratio can be determined by following the formula:

$$\bar{P}_0 = \frac{1,2}{K_{\text{крейс}}} \left[1 + \sqrt{0,3 + \frac{(0,95 - \bar{\sigma}_{\text{т.расх}}) (H_{\text{крейс}} + V_{\text{крейс}}^2 / 2g) K_{\text{крейс}} c_{\text{р.крейс}}}{\epsilon V_{\text{крейс}} \gamma_{\text{дв}} \bar{\sigma}_{\text{т.расх}}}} \right], \quad (8.11)$$

where $K_{\text{крейс}}$ - aerodynamic aircraft quality/fineness ratio at cruising speed;

$\bar{G}_{\text{т.пакх}} = G_{\text{т.пакх}}/G_{\text{т}}$ - the over-all payload ratio of the fuel/propellant, spent for the time of entire flight;

$H_{\text{крейс}}$ - initial cruising heightⁱⁿ m;

$V_{\text{крейс}}$ - cruising speed in m/s;

$c_{\text{р.крейс}}$ - specific hourly consumption of fuel/propellant in cruise in kgf/kgf·h;

$\gamma_{\text{лв}}$ - starting weight per horsepower.

The values of dimensionless coefficient ϵ and value $K_{\text{крейс}}$ depending on the cruising Mach number are taken from of following table¹;

| | | | |
|--------------------|-------|------|------|
| $M_{\text{крейс}}$ | 2-3,5 | 6,0 | 9,0 |
| ϵ | 2700 | 3500 | 4700 |
| $K_{\text{крейс}}$ | 6-9* | 5-7 | 4-6 |

FOOTNOTE.¹ Smaller values $K_{\text{крейс}}$ are characteristic for the aircraft of small flying range, large - for the aircraft of large distance.

ENDFOOTNOTE.

FOOTNOTE 1. V. F. Mishin. Selection of engine in the period of the preliminary development of aircraft. Publ. MAI, 1968. ENDFOOTNOTE.

§3. Determination of full of (takeoff) weight aircraft.

Determination of the takeoff weight of aircraft - one of the basic tasks during the first stage of design. The degree of accuracy with which is determined G_0^2 , has special importance, since this value affects basic flight-performance data of aircraft.

FOOTNOTE 2. Here has in mind the approximate determination G_0 .
ENDFOOTNOTE.

First of all it is necessary to keep in mind that the wing area S is determined on the basis of the selected for the design/projected aircraft value of specific load p_0 ; therefore examining effect on the flight characteristics of gross weight G_0 , it is necessary to accept always $p_0 = \text{const}$.

Page 147.

The overestimate of the takeoff weight of the design/projected

or constructed aircraft always makes its flight characteristics worse. Calculation shows, for example, that during a gain in weight G_0 by 100/o number M_{max} it descends at supersonic speeds by approximately 120/o. The overestimate of weight G_0 can be obtained either in the initial stage of design - during the determination of gross weight, or in design - construction/design. If the overestimate of weight was obtained only as a result of the weight increase of construction/design, then with invariability G_0 \bar{G}_K will increase, \bar{G}_T , $\bar{G}_{c.y}$ and thrust-weight ratio \bar{P}_0 decrease and flight characteristics will deteriorate.

As is known, gross weight of aircraft encompasses empty weight G_{nyct} and weight of full load G_H . In turn, empty weight G_{nyct} includes in itself the weight of the structure of aircraft G_K , the weight of power plant $G_{c.y}$, the weight of equipment and control $G_{ob.yup}$. The weight of full load G_H consists of the fuel load G_T , of payload weight $G_{n.n}$, by representing by itself the weight of the various kinds of loads, passengers and weight of official load $G_{c.nyk}$ (crew and equipment) (Fig. 8.1). Thus,

$$G_0 = G_{nyct} + G_H = G_K + G_{c.y} + G_{ob.yup} + G_T + G_{n.n} + G_{c.nyk}$$

The determination of gross weight becomes complicated by the fact that some of its term/component/addends are the functions of the weight itself G_0 , furthermore, determination $G_{c.y}$ and G_T directly at the very beginning of design is impossible, since for this it is

necessary to know the value of weight G_0 .

For determining the weight of the structure of aircraft G_R it is also necessary to know G_0 , since the sufficiently precision determination of the weight of structure G_R possibly if and only if are known the basic dimensions of aircraft; size/dimensions can be determined only on the basis of weight G_0 . Therefore in the first approximation, gross weight is best to determine from the equation of the over-all payload ratios:

$$\bar{G}_R + \bar{G}_{c.y} + \bar{G}_T + \frac{G_{c.z.r}}{G_0} = 1,$$

where $G_{c.z.r} = G_{об.упр} + G_{п.н} + G_{служ}$ - the sum, determined sufficiently accurately on the basis of the lists of equipment, catalogs and data of statistics, moreover $G_{п.н}$ and $G_{служ}$ - are assigned; $\bar{G}_{c.y}$ and \bar{G}_T are determined from formulas. Determination \bar{G}_R is possible only when in the first approximation, gross weight of aircraft is known. Calculation is conducted as follows.

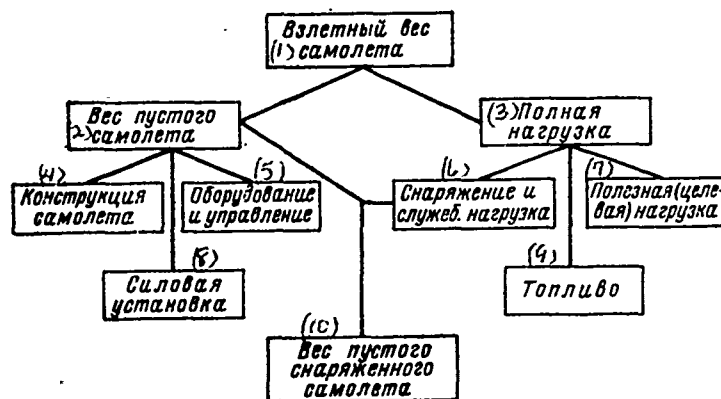


Fig. 8.1. Layout chart gross weight aircraft G_0 to components.

Key: (1). The takeoff weight of aircraft. (2). Empty weight. (3). Full load. (4). Construction of aircraft. (5). Equipment and control. (6). Equipment and duty load. (7). Useful (purposeful) load. (8). Power plant. (9). Fuel/propellant. (10). Weight of empty equipped aircraft.

Page 148.

According to formulas (2.21) and (2.23) they determine $\bar{G}_{c,y}$ and \bar{G}_T , then by formula (2.26); (2.26') or (2.26''), after assigning the probable value gross weight aircraft G_0' (utilizing statistics), is found the value of the over-all payload ratio of construction/design in the first approximation, \bar{G}'_k . Since weight $G_{c,y,r}$ is known, they obtain $G_{c,y,r}/G_0'$ and is found the sum

$$\bar{G}'_k + \bar{G}_{c,y} + \bar{G}_T + G_{c,y,r} = \Sigma \bar{G}'$$

which will be more or lesser than unity (or it is equal to unity). If sum will be equal to unity, then G_0^1 will be the first approximation of the unknown value gross weight aircraft. If sum is not equal to unity, they are assigned by the second value of gross weight G_0^{11} , they find \bar{G}_x and $G_{c.s.r}/G_0^1$ and they compute sum $\bar{G}_x + \bar{G}_{c.y} + \bar{G}_r + G_{c.s.r}/G_0^1 = \Sigma \bar{G}^1$. Further is constructed dependence $G_0 = f(\Sigma \bar{G})$ (Fig. 8.2), will be deposited points with coordinates $G_0^1, \Sigma \bar{G}^1, G_0^2, \Sigma \bar{G}^2$ and is carried out through these points smooth curve. Intersection of curve with axle/axis G_0 gives the value gross weight aircraft in the first approximation, G_0^1 .

For determination $\bar{G}_{c.y}$ it is necessary to know the required thrust-weight ratio \bar{P}_0 and specific gravity/weight of SU. The required thrust-weight ratio \bar{P}_0 is defined in the manner that it was indicated above. Specific gravity/weight of the power plant r_0 can be determined for TRD by the formula

$$r_0 = \gamma_{AB} + \Delta \gamma_{AB}, \quad (8.12)$$

where $\Delta \gamma_{AB} = \varphi \bar{G}_r / \bar{P}_0$ ($\varphi = 0.09$ for small aircraft with fuselage tanks; $\varphi = 0.13$ for large aircraft with wing tanks);

\bar{G}_r and \bar{P}_0 are taken according to statistics or given above calculation;

$\gamma_{\text{дв}}$ - weight per horsepower can be accepted according to static data ($\gamma_{\text{дв}}=0,16-0,20$).

The over-all payload ratio of fuel/propellant \bar{G}_r is determined in accordance with the fact, is assign/prescribed duration of flight t^* or distance L_{max} - according to formulas (2.22) or (2.23) and (2.23'). The entering the formulas coefficients ξ and ψ are determined from the appropriate curve/graphs. Coefficient c_x depending on speed can be undertaken from the testing of model in wind tunnel of similar to that design/projected aircraft or is calculated from the approximation formulas. Coefficient c_x is equal to $c_x=c_{x_0}+D_0\rho^2/q^2$. For aircraft with piston and turboprop engines, the over-all payload ratio of fuel/propellant is determined from formula (2.23'').

Frequently the engine for the design/projected aircraft is assign/prescribed. Then in the beginning of design are accurately known $\gamma_{\text{дв}}, c_{x_0}$, to function $\xi=f_1(M)$ and $\psi=f_2(M)$ task is reduced to check by calculation in the first approximation, will be carried out requirements for flight characteristics. If during the design of aircraft is not assign/prescribed concrete/specific/actual engine, then it is necessary to make selection from several adequate/approaching. For the solution in the first approximation, of a question of the satisfaction of requirements concerning M_{max} are constructed the plotted functions $c_x(M)$ and $c_p(M)$.

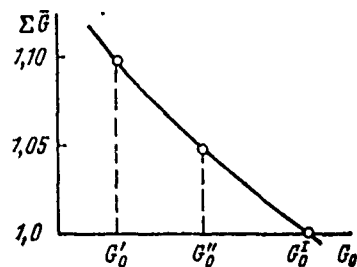


Fig. 8.2. Graphic method of determining gross weight aircraft G_0 during sketch design.

Page 149.

Thrust coefficient c_p is determined from the formula

$$c_p = \frac{P_{HI} n_{en} \rho_0}{G_0^1 q}$$

where P_{HI} - an engine thrust at rated altitude H with assigned/prescribed flight mach number;

n_{en} - quantity engine;

G_0^1 - gross weight of aircraft in the first approximation;

q - velocity head.

Through the characteristics of the selected engine, is found the

weight of power plant $G_{c,y} = P_{01} n_{дв} r_0 (P_{01}$ - the boost for launching of engine) and fuel load

$$G_T \approx G_0^I \left(SR \psi c_{p0} \frac{L_{max} \sqrt{c_{x_0} D_0}}{M_{крейс}} + u \right),$$

where ψc_{p0} - specific fuel consumption per $H_{крейс}$ and $M_{крейс}$, c_{x_0} and D_0 - for $H_{крейс}$ and $M_{крейс}$ (see Chapter II).

The value of number $M_{крейс}$ is determined graphically by construction in coordinates $M_{зад}$ and $M_{нст}$ curved $M_{крейс}$, computed from formula $M_{крейс} = 0,012 \sqrt{\frac{P_{01} n_{дв} P_0 \xi}{G_0^I c_{x_0}}}$, and ray/beam from the origin of coordinates at angle of 45° to the axle/axes (see Fig. 2.17). By the intersection with curve and ray/beam will be determined value $M_{крейс}$ at cruising altitude $H_{крейс}$, to which it will correspond

$$\Delta_{крейс} = \Delta_{нв} = \frac{1,76 G_0^I \sqrt{c_{x_0} D_0}}{P_{01} n_{дв} \xi},$$

where $P_0 \xi$ - thrust of selected engine on $M_{крейс}$ the engine characteristic for $H=0$ (coefficient ξ calculates a change in the thrust on the basis of speed, and also thrust losses of input devices of SU with $M > 1$).

After refining values $G_{c,y}$, G_T and \bar{G}_K , is determined gross weight in the second approach/approximation

$$G_0^{II} = \frac{G_{c,y,r} + G_{c,y} + G_T}{1 - \bar{G}_K}. \quad (8.13)$$

Then is found value $S = G_0^{II} / p_0$.

Knowing S , they begin the layout of aircraft, they select and more precisely formulate all size/dimensions and parameters of aircraft components, they develop/process and more precisely formulate its general view and is calculated the weight of the structure of aircraft components, utilizing for this weight formulas (for a wing, a fuselage, tail assembly, chassis/landing gear, etc.). After this is determined gross weight in the third approach/approximation:

$$G_0^{III} = G_{c.s.r} + G_{c.y} + G_r + G_k$$

they further compose the combined weight (see Appendix I).

Page 189.

Chapter XI.

SPECIAL FEATURES OF THE DESIGN OF AEROSPACE AIRCRAFT.

The continuous increase in the space flights sharply raises the question of the cost/value of delivery/procurement in space of the payload by rocket systems. This leads to the search of the fundamentally new systems which would make it possible to obtain the economically feasible cost/value of flights. ^{new}Such system is the aerospace aircraft (VKS). Besides the delivery/procurement of people and loads from the Earth to orbital stations and back, VKS will be necessary for servicing of scientific space laboratories, for the assembly of interplanetary space vehicles or for their discharging after return to the earth's orbit and so forth [38].

In order to fulfill assigned missions, the aerospace aircraft must satisfy the following basic requirements.

1. VKS must be by repeatedly utilized flight vehicle.

2. VKS must derive/conclude payload in orbit with a height/altitude of $H=150-500$ km.

3. VKS must possess good maneuverability in the atmosphere for liquidation of possible parallax of orbit (after start) and for accomplishing landing on assigned/prescribed airfield (as usual aircraft).

4. VKS must possess sufficient maneuverability in space in order to complete orbital rendezvous and accomplish mating with given object.

The use of an aerodynamic lift will make it possible to substantially lower g-forces and to select glide path, suitable with regard to aerodynamic heating. Calculations show that even with hypersonic aerodynamic aircraft quality/fineness ratio $K_r=0,5-1$ deorbit it is possible to carry out with g-force less than 2, in this case, it will not be required the special orientation of crew relative to the vector of g-force and substantially will be lowered heat transfer rate in comparison with ballistic entry.

The problem of the guarantee of landing of VKS in the assigned

place of the Earth will be reduced to the guarantee of the necessary lateral distance in hypersonic gliding/planning, since the guarantee of longitudinal distance will not apparently cause complications.

§1. Special feature/peculiarities of the flight of the aerospace aircraft.

For the aerospace aircraft there is a specific region of possible flights in the atmosphere and in space. Upper boundary of flights in the atmosphere for VKS as winged flight vehicle is determined by the combined action of the force of gravity, aerodynamic force and centrifugal force, caused by the spherical surface of the Earth. Lower boundary of flights is determined by structural strength and by permissible temperature of aerodynamic heating (Fig. 11.1).

The lower boundary of the region of flights is common/general/total for all winged flight vehicles. Upper boundary of the region depends on the special feature/peculiarities of diagram (from the value of the specific wing load and the coefficient of aerodynamic lift).

To determine upper boundary of flights of VKS in the atmosphere is possible, examining the conditions for level flight (gliding/planning) at given height/altitude. In level flight, as is known, the weight of winged flight vehicle is balanced by two forces - aerodynamic lift and centrifugal force, which appears as a result of moving the apparatus along curved path relative to the center of the Earth,

$$G = Y + P_u = \text{weight} \quad (11.1)$$

This equality will determine upper boundary of flights of VKS.

Expression for aerodynamic lift is widely-known

$$Y = c_y S \frac{\rho V^2}{2}.$$

Expression for centrifugal force in level flight it is possible to write thus:

$$P_u = \frac{G (V_{r.u} \pm V_{B.3} \cos \varphi)^2}{g (R + H)}, \quad (11.2)$$

where $V_{r.u}$ - a speed of level flight;

$V_{B.3}$ - speed of rotation of the Earth;

φ - angle of the slope of the plane of flight (orbit) to equatorial plane (orbit inclination);

H - flight altitude above the surface of the Earth (above sea

level);

R - average radius of the Earth, $R \sim 6370$ km;

g - acceleration of gravity at height/altitude H

$$g = g_0 \frac{R^2}{(R + H)^2} = 9,81 \frac{R^2}{(R + H)^2}.$$

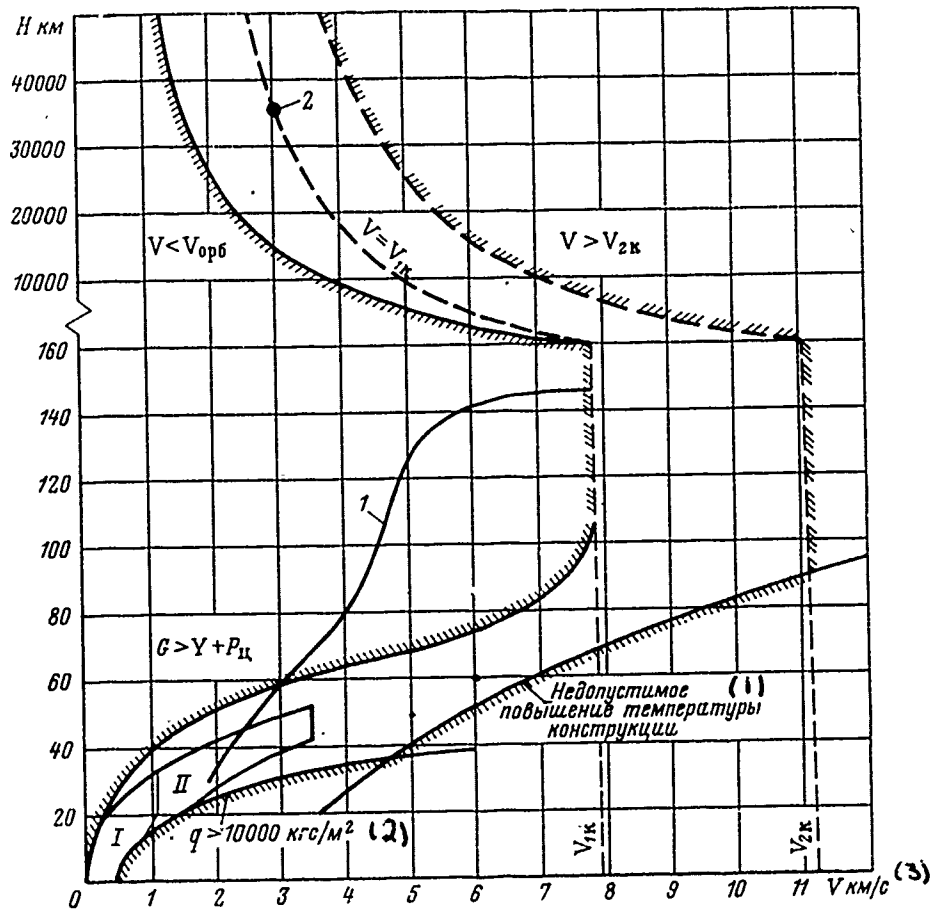


Fig. 11.1. The region of possible flights of VKS (I - region of the flights of contemporary aircraft; II - region of the flights of hypersonic aircraft): 1 - one of the possible ballistic trajectories of output/yield of VKS into space (with start from hypersonic carrier aircraft); 2 - synchronous orbit (rotating around the Earth on this orbit, flight vehicle will constantly remain above one point of equator) ($V_{орб}$ - minimum speed at which VKS can accomplish flight in

space, moving over circular or elliptic orbit; v_{1k} - orbital velocity (circular); v_{2k} - escape velocity (parabolic)].

Key: (1). Inadmissible increase of construction/design temperature.
(2). kgf/m². (3). km/s.

Page 191.

For flight altitudes where the aerodynamic force still has essential value ($H < 100$ km), expression for centrifugal force with a sufficient degree of accuracy it is possible to write thus:

$$P_{\pi} = \frac{G (V_{r,\pi} + 460 \cos \varphi)^2}{62.106} \quad (11.3)$$

Here $V_{r,\pi}$ m/s.

In flight of usual aircraft ($V < 1$ km/s) on centrifugal force it is possible to disregard (Fig. 11.2). On leaving into space, it is necessary to consider not only centrifugal force, but also angle of orbit φ . If orbit considerably differs from polar, then to launch flight vehicle is more favorable toward the diurnal rotation of the Earth. The possible angle of the orbit inclination to equatorial plane with start from any point of the Earth will be found in the range

$$\varphi_{\text{мест}} \leq \varphi \leq 90^\circ,$$

where $\varphi_{\text{мест}}$ - a local angle of the latitude (northern or southern) of

launching point.

Solving equation (11.1) relative to value ρ , we determine the value of mass air density, and consequently, let us find the necessary height/altitude, on which at given speed is feasible the level flight

$$\rho = \frac{p}{c_y} \frac{62 \cdot 10^6 - (V_{r,n} \pm 460 \cos \varphi)^2}{31 \cdot 10^6 V_{r,n}^2} \quad (11.4)$$

where $p=G/S$ - specific load on lifting surface.

Expression (11.4) determines so-called equilibrium height of flight.

Figures 11.3 show the effect of speed (but for value $p/c_y = 1000$ and angle of orbit inclination) to the upper boundary of the region of flights of VKS.

In flight in space, the aerospace aircraft becomes artificial Earth satellite. The motions of any celestial bodies (including artificial) are realized/accomplished, as is known, according to the laws of celestial mechanics at basis of which lie/rests the law of universal gravitation of Newton. Therefore the region of the steady flights of VKS in space will not have vital differences from a similar region of flights of contemporary artificial Earth satellites.

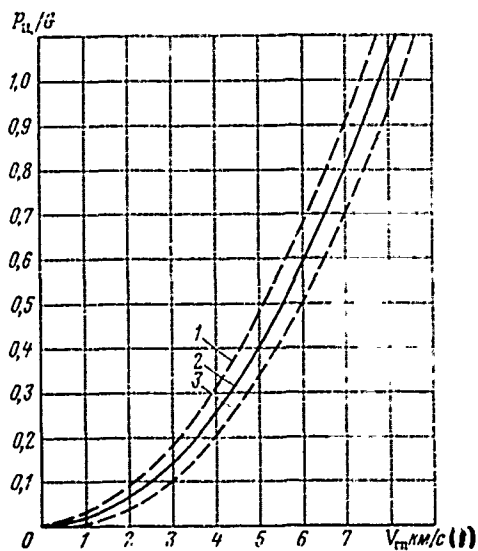


Fig. 11.2. The dependence of relation P_n/G on the speed of the level flight: 1 - flight in equatorial plane toward the diurnal rotation of the Earth ($\phi=0$); 2 - flight in the plane of the poles of the Earth ($\phi=90^\circ$); 3 - flight in equatorial plane to opposite from the rotation of the Earth side ($\phi=0$).

Key: (1). km/s.

Page 192.

Flight trajectories of VKS.

The motion of the aerospace aircraft is in general described by the system of six differential equations three of which reflect the condition of equilibrium of forces in projections on the axle/axis of inertial coordinate system, and three - moment condition of equilibrium relative to these axle/axes

$$\begin{aligned} m \left(\frac{dV_x}{dt} + V_z \omega_y - V_y \omega_z \right) &= X; & m \left(\frac{dV_y}{dt} + V_x \omega_z - V_z \omega_x \right) &= Y; \\ m \left(\frac{dV_z}{dt} + V_y \omega_x - V_x \omega_y \right) &= Z; & J_x \frac{d\omega_x}{dt} + (J_z - J_y) \omega_y \omega_z &= M_x; \\ J_y \frac{d\omega_y}{dt} + (J_x - J_z) \omega_x \omega_z &= M_y; & J_z \frac{d\omega_z}{dt} + (J_y - J_x) \omega_x \omega_y &= M_z, \end{aligned}$$

where X, Y and Z - projection of all external forces (including reaction force) to the appropriate coordinate axes;

M_x, M_y and M_z - moments of external and reaction forces relative to the coordinate axes.

Since the mass and the moments of inertia of VKS in the course of time change, then during the solution of equations of motion it is necessary to accept

$$m = m(t); \quad J_x = J_x(t); \quad J_y = J_y(t); \quad J_z = J_z(t).$$

To solve the system of equations of motion indicated is possible, if we present in the expanded/scanned form of the expression of the projections of external forces and torque/moments, entering the right sides of the equations.

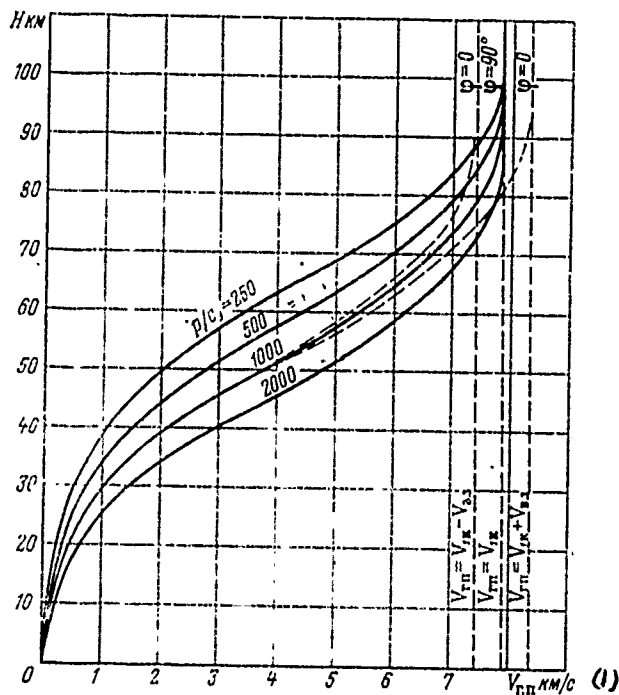


Fig. 1.3. Dependence of upper boundary of flights of VKS on speed.

Key: (1). km/s.

Page 193.

On flight vehicle act the following external forces:

- mass external forces, caused by the attraction of the Earth, sun and moon;

- aerodynamic forces (in flight in the sufficiently dense layers of the atmosphere);

- thrust of engine (in its work).

During the detailed analysis of the dynamics of flight of VKS (for example, during navigational calculations) in resolving differential equations of motion it is necessary to consider all external forces, which act on flight vehicle. However, in the period of preliminary design of VKS (when selecting of the diagram and basic parameters) it is possible to introduce the row/series of the assumptions which will make it possible to considerably simplify the system of equations of motion. For example, if we do not examine the interplanetary flight of vehicle, then it is possible to be restricted to the account only of the mass attracting force of the Earth.

Considering flight of VKS in vertical plane as the point of variable mass, we disregard the expenditure of fuel/propellant for balance and for the compensation for the random moments of roll and yaw in the process of injection into orbit. In this case are considered following forces: G , Y , X , P , moreover the thrust of

engine P they in general accept that directed along its axle/axis and sloped toward the axle/axis of aircraft (to wing chord) at angle ψ (Fig. 11.4).

At high velocities of flight (see Fig. 11.2) it is necessary to also consider centrifugal force $P_{\text{ц}}$.

Besides the enumerated forces, to flight vehicle will act Coriolis's force, caused by the diurnal rotation of the Earth. With $V \sim 3$ km/s this force is approximately 0.02 G, while when $V = V_{\text{III}}$ it reaches $\sim 10\%$ of gravitational force. Coriolis's force depends on the place of start and heading and it must be considered during navigational calculations. For the proximate analysis of motion of VKS by Coriolis's forces, it is possible to disregard.

Design/projecting the forces, which act on VKS, on the axle/axis of the high-speed/velocity coordinate system and adding to the obtained equations of motion kinematic constraints (communication/connection of change in altitude and flying range with speed and flight path angle), we will obtain the necessary system of differential equations, which makes it possible to determine the basic parameters of the trajectory:

$$\frac{dV}{dt} = \left[\frac{P \cos(\alpha + \psi) - X}{G} - \sin \theta \right] g; \quad (11.5)$$

$$\frac{d\theta}{dt} = \left[\frac{P \sin(\alpha + \psi) + Y + \frac{GV^2 \cos \theta}{g(R + H)}}{G} - \cos \theta \right] \frac{57,3g}{V}; \quad (11.6)$$

$$dH/dt = V \sin \theta; \quad (11.7)$$

$$dL/dt = V \cos \theta, \quad (11.8)$$

where α - angle of attack; θ - flight path angle to the local horizon.

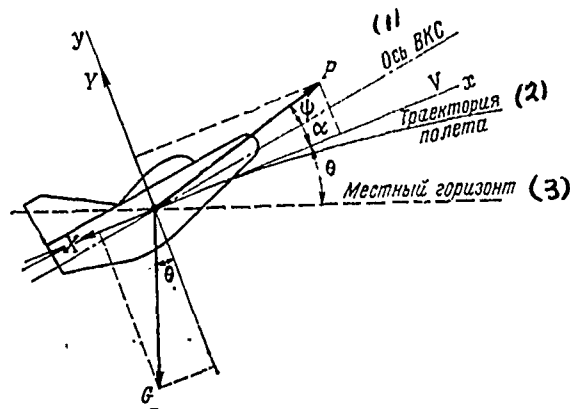


Fig. 11.4. Forces, which act on VKS in flight in vertical plane.

Key: (1). Axle/axis of VKS. (2). Flight trajectory. (3). Local horizon.

Page 194.

This system of equations can be solved by numerical integration with use the computers (during diploma design it is possible to use usual slide rule).

For the definition of the parameters of trajectory of VKS at return from space entire phase of flight can be considered as equilibrium gliding/planning, in this case, are valid following of the assumption:

$$P=0; \sin \theta \approx \theta=0; \cos \theta = 1; G = \text{const.}$$

Motion of VKS in the section of gliding/planning will be described by equations (11.1) and (11.5). The latter will take the form

$$\frac{dV}{dt} = -\frac{X}{G} g. \quad (11.9)$$

From (11.9) it follows

$$t_{\text{пл}} = \frac{G}{g} \int_{V_{\text{н.пл}}}^V \frac{dV}{-X}, \quad (11.10)$$

where $V_{\text{н.пл}}$ — a speed at the initial moment of gliding/planning (when $t_{\text{пл}}=0$).

Solving together equations (11.1) and (11.10), we will obtain expression for determining the time of the gliding/planning

$$t_{\text{пл}} = K_r \frac{R+H}{2V_{\text{IK}}} \ln \frac{(V_{\text{н.пл}} + V_{\text{IK}})(V_{\text{к.пл}} - V_{\text{IK}})}{(V_{\text{н.пл}} - V_{\text{IK}})(V_{\text{к.пл}} + V_{\text{IK}})}, \quad (11.11)$$

where $K_r = c_y/c_x$ — hypersonic lift-drag ratio of VKS;

V_{IK} — orbital velocity;

$V_{\text{к.пл}}$ — speed at the end of gliding.

In order to pass from orbital flight to the conditions/mode of

equilibrium gliding/planning, it is necessary to apply the retro impulse, which ensures

$$\Delta V_r = 30 - 70 \text{ m/c.}^{(1)}$$

Key: (1). m/s.

The speed in the beginning of gliding/planning will be equal to

$$V_{H.HH} = V_{IK} - \Delta V_r.$$

The conditions/mode of equilibrium gliding/planning begins at height/altitude $H=90-100$ km (see Fig. 11.3). For precomputations, set/assuming $R=6370$ km; $V_{IK}=7850$ m/s; $V_{H.HH} \approx 0$, it is possible to determine the complete time of gliding/planning by the approximate dependence, obtained from (11.11),

$$t_{H.HH} = 2300 \cdot K_r \text{ c.}^{(1)} \quad (11.12)$$

Key: (1). s.

It must be noted that 75-80% of time the gliding/planning occurs at speed $V > 5$ km/s (Fig. 11.5).

Glide path always can be broken in individual sections with $K_r = \text{const}$, then gliding distance can be found from (11.9), having preliminarily multiplied left and right side by V and after expressing G from (11.1):

$$\frac{1}{2} \frac{dV^2}{dt} = -\frac{g}{K_r} \left[1 - \frac{V^2}{g(R+H)} \right], \quad (11.13)$$

whence

$$L_{\text{пл}} = K_r \frac{R}{2} \ln \frac{V_{1к}^2 - V_{к.пл}^2}{V_{1к}^2 - V_{н.пл}^2}. \quad (11.14)$$

Page 195.

Equations (11.11) and (11.14) make it possible to determine $t_{\text{пл}}$ and $L_{\text{пл}}$ in any trajectory phase (i.e. for any values $V_{н.пл}$ and $V_{к.пл}$).

For precomputations the gliding distance of VKS from the torque/moment of orbit ejection to touchdown can be determined from the formula

$$L_{\text{н.пл}} = 13800 \cdot K_r \text{ км.} \quad (11.15)$$

Let us note that ~90% of entire time of gliding/planning (on distance) occurs at speed $V > 5$ км/с (Fig. 11.6).

The distance of lateral maneuver depends on value $K_r^{1.5}$. In precomputations the complete distance of lateral maneuver can be determined by the formula

$$L_{\text{п.бок}} = 1400 \cdot K_r^{1.5} \text{ км.} \quad (11.15')$$

Task regarding the flight trajectory of VKS in space coincides with the task of the determination of the orbits of celestial bodies (Kepler's task). The motion of body is examined in polar coordinate system with pole in the center of the Earth. The equations of motion of flight vehicle in polar coordinate system can be obtained,

design/projecting the external forces, which act on apparatus, to the direction of radius-vector and tangent to the circumference, described by radius-vector.

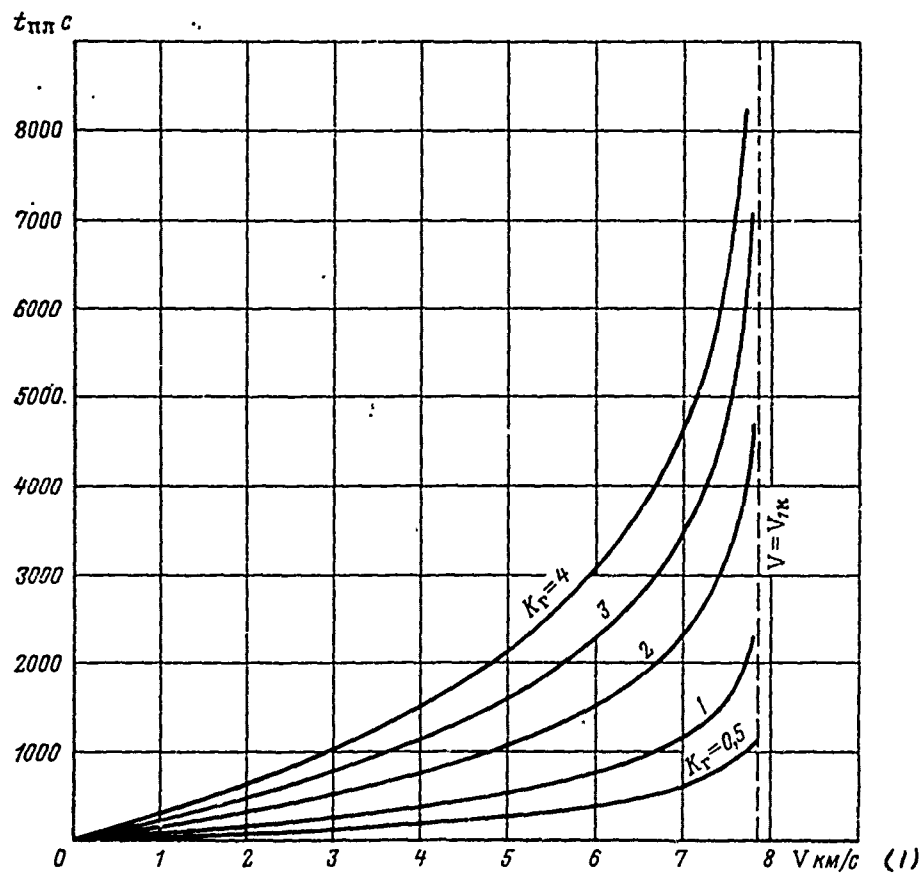


Fig. 11.5. Dependence of the time of gliding/planning on speed and hypersonic lift-drag ratio of VKS.

Key: (1). km/s.

Page 196.

In particular, equations of motion of VKS in space (in the absence of

aerodynamic forces and thrust) will take the form

$$\frac{dV_s}{dt} + V_r \frac{dx}{dt} = 0; \quad (11.16)$$

$$\frac{dV_r}{dt} - V_s \frac{dx}{dt} = -g_0 \frac{R^2}{r^2}, \quad (11.17)$$

where V_s — peripheral component of velocity;

V_r — radial component of speed;

x — angle of rotation of radius-vector (vectorial angle),
calculated off polar axis, certain initial constant/invariable in
space direction of radius-vector;

r — distance from VKS to the center of the Earth
(radius-vector).

The theory of the motion of body under conditions of space under the action of the forces of gravitation is called of elliptical theory. A great use at present elliptical theory finds during the solution of such basic tasks of cosmonautics as the determination of the orbits of artificial Earth satellites, the orbits of interplanetary flight vehicles, etc.

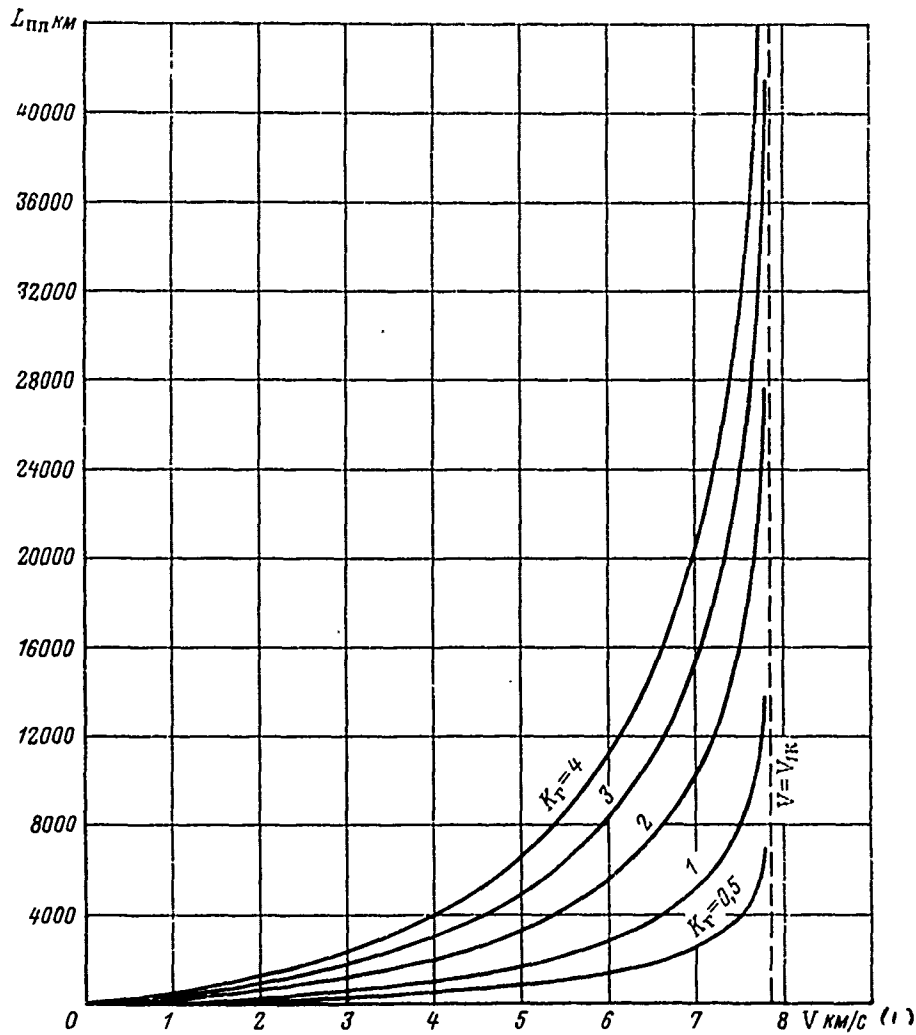


Fig. 11.6. Dependence of gliding distance on speed and hypersonic lift-drag ratio of VKS.

Key: (1) . km/s.

Page 197.

This theory determines the flight trajectories of VKS in space. So, the equation of orbit in polar coordinates can be obtained, solving the system of differential equations (11.16) and (11.17):

$$r = \frac{p}{1 + e \cos(x - x_0)}, \quad (11.18)$$

where p - a focal orbital parameter;

e - orbital eccentricity;

x_0 - initial value of angle x .

During motion in terrestrial gravitational field when the focus of orbit is arranged/located in the center of the Earth, value of the focal parameter and eccentricity will be equal to

$$p = \frac{V_0^2 r_0^2 \cos^2 \theta_0}{f M_3}; \quad (11.19)$$

$$e = \sqrt{1 - \frac{2V_0^2 r_0^2 \cos^2 \theta_0}{f M_3} + \frac{V_0^4 r_0^2 \cos^2 \theta_0}{f^2 M_3^2}}. \quad (11.20)$$

Substituting these values in (11.18), we will obtain the final equation of orbit of VKS (artificial Earth satellite)

$$r = \frac{\frac{V_0^2 r_0^2 \cos^2 \theta_0}{f M_3}}{1 + \sqrt{1 - \frac{2V_0^2 r_0 \cos^2 \theta_0}{f M_3} + \frac{V_0^4 r_0^2 \cos^2 \theta_0}{f^2 M_3^2} \cos(x - x_0)}}, \quad (11.21)$$

where $r_0 = R + H$ - initial distance from the center of the Earth;

V_0 - the initial velocity in orbit (at height/altitude H from the surface of the Earth);

θ_0 - flight path angle to the local horizon at initial point;

$f M_3$ - constant of the gravitational field of the Earth;

f - gravitational constant;

M_3 - mass of the Earth.

According to the law of universal gravitation, the weight of any body at height/altitude H from the surface of the Earth is equal to

$$G = f \frac{M_3 m}{(R + H)^2}, \quad (11.22)$$

where m - a mass of body.

The constant of gravitational field, therefore, will be equal to

$$fM_3 = g_0 R^2.$$

It is known that the form of the curve of the second order is caused by the value of its eccentricity. With $e=0$ equation (11.18) is the equation of circumference, when $e < 1$ - equation of ellipse, when $e = 1$ - equation of parabola and finally when $e > 1$ - equation of hyperbola.

One of injection condition in orbit of VKS will be equality $\theta_0 = 0$; therefore it is possible to consider that the orbit eccentricity is determined by the speed and height/altitude in the initial point of the orbit

$$e = e(V_0, H).$$

Page 198.

Let us find the necessary initial velocity for motion along circular orbit. This speed is called of circular, or firstly space (V_{IK}).

For case $e=0$ from (11.20) we will obtain

$$V_0 = V_{IK} = \sqrt{\frac{g_0 R^2}{R + H}}. \quad (11.23)$$

Circular orbit is the special case. For its realization are necessary specified conditions ($V_0 = V_{IK}$ and $\theta_0 = 0$). Furthermore, as a

result of the disturbance/perturbations, called mainly by the flattening of the form of the Earth, appear the deviations, which distort orbit shape. Therefore strictly circular orbit can be obtained only in equatorial plane. However, during the determination of the parameters of VKS the form of the Earth can be considered sphere and orbital velocity determined from formula (11.23).

For example, for height/altitude $H=100$ km the numerical value of orbital velocity (at $\phi=90^\circ$)

$$V_{ik}=7,85 \text{ km/c.}$$

At the values of eccentricity

$$0 < e < 1$$

equation (11.18) is the equation of ellipse. Ellipse, as is known, besides eccentricity and focal parameter, is characterized still by the large (a) and low (b) semi-axis

$$a = \frac{p}{1-e^2}; \quad b = a\sqrt{1-e^2}.$$

Equation (11.19) and (11.20) they make it possible to find the major axis of the elliptic orbit

$$2a = \frac{R+H}{1 - \frac{V_0^2(R+H)}{2g_0R^2}}. \quad (11.24)$$

During motion along elliptic orbit, flight altitude will continuously vary from minimum H (perigee) to the the maximum $H+\Delta H$ (apogee).

From expression (11.24) it is evident that when $V_0=V_{1K}$ the transverse will be equal to $2a=2(R+H)$, i.e., orbit is converted into circumference.

At the speed, equal parabolic, or secondly space (V_{2K}), the flight trajectory becomes parabola. Flight vehicle, which developed flight speed $V \geq V_{2K}$, to the earth does not return.

Escape velocity is determined as follows:

$$V_{2K} = \sqrt{2} \cdot V_{1K} = \sqrt{\frac{2g_0 R^2}{R+H}}. \quad (11.25)$$

For the height/altitude of 100 km $V_{2K} = 11.1$ km/s.

Figures 11.7 show the possible orbits of space vehicle.

The time of one revclution of VKS around the Earth with circular orbit at height/altitude H is equal

$$t_{Kpyr} = \frac{2\pi(R+H)}{V_{1K}} = \frac{2\pi}{\sqrt{g_0 R^2}} (R+H)^{3/2}. \quad (11.26)$$

For elliptic orbits the orbital period is determined analogously, but instead of $(R+H)$ into expression (11.26) it is necessary to substitute the value of the large semi-axis of the ellipse

$$t_{\text{orb}} = \frac{2\pi}{\sqrt{g_0 R^2}} a^{3/2}. \quad (11.27)$$

After output/yield into space, can arise the need in certain change in the orbital parameters. To change the parameters of orbit (i.e. to pass from circular orbit to elliptical and back, or to change the angle of the orbit inclination) is possible, changing value and direction of flight speed.

If it is required, for example, to increase flight altitude by value ΔH , then it is necessary to impart to flight vehicle supplementary speed ΔV_H , equal to

$$\Delta V_H = V_0 \left(\sqrt{\frac{R+H+\Delta H}{R+H+\Delta H/2}} - 1 \right). \quad (11.28)$$

Orbit will be elliptical and flight speed will be changed from V_{max} at height/altitude H (perigee of orbit) to V_{min} at height/altitude $H+\Delta H$ (apogee of orbit).

During the motion of body along orbit a change in the kinetic

energy is equal to a change potential energy

$$d\left[\frac{mV^2}{2} - mg(R+h)\right] = 0,$$

where h - height of the point of the orbit, the flight speed in which is equal to V . Since the mass of flight vehicle remains constant, then

$$\frac{V^2}{2} - \frac{g_0 R^2}{R+h} = \text{const.} \quad (11.29)$$

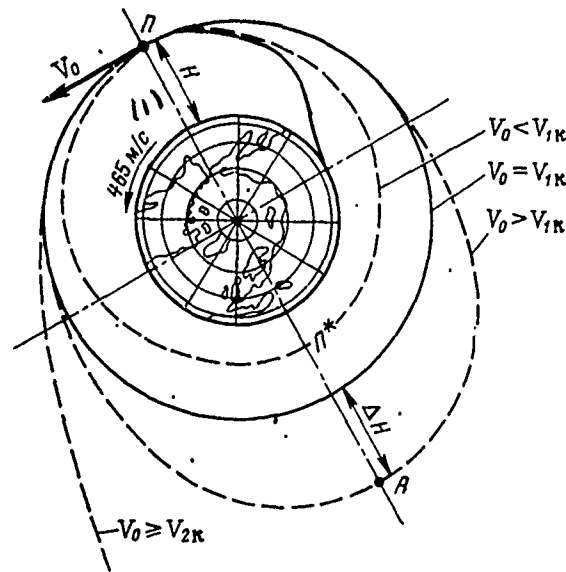


Fig. 11.7. The diagram of the removal of flight vehicle in equatorial orbit ($\phi=0$) during the maximum use of diurnal rotation of the Earth: P - perigee of orbit; A - apogee of orbit; P* - perigee of new orbit (when $v_0 < v_{1K}$ and at sufficiently large value of H).

Key: (1). m/s.

Page 200.

This expression, called the integral of energy, shows that the flight speed will depend only on trajectory height at the particular point.

From equation (11.29) we will obtain the apogee velocity of orbit (at height/altitude $H+\Delta H$)

$$V_{\min} = \sqrt{V_{\max}^2 - \frac{2\Delta H g_0 R^2}{(R+H)(R+H+\Delta H)}}, \quad (11.30)$$

where V_{\max} - the speed in the perigee of orbit.

The speed in the perigee of orbit (i.e. new speed at height/altitude H), will be, obviously, is equal to $V_{\max} = V_0 + \Delta V_H$.

At height/altitude $(H+\Delta H)$ occurs inequality $V_{\min} < V_{1H}$, therefore, if it is required to increase flight altitude, after preserving circular orbit, then flight speed at height/altitude $(H+\Delta H)$ must be increased to value V_{1H} at given height/altitude.

The simplest maneuver with respect to a change in the angle of orbit inclination to angle $\Delta\phi$, without changing flight altitude, can be fulfilled by a change in the direction of flight speed in angle $\Delta\phi$. For a similar maneuver to flight vehicle it is necessary to impart supplementary speed ΔV_φ , directed at angle $(90^\circ + (\Delta\phi/2))$ to the plane of initial orbit (Fig. 11.8). The value of the supplementary speed in this case will be equal to

$$\Delta V_\varphi = V_0 \frac{\sin \Delta\varphi}{\cos \frac{\Delta\varphi}{2}}. \quad (11.31)$$

During design of VKS a possible change in the speed for one or

DOC = 79052107

PAGE

~~34~~ 345

the other maneuver in space must be considered, since it requires the supplementary consumption of fuel sometimes of very essential.

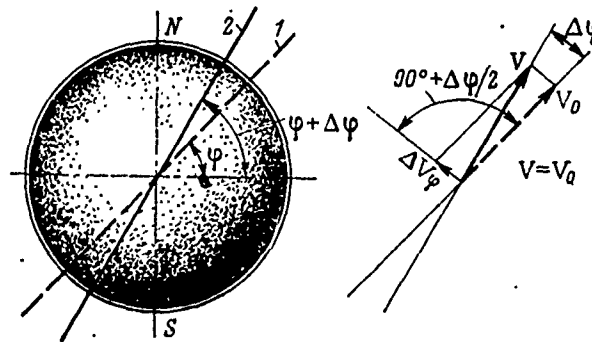


Fig. 11.8. A change in the orbital plane with $H=\text{const}$: 1 - initial orbit; 2 - new orbit.

Aerodynamic heating.

The distinctive special feature/peculiarity of flight of VKS in the atmosphere is flight at high temperatures. The external sources of heating are: aerodynamic (kinetic) heating, solar radiation, radiation of the Earth and its atmosphere. Furthermore, are other sources, heat, placed within flight vehicle. The determining value for VKS will have aerodynamic heating. Other (external and internal) sources of heating can be disregarded.

Page 201.

The bulk of heat to sheathing/skin of apparatus is fed from

boundary layer. The temperature of boundary-layer air is close to temperature of stagnation. Considering air as perfect gas (with $T < 2000$ K) and taking into account heat exchange in boundary layer, it is possible to find temperature on the internal boundary/interface of the boundary layer:

$$\left. \begin{array}{l} \text{a) the laminar boundary layer } T_{n.c} = T_H(1 + 0,17 M^2); \\ \text{b) turbulent boundary layer. } T_{n.c} = T_H(1 + 0,18 M^2). \end{array} \right\} (11.32)$$

Here T_H — the temperature of air at height/altitude H .

Determination of the temperature of skin heating. Under the conditions when heat exchange is determined by the combined action of convection, thermal conductivity and emission, the temperature of sheathing/skin of flight vehicle can be determined from the equation of the balance of the heat:

$$q_{n.c} - q_{изл} = c \gamma \delta \cdot \frac{dT_{об}}{dt}, \quad (11.33)$$

where $q_{n.c}$ — heat transfer rate from boundary layer, i.e., the quantity of heat, which enters the sheathing/skin the unit of area per unit time in kcal/m²s;

$q_{изл}$ — heat transfer rate, emitted by sheathing/skin into the

surrounding space;

c - specific heat of skin material in kcal/kgf·deg;

γ - the specific gravity/weight of skin material in kgf/m³;

δ - thickness of sheathing/skin m;

t - time in s;

T_{06} - the temperature of the external surface of sheathing/skin in deg K.

Equation (11.33) describes the unsteady thermal process, by which the temperature of surface of body changes in the course of time. The solution of this nonlinear differential equation can be obtained by the methods of numerical integration.

The greatest temperature of sheathing/skin will be when $dT_{06}/dt=0$. In this case occurs the steady heat exchange and the equilibrium temperature of sheathing/skin which is establish/installed during endurance flight under constant/invariable conditions. In this case, $q_{n,c} = q_{n,n}$.

Emitted by sheathing/skin heat transfer rate is determined according to the law of stefana - Boltzmann

$$q_{\text{изл}} = \varepsilon \sigma T_{06}^4, \quad (11.34)$$

where ε - radiation coefficient, or emissivity factor of sheathing/skin;

$\sigma = 1.37 \cdot 10^{-11}$ kcal/m²s•deg⁴ - radiation coefficient of blackbody.

Coefficient ε estimates the radiating capacity of body (sheathing/skin) in comparison with blackbody. It depends on material of surface and its treatment, and also on temperature. For the sheathing/skin of VKS, it is possible to accept $\varepsilon \approx 0.9$.

Heat transfer rate, which enters the sheathing/skin from boundary layer, in accordance with Newton's law, is determined as follows:

$$q_{\text{n.c}} = \alpha (T_{\text{n.c}} - T_{06}), \quad (11.35)$$

where α - a local coefficient of convection heat transfer on boundary/interface air - sheathing/skin in kcal/m•deg.

Considering equalities $q_{\text{изл}}$ and $q_{\text{n.c}}$, we will obtain the equation, which makes it possible to determine the temperature of

sheathing/skin during the steady heat exchange,

$$\epsilon\sigma T_{ob}^4 + \alpha T_{ob} - \alpha T_{u.c} = 0. \quad (11.36)$$

Page 202.

The coefficient of convection heat transfer α has different values for a plate and for the critical point of spherical body. The approximation of the coefficient of heat transfer for a plate takes the form:

$$\alpha \approx 0,5g\rho V c_p c_f Pr^{-1/4}, \quad (11.37)$$

where c_p - heat capacity of the air at a constant pressure in kcal/kg·deg;

c_f - the coefficient of air friction against the surface of sheathing/skin, depending on Reynolds number and structure of boundary layer;

$Pr = \mu c_p g / \lambda$ - Prandtl number;

μ - coefficient of the ductility/toughness/viscosity of air in kg·s/m²;

λ - coefficient of thermal conductivity of air in kcal/m·s·deg.

The physical constants of the air ρ , μ , λ , which depend on temperature, must be taken for the so-called determining temperature

$$T_{on} = T_H + 0,72(T_{n.c} - T_H). \quad (11.38)$$

Prandtl number depends on the temperature of air (table 11.1). At large temperatures ($T_{on} > 1250$ K) Prandtl number can be considered constant.

For the approximate estimate of the temperature of sheathing/skin the coefficient α can be determined thus:

the laminar boundary layer

$$\alpha = 31,6 g \rho V c_p (\rho V x / \mu)^{-0,5} Pr^{-0,67}; \quad (11.39)$$

the turbulent boundary layer

$$\alpha = 0,184 g \rho V c_p (\rho V x / \mu)^{-0,2} Pr^{-0,67}, \quad (11.40)$$

where

$$x \approx \frac{0,0038}{\left(1 + \frac{120}{T_H}\right) \rho M}. \quad (11.41)$$

The given formulas are valid for determining the temperature of the wing skin, tail assembly and cylindrical of the part of the

fuselage (housing).

For the coefficient of convection heat transfer near critical point with laminar boundary layer, it is possible to accept the following expression:

$$\alpha = 0,54 Pr^{-0,66} g c_p \sqrt{\beta \rho \mu V / r}, \quad (11.42)$$

where r - a radius of the nose section of the body:

$$\beta = 2,82 \sqrt{\frac{p}{p_c} \frac{1}{(1 + 0,2M^2)^{2,5}}}. \quad (11.43)$$

Here p and p_c the pressure of the flow before and after the normal shock of pressure. Relation p/p_c is determined from of known to the formula gas dynamics

$$\frac{p}{p_c} = 11,3 \frac{(1 + 0,2M^2)^{3,5}}{1,167M^2 - 0,167} \left[\frac{2,43(1 + 0,2M^2) - 2,5}{M^2} \right]^{3,5}.$$

Using equation (11.36) and given above formulas, it is possible to calculate the equilibrium temperature of the sheathing/skin of VKS (and also any other aircraft) during aerodynamic heating.

Table 11.1.

| | | | | |
|------------|------|-------|-------|------|
| T_{on} K | 500 | 750 | 1000 | 1250 |
| Pr | 0,69 | 0,665 | 0,655 | 0,65 |

Page 203.

Figures 11.9 give approximate values of equilibrium temperature for the probable region of flights of VKS (for small angles of attack).

The intensity of the aerodynamic heating of surface substantially decreases during an increase in the distance from leading wing edge (from the leading edge/nose of fuselage) and during an increase in the sweep angle of wing (tail assembly). Figures 11.10 show isotherms on the surface of hypersonic aircraft in cruise at the height/altitude of 34 km with $M=8$. Should be focused attention on the temperature distribution on lower intake plane (temperature distribution on plane at permanent angle of attack and zero angle of sweepback).

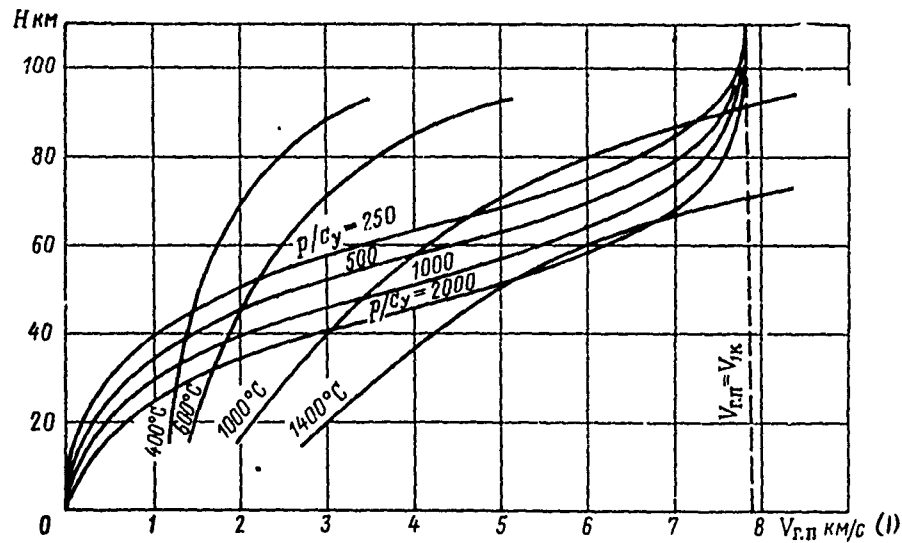


Fig. 11.9. Equilibrium temperature of flat surface at a distance $x=1.5$ m from leading edge ($\xi > c$).

Key: (1). km/s.

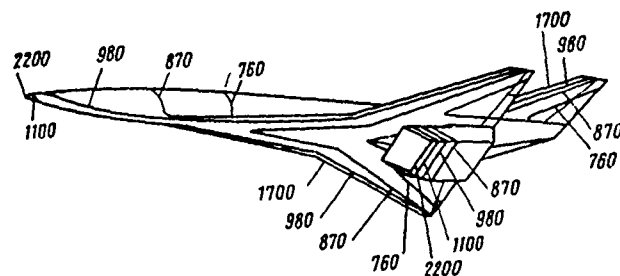


Fig. 11.10. Steady temperature in surface of aircraft (in $^{\circ}\text{C}$) during endurance flight ($V=2400$ m/s $H=34$ km).

Page 204.

§2. Selection of the diagram of the aerospace aircraft.

If we by payload understand the weight of the apparatus, concluded in orbit (without considering, naturally, the weight of the structure of the last/latter step/stage of accelerator, which will also reach orbital speed), then the most adequate/approaching criterion for analysis and selection of diagram will be payload fraction

$$\bar{G}_{n,n} = G_{n,n}/G_0,$$

where $G_{n,n}$ - the weight of the apparatus, concluded in orbit;

G_0 - launching weight of system.

Although this criterion is not exhausting (more common/general/total criterion is the cost/value of system), nevertheless it plays main role, since on $\bar{G}_{n,n}$ depends, other conditions being equal, the cost/value of the delivery/procurement 1 kg of the payload in orbit.

At the assigned/prescribed value of payload weight evaluation criteria of diagram of VKS will be, obviously, the value of launching weight of system.

Possible diagrams of the aerospace aircraft. The most important aircraft characteristics for the delivery/procurement of load in orbit is the minimally necessary flight speed in orbit V_{op0} (for flight altitude $H < 500$ on km $V_{op0} \approx V_{IK}$). A strict guarantee of assigned/prescribed flight speed not for one flight vehicle has this important value as for space vehicles. For example, if aircraft was design/projected for the flight speed $V = 3185$ cf km/h ($M = 3$), but in actuality speed render/showed to 10/o less, i.e., $V = 3153$ km/h ($M = 2.97$), then this virtually in any way will not be reflected in the effectiveness of this aircraft. For an orbital apparatus the error in speed to 10/o (i.e. instead of 7.8 km/s to obtain 7.72 km/s) indicates starting/launching idle, since apparatus will not be held in orbit and it will complete landing, having fulfilled not one turn around the Earth. Therefore the most important and necessary flight condition on orbit is the achievement of corresponding to speed of flight. This condition will to a considerable degree determine the diagram and the basic parameters of orbital flight vehicles.

To find communication/connection of orbital speed with the basic parameters of flight vehicle is possible, analyzing the process of

acceleration/dispersal and climb on leaving in orbit.

In the process of acceleration/dispersal and climb, flight vehicle acquires the speed which in general can be written thus:

$$V = V_n - \Delta V_n + V_{cr}, \quad (11.44)$$

where V_n - the ideal velocity of apparatus, i.e., the speed which the apparatus would obtain in the absence of force of gravity and aerodynamic drag;

ΔV_n - total speed losses from the action of gravitation and aerodynamic drag;

V_{cr} - the starting speed of apparatus (for single-stage apparatuses with start from the Earth, obviously $V_{cr}=0$).

The ideal velocity of apparatus is determined from known formula of K. E. Tsiolkovskiy

$$V_n = W_e \ln m_{HA} / m_{KH}$$

where W_e the effective exhaust velocity;

m_{HA} the initial mass of apparatus;

$m_{\text{КОН}}$ - the finite mass of apparatus (after burnout).

Expressing effective discharge velocity through the specific impulse (the specific thrust of engine), and the mass of the flight vehicle through weight, we will obtain

$$V_{\text{II}} = g_0 J_{\tau} \ln \frac{G_{\text{НАЧ}}}{G_{\text{КОН}}} = 9,81 J_{\tau} \ln \frac{1}{1 - \bar{G}_{\tau}}, \quad (11.45)$$

where J_{τ} - specific jet firing (on fuel/propellant);

$\bar{G}_{\tau} = G_{\tau} / G_{\text{НАЧ}}$ - the over-all payload ratio of fuel/propellant.

Page 205.

On value ΔV_{τ} especially essential effect has the velocity of start.

For the concrete/specific/actual diagram of flight vehicle on leaving in orbit according to the specific trajectory value ΔV_{τ} can be determined, integrating equations of motion (11.5)-(11.7).

In the period of preliminary design this value can be accepted approximately; with a sufficient degree of accuracy of its it is possible to remove/take from the curve/graph of Fig. 11.11 which we get as a result of the trajectory calculation of injection into orbit

with a height/altitude of $H=120-200$ km; in this case were examined different diagrams of flight vehicles with the actually possible parameters.

Injection into orbit with $H>200$ km can be broken into two stages:

1) output/yield to $H\sim 150$ km;

2) maneuver on an increase in altitude of orbit by value ΔH [see (11.28)].

A required quantity of fuel/propellant $G_{\tau, \text{HOT}}$ for injection into orbit we will obtain, accepting in (11.44) $V=V_{1K}$ and deciding together (11.44) and (11.45) relatively \bar{G}_{τ} ,

$$\ln \frac{1}{1 - \bar{G}_{\tau, \text{HOT}}} = \frac{V_{1K} + \Delta V_{II} - V_{CT}}{9.81 J_{\tau}},$$

or

$$\bar{G}_{\tau, \text{HOT}} = 1 - \frac{1}{e^{\frac{V_{1K} + \Delta V_{II} - V_{CT}}{9.81 J_{\tau}}}}, \quad (11.46)$$

where $\bar{G}_{\tau, \text{HOT}} = G_{\tau, \text{HOT}} / G_{\text{HAY}}$;

G_{HAY} the initial weight of apparatus (when $V=V_{CT}$), for single-stage

apparatuses $V_{cr}=0$ and $G_{HAY}=G_0$.

Figures 11.12 depict the graphic interpretation of equation (11.46) for several values of starting speed.

Possible values \bar{G}_r and \bar{G}_n for contemporary aircraft and aircraft of the nearest future are given in Fig. 11.13.

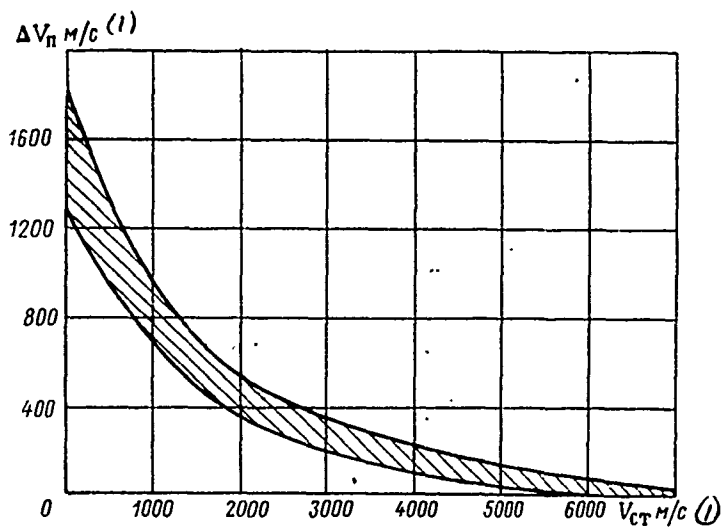


Fig. 11.11. Effect of the speed of start on total speed losses from the action of gravitation and aerodynamic drag (for orbits $H=120-200$ km).

Key: (1). m/s.

Page 206.

For injection into orbit, flight vehicle with ZhRD when $J_T = 250-450$ s must have the over-all payload ratio of fuel/propellant $\bar{G}_T = 0,98-0,87$ when $M_{CT} = 0$ (see Fig. 11.12).

If flight vehicle will start from hypersonic carrier aircraft (for example, when $M_{CT} = 6-12$), then the necessary fuel reserve for injection into orbit decreases; however, also in this case it will be equal to $\bar{G}_{T, \text{not}} = 0,78-0,64$ for $J_T = 450$ s (fuel/propellant H_2+O_2).

Only start with $M_{CT} \geq 18$ gives the possibility of injection into orbit ($\bar{G}_{T, \text{not}} \leq 0,45$).

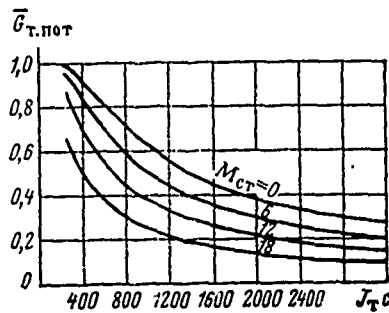


Fig. 11.12.

Fig. 11.12. Dependence of the over-all payload ratio of fuel/propellant, required for injection into orbit ($H=120-200$ km), from specific jet firing.

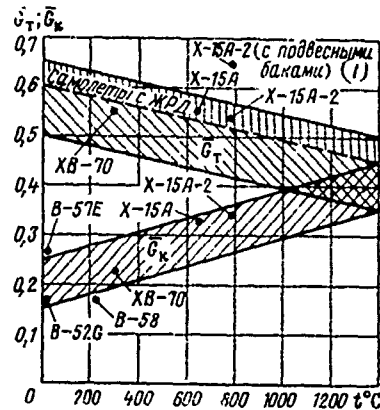


Fig. 11.13.

Fig. 11.13. Change in over-all payload ratio of fuel/propellant and construction of aircraft in dependence on operating temperature of construction/design.

Key: (1). suspension tanks. (2). Airplanes with liquid propellant rocket engines.

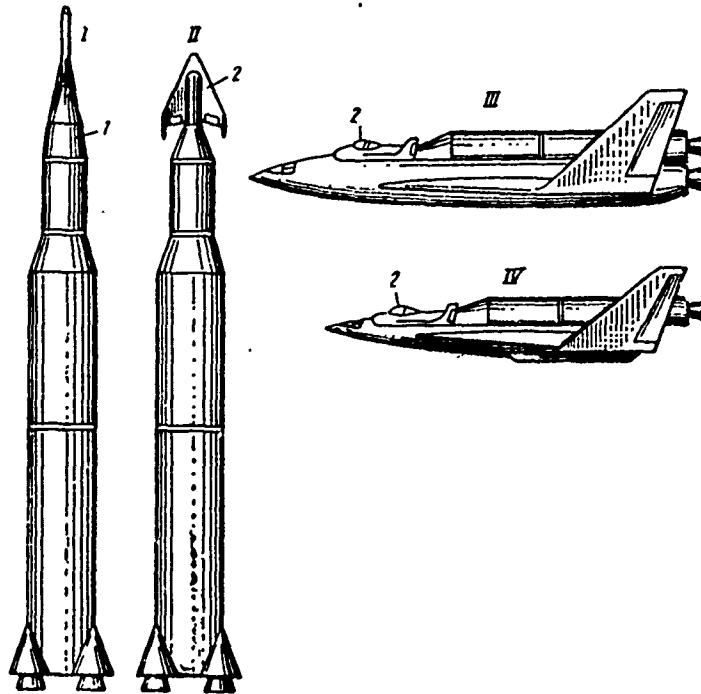


Fig. 11.14. The possible diagrams of flight vehicles for the delivery/procurement of the payload in orbit (as fuel for all engines is utilized liquid hydrogen): 1 - space ship with ballistic entry into the atmosphere; 2 - VKS.

Page 207.

Therefore it is possible to draw a conclusion relative to the diagram of the apparatus: to supply the payload in orbit and to complete return and landing to the earth at present (when $J_T \approx 450 s$) can only multistage flight vehicles. Figures 11.14 show the possible

diagrams of such flight vehicles.

Payload in diagram I is space vehicle with ballistic entry into the atmosphere; landing to the earth is conducted with the use of parachutes. The apparatuses of diagrams II, III and IV have identical payload - the aerospace aircraft, which accomplishes planning/gliding entry into the atmosphere and horizontal landing to the earth.

Diagrams I and II are identical and are characterized by only payload. These diagrams are based on the principle of the maximum use of the existing construction/designs of rockets. The high cost/value of carrier rocket leads to the need for the searches of the repeated use of step/stages. Is most expedient the rescue of first stage, since in this case from 75 to 80% of weight of an entire structure of carrier rocket it returns conversely.

The best possibilities in the creation of the repeatedly utilized space systems gives the hypersonic carrier aircraft (booster), piloted by crew and which independently returns to the place of start after the starting/launching of space vehicle (diagram III and IV). Upon transfer from ballistic ones to the winged aerospace systems of repeated application/use, the cost/value of the delivery/procurement of the payload in orbit considerably will be lowered.

Diagram III is one of the possible versions of the rescue of the first booster stage with ZhRD.

Diagram IV is most promising. During use in the process of the acceleration/dispersal or high specific impulse, VRD can be obtained very large gain in useful load, concluded in orbit, in comparison with the carriers, equipped with ZhRD. Carrier with VRD will be close to aircraft in diagram and accomplishing of operations.

The effectiveness of carrier with VRD is visible from Fig. 11.15.

Certain representation of the weight distribution of the apparatuses of the examined diagrams gives Fig. 11.16.

It should be noted that diagram IV provides not only the repeated use of the expensive first step/stage, it makes it possible to substantially raise value $\bar{G}_{\text{нн}}$. For an orbital injection one and the same of payload the launching weight of the flight vehicle, designed by diagram IV, will be two times less in comparison with the best specimen/samples of the contemporary carrier rockets:

$$\begin{aligned}\bar{G}_{\text{нн}} &= 0,10-0,12 \text{ (diagram IV);} \\ \bar{G}_{\text{нн}} &= 0,05-0,06 \text{ (diagram I, II),}\end{aligned}$$

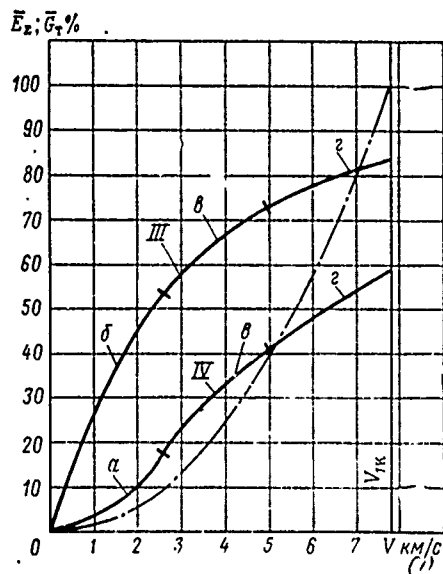


Fig. 11.15. The dependence of relative energy, to the communicated payload on leaving in orbit, and the relative fuel consumption on speed for diagrams III and IV in Fig. 11.14 (as fuel for all engines is utilized liquid hydrogen): a) carrier aircraft with VRD; b) first stage with ZhRD; c) the second step/stage with ZhRD; d) the third step/stage with ZhRD

$$\begin{aligned} \text{---} & \text{---} \bar{E}_r = E_r / E_{r0p6} \\ \text{---} & \text{---} \bar{G}_r = G_r / G_0 \end{aligned}$$

Key: (1) . km/s.

Page 208.

During the use of nuclear rocket engines (YaRD) whose specific impulse will considerably exceed specific impulse ZhRD, diagram IV

will change toward the decrease of a quantity of step/stages.

So, when $J_T \approx 1000$ s VKS with YARD, starting from carrier aircraft, will leave in orbit without supplementary accelerators. When $J_T \approx 2000$ s drops off the necessity also for carrier aircraft, since VKS according to equation (11.46) can independently (starting from the Earth) emerge in orbit.

During wide use YARD with specific impulse ~ 2000 s the era of rockets as flight vehicles for the conclusion/derivation of payload in orbit, apparently, it will end, since the key advantage of rocket step/stages - a high load ratio on fuel/propellant - it will lose its value, since required fuel load for injection into orbit when $J_T > 2000$ s will be $\bar{C}_{r, \text{not}} < 0,4$ (see Fig. 11.12).

The diagram of the aerospace aircraft must provide:

- obtaining the necessary value of lift-drag ratio in hypersonic and subsonic flight conditions;
- light thermal loads upon entry into the atmosphere.

Apparatus with $K_r = 0$ is experience/tested upon entry into the atmosphere g-force from 8 to 10. An increase in the lift-drag ratio

DOC = 79052108

PAGE

369

in all to 0.5 makes it possible to decrease the g-force in an entire line of descent to two.

Investigations showed that in the majority of the cases the hypersonic lift-drag ratio VKS can be restricted by value

$$K_r = 1 - 2.$$

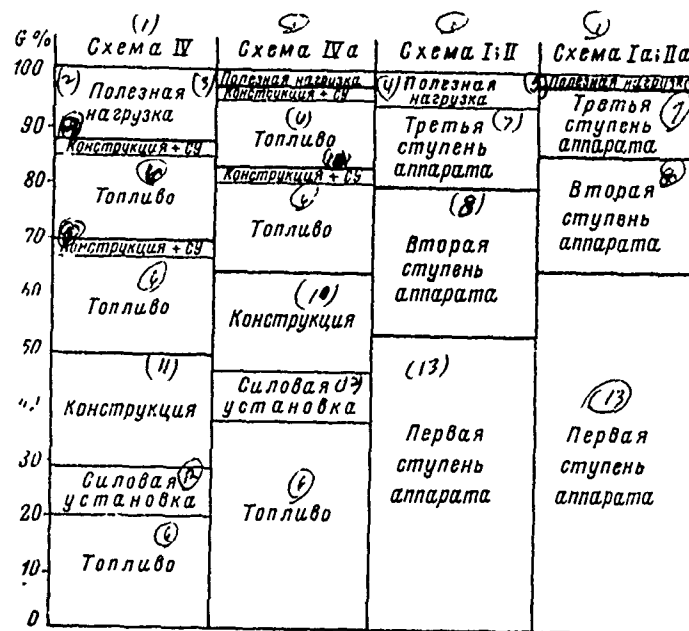


Fig. 11.16. The diagram of the weight distribution of flight vehicles for the delivery/procurement of the payload in orbit (with start from the Earth), in diagrams all I, II, IV engines work on liquid hydrogen, in diagrams Ia, IIa, IVa, all engines work on kerosene.

Key: (1). Diagram. (2). Payload. (3). Payload of construction. (4). Payload. (5). Useful load. (6). Fuel/propellant. (7). Third step/stage of apparatus. (8). Second step/stage of apparatus. (9). Construction/design. (10). Construction/design. (11). Construction/design. (12). Power plant. (13). First stage of apparatus.

Figures 11.17 show a change of the physical characteristics VKS in dependence on value K_r . A gain in weight of apparatus during an increase in the hypersonic lift-drag ratio is connected with an increase in the relation to surface area toward working volume, with an increase in the duration of flight, which leads to large common/general/total thermal loads.

Acceptable landing data VKS are provided with the value of subsonic lift-drag ratio not less than four.

At present are conducted the widespread investigations of the aerodynamic shapes of the maneuvering aerospace apparatuses of repeated application/use, in this case, special attention is given to the apparatuses with lifting body. The major advantage of such apparatuses (in comparison with winged ones) is the less complicated resolution of the problem of the thermal insulation of construction/design. For an improvement in the subsonic and landing data VKS with lifting body, it is proposed to utilize a special wing with the subsonic airfoil/profile (with $M > 1$ wing is removed).

The evolution of diagram VKS is shown in Fig. 11.18.

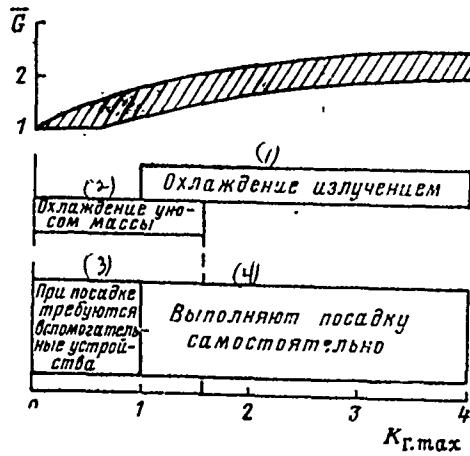


Fig. 11.17. Effect of hypersonic lift-drag ratio on characteristics VKS.

Key: (1). Radiation cooling. (2). Cooling by ablation. (3). During landing are required auxiliary devices. (4). Is fulfilled landing independently.

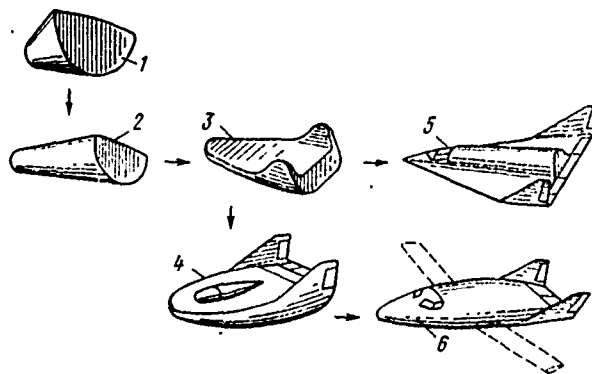


Fig. 11.18. The evolution of diagram VKS: 1 - blunted semicone with the aperture angle of 60°; 2 - blunted semicone with the aperture

angle of 30° ; 3 - semicone with the endplates; 4 - VKS with lifting body (lower surface oval); 5 - winged VKS; 6 - VKS with lifting body (lower surface flat/plane)

| Cxcms | P | | Cxcms | P | |
|-------|-------------|--------------|-------|-------------|------------|
| | M > 10 | M < 1 | | M > 10 | M < 1 |
| 1 | $K_r = 0.5$ | $K \sim 0.8$ | 4 | $K_r = 1.3$ | $K \sim 4$ |
| 2 | $K_r = 1.2$ | $K \sim 2$ | 5 | $K_r = 2$ | $K \sim 8$ |
| 3 | $K_r = 1.2$ | $K \sim 4$ | 6 | $K_r = 2$ | $K \sim 8$ |

Key: (1). Diagram.

Page 210.

§ 3. Determination of the basic parameters of the aerospace flight vehicle.

Let us examine the basic parameters for panoramic sketches.

Let us consider that the optimum parameters correspond $(\bar{G}_{II})_{\max}$ in acceleration/dispersal to V_{III} .

Figures 11.19 show the project VKS, designed for 10-12 people.
Apparatus of multistage circuit.

The diagram of apparatus they will in general determine: carrier aircraft (retained step/stage), accelerators (nonrecoverable

step/stages) and VKS (retained step/stage) (see Fig. 11.14, diagram IV).

Launching weight of apparatus is equal to

$$G_0 = G_{c.H} + G_{y1} + \dots + G_{ym} + G_{BKC}, \quad (11.47)$$

where $G_{c.H}$ - weight of carrier aircraft;

G_{y1} - weight of the first accelerator;

G_{ym} - weight of the m accelerator;

G_{BKC} - weight VKS;

m - number of accelerators.

For determining the optimum values of the parameters of a similar flight vehicle, it is necessary to answer two questions:

- 1) what payload and to what speed (in these parameters) it is capable to drive away carrier aircraft;
- 2) what part of this load it is capable of leaving on near earth orbit. In other words, it is necessary, providing the maximum of criterion $\bar{C}_{H.H} = G_{BKC}/G_0$, to find minimum launching weight of system, if is assign/prescribed

concrete/specific/actual weight VKS or, if has in mind concrete/specific/actual carrier aircraft, to find maximally possible weight VKS, capable of leaving in orbit with start from this carrier aircraft.

Let us introduce following of concept and designation:

G_i - weight of the i step/stage;

G_{Hi} - useful load, accelerate/dispersed with the i step/stage to speed $V = V_{cti} + \Delta V_i$ and height/altitude $H = H_{cti} + \Delta H_i$ (V_{cti} and H_{cti} - respectively speed and height/altitude of the start of the i step/stage; ΔV_i and ΔH_i - supplementary speed and height/altitude, acquired by load G_{Hi} due to the fuel/propellant i step/stages);

G_{Ti} - fuel load of the i step/stage, required for the acceleration/dispersal of load with a weight of G_{Hi} (on value ΔV_i and ΔH_i);

$$\bar{G}_{Ti} = \frac{G_{Ti}}{G_i + G_{Hi}}; \quad \bar{G}_{Ti}^* = \frac{G_{Ti}}{G_i}.$$

For carrier aircraft let us have:

$$G_{n.c.H} = G_{y1} + \dots + G_{ym} + G_{BKC};$$

$$\bar{G}_{T.c.H} = \frac{G_{T.c.H}}{G_{c.H} + G_{n.c.H}} = \frac{G_{T.c.H}}{G_0}; \quad \bar{G}_{T.c.H}^* = \frac{G_{T.c.H}}{G_{c.H}}.$$

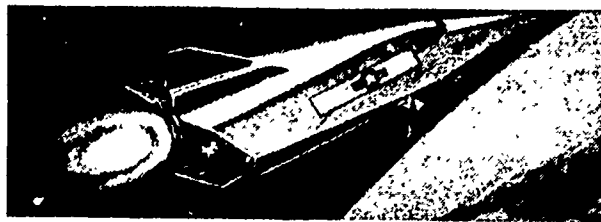


Fig. 11.19. VKS of firm "Lockneed", USA (figure).

Page 211.

For the first accelerator:

$$G_{n,y1} = G_{y2} + \dots + G_{ym} + G_{BKC};$$

$$\bar{G}_{\tau,y1} = \frac{G_{\tau,y1}}{G_{y1} + G_{n,y1}}; \quad \vec{G}_{\tau,y1} = \frac{G_{\tau,y1}}{G_{y1}}.$$

For the i accelerator:

$$G_{n,y m} = G_{BKC}; \quad \bar{G}_{\tau,y m} = \frac{G_{\tau,y m}}{G_{y m} + G_{BKC}}; \quad \vec{G}_{\tau,y m} = \frac{G_{\tau,y m}}{G_{y m}}.$$

The supplementary speed, communicated by the i step/stage to the accelerate/dispersed load, will be in general equal to

$$\Delta V_i = V_{ni} - \Delta V_{ni},$$

where V_{ni} - the ideal velocity, which communicates the i grade of load G_{ni} ;

ΔV_{ni} - speed losses from the action of gravitation and aerodynamic drag in acceleration phase from V_{cri} to V_{cri+1} .

It is easy to show that

$$\bar{G}_{\tau i} = \frac{G_{\tau i}}{G_i + G_{ni}} = \bar{G}_{\tau i}^* \left(1 - \frac{G_{ni}}{G_i + G_{ni}} \right),$$

and consequently, according to equation (11.46), will occur the equality

$$\bar{G}_{\tau i}^* \left(1 - \frac{G_{ni}}{G_i + G_{ni}} \right) = 1 - \frac{1}{e^{\frac{\Delta V_i + \Delta V_{ni}}{9.81 J_{\tau i}}}}.$$

From this equality let us find the weight of apparatus when V_{cri} at the moment of firing the engines of the i step/stage (after the isolation/evolution from $i-1$ of step/stage),

$$G_i + G_{ni} = \frac{\bar{G}_{\tau i}^*}{\bar{G}_{\tau i}^* - 1 + \frac{1}{e^{\frac{\Delta V_i + \Delta V_{ni}}{9.81 J_{\tau i}}}}} G_{ni}. \quad (11.48)$$

Since for each preceding/previous step/stage the accelerate/dispersed load is the sum of all subsequent step/stages, then on the basis of dependence (11.48) launching weight of multistage flight vehicle will be equal to

$$G_0 = \left(\prod_{i=1}^{n-1} \frac{\bar{G}_{\tau i}^*}{\bar{G}_{\tau i}^* - 1 + \frac{1}{e^{\frac{\Delta V_i + \Delta V_{ni}}{9.81 J_{\tau i}}}}} \right) G_{n,n}. \quad (11.49)$$

where n - a number of step/stages of apparatus;

sign $\prod_{i=1}^{n-1}$ - indicates product (n-1) of terms;

$n-1=m+1$ - number of the "working" step/stages of the apparatus (fuel/propellant of which is expend/consumed in the process of acceleration/dispersal);

$G_{n,n}$ - payload weight, concluded in orbit.

Page 212.

As was accepted, $G_{n,n}=G_{BKC}$, the aerospace aircraft is the last/latter step/stage of multistage orbital apparatus, moreover the fuel/propellant of this step/stage in the process of acceleration/dispersal is not expend/consumed (speed V_{IK} is reached at the end of the work of the m accelerator). If VKS in final trajectory emerges in orbit due to its own fuel/propellant, then the m accelerator will accelerate/disperse VKS to the speed

$$V = V_{IK} - \Delta V_{BKC}$$

Value ΔV_{BKC} is defined as

$$\Delta V_{BAC} = 9.81 J_{T.BKC} \ln \frac{1}{1 - \Delta \bar{\sigma}_{T.BKC}} - \Delta V_{n.BKC}, \quad (11.50)$$

where $\Delta \bar{\sigma}_{T.BKC} = \frac{\Delta G_{T.BKC}}{G_{BKC}}$ - the over-all payload ratio of fuel/propellant VKS, expendable in process injection into orbit;

$$\Delta V_{n.BKC} = f(V) - \text{with } V > 6.5 \text{ km/s } \Delta V_{n.BKC} \approx 0.$$

One should note that in this diagram (multistage apparatus) it is conformable, since this increases the weight of structure VKS and substantially is decreased its maneuverability in open space.

The solution of task for the optimization of the parameters of flight vehicle in the minimum of value G_0 with to assigned magnitude $G_{n.H}$ is reduced to solution of system $dG_0/di_1, \dots, i_k = 0$ during known limitations (here i - parameter). A strict solution of this task is very bulky, since the majority of variables, determining value G_0 , is in turn, the functions of unknown parameters and characteristics of the separate step/stages of flight vehicle, for example:

$$\Delta V_{n.l} = \Delta V_{n.l}(V_{ct.l}, \bar{P}_l, K_l, \theta_l, H_l, \dots);$$

$$J_{T.C.H} = J_{T.C.H}(H, V, \bar{P}_0, c_p, \gamma_{zn}, \dots) \text{ and so forth.}$$

This problem in sketch design it is better to solve by the approximation method which considerably simplifies the solution in it

at the same time gives the necessary for sketch design accuracy/precision.

The essence of method consists in the fact that in equation (11.49) the variables are record/fixed. Matter is facilitated by the fact that some variables with sufficient accuracy/precision can be determined on the basis of experiment in the design of identical flight vehicles, other variables during deviation from optimum exert insignificant error to the solution of task as a whole.

For preliminary design it is possible to accept $\bar{G}_{\tau,y}^* = 0,85 - 0,92$ (this value of load ratio on fuel/propellant they have the upper stages of modern carrier rockets); $J_{\tau,y} = \text{const}$ (for example, for the fuel/propellant $H_2 + O_2$, $J_{\tau,y} \approx 450 \text{ s}$);

$$\Delta V_{y_1} = \dots = \Delta V_{y_m} = \frac{V_{1k} - V_{cr,y_1}}{m},$$

or $\Delta V_{y_1} = \dots = \Delta V_{y_m} = \frac{V_{1k} - V_{cr,y_1} - \Delta V_{BKC}}{m}$ (if the part of the fuel/propellant VKS is spent on acceleration/dispersal),

where V_{cr,y_1} - a speed of the start of the first accelerator (i.e. the speed which communicates carrier aircraft to the accelerate/dispersed by it load).

Increase $\Delta V_{nt} = f(V_{cr,t})$ is taken either from curve/graph in Fig.

11.11 or from the calculation of the optimum trajectory of injection into orbit.

Page 213.

A number of all step/stages of flight vehicle let us find, after determining a number of accelerators, since $n=m+2$.

Value $\bar{G}_{n,n}$ will be, obviously, is greater, the greater percentage it will compose payload weight, concluded in orbit, from weight of load, accelerate/dispersed with carrier aircraft (respectively smaller percentage will compose the weight of accelerators). From this condition should be determined value m .

Criterion $\bar{G}_{n,n}$ can be presented as

$$\bar{G}_{n,n} = \bar{G}'_{n,n} (1 - \bar{G}_{c,n}),$$

where

$$\bar{G}'_{n,n} = G_{n,n} / G_{n,c,n}, \quad \bar{G}_{c,n} = \frac{G_{c,n}}{G_{c,n} + G_{n,c,n}} = \frac{G_{c,n}}{G_0}.$$

Value $\bar{G}'_{n,n}$ it is easy to determine from equation (11.49), which will take the form

$$\bar{\sigma}_{n,n} = \prod_{l=1}^m \frac{\bar{\sigma}_{r,l}^* - 1 + \frac{1}{e^{\frac{\Delta V_l + \Delta V_{n,l}}{9.81 J_{r,l}}}}}{\bar{\sigma}_{r,l}^*} \quad (11.51)$$

From equation (11.51) it is possible to determine, what part of the load, accelerate/dispersed with carrier aircraft, is capable of leaving to near earth orbit.

Varying by the speed of the start of the first accelerator and by Mach number, it is possible to determine the appropriate values of value $\bar{\sigma}_{n,n}$.

In Fig. 11.20 shown graphical solution of equations (11.51).

Analyzing the obtained dependence, it is possible to draw the conclusion: for the real values of the parameters of accelerators, an increase in number $m > 2$ virtually to an increase in criterion $\bar{\sigma}_{n,n}$ does not lead; therefore for a multistage orbital apparatus should be accepted a number of accelerators $m=2$ and a number of all step/stages, therefore, $n=4$.

Equation (11.49), which is determining launching weight of multistage apparatus, in that case will take the form

$$G_0 = \frac{\bar{G}_{T.C.H}^*}{\bar{G}_{T.C.H}^* - 1 + \frac{1}{e^{\frac{\Delta V_{C.H} + \Delta V_{H.C.H}}{9.81/T.C.H}}}} \frac{\bar{G}_{T.Y_1}^*}{\bar{G}_{T.Y_1}^* - 1 + \frac{1}{e^{\frac{\Delta V_{Y_1} + \Delta V_{H.Y_1}}{9.81/T.Y_1}}} \times$$

$$\times \frac{\bar{G}_{T.Y_2}^*}{\bar{G}_{T.Y_2}^* - 1 + \frac{1}{e^{\frac{\Delta V_{Y_2} + \Delta V_{H.Y_2}}{9.81/T.Y_2}}} G_{BRC}. \quad (11.52)$$

It is obvious, for each value $V_{cr.y}$, there is optimum value $V_{cr.y}$, which is determining the optimum distribution of the total weight of accelerators (between the first and second accelerator). However, the error in the determination of the maximum of criterion $\bar{G}_{H.H}$, obtained during the replacement of optimum value $V_{cr.y}$, by the recommended value

$$V_{cr.y_2} = V_{cr.y_1} + \Delta V_{y_1} = \frac{V_{IK} + V_{cr.y_1}}{2},$$

will be insignificant (Fig. 11.21).

Page 214.

Thus, solving assigned mission by the proposed approximation method, it is possible to find with sufficient accuracy/precision the optimum value G_0 and the row/series of the important parameters of orbital apparatus, without resorting to the determination of the extremum of the function of many variables.

Determining optimum weight of the i step/stage from equation (11.48)

$$G_i = \left(\frac{\bar{G}_{\tau,i}^*}{\bar{G}_{\tau,i}^* - 1 + \frac{1}{e^{\frac{\Delta V_i + \Delta V_{n,i}}{9,81 J_{\tau,i}}}}} - 1 \right) G_{n,i}, \quad (11.53)$$

let us find the weights of the separate step/stages of multistage flight vehicle.

If is assign/prescribed payload weight G_{BKC} of concluded in orbit, and is required to determine the minimum launching weight G_0 , then the sequence of determining the weight of separate step/stages must be similar: the weight of the second accelerator; the weight of the first accelerator; the weight of carrier aircraft.

From equation (11.52) we will obtain:

- weight of the second accelerator

$$G_{y2} = \left(\frac{\bar{G}_{\tau,y2}^*}{\bar{G}_{\tau,y2}^* - 1 + \frac{1}{e^{\frac{\Delta V_{y2} + \Delta V_{n,y2}}{9,81 J_{\tau,y2}}}}} - 1 \right) G_{BKC}; \quad (11.54)$$

- the weight of the first accelerator

$$G_{y1} = \left(\frac{\bar{G}_{\tau,y1}^*}{\bar{G}_{\tau,y1}^* - 1 + \frac{1}{e^{\frac{\Delta V_{y1} + \Delta V_{n,y1}}{9,81 J_{\tau,y1}}}}} - 1 \right) (G_{y2} + G_{BKC}); \quad (11.55)$$

- weight of carrier aircraft

$$G_{c.H} = \left(\frac{\bar{G}_{T.C.H}^*}{\bar{G}_{T.C.H}^* - 1 + \frac{1}{e \frac{\Delta V_{c.H} + \Delta V_{H.C.H}}{9.81 J_{T.C.H}}}} - 1 \right) (G_{y1} + G_{y2} + G_{BKC}). \quad (11.56)$$

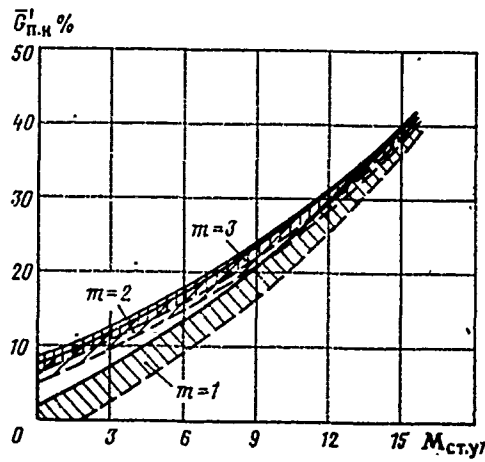


Fig. 11.20.

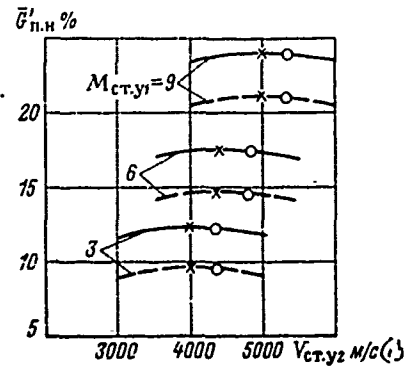


Fig. 11.21.

Fig. 11.20 effect of a number of accelerators and velocity of start from carrier aircraft to value $\bar{G}'_{п.н}$. (fuel/propellant H_2+O_2 , $J_{r.y.}=450$ g):

———— $\bar{G}_{r.y}^* = 0.9$; - - - $\bar{G}_{r.y}^* = 0.85$

Fig. 11.21. Effect of speed of start of second accelerator on value

$\bar{G}'_{п.н}$: ——— $\bar{G}_{r.y}^* = 0.9$; - - - $\bar{G}_{r.y}^* = 0.85$; ○ — $V_{cr.y2} = \frac{V_{1k} + V_{cr.y1}}{2}$; x — $V_{cr.y2}^{opt}$

Key: (1) m/s.

Page 215.

From equation (11.56) it is possible to determine, what load and to what speed it is capable to drive away the carrier aircraft

$$\bar{G}_{\text{T.C.H}} = \frac{G_{\text{H.C.H}}}{G_0} = \frac{\bar{G}_{\text{T.C.H}}^* - 1 + \frac{1}{e^{\frac{\Delta V_{\text{C.H}} + \Delta V_{\text{H.C.H}}}{9.81 J_{\text{T.C.H}}}}}}{\bar{G}_{\text{T.C.H}}^*}. \quad (11.57)$$

In order to solve system of equations (11.52) - (11.57), it is necessary to know value \bar{G}_r^* and value J_r for of all working step/stages. If for accelerators value $\bar{G}_{r,y}^*$ is determined only by the perfection of construction/design and its possible value is actually known (this load ratio on the fuel/propellant of upper stages of contemporary multistage rockets), then for carrier aircraft value $\bar{G}_{\text{T.C.H}}^* = G_{\text{T.C.H}}/G_{\text{C.H}}$ determine in the stage of sketch design is considerably more complicated. The necessary fuel load will depend (besides the perfection of construction/design) from the characteristics of power plant, from the maximum speed of flight, from the parallax of orbit, from the conditions of takeoff, etc. Therefore the final value of value $\bar{G}_{\text{T.C.H}}^*$ can be establish/installed only as a result of working design.

It is exactly the same also concerning specific impulses on fuel/propellant. For power plant with ZhrD value $J_r = \text{const}$, and its value for different fuel/propellants it is known. For the power plant of carrier aircraft with VRD, value $J_{\text{T.C.H}}$ in the given equations is not true specific impulse on fuel/propellant for VRD. ^{In this case} $J_{\text{T.C.H}}$ - required conditional momentum/impulse/pulse VRD, i.e., this is the specific

impulse of conditional ZhRD, which, fulfilling, the same work, would consume the same quantity of fuel/propellant (by weight), that also VRD. The values of the required of true and conditional specific impulses VRD do not coincide due to different value of the optimum thrust-weight ratio of aircraft with VRD and ZhRD. The true specific impulse VRD, defined as

$$J_{T.BPD} = \frac{3600}{c_p}$$

must be considerably more than value $J_{T.C.H}$ in order to compensate large weight VRD.

In the period of the preliminary design of value $\bar{G}_{T.C.H}^*$ and $J_{T.C.H}$ it is possible to find, after determining the over-all payload ratio of fuel/propellant, required for acceleration/dispersal and climb, i.e., value $\bar{G}_{T.C.H} = \bar{G}_{T.C.H} / G_0$.

With the sufficient for a preliminary design accuracy/precision

$$\bar{G}_{T.C.H} = \frac{(H_{cr.y1} + V_{cr.y1}^2 \cdot 2g) c_{p,cr}}{1300V_{cr.y1}} \frac{\bar{P}_0 K_{cr}}{\bar{P}_0 K_{cr} - 1}, \quad (11.58)$$

where $H_{cr.y1}$ and $V_{cr.y1}$ - height/altitude and speed of the start of the first accelerator respectively in m and m/s;

$c_{p,cr}$ - specific fuel consumption by the engines of carrier aircraft at the moment of the start of the first accelerator in

kg/kg•s;

Page 216.

$\bar{P}_0 = P_0/G_0$ - starting (takeoff) thrust-weight ratio of flight vehicle;

K_{cr} - lift-drag ratio of apparatus (aircraft with the accelerate/dispersed load) at the moment of the start of the first accelerator.

For preliminary (or diploma) design it is possible to use data of Fig. 11.22.

Value $\bar{G}_{r.c.n}^*$ let us find, solving the equation of the weight balance

$$\bar{G}_{r.c.n}^* = \frac{\bar{G}_{r.c.n}}{\bar{G}_{c.n.пуст} + \bar{G}_{r.c.n}}, \quad (11.59)$$

where $\bar{G}_{c.n.пуст} = \frac{\bar{G}_{c.n.пуст}}{G_0}$;

$\bar{G}_{c.n.пуст}$ - weight of carrier aircraft without the accelerate/dispersed load and without the fuel/propellant, spent to acceleration/dispersal to $V_{cr.yl}$.

For the heavy supersonic and hypersonic aircraft

$$\bar{G}_{\text{с.н.пер}} = 0,3-0,4.$$

The required conditional momentum/impulse/pulse VRD of carrier aircraft it is easy to determine from equation (11.46), knowing value $\bar{G}_{\text{т.с.н}}$:

$$J_{\text{т.с.н}} = \frac{\Delta V_{\text{с.н}} + \Delta V_{\text{п.с.н}}}{9,81 \ln \frac{1}{1 - \bar{G}_{\text{т.с.н}}}} \quad (11.60)$$

After determining thus for all step/stages of the flight vehicle of value $\bar{G}_{\text{т}}$ and $J_{\text{т}}$, it is possible to solve equations (11.52) - (11.57).

Figures 11.23 and 11.24 show the effect of the velocity of the start of the first accelerator on value $\bar{G}_{\text{н.с.н}} = \frac{\bar{G}_{\text{н.с.н}}}{G_0}$ and $\bar{G}_{\text{п.н}} = \frac{G_{\text{ВКС}}}{G_0}$ (for the recommended above range of the characteristics of carrier aircraft and accelerators).

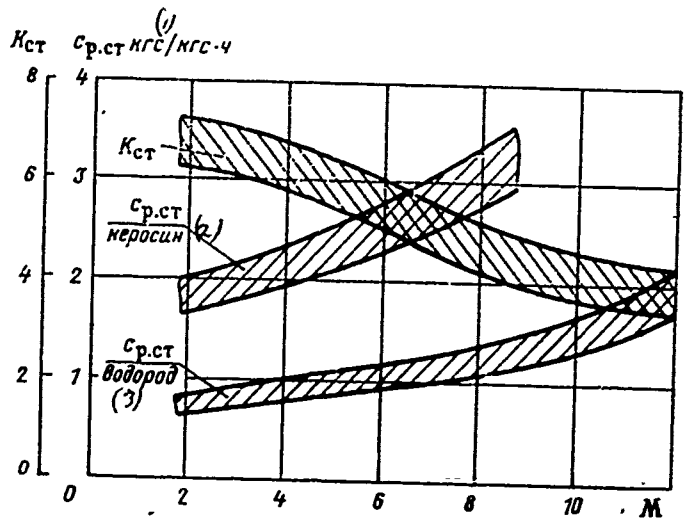


Fig. 11.22. Dependence of values K_{ct} and $C_{p.ct}$ on Mach number.

Key: (1). $kg/kg \cdot h$. (2). kerosene. (3). hydrogen.

Page 217.

Equations (11.52) - (11.57) for the diagram of flight vehicle in question make it possible to determine the optimum speed of acceleration/dispersal with the aid of carrier aircraft (speed of the start of the first accelerator):

for cryogenic fuel $M_{opt}=8-10$;

for Λ ^{hydrocarbon} fuel $M_{opt}=4-6$.

Payload weight. The most important factor during the design of orbital flight vehicle is, obviously, the weight of the true payload, concluded in orbit.

If we under payload VKS understand the weight of the cosmonauts and transported cargo, then value $\bar{G}_{\text{п.н.ВКС}} = G_{\text{п.н.ВКС}}/G_{0\text{ВКС}}$ can be determined, using the equation of the weight balance

$$\bar{G}_{\text{п.н.ВКС}} = 1 - (\bar{G}_{\text{ВКС н.ст}} + \bar{G}_{\text{Т ВКС}}),$$

where $\bar{G}_{\text{ВКС н.ст}} = G_{\text{ВКС н.ст}}/G_{0\text{ВКС}}$ - the over-all payload ratio of empty VKS (without load and fuel/propellant);

$\bar{G}_{\text{Т ВКС}} = G_{\text{Т ВКС}}/G_{0\text{ВКС}}$ - the over-all payload ratio of full of reserve fuel/propellant VKS;

$G_{0\text{ВКС}}$ - weight of completely filled/charged VKS.

On the value $\bar{G}_{\text{п.н.ВКС}}$ essential effect exerts requirement for maneuverability in orbit (necessary fuel reserve for a maneuver) and requirement for maneuverability in the atmosphere at the hypersonic speeds (since on the value of hypersonic lift-drag ratio K_r depends the weight of structure VKS).

During design VKS (in the first approximation,) it is possible to bear in mind following of the value of the weight characteristics (see Table 11.2).

In Fig. 11.25 is shown value $\bar{G}_{n,BKGC}$ depending on the hypersonic lift-drag ratio of apparatus.

Fuel load. Gross weight of the fuel/propellant of separate (the i-th) step/stage will be in general defined as the sum

$$G_{T,i} = G_{T,p} + G_{T,m} + G_{T,b} + G_{T,n.s.}$$

where $G_{T,p} = G_{T,i}$ - the fuel load, required for the acceleration/dispersal of load $G_{H,i}$ (to value ΔV_i and ΔH_i);

$G_{T,m}$ - fuel load, required for maneuver accomplishment;

$G_{T,b}$ - fuel load for a return to base;

$G_{T,n.s.}$ - navigational fuel reserve.

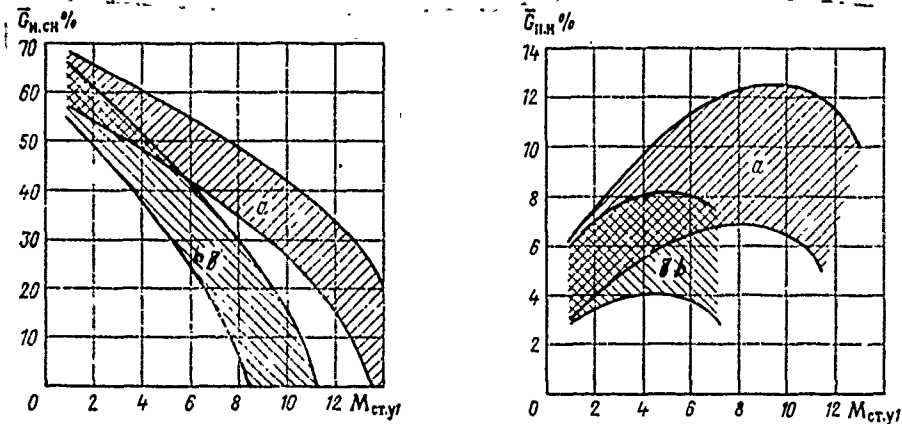


Fig. 11.23. Dependence of the over-all payload ratio of the load, accelerate/dispersed with carrier aircraft with VRD, from the speed of the acceleration/dispersal: a) engines work on hydrogen; b) engines work on kerosene.

Fig. 11.24. Dependence of payload fraction, concluded in orbit, from speed of start of first accelerator: a) engines of all step/stages work on hydrogen; b) engines of carrier aircraft work on kerosene, booster engines - on hydrogen.

Page 218.

Let us examine components full of reserve fuel/propellants for the separate step/stages of multistage orbital apparatus.

Knowing launching weights of separate step/stages and value $G_{T,1}$, let us find fuel load, required for the acceleration/dispersal of the load $G_{c,II}$:

$$G_{T,p} = \bar{G}_{T,1} G_{c,II}$$

Virtually entire fuel/propellant of accelerators will be expend/consumed on an increase in the energy of the accelerated load; therefore for accelerators as one-time stage $\bar{G}_{T,M} + G_{T,B} + G_{T,H,3} = 0$.

The fuel/propellant, required to carrier aircraft with VRD for maneuver accomplishment after the starting/launching of load and for a return on airport of departure in the first approximation, it is equal (fuel/propellant - hydrogen)

$$\bar{G}_{T,M} + G_{T,B} + G_{T,H,3} \approx (0,02 - 0,03) G_{c,II}$$

If in the process of injection into orbit fuel/propellant VKS is not expend/consumed, then gross weight of fuel/propellant VKS will be equal to

$$G_{T,BKC} = G_{T,M} + G_{T,B} + G_{T,H,3}$$

The fuel load, required for execution of maneuver in space, depends substantially on the means of the maneuver which in turn, is determined by value ΔV_M - by a change in the velocity vector. The relationship/ratio between value ΔV_M and required fuel load can be

obtained from equation (11.45):

$$G_{T,M} = G_{BKC} \left(1 - \frac{1}{e^{\frac{\Delta V_M}{g_{81/T,BKC}}}} \right). \quad (11.61)$$

Here G_{BKC} - initial weight of apparatus in orbit (before the maneuver);

$\bar{J}_{T,BKC}$ - specific jet firing VKS, with the aid of which is fulfilled the maneuver.

Table 11.2. Weight characteristics VKS.

| Относительный вес (1) | $K_r = 1,0$ | $K_r = 2,3$ |
|---|-------------|-------------|
| Конструкция (с тепло- изоляцией), оборудова- ние, системы (2) | 0,52—0,37 | 0,55—0,41 |
| Двигательная уста- новка (3) | 0,015—0,03 | |
| Шасси (4) | 0,02—0,035 | |
| Управление (аэроди- намическое) (5) | 0,015—0,02 | |
| Управление (газо- струйное) (6) | 0,01—0,015 | |
| Топливо (7) | 0,30—0,35 | |
| Полезная нагрузка (8) (космонавты и грузы) | 0,12—0,18 | 0,09—0,14 |

Key: (1). Over-all payload ratio. (2). Construction/design (with thermal insulation), equipment, system. (3). Engine plant. (4). Chassis/landing gear. (5). Control (aerodynamic). (6). Control (gas-jet). (7). Fuel/propellant. (8). Payload (cosmonauts and loads).

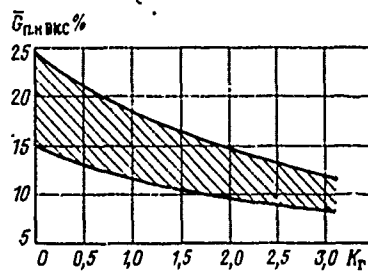


Fig. 11.25. Dependence of payload fraction VKS on hypersonic lift-drag ratio.

The representation of the numerical value of value ΔV_M and corresponding value $\bar{G}_{T.M}$ gives Table 11.3, in which are shown the expenditures of fuel/propellant (when $J_{T.BKC}=450$ s) for an increase in altitude ΔH or on a change in the angle of the slope $\Delta\phi$ of orbit.

Fuel/propellant for a return will be composed of three parts:

$$G_{T.R} = G_{T.CX} + G_{T.CTAS} + G_{T.NOC},$$

where $G_{T.CX}$ - a fuel load for an orbit ejection (for the creation of retro impulse);

$G_{T.CTAS}$ - fuel/propellant for stabilization (and control) in the initial stage of gliding/planning;

$G_{T.NOC}$ - fuel/propellant for landing on assigned/prescribed airfield.

Value $G_{T.CX}$ is determined by equation (11.61), it is necessary to have $\Delta V_M = \Delta V_T = 30-70$ m/s (see § 2).

In the period of preliminary design VKS, it is possible to accept:

$$G_{T.CTAS} \approx (0,015 - 0,025) G_0 \text{ BKC};$$

$$G_{T.NOC} \approx (0,015 - 0,030) G_0 \text{ BKC};$$

$$G_{T.H.3} \approx (0,010 - 0,015) G_0 \text{ BKC}.$$

Required thrust-weight ratio of multistage apparatus. The starting thrust-weight ratio of multistage flight vehicle is defined as the relation

$$\bar{P}_0 = \frac{P_0}{G_{c.n} + G_{n.c.n}} = \frac{P_0}{G_0},$$

where P_0 - total boost for launching of the engines of carrier aircraft.

The optimum value of value \bar{P}_0 must correspond to the maximum of criterion $\bar{G}_{n.n}$. Therefore selected the starting thrust-weight ratio of multistage flight vehicle should be in such a way, as, other conditions being equal, to obtain the maximum value of value $G_{n.c.n}$, and this can be made, after ensuring for carrier aircraft the minimum of sum $(G_{t.c.n} + G_{d.v.y})$.

Since $G_{t.c.n} = f(\bar{P}_0)$ and $G_{d.v.y} = \psi(\bar{P}_0)$, then expressing the indicated values through the characteristics of aircraft and solving the equation

$$\frac{d\bar{G}_{n.c.n}}{dP_0} = 0,$$

we will obtain the functional connection of optimum starting thrust-weight ratio with the fundamental characteristics of the carrier aircraft:

$$\bar{P}_0 = \frac{1}{K_{cr}} + \sqrt{\frac{\left(H_{cr.y1} + \frac{V_{cr.y1}^2}{2g}\right) c_{p cr}}{1690V_{cr.y1} \gamma_{th} K_{cr}}}, \quad (11.62)$$

DOC = 79052108

PAGE 400

where $K_{ст}$ and $C_{рст}$ - see (11.58) and Fig. 11.22;

$\gamma_{дв}$ - the weight per horsepower of the power plant of carrier aircraft.

Table 11.3. The initial orbit: H=200 km:

 $V_0 = V_{1k} = 7790 \text{ m/s.}$

| | | | | | | | |
|---|-------|------|------|---|------|------|------|
| $\Delta H \text{ в км } (1)$ | 10 | 100 | 300 | $\Delta \psi^\circ$ (2) | 1 | 7 | 15 |
| $\Delta V_M = \Delta V_H \text{ в м/с}$ | 10 | 85 | 200 | $\Delta V_M = \Delta V_\varphi \text{ в м/с}$ | 140 | 950 | 2050 |
| $G_{T.M}/G_{BKC}$ | 0,002 | 0,02 | 0,05 | $G_{T.M}/G_{BKC}$ | 0,03 | 0,19 | 0,38 |

Key: (1). in km. (2). in m/s.

Page 220.

The starting thrust-weight ratio of accelerators and VKS will be defined as the relation

$$\bar{P}_{y1} = \frac{P_{y1}}{G_{y1} + G_{n.y1}} = \frac{P_{y1}}{G_{n.c.H}};$$

$$\bar{P}_{y2} = \frac{P_{y2}}{G_{y2} + G_{n.y2}} = \frac{P_{y2}}{G_{n.y1}}; \quad \bar{P}_{BKC} = \frac{P_{BKC}}{G_{BKC}},$$

where P_{y1} - the boost for launching of the first accelerator;

P_{y2} - the boost for launching of the second accelerator;

P_{BKC} - boost for launching VKS.

If on accelerators and VKS are establish/installed ZhRD, then thrust-weight ratio will not be limited by the weight of engine plant, since the specific gravity/weight of contemporary ZhRD is

considerably lesser than the specific gravity/weight VRD

$$\frac{\gamma_{\text{AB ЖРД}}}{\gamma_{\text{AB ВРД}}} \approx 0,05.$$

Therefore the thrust-weight ratio of the accelerators (without fearing overboost of engine plant) should be selected from the condition of guaranteeing the acceptable g-force upon acceleration/dispersal and the speed losses to gravitation and aerodynamic drag $\Delta V_{n,y}$, which, other conditions being equal, will determine value $\bar{G}'_{n,n}$. Figure 11.26 shows the effect of the starting thrust-weight ratio of the first accelerator on value $\bar{G}'_{n,n}$ (for $M_{\text{ст.}y1}=6$).

In the period of preliminary design, taking into account possible g-limitations, it is possible to ac...

$$\bar{P}_{y1} \approx \bar{P}_{y2} \approx \bar{P}_{\text{BKC}} = 1,5 - 2,0.$$

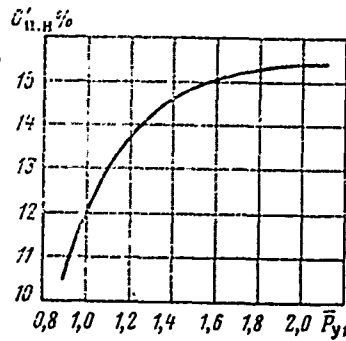


Fig. 11.26. Effect of the starting thrust-weight ratio of the first accelerator on value $\bar{G}'_{н.н.}$ ($M_{ст. y1}=6$)

Aerospace aircraft with YaRD [38].

The aerospace aircraft with nuclear rocket engine (YaRD), as it was shown above, can leave to Earth-circling orbit without the aid of intermediate step/stage-accelerators, and when $J_{т.ярд} > 2000$ with and without the aid of carrier aircraft. The over-all payload ratio of fuel/propellant, required for injection into orbit of single-stage VKS, is determined by equation (11.46), which will take the form

$$\bar{G}_{т.пост} = \frac{G_{т.пост}}{G_{0 \text{ ВКС}}} = 1 - \frac{1}{e^{\frac{V_{1к} + \Delta V_{н}}{9.81 J_{т.ярд}}}} \quad (11.63)$$

Here $G_{0 \text{ ВКС}}$ - launching weight of VKS with YaRD (when $(\text{при } V_{cr}=0)$);

$\Delta V_{н}$ - see Fig. 11.11 (when $V_{cr}=0$).

Effect $J_{т.ЯРД}$ on value $\bar{G}_{т.пост}$ is shown in Fig. 11.12 (when $M_{сг}=0$).

If we payload weight, concluded in orbit, consider the weight of repeated flight vehicle when $\bar{V}_{пн}$, then for single-stage VKS with YaRD payload will be equal to

$$G_{п.н} = \bar{G}_{ВКС} = G_{0 ВКС} - G_{т.пост},$$

and value $\bar{G}_{п.н}$ is equal to

$$\bar{G}_{п.н} = \frac{G_{ВКС}}{G_{0 ВКС}} = \frac{1}{\frac{V_{пк} + \Delta V_{п}}{e^{9,81 J_{т.ЯРД}}}} \quad (11.64)$$

Page 221.

If payload for single-stage VKS is understood just as for a usual aircraft, then in that case payload will be determined by the equation of weight balance, solving which together with (11.63), it is possible to find the over-all payload ratio of the true payload, concluded in orbit; and, consequently, the weight of single-stage VKS with YaRD

$$\bar{G}_{п.н} = \frac{G_{п.н}}{G_{0 ВКС}} = \frac{1}{\frac{V_{пк} + \Delta V_{п}}{e^{9,81 J_{т.ЯРД}}}} - (\bar{G}_{ВКС.пост} + \bar{G}_{т.резерв}), \quad (11.65)$$

where $\bar{G}_{т.резерв} = \bar{G}_{т.} - \bar{G}_{т.пост}$ - the over-all payload ratio of standby fuel/propellant.

In the period of preliminary design VKS with YaRD the tentative value of relative empty weight (taking into account biological protection) can be taken in limits $G_{ВКС.пост} = 0,40 - 0,65$.

Value $\bar{G}_{\text{т.резерв}}$ will be equal to

$$\bar{G}_{\text{т.резерв}} = \frac{G_{\text{т.м}} + G_{\text{т.н}} + G_{\text{т.н.э}}}{G_{0 \text{ ВКС}}} = \bar{G}_{\text{т.м}} + \bar{G}_{\text{т.н}} + \bar{G}_{\text{т.н.э}}$$

Fuel load for maneuver accomplishment in space is also determined by equation (11.61), and value $\bar{G}_{\text{т.в}}$ and $\bar{G}_{\text{т.н.э}}$ in the first approximation, can be taken $\bar{G}_{\text{т.в}} + \bar{G}_{\text{т.н.э}} = 0,03 - 0,06$. If single-stage VKS has combined engine plant (VRD + YaRD) and YaRD is included when $V_{\text{ст}} \neq 0$, then the over-all payload ratio of the true payload, concluded in orbit, analogous (11.65) will be determined then:

$$\bar{G}_{\text{п.н}} = \frac{G_{\text{п.н}}}{G_{0 \text{ ВКС}}} = \frac{1 - \bar{G}_{\text{т.в.рл}}}{\frac{V_{\text{н}} + \Delta V_{\text{п}} - V_{\text{ст}}}{e^{9,81 J_{\text{т.ЯРД}}}}} - (\xi + \bar{G}_{\text{т.резерв}}). \quad (11.66)$$

Here $\bar{G}_{\text{т.в.рл}} = \frac{G_{\text{т.в.рл}}}{G_{0 \text{ ВКС}}}$ - over-all payload ratio of fuel/propellant VRD, required for output/yield to height/altitude and speed at which it is included by YaRD. Value $\bar{G}_{\text{т.в.рл}}$ is determined from equation (11.58), in which the torque/moment of the start of the first accelerator is the torque/moment of connection/inclusion YaRD;

$\Delta V_{\text{н}}$ - corresponds to value $V_{\text{ст}}$ (see Fig. 11.11)

$$\xi = \bar{G}_{\text{ВКС.пуст}} + \bar{G}_{\text{ав.у.ВРД}},$$

where $\bar{G}_{\text{ав.у.ВРД}} = G_{\text{ав.у.ВРД}} / G_{0 \text{ ВКС}} \approx 1,3 \bar{P}_{0 \text{ ВРД}}$ [coefficient 1.3 considers the weight of air intakes, air ducts, etc.]. Starting thrust-weight ratio $\bar{P}_{0 \text{ ВРД}} = P_{0 \text{ ВРД}} / G_{0 \text{ ВКС}}$ is determined by equation (11.62).

Finally, if VKS has YaRD with $J_{\text{т.ЯРД}} < 2000$ s and for injection

into orbit, is required the carrier aircraft, which accelerate/disperses VKS to necessary value V_{ct} , then this flight vehicle can be considered as multistage with $m=0$. Due to its own fuel/propellant VKS, it must increase speed by value $\Delta V_{BKC} = V_{IK} - V_{ct}$.

Page 222.

Gross weight of fuel/propellant of VKS in this case will be equal to $G_{T.BKC} = G_{T.HOT} + G_{T.M} + G_{T.B} + G_{T.H.S}$, where $G_{T.HOT}$ - the fuel load, required for output/yield VKS in orbit after start from carrier aircraft [see (11.46)]. All parameters of two-stage flight vehicle are determined by the given above dependences.

Special feature/peculiarities of the selection of geometric parameters VKS.

On geometry VKS, is had simultaneous effect of requirements, presented to flight characteristics during hypersonic gliding/planning, and the requirements ^{imposed on landing characteristics of craft. The same requirements in the} _{final analysis} are expressed by the value of the hypersonic and subsonic lift-drag ratio (takeoff data have smaller value, since for the takeoff of the aerospace flight vehicle to more expediently apply special rocket dolly).

Important effect on geometry VKS will exert aerodynamic reentry heating. The solution of task requires compromises between geometry at hypersonic and subsonic flight speeds. A change in the hypersonic configuration affects subsonic characteristics and vice versa. This interdependence and incongruence of characteristics for hypersonic and subsonic flight substantially complicates aerodynamic development and requires often the application/use of the variable geometry. Therefore large value in design VKS obtained the idea of the "separation of hypersonic and subsonic conditions/modes". The configuration of the apparatus, designed according to this principle facilitates the problem of aerodynamic investigations and provides the achievement of subsonic flight characteristics, close to usual aircraft ones.

As the example VKS with the divided flight conditions can serve the project of apparatus VL-3A (Fig. 11.27).

The given VKS has the advanced wings for the separation of hypersonic and subsonic conditions/modes. The hypersonic lift-drag ratio of apparatus is equal to $K_r = 2,3$, at subsonic speed with the pushed forward wings $K = 8$.

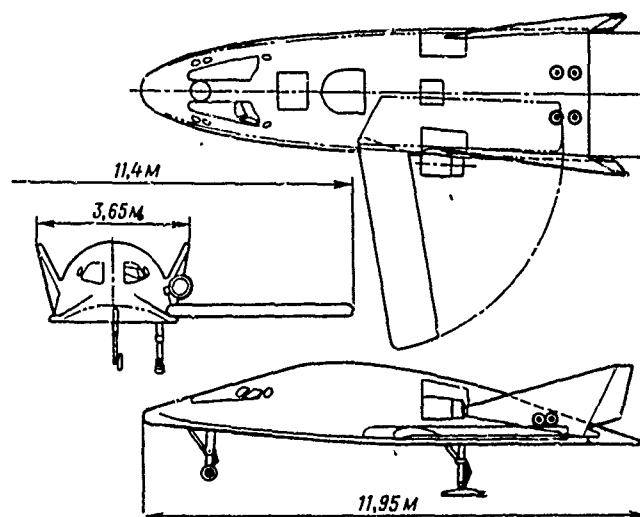


Fig. 11.27. Diagram VKS VL-3A.

Page 223.

After the completion of the hypersonic phase of gliding/planning, the wings partially are advanced for the attitude control center of pressure in transonic region. At subsonic speed the wings are advanced completely. Are advanced and are started two TRD, which ensure aircraft landing. There is a reserve of fuel (on 10 min of flight with full thrust) for approach guidance, "pulling" and attendance/departure to the second circle. For crash landing and splashdown, is applied the parachute. Landing shock with parachute is absorbed by the tail section of the apparatus which concerns the

earth/ground of the first.

One of the most important geometric parameters of flight vehicles is the specific wing load or on lifting surface (for apparatuses with lifting body). By lifting surface, is understood the projected area of apparatus in plan/layout. For VKS during hypersonic flight, the specific load on lifting surface will depend on equation (11.1), therefore, the value of this parameter, necessary for equilibrium flight (gliding/planning) at given speed at given height/altitude, it is possible to determine from equation (11.4)

$$p = \frac{31 \cdot 10^6 \rho V_{r,n}^2 c_y}{62 \cdot 10^6 - (V_{r,n} \pm 460 \cos \varphi)^2} \quad (11.67)$$

Values $c_y(\alpha)$ and $K_r(\alpha)$ are given in Fig. 11.28. For calculation of load on the m^2 of surface VKS one should accept c_y appropriate $K_{r \max}$.

The task of the selection of the specific wing load, necessary for obtaining of acceptable subsonic characteristics of VKS (mainly landing), does not have vital differences from analogous task for a usual aircraft. Figure 11.29 gives an example of subsonic aerodynamic characteristics VKS with lifting body.

On exterior form VKS, essential effect exerts aerodynamic heating. Heat transfer rate, which enters the sheathing/skin from boundary layer, as is known, it is proportional to the local coefficient of convection heat transfer on boundary/interface an air-

sheathing/skin [see equation (11.35)], which depends substantially on the sweepback of the body (during an increase in the sweepback the coefficient of heat transfer sharply decreases, Fig. 11.30).

Therefore all speakers into the flow of part VKS must have the large sweepback (from these considerations the control surfaces, therefore, must not be deflect/diverted to large angles). Sweep angle should be accepted not less than 70-75°.

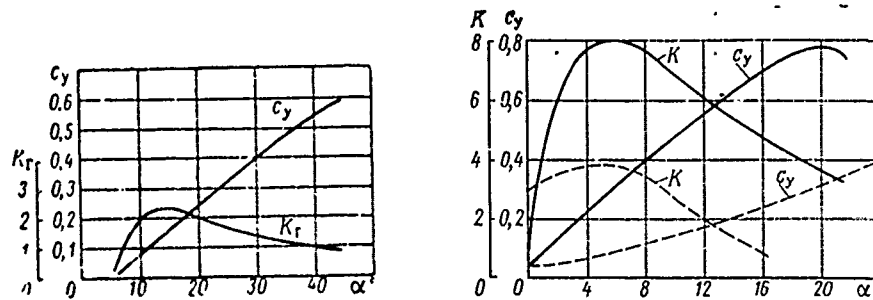


Fig. 11.28. Hypersonic aerodynamic characteristics VKS with lifting body in trim position center of gravity (apparatus VL-3A, $V=6080$ m/s; $H=60.8$ km).

Fig. 11.29. Subsonic aerodynamic characteristics of VKS with lifting body (apparatus VL-3A; $\overline{S}_{Hn} = 28,1$ m²; $S_{Hn} = 9,7$ m²): ---- with wing; --- without wing.

Page 224.

The coefficient of convection heat transfer near critical point depends on a radius of the nose section of the body. Solving together the equation, which describes heat transfer by heat radiation, and the equation, which describes aerodynamic heating in critical point on sphere, it is possible to obtain the approximate dependence, which connects a radius of forebody VKS with the parameters of the hypersonic flight

$$r = \frac{0,00019 \cdot q [(V/1000)^2 + 0,6T_{Hn}/1000]^2}{\epsilon^2 (T_{Hn}/1000)^8}, \quad (11.68)$$

where r - a radius of nose section m;

q - velocity head in the undisturbed flow in kgf/m^2 ;

V - flight speed in m/s;

$T_{\text{нон}}$ - temperature of external surface in $^{\circ}\text{K}$;

$\bar{\epsilon}$ - coefficient of the heat radiation of material of nose section.

During the design of exterior form VKS, usually are examined two systems of heat shielding from aerodynamic heating - ablation and radiation. It considers that for apparatuses $K_r < 1,3$ advantage in ratio by weight has the ablation system of heat shielding, whereas for apparatuses with the higher value of hypersonic lift-drag ratio is required more complicated radiation system. Deserves considerable attention the combined heat shielding, when ablation system is utilized only for the protection of lower surface VKS. The detachable lower heat shield, covered with ablating material, shields well construction/design VKS from high temperatures on lower surface.

As an example of the combined system of heat shielding can serve the system of heat shielding VKS VL-3A (Fig. 11.31 and 11.32).

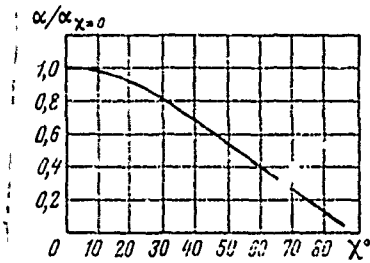


Fig. 11.30. Dependence of the coefficient of heat transfer in the zone of leading edge on sweep angle.

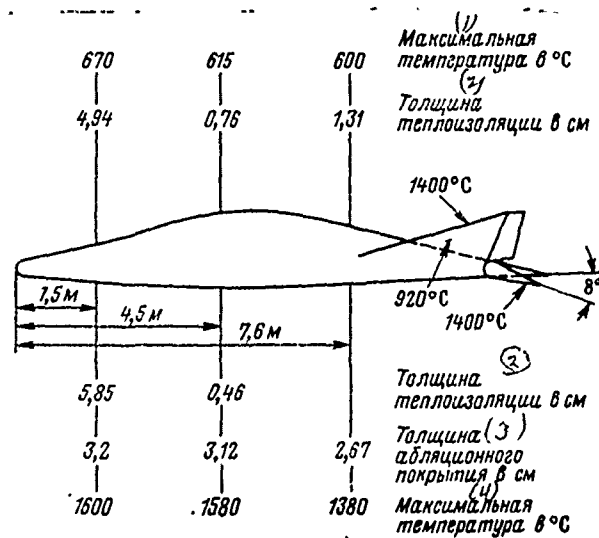


Fig. 11.31. System of heat shielding apparatus LV-3A (ablation coating - purple mixture NASA, density of 650 kg/m^3 ; thermal insulation - micro-quartz, density of 70 kg/m^3).

Key: (1). Maximum temperature in $^\circ\text{C}$. (2). Thickness of thermal insulation in cm. (3). Thickness of ablation coating in cm. (4). Maximum temperature in $^\circ\text{C}$.

Page 225.

The given in present chapter recommendations are not, of course, the comprehensive material according to the design of the aerospace aircraft. Nevertheless they allow in the period of the preliminary design of apparatus to solve many important problems.

For example, is required to design the multistage flight vehicle, capable of delivering to the near earth orbit $H \sim 150$ km of 10 cosmonauts and 500 kg of load ($G_{\text{п.ВКС}} = 1500$ kg). The last/latter step/stage of apparatus - VKS must increase orbit altitude to 500 km and change orbit inclination by angle to 7° . With return, in the process of hypersonic gliding/planning, VKS must fly not less than 16500 km and accomplish lateral maneuver, reaching in this case lateral distance $L_{\text{п.ВКС}} = 4000$ km. Maximum equilibrium temperature on the surface VKS, not shielded by ablation coating, must not exceed 1400°C , and the time of action of temperature $t \geq 1000^\circ\text{C}$ must not exceed 70 min. It is required to determine the optimum values of the basic parameters and flight characteristics VKS and multistage flight vehicle as a whole. As fuel in the engines of all step/stages to accept liquid hydrogen.

Utilizing the given in this chapter formulas and graphic dependences, we find:

a) the aerospace aircraft

$$\begin{aligned} G_{0\text{BKC}} &= 12 \text{ t}^{(1)}; \bar{G}_{\text{п.н. BKC}} = 0,125; P_{\text{BKC}} = 20 \text{ TC}^{(1)}; \\ G_{\text{т. BKC}}^{\text{н}} &= 3520 \text{ кгс}^{(2)}; \bar{G}_{\text{т. BKC}} \approx 0,3; S_{\text{BKC}} = 52 \text{ м}^2 \\ P_{\text{BKC}} &= 230 \text{ кгс/м}^2; K_{\text{r}} = 2; V_{\text{лк}} = 7810 \text{ м/с}^{(4)}; \\ \Delta V_{\text{H}} &= 109,4 \text{ м/с}^{(2)}; \Delta V_{\text{p}} = 954 \text{ м/с}^{(2)} \end{aligned}$$

Key: (1). t. (2). kg. (3). kgf/m². (4). m/s.

b) the second accelerator

$$\begin{aligned} G_{y_2} &= 11,9 \text{ TC}^{(1)}; P_{y_2} = 41 \text{ TC}^{(2)}; G_{\text{т. } y_2} = 10,7 \text{ TC}^{(1)}; \\ V_{\text{ср. } y_2} &= 5255 \text{ м/с}^{(2)}; \Delta V_{y_2} = 2555 \text{ м/с}^{(2)} \end{aligned}$$

Key: (1). t. (2). m/s.

c) the first accelerator

$$\begin{aligned} G_{y_1} &= 29,2 \text{ TC}^{(1)}; P_{y_1} = 90 \text{ TC}^{(2)}; G_{\text{т. } y_1} = 24,9 \text{ TC}^{(1)}; \\ V_{\text{ср. } y_1} &= 2700 \text{ м/с}^{(2)}; \Delta V_{y_1} = 2555 \text{ м/с}^{(2)} \end{aligned}$$

Key: (1). t. (2). m/s.

d) the hypersonic carrier aircraft

$$\begin{aligned} G_{\text{с.н}} &= 77,7 \text{ т}^{(1)}; P_{\text{с.н}} = P_0 = 76 \text{ TC}^{(2)}; G_{\text{т.с.н}}^{\text{н}} = 33,8 \text{ TC}^{(2)}; \\ \bar{G}_{\text{т.с.н}} &= 0,244; \bar{G}_{\text{т.с.н}}^{\text{н}} = 0,411; J_{\text{т.с.н}} = 1422 \text{ с}^{(3)}; M_{\text{max}} = 9; \end{aligned}$$

Key: (1). t. (2). t. (3). s.

e) the multistage flight vehicle

$$G_0 = 130,8 \text{ t (with } m=1; G_0=175 \text{ t);}$$

$$\bar{Q}_{11,11} = G_{BRC}/G_0 = 0,0917; \bar{P}_0 = 0,58 \text{ so forth.}$$

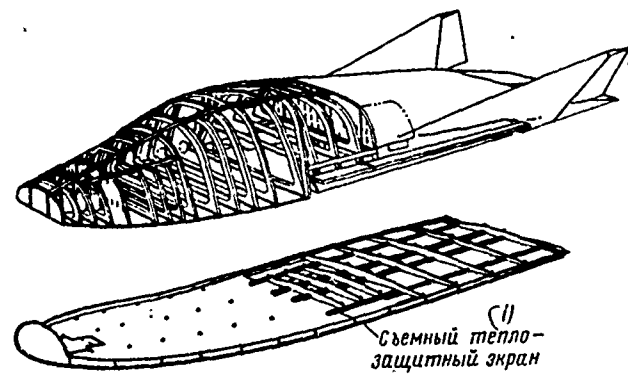


Fig. 11.32. Construction/design VKS VL-3A.

Key: (1). Detachable heat shield.

DISTRIBUTION LIST

DISTRIBUTION DIRECT TO RECIPIENT

| <u>ORGANIZATION</u> | <u>MICROFICHE</u> | <u>ORGANIZATION</u> | <u>MICROFICHE</u> |
|----------------------------------|-------------------|---------------------|-------------------|
| A205 DMATC | 1 | E053 AF/INAKA | 1 |
| A210 DMAAC | 2 | E017 AF/INDXTR-W | 1 |
| B344 DIA/RDS-3C | 9 | E403 AFSC/INA | 1 |
| C043 USAMIIA | 1 | E404 AEDC | 1 |
| C509 BALLISTIC RES LABS | 1 | E408 AFWL | 1 |
| C510 AIR MOBILITY R&D LAB/FIO | 1 | E410 ADTC | 1 |
| C513 PICATINNY ARSENAL | 1 | FTD | |
| C535 AVIATION SYS COMD | 1 | CCN | 1 |
| C591 FSTC | 5 | ASD/FTD/NIIS | 3 |
| C619 MIA REDSTONE | 1 | NIA/PHS | 1 |
| D008 NISC | 1 | NIIS | 2 |
| H300 USAICE (USAREUR) | 1 | | |
| P005 DOE | 1 | | |
| P050 CIA/CRB/ASD/SD | 2 | | |
| NAVORDSTA (50L) | 1 | | |
| NASA/NST-44 | 1 | | |
| AFIT/LD | 1 | | |
| IIL/Code L-389 | 1 | | |
| NI 1/1213/TDL | 2 | | |